DOCTOR OF PHILOSOPHY

Detection of saline intrusions in coastal and estuarine sediments.

Soomro, Saeed Ahmed

Award date:
1993

Awarding institution:
Bangor University

Title: DETECTION OF SALINE INTRUSIONS IN COASTAL AND ESTUARINE SEDIMENTS

A thesis submitted in accordance with the requirements of the University of Wales for the degree of Doctor of Philosophy.

By: SAEED AHMED SOOMRO

University College of North Wales,

School of Ocean Sciences,

Menai Bridge, Gwynedd.

U.K. LL59 5EY.

December, 1993.

بِسْمِ اللّٰهِ الرَّحْمٰنِ الرَّحِيْمِ

In the name of ALLAH (GOD),

THE MOST BENEFICENT, THE

MOST MERCIFUL

وَهُوَ الَّذِيْ مَرَجَ الْبَحْرَيْنِ هٰذَا

عَذْبٌ فُرَاتٌ وَّهٰذَا مِلْحٌ اُجَاجٌ

وَجَعَلَ بَيْنَهُمَا بَرْزَخًا وَّحِجْرًا مَّحْجُوْرًا

(52) It is HE (ALLAH) Who has let free the two bodies of flowing water: one palatable and sweet, and the other salt water and bitter; yet He has made a barrier between them. A barrier that is forbidden to be passed (Qura-an, s.xxv. 52).

DEDICATION

Dedicated to my late father who always wanted me to seek higher education and to my loving mother whose blessings I live on.

ACKNOWLEDGEMENTS

I thank Professor Denzil Taylor Smith who despite his multifarious engagements as head of School of Ocean Sciences, University of Wales, took time to supervise. His positive and constant encouragement enabled me to finish this project.

My special thanks are due to Mr. Roger Cratchley for his constant support, encouragement and enlightening discussions.

I am thankful to Mr. Sinclair Buchan, Dr. Jim Bennell, Dr. Angela Davis, Dr. J.Scourse and D. J.Wrench who helped me at every stage of this work.

I would also like to thank Mr. F.C.D. Dewes, A.Nield, David Boon and especially Mr. G.Williams.

I am grateful to Dr. David Laidman and Mrs. Peggy Laidman for their constant encouragement and making my family's stay in Bangor a comfortable one.

I am thankful to my colleagues and friends especially Lal Bakhsh Bozdar, Allah Dino Memon, Mohammed Ali Baryar, Asif Ali Kazi, Dr. M.R. Ahmed, Abdul Rehman Mughal, Khalil-ur-Rehman Mughal, Ali Mohammed Jokhio and Sarfraz Solangi at the University of Sindh; and Mir Lutuf Ali Talpur and Ahmed Saeed Abbassi at the Cooperation Department, Government of Sindh, for their constant moral support.

I also thank Mrs. Rose & Mr. Joe Evans for their encouragement and making my stay for the last few months at their home a comfortable one.

I am extremely grateful to my brother Atta Mohammed Soomro for his continuous and unending encouragement through moral and material support.

In the last but not the least I am highly indebted to my wife Hasina Soomro and children Kashif, Faisal, Mehwish and Shafqat Soomro, who made me take up this challenging task: their continued silence and undemanding support after returning to Pakistan made it possible to finish this project.

I acknowledge with many thanks the special permission granted by the Countryside Council for Wales for the survey on Malltraeth beach and Newborough forest area.

I am grateful to the University of Sindh, Pakistan, for their very valuable financial support during this research.

SUMMARY

In the years 1991 and 1992 combined vertical electric (VES) and electromagnetic (EM) soundings, complemented by chemical analyses of borehole water samples, were made with the aim of detecting and mapping saline-fresh water interfaces in coastal and estuarine sediments. Two coastal areas, one at Morfa Bychan at the northern edge of Cardigan Bay and another on the College Farm at Aber on the Menai Strait, and one estuarine area on the northern bank of the Afon Cefni at Malltraeth, were chosen for detailed study.

The VES and EM data show close agreement to themselves as well as to the salinity of the groundwater determined by chemical means. On the basis of these and borehole data it has been possible to define an aquifer at each site, boundaries of saline intrusion into groundwater, and zones of mixing between the two. An aquifer filled with fresh groundwater has a resistivity of more than 35 ohm.m (chlorides less than 250 ppm), the zone of mixing water (transition zone) has resistivities ranging between 8 ohm.m to 35 ohm.m (chlorides between 250 to 500 ppm), and saline water has a resistivity of 7 ohm.m or less (chlorides 500 ppm or more). These data cast some doubt on the applicability of the Ghijben-Herzberg Relationship in defining the position of the saline-fresh water interface.

In addition to these observations, pumping tests were carried out which not only gave permeability values but also showed the modification of the saline interface caused by pumping. Permeabilities were also measured both in-situ and in the laboratory on collected samples using standard techniques; permeabilities were also estimated using electrical formation factor considerations. In general close similarities existed between the various techniques. The permeabilities of the aquifers range from 3.2×10^{-4} m /sec to 1.3×10^{-3} m/sec which can be classified as moderate.

It is clear that in the sites examined a combination of permeability and an abundance of fresh water from the land (from rainfall and rivers) prevent any extensive saline intrusion. However the intrusive zone is extended during the period when spring tides operate.

The overall conclusion is that VES and EM techniques are dependable practical tools for the determination and mapping of any saline intrusion. Importantly they can also provide values of porosity and permeability which agree closely with those parameters obtained by traditional hydrological methods. This opens a way forward for the use of electrical techniques as precursors to any detailed investigation such as pumping tests. They can also be used in a monitoring mode for detecting changes in aquifer salinity caused by abstraction of groundwater allowing saline intrusion to occur. Such a procedure can be of considerable significance in Pakistan to assess the severity of the twin problems of waterlogging and commensurate salinity changes.

CONTENTS

CHAPTER 1. INTRODUCTION

Saline water is the most common pollutant in fresh groundwater. The pollution can occur in deep aquifers with the upward advance of saline waters of geologic origin, in shallow aquifers from surface waste discharges, and in coastal aquifers from an invasion of seawater.

Increasing demands are being made on the water resources of many countries particularly Third World countries because of their expanding population, especially in coastal areas. Proper management, development and use of fresh water in such areas is necessary to prevent contamination of existing water supplies. Sound management decisions can be made when based on available information; therefore, it is desirable to gather as much data as is economically reasonable to support these decisions.

A typical inland groundwater salinity problem is that exhibited in Pakistan, which geologically comprises mostly marine beds with thick overlying alluvial deposits. Since the introduction of canal irrigation systems, the canals have gradually silted up such that their beds have been raised to the same level as the ground surface and, in some instances, even higher. This caused a lot of seepage of canal water into the ground which raised the level of the water table. Groundwater with dissolved Na, K, Mg, Ca, SO_4, or Cl, etc., is abundantly present in the lower layers; when this water, rich in SO_4 and/ or Cl, reaches the ground surface it evaporates and leaves behind a thin crust of salt on the surface causing the twin problems of surface waterlogging and salinity.

In the seventies almost one hundred thousand acres of land went out of cultivation annually because of this twin menace. The subsequent installation of tube wells in large numbers, reduced this menace to some extent. However the problem of extraction of saline water and its use for watering agricultural lands on the one hand lowered the water table but on the other hand aggravated further the salinity on the surface. To overcome this new problem, the World Bank with the aid of O.D.A. (U.K) and other donor agencies, started a gigantic drainage project in the late eighties involving the construction of many surface drains to drain out highly saline water (initially pumped out by tube wells) into the sea. Work on this project is still going on and the results are yet to be seen (Water and Power Development Agency,Pakistan. Water logging and salinity. Annual Reports, 1970; 1988; and 1989).

Braithwaite (1855), which historically may be the first published reference on the problem, illustrated the salinity problems caused by pumping in London and Liverpool. He suggested that the infiltration of seawater was caused by lowering the groundwater level below that of the sea. Herzberg (1901), Oscar Meinzer (1945), Wentworth (1951), Schmorak and Mercado (1969), on the basis of various field observations, remarked that pumping caused a continuous encroachment of salt water. More than 90 years ago Badon Ghijben (1889) in Holland and Herzberg (1901) in Germany, working independently, found that fresh groundwater floats above salt water because of its lower density. Field measurements at Miami (Cooper et al., 1964) and experimental studies (Cahill, 1967; Goswami, 1968) have confirmed a considerable amount of shift in the saline-fresh water interface due to changing tidal patterns.

The most common method of monitoring salt water movement in coastal areas is

by periodically measuring the chloride concentration in water from observation wells. Properly-constructed observation wells are expensive and, thus, the number that can be drilled is highly restricted. An alternative method of monitoring is to use geophysical electrical resistivity surveying techniques. This method allows monitoring of a large area at a comparatively small cost. In addition, surface resistivity measurements can be used to give supplemental water quality control in areas between observation wells.

As chloride is a dominant ion of ocean water, and usually plays only a minor role in groundwater, an increase in chloride content is the most reliable indicator of the first stages of salt water intrusion into groundwater. Hagemeyer (1988) has shown that water quality control data are essential to differentiate saline water from mineralized water.

As early as 1937, Swartz (1937) used direct-current resistivity method to locate fresh water lenses in salt water bodies. Since then, much resistivity work on the detection of fresh-saline water interface has been continuously carried out in various parts of the world (Flathe, 1970; Zohdy et al., 1974; Gorhan, 1976; and Worthington, 1977). Since the late 1960's, numerous studies in the United States have been performed to locate and map contaminated waters (Cartwright et al., 1968; Fretwell and Stewart, 1981; and Stewart et al., 1982).

It follows from the above that it should be possible to develop combined vertical electric (VES) and electromagnetic (EM) soundings together with chemical methods to detect and map the fresh-saline water interface in coastal and estuarine sediments. At the same time the separate effects of pumping and spring tides can be studied on the saline-

fresh water interface.

1.1 Aims of the thesis:

To detect/ map the saline-fresh water interface in coastal and estuarine sediments at different sites in North Wales using geophysical and chemical methods, and to compare the characteristics of these sites,

(2) To investigate the movement of the interface due to tidal and pumping effects,

(3) To examine the effect of permeability and transmissivity on the saline intrusions, while at the same time to compare the value of permeability derived from the electrical observations to those obtained by conventional means.

To achieve these aims:

(1) Combined vertical electric and electromagnetic soundings were carried out in three areas, where some sediment parameter data from previous investigations was available. These were Aber College Farm, Malltraeth and Morfa Bychan during the years 1991 and 1992. In addition, boreholes and auger holes were drilled to carry out field pumping (one site only), permeability and hydro-chemical tests.

(2) Laboratory measurements of some sediment parameters from these sites were made (to supplement the data already on file) to examine the effect of porosity and permeability on saline intrusion.

CHAPTER 2. SALINE INTRUSION IN GROUNDWATER

Intrusion of seawater into coastal aquifers is a natural consequence of the density contrast between fresh and saline water, the denser seawater often forming a deep wedge that can extend for many kilometres inland (Bear, 1972; Raudikivi and Callander, 1976).

The first known published reference in history may be that of Braithwaite (1855) who illustrated the salinity problems caused by pumping in London and Liverpool. He suggested that the infiltration of seawater was caused by lowering the groundwater level below that of the sea. But according to our present knowledge, it is well established that salt water invasion may still take place even when the water table level is slightly higher than that of the sea (Kashef, 1968a).

2.1 Nature and Position of saline-fresh water bodies and Ghijben-Herzberg Relationship

More than 90 years ago two investigators Badon Ghijben (1889) in Holland and Herzberg (1901) in Germany, working independently along the European coast, found that fresh groundwater floats above salt water because of its lower density. Their principle is now well known as the Ghijben-Herzberg Relationship. If the height of the water table level is h_f above the mean sea level (MSL), then at the same site the fresh water should extend to a distance z below the MSL such as shown in Figure 2.1. This distribution was attributed to hydrostatic equilibrium existing between the two fluids of different densities neglecting the fresh water movement. The hydrostatic balance between fresh and saline water can further be illustrated by the U-tube shown in Figure

2.2. Pressures on each side of the tube must be equal; therefore,

$$\rho_s g z = \rho_f g (z + h_f) \qquad (2.1)$$

where ρ_s is the density of the saline water, ρ_f is the density of the fresh water, g is the acceleration of gravity, and z and h_f are as shown in Figure 2.2. Solving for z yields

$$z = \frac{\rho_f}{(\rho_s - \rho_f)} h_f \qquad (2.2)$$

which is the Ghijben-Herzberg relationship. For typical seawater conditions, let ρ_s=1.025 and ρ_f=1.000, so that

$$z = 40 h_f \qquad (2.3)$$

Translating the U-tube to a coastal situation shown in Figure 2.1., h_f becomes the elevation of the water table above sea level and z is the depth to the fresh-saline water interface below sea level. Herzberg (1901) gave an approximate value for z as 37. Wentworth (1939) stressed the relation of ground and sea temperatures to measurements of the specific gravity in his application of the Ghijben-Herzberg relationship. He favoured using a value z = 38. Hubbert (1940) considered the dynamic rather than the hydrostatic equilibrium of the fresh-salt water interface because fresh water is flowing

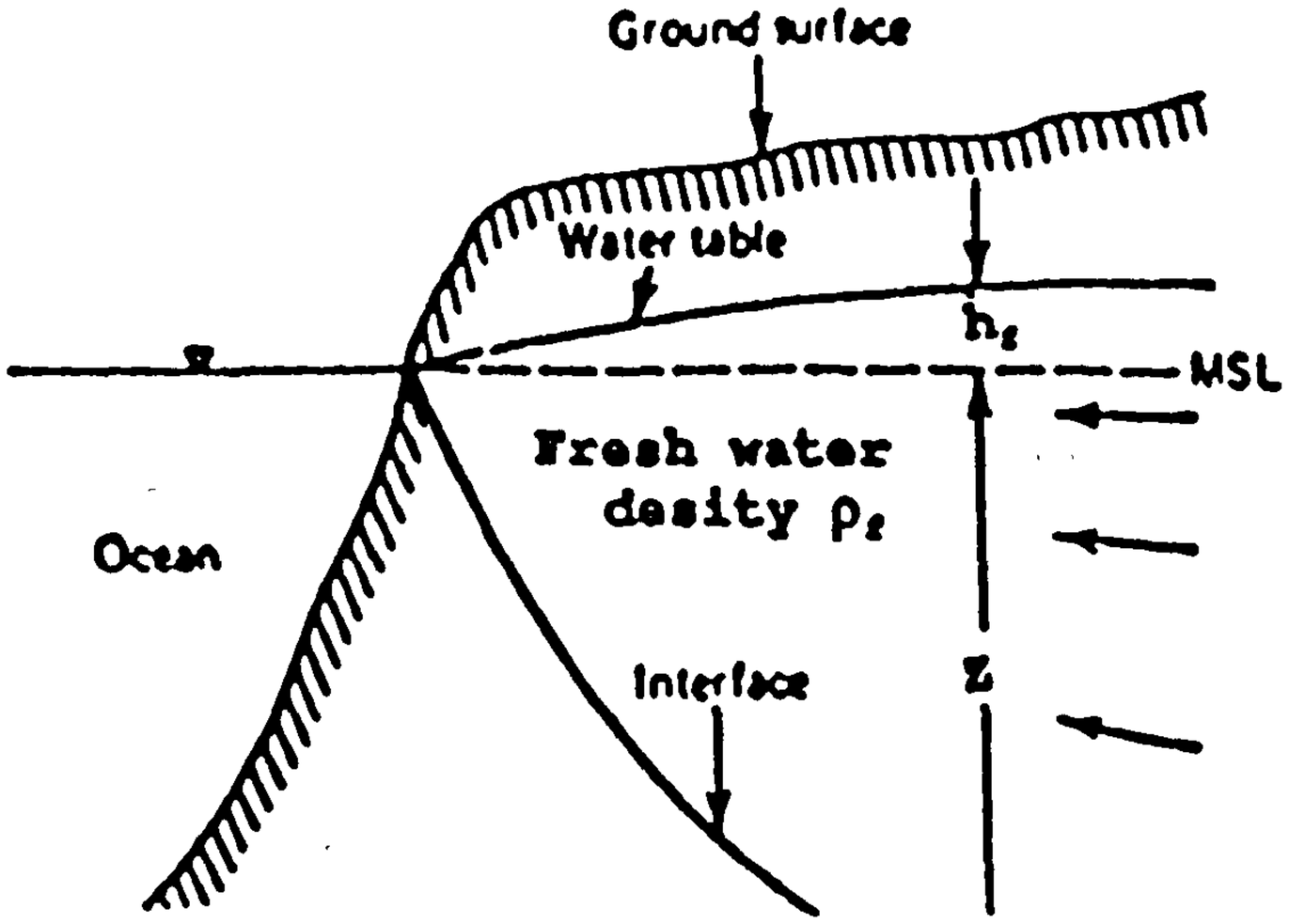

Figure 2.1 Idealized sketch of occurrence of fresh and saline groundwater in an unconfined coastal aquifer(after Todd, 1980).

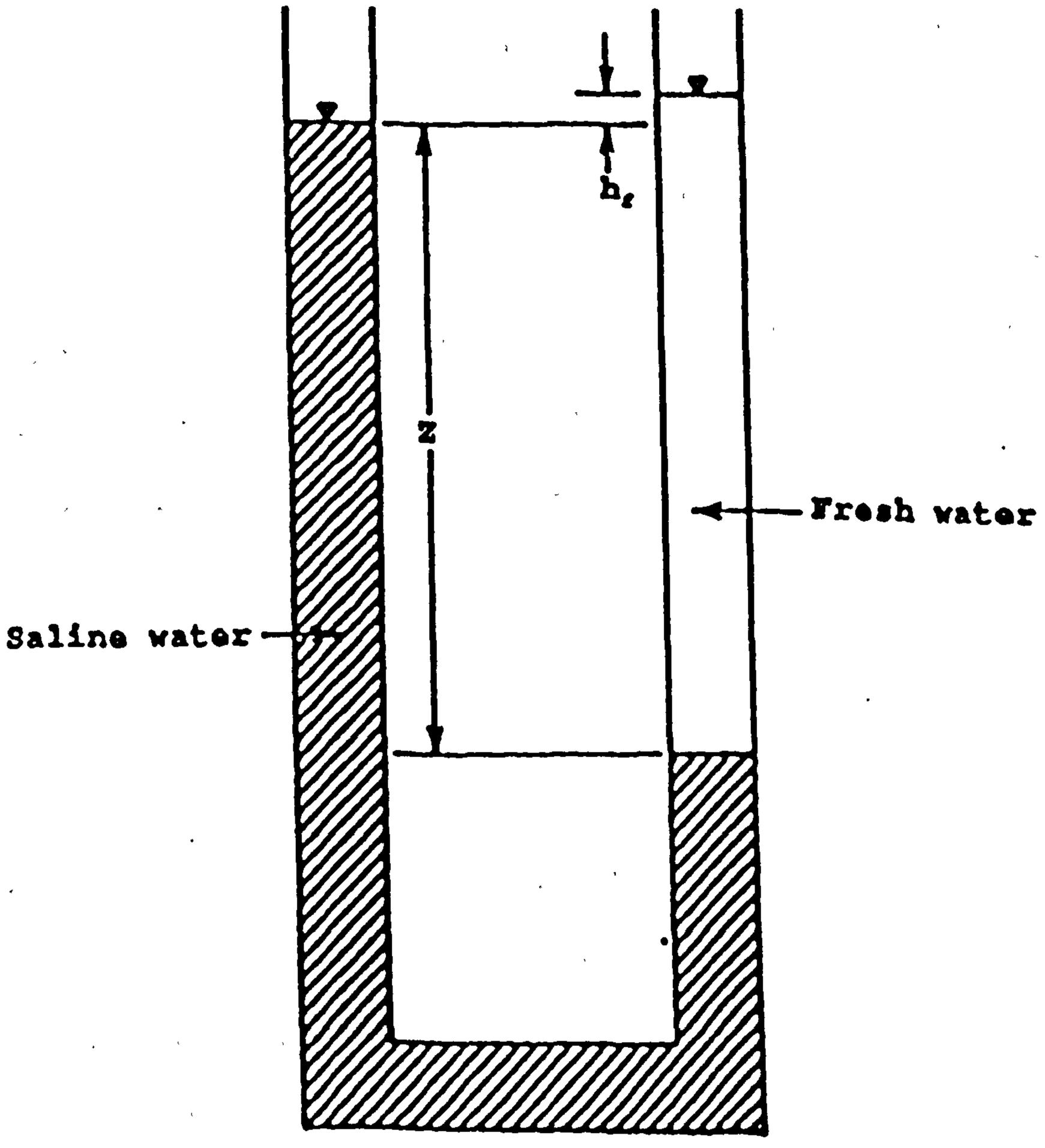

Figure 2.2 Hydrostatic balance between fresh water and saline water illustrated by a U-tube (after Todd, 1980).

toward the sea. Hubbert (1940) also showed that where the flow is nearly horizontal, the Ghijben-Herzberg relationship gives satisfactory results. His analyses indicated that the actual interface should be located below that determined by Ghijben- Herzberg (Figure 2.3). For confined aquifers the above derivation can also be applied by replacing the water table by the piezometric surface. It is important to note from the Ghijben-Herzberg relationship that fresh-salt water equilibrium requires that the water table, or piezometric surface, (1) lies above sea level, and (2) slopes downward toward the ocean. Without these conditions, seawater will advance directly inland.

Starting from the work of Hubbert (1940), the Ghijben-Herzberg relationship has been generalized by Lusczynski, 1961; and Lusczynski et al., 1966, for situations where the underlying saline water is in motion with heads above or below sea level.

Since the original studies, others have appeared based on observations of coastal wells, which have been in agreement with the Ghijben-Herzberg relationship. These studies have included further work in Holland by Pennink (1905), in Belgium by D'Andrimont (1902), in Florida by Brown and Parker (1945), and in the Marianas Islands by Ohrt (1947). It is manifest that sea water does not exist everywhere under continental areas, so that the extent and continuity of the primary aquifers impose a natural boundary upon the application of the principle (Brown, 1925; Nomitsu, Toyohara and Kamimoto, 1927).

Krul and Liefrinck (1946) have recognized that the Ghijben-Herzberg relationship is really a great simplification of the actual ground-water picture. Sympathetic tidal fluctuations in coastal aquifers (Brown, 1925; Isaacs and Bascom, 1949) continuously shift the fresh-water interface. Diffusion introduces the problem of

density changes. In beach zones this effect may be of sufficient magnitude to introduce discrepancies in identification of interfaces (Toyohara, 1935) or to obscure completely the interface between fresh and salt water. Nevertheless, most observations have confirmed the Ghijben-Herzberg relationship. However, where steep potential gradients frequently occur, as near coastal areas, pumping wells, rivers and canals, large errors may be incurred.

Further recent developments have indicated that the actual theoretical interface should always be lower than the Ghijben-Herzberg interface. The difference in location is due to the effect of the 'seepage forces' produced by the water movements (Kashef, 1968b).

2.2 Structure of the Fresh-Salt water Interface

2.2.1 Shape of Interface

In deriving the Ghijben-Herzberg relationship, it was implicitly assumed that the fresh-salt water interface sloped downward from the coast. The interface shape and slope can be inferred for the case where flow occurs in the fresh water zone only. Denoting the water table slope, as shown in Figure 2.4, then from Darcy's law

$$Sin\beta = \frac{dh}{d_s} = \frac{V}{K} \qquad (2.4)$$

where V is velocity and k is the coefficient of permeability. Along this slope the water table elevation decreases in the direction of flow, consequently according to equation

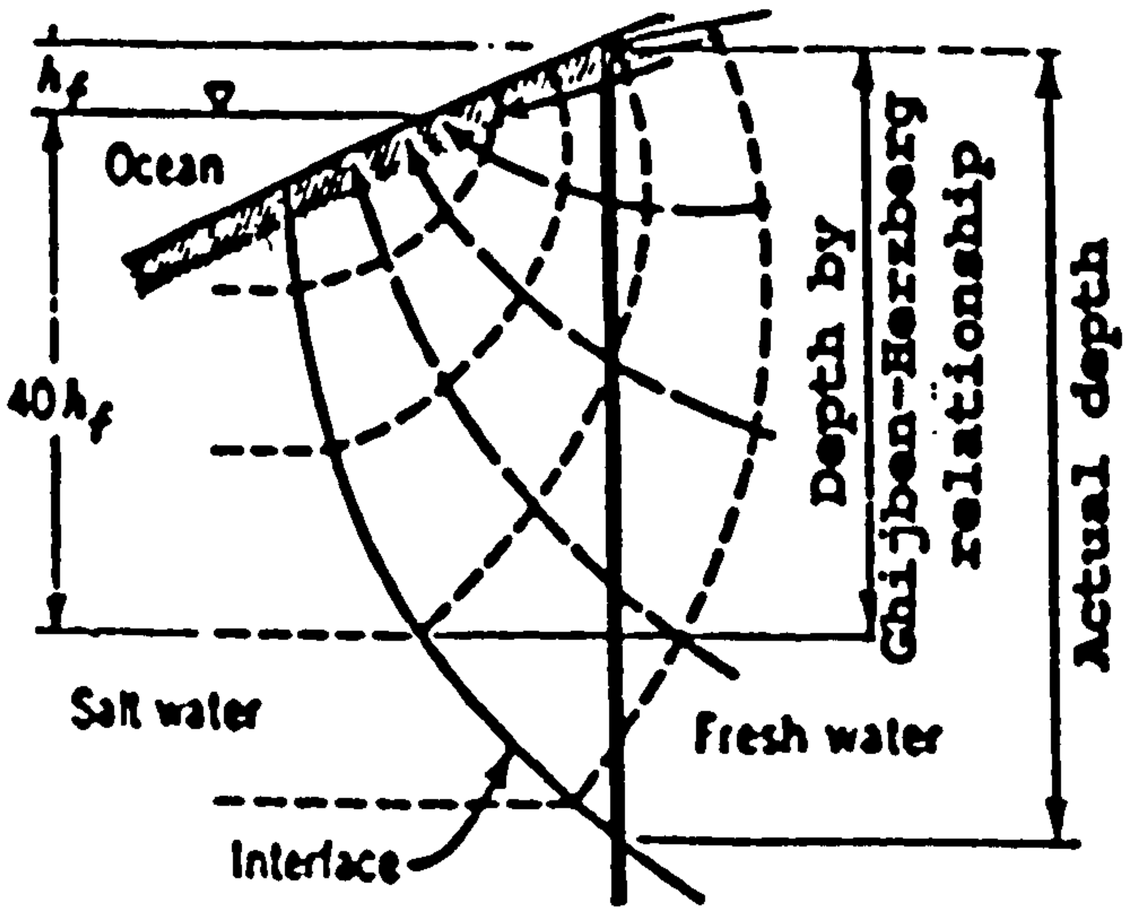

Figure 2.3. Discrepancy between actual depth to salt water and depth calculated by the Ghijben-Herzberg relationship (after Hubbert, 1940).

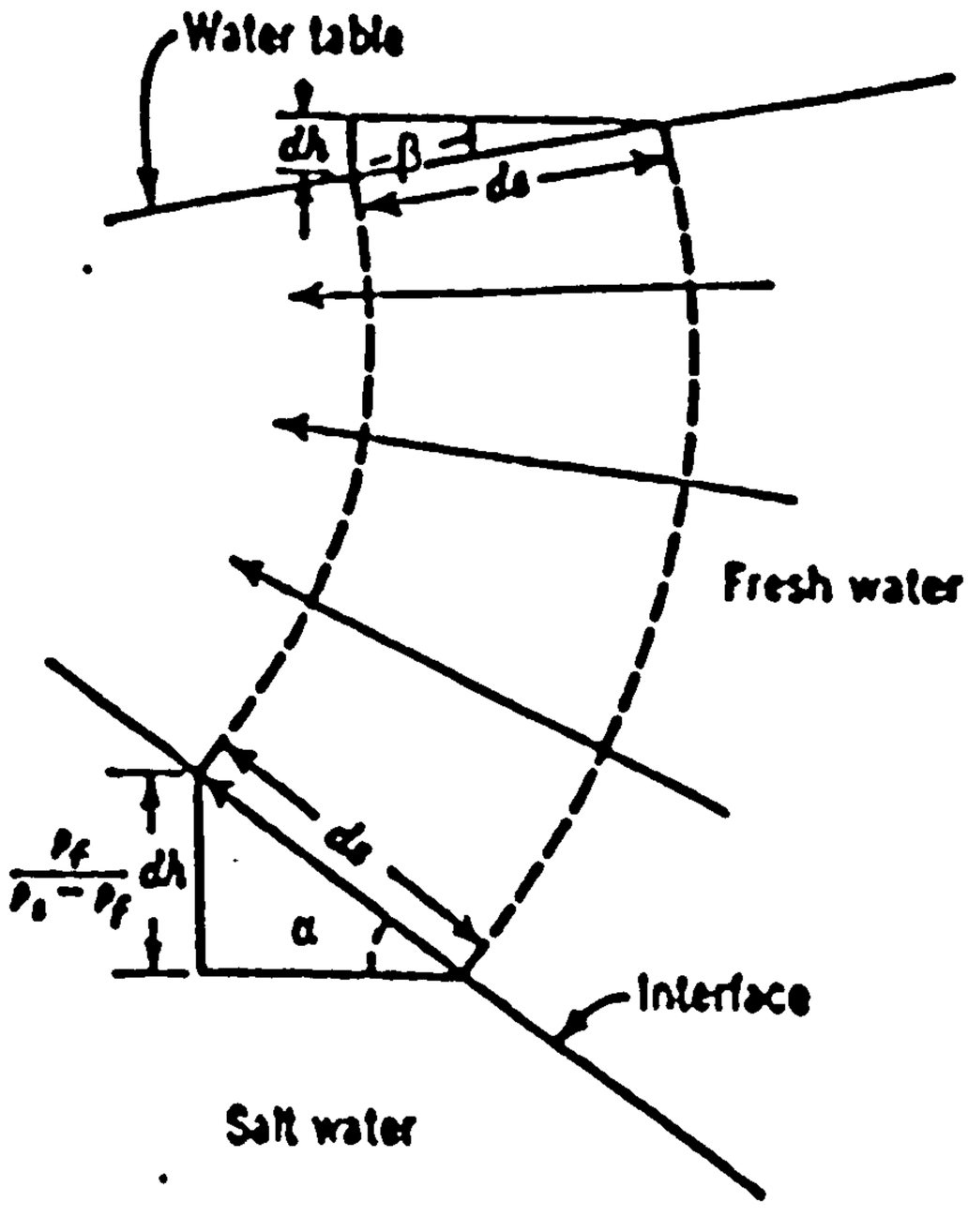

Figure 2.4. Relation between slopes of the water table and the fresh-salt water interface.

2.2., the fresh-salt water boundary must rise. Its slope (Figure 2.4) is given by

$$Sin\ \alpha = \frac{\rho_f}{\rho_s - \rho_f}\frac{V}{K} \qquad (2.5)$$

Because of the converging boundaries, V must increase with distance. It follows, therefore that the magnitude of the slopes increase accordingly. This results in a concave interface with respect to the fresh water. A more rigorous derivation of the above reasoning is given by Hubbert (1940).

Recognizing the approximations inherent in the Ghijben-Herzberg relationship, more exact solutions for the shape of the interface have been developed from potential flow theory (Charmonman, 1965; Cooper et al., 1964). The result (by Cooper et al., 1964) has the form for the depth of the interface beneath the shoreline z_o occurs, where x = 0 (see Figure 2.5) so that

$$z_o = \frac{\rho q}{\Delta_\rho K} \qquad (2.6)$$

where z and x are as shown in Figure 2.5., K is the hydraulic conductivity of the aquifer, q is the fresh water flow per unit length of shoreline and $\Delta_\rho = \rho_s - \rho_f$.

Steady state solutions for the size and shape of the lens, assuming a fixed boundary and sharp interface have been given by Henry, 1964; Todd, 1980; and Van Der Veer, 1977.

2.2.2 Length of the Intruded Wedge

Reasoning from the Ghijben-Herzberg relationship, a salt water wedge must exist at the intersection of an aquifer with the ocean. Assuming that a seaward fresh water flow q per foot of ocean front exists, then the approximate relation for a confined aquifer can be derived

$$q=\frac{1}{2}\frac{(\rho_s-\rho_f)}{\rho_f}\frac{kb^2}{L} \qquad (2.7)$$

Starting from Darcy's law, where ρ_f and ρ_s are fresh and salt water densities respectively, b and L are as defined in Figure 2.6., and k is the coefficient of permeability. Equation 2.7. indicates for uniform aquifer and fluid conditions that the length of the intruded wedge is inversely proportional to the fresh water flow. The equation can also be applied to unconfined aquifers by replacing b by the saturated thickness, providing the flow does not deviate greatly from the horizontal.

2.2.3 Trans-Interface Flow/Mixing zone

Interfaces are generally treated as fluid boundaries. At actual ground water interfaces, however, processes occur which introduce passage of fluids across the interface. The most important of these are percolation and evaporation across the upper interface and diffusion across the lower interface. Water percolating downward from the ground surface flows through partially saturated pores until reaching the fresh-water (upper) interface. Here it combines with the fresh-water flow in completely saturated

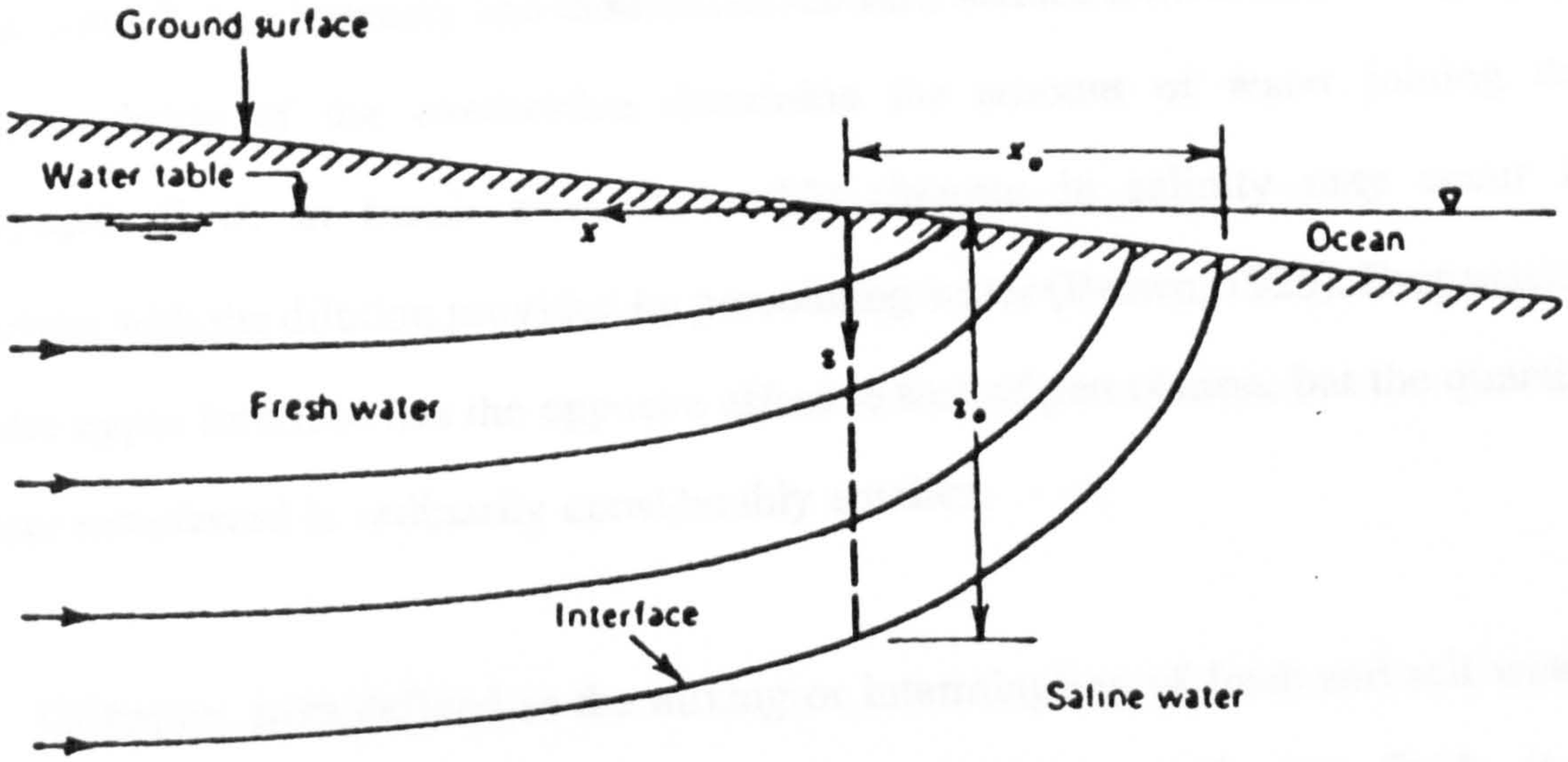

Figure 2.5 Flow pattern of fresh water in an unconfined coastal aquifer(after Todd, 1980).

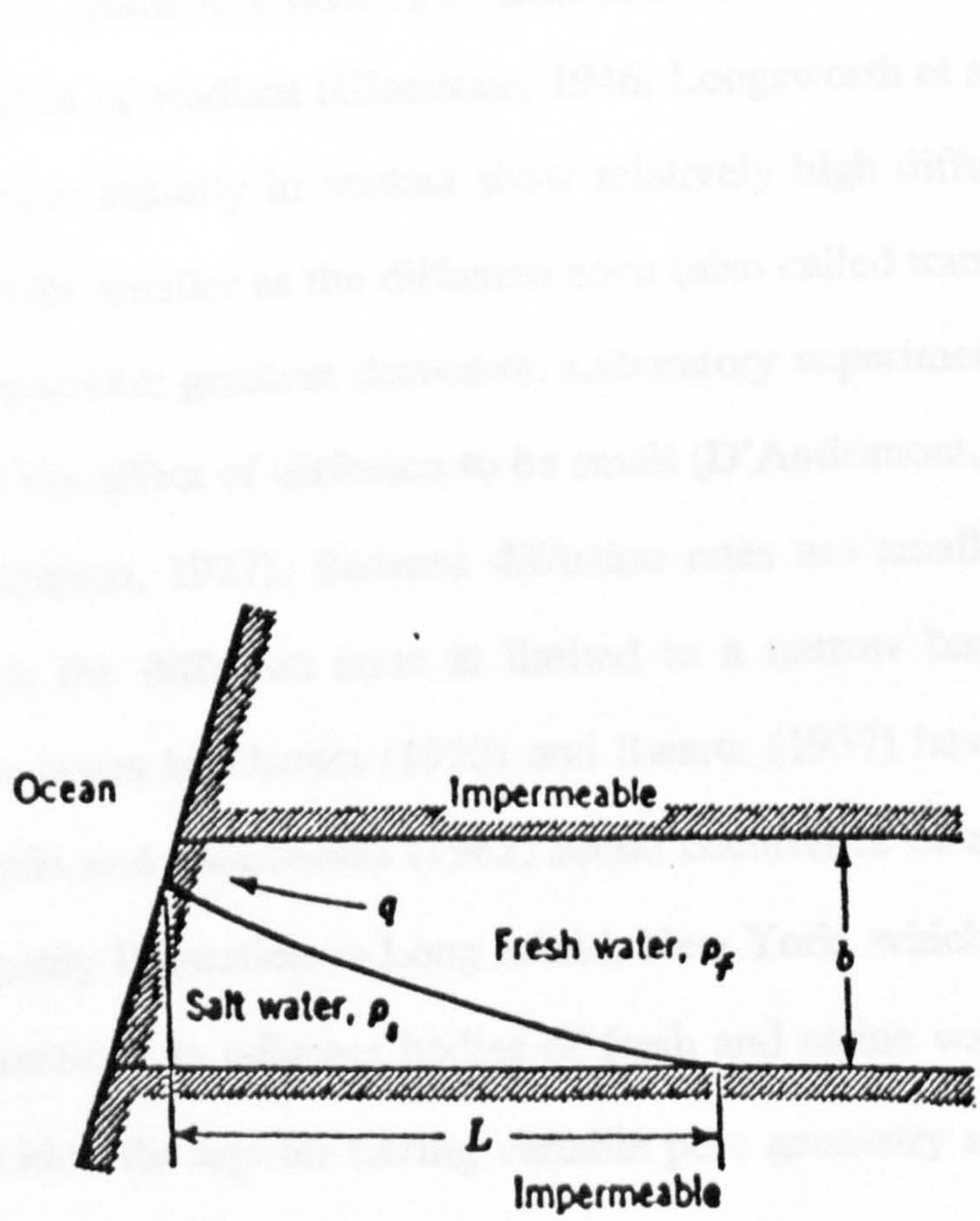

Figure 2.6. Salt water wedge in a confined aquifer.

pores. Jacob (1950) has pointed out this process causes ground-water streamlines to form very flat angles with the interface. This added water raises the interface in proportion to the volume of surcharge, as is commonly observed after periods of above-average rainfall. The intensity and duration of rainfall, surface infiltration, stratigraphy, and permeability of the overburden determine the amount of water joining the groundwater flow. In beach areas noticeable changes in salinity may occur in connection with the dilution provided by percolating water (Brown, 1925). Evaporation from the upper interface has the opposite effect to that of percolation, but the quantity of water transferred is ordinarily considerably smaller.

Diffusion, here defined as the mixing or intermingling of fresh and salt waters at their interface resulting from molecular dispersion between the two fluids, is an instance of a fluid interface not serving as a complete boundary. The rate of diffusion between two fluids in a vertical column of uniform cross section is proportional to the concentration of gradient (Glasstone, 1946; Longsworth et al., 1945). Thus freshwater and saltwater initially in contact show relatively high diffusion rates, which become progressively smaller as the diffusion zone (also called transition zone), increases and the concentration gradient decreases. Laboratory experiments in this connection have indicated the effect of diffusion to be small (D'Andrimont, 1905; Nomitsu, Toyohara, and Kamimoto, 1927). Because diffusion rates are smaller than usual groundwater velocities, the diffusion zone is limited to a narrow band. Field measurements of diffusion zones by Brown (1925) and Swartz (1937) have confirmed this. However Lusczynski and Swarzenski (1962) found occurrence of a broad zone of diffusion in the Magothy Formation in Long Island, New York, which they attributed to opposing flow directions in adjacent bodies of fresh and saline water, effects of movement of water within the aquifer having variable pore geometry and molecular diffusion.

Cooper (1959) advanced the hypothesis of Ghijben and Herzberg that under dynamic conditions salt water is not static but flows perpetually in a cycle from the floor of the sea into a zone of diffusion and back to the sea, and that this flow tends to lessen the extent to which the salt water occupies the aquifer. Under the zone of diffusion Cooper (1959) suggested that there is a zone of substantial thickness in which there is a gradation of the salinity from that of salt water to that of fresh water. Thus, diluted sea water having become less dense than native sea water, rises along a seaward path. Meanwhile, the salts that are introduced into the fresh water environment are carried back to the sea by the flow of the fresh water system.

Where inhomogeneities occur in coastal aquifers, stratifications and irregularities in the distribution of fresh and saline waters occur (Harris, 1967; and Perlmutter and Geraghty, 1963). Considerable research has been done on seawater intrusion in layered aquifers (Collins and Gelhar, 1971; and Rumer and Harleman, 1963), and on unsteady movement of the transition zone (Bear and Dagan, 1964; Hantush, 1968; and Pinder and Cooper, 1970).

Figure 2.7 shows a transition zone in a highly permeable limestone aquifer in Miami, Florida. Note the numbered lines are iso-chlors (water areas having the same chloride or salinity value) which approach the base of the aquifer perpendicularly ; this results because the flow parallels the base of the aquifer, thereby restricting vertical mixing (Cooper et al., 1964). This is a case where the sharp interface approximation is not justified. Figure 2.8, after Todd (1974), schematically illustrates the flow patterns in the three subsurface zones.

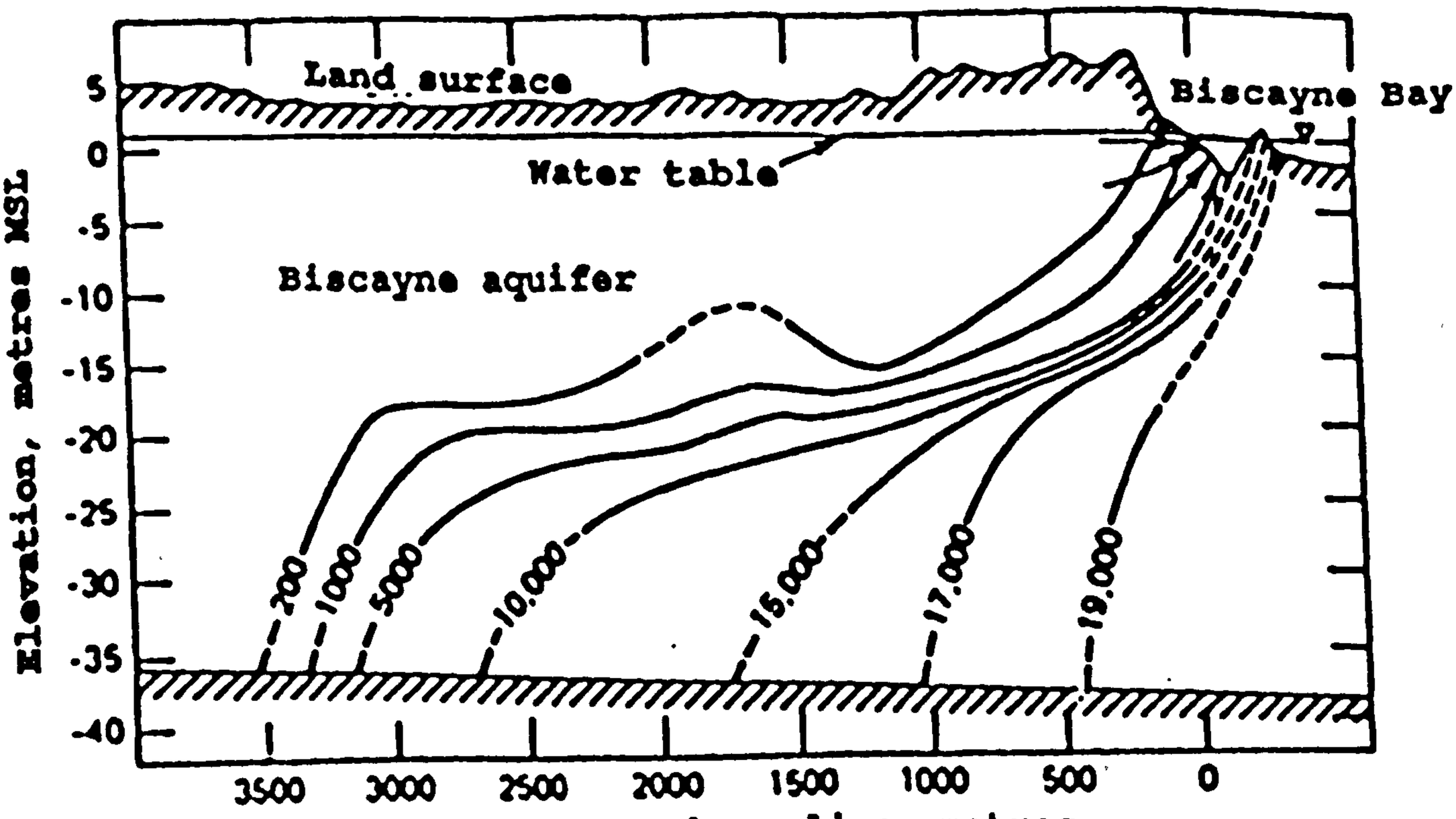

Figure 2.7. Cross section through the transition zone of the Biscayne aquifer near Miami, Florida. Numbered lines are isochlors in mg /l (after Cooper, et al. 1964).

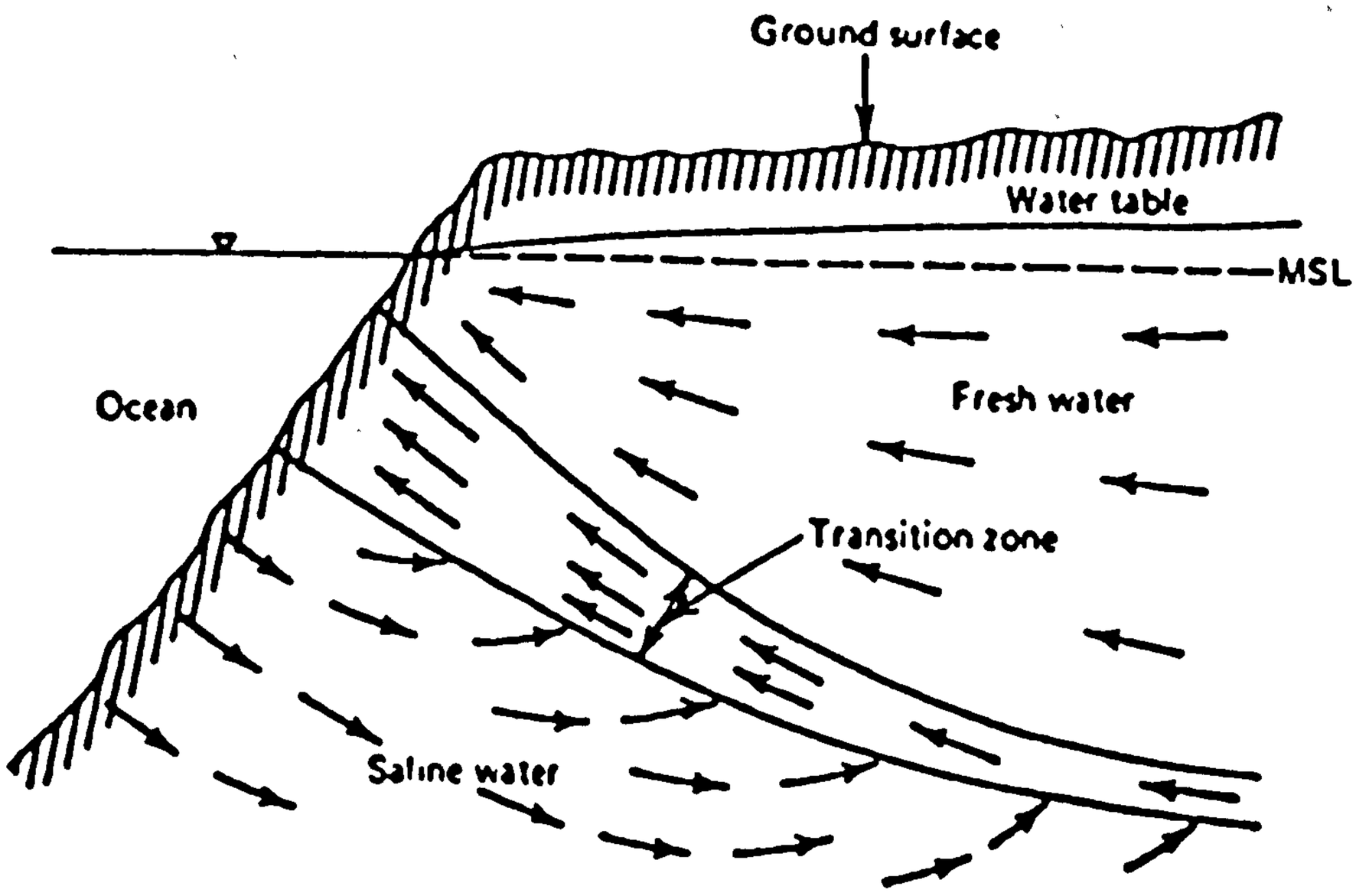

Figure 2.8 Vertical cross section showing flow pattern of fresh and saline water in an unconfined coastal aquifer(after Todd, 1974).

2.3 Change in shape and position of interface

2.3.1 Due to Tidal Effect

The hydrodynamic balance between saline and freshwater in a beach area is governed by the broad principles of rise and fall of sea level, the principal and important results of which are evident locally in the patterns of coastal erosion or beach build up. It has also been observed that every year during winter in some regions, and in summer and monsoon periods in other regions, the coastal beaches as well as shore lines get eroded due to the action of large tidal waves causing a considerable change in the morphology of the coastal area. Obviously, a study of the stability relationship of the interface over an interval of time and space could materially indicate the areal extent and depth of variation of the interface, vis-a-vis the activities of the sea.

Herzberg (1901) noted that equation 2.2 did not hold exactly in all cases and that it is strongly influenced by the fineness or coarseness of the dune sands which were the media of his field tests. He also recognised the rise and fall of water levels due to the tidal effects and that the response lagged three to four hours behind the tides.

Field measurements at Miami (Cooper et al., 1964) and experimental studies (Cahill, 1967) have confirmed the landward movement of the saline water body. Where tidal action is the predominant mixing mechanism, fluctuations of groundwater, and hence the thickness of the transition zone, become greatest near the shore line.

Goswami (1968) after study of many continuous years on coastal areas, observed that spring tides caused lot of erosion of beaches and this resulted in considerable amount of shift in saline and fresh water interface. He further observed that the daily tidal effect and groundwater variations caused minor movement of the saline and fresh

water interface.

2.3.2 Due to Pumping

A sharp interfacial boundary between fresh and saline water does not occur under field conditions. Instead, a brackish transition zone of finite thickness separates the two fluids. This zone develops from dispersion by flow of the fresh water plus unsteady displacements of the interface by external influences such as tides, recharge and pumping of wells (Wentworth, 1951). In general the greatest thickness of transition zones are found in highly permeable coastal aquifers subjected to heavy pumping. Observed thicknesses vary from less than 1 m to more than 100 m. As an extreme case, concentrated pumping in the Honolulu-Pearl Harbour area of Hawaii has created localized transition zones more than 300 m thick.

Herzberg (1901) remarked that the salinity of the groundwater increased during a dry season and periods of heavy pumping. Pennink (1905) through his detailed studies and drawings, indicated how the salt water may be sucked into a well even when the bottom of the screen is above the original salt water level, a conclusion which is presently accepted. Oscar Meinzer (1945) warned of over pumping in coastal aquifers on the basis of various field observations and predicted a continuous encroachment of salt water.

Pumping a well in a fresh water zone underlain by salt water causes the salt water front to rise locally below the well. This phenomenon is also known as 'upconing' and is in response to the pressure depression around the well (Diersch et al., 1984; Schmorak and Mercado, 1969). While working on the upconing mechanism,

Schmorak and Mercado (1969) defined a certain elevation above the initial interface (which they assumed horizontal) and called it the 'critical rise', Figure 2.9. As pumping increases the interface forms an expanding mound with a maximum height below the axis of the partially penetrating wells. Once the maximum height reaches the critical rise, a sudden rise of salt water to the well would take place. They prepared two graphs from which the maximum permissible pumping and rise of interface may be obtained.

2.4 Sources of Salinity in Groundwater

As a result of chemical and biochemical interactions between groundwater and the geological materials through which it flows, and to a lesser extent because of contribution from the atmosphere and surface water bodies, groundwater contains a wide variety of dissolved inorganic chemical constituents in various concentrations (Foster, M.D. 1942). The concentrations of total dissolved solids (TDS) in groundwater is determined by weighing the solid residue obtained by evaporating a measured volume of filtered sample to dryness. The solid residue almost invariably consists of inorganic constituents and very small amounts of organic matter. The TDS concentrations in groundwater vary over many orders of magnitude. A simple but widely used scheme for categorising groundwater based on TDS is presented in Table 2.1 (Freeze and Cherry, 1979). To put the concentration ranges in perspective, it may be useful to note that water containing more than 2000-3000 mg/l TDS is generally too salty to drink. The TDS of seawater is approximately 35,000 mg/l. Milligrams per litre is numerically equivalent to weight in parts per million (ppm).

Groundwater can be viewed as an electrolyte solution because nearly all its major and minor dissolved ionic constituents can be obtained by determining the

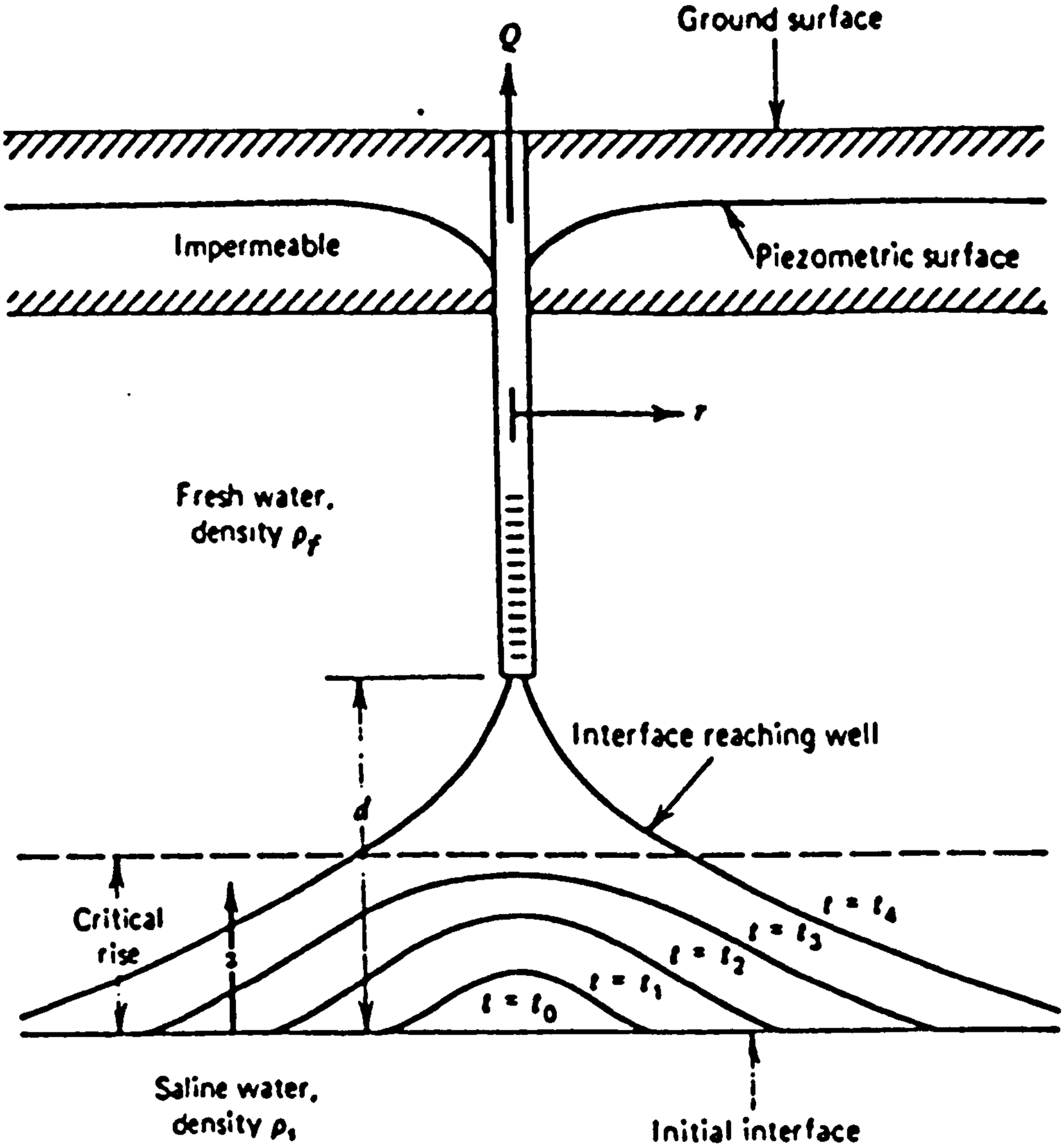

Figure 2.9 Diagram of upconing of underlying saline water to a pumping well (after Schmorak and Mercado, 1969).

Category	Total Dissolved Solids (mg / l or g /m³)
Fresh water	0 - 1000
Brackish water	1000 - 10,000
Saline water	10,000 - 100,000
Brine water	> 100,000

Table 2.1 Simple Groundwater Classification Based on Total Dissolved Solids (After Freeze and Cherry, 1979).

capability of the water to conduct an applied electrical current. The electrical conductance or conductivity of a material is the ability of that substance to conduct an electric current. The specific electrical conductance of a substance (EC) is the conductance of a body of unit length and unit cross section at a specified temperature. This term is synonymous with volume conductivity and is the reciprocal of volume resistivity. A rapid determining of TDS can be made by measuring the electrical conductivity of a groundwater sample. The relationship between the various parameters such as TDS and EC are worked out in order to express the groundwater quality. It is given by the formula (Hem, 1970):

$$TDS = A \times EC \qquad (2.8)$$

where TDS is expressed in mg/ l, EC is in µS/ cm and A is a conversion constant. According to Hem (1970), the range of A is from 0.54 to 0.96 representing most types of natural water. Conductance in preference to resistance is used because it increases with salt content, its units are known as siemens (S) or microsiemens (µS) in the SI system. In the past these units have been known as millimhos and micromhos. Conductivity (microsiemens) and resistivity (ohm.m) of a fluid R_w could be interchanged by the formula

$$Conductivity = \frac{10^4}{R_w} \qquad (2.9)$$

As conductance is a function of water temperature hence a standard temperature (usually 25°C) must be specified in reporting conductivities. The major constituents

which occur in groundwater are mainly in ionic form and are commonly referred to as the major ions (Na^+, Mg^{2+}, Ca^{2+}, Cl^-, HCO_3^-, $S0_4^{2-}$). The total concentration of these six major ions normally comprises more than 90% of the total dissolved solids in the water, regardless of whether the water is dilute or has salinity greater than seawater (Davis and DeWiest, 1966).

2.4.1 Recognition of Sea water in Groundwater

As chloride is a dominant ion of ocean water and usually plays only a minor role in groundwater, an increase in chloride content is the most reliable indicator of the first stages of salt water intrusion into groundwater. Bicarbonate is usually the most abundant negative ion in groundwater, and as there is such a large difference between the proportions of chloride-bicarbonate ratio in normal groundwater and in ocean water, the ratio between these two ions is a useful index of the presence of seawater (Roger Revelle, 1941).

The concept of an equivalent salinity is frequently used in discussing the resistivity of groundwater. The equivalent salinity of a solution is defined as the salinity of a sodium chloride solution which would have the same resistivity as that of the particular solution for which the equivalent salinity is being expressed. The equivalent salinity should be fairly close to the true salinity since mobilities of ions do not vary widely. The use of equivalent salinity has the advantage that only tables (or graphs) for a single salt are needed to determine the resistivity of a solution (Keller and Frischknecht, 1966).

Goswami (1968) presented field studies at Digha, India, and making use of the

chloride content of water samples, he delineated the saline groundwater body by an isochlor of 500 ppm (TDS 1000 ppm) and chloride/bicarbonate ratio of 2.3; and the zone bounded by the 300 and 500 isochlors demarcated the zone of diffusion.

Kwader (1986) worked out an equation relating R_w the resistivity of groundwater to chloride concentration in ppm, while working on the Floridan Aquifer in areas where the water was predominantly calcium bicarbonate rich:

$$Chloride(ppm) = \left(\frac{3100}{R_w}\right) - 88 \qquad (2.10)$$

Hagemeyer and Stewart (1990), found that there were two sources of salinity in the groundwater: seawater intrusion (contributing chlorides), and deep mineralized water (contributing sulfates). The resistivity and the available water quality data showed that three groundwater masses are present: fresh, saline and mineralized. They observed that water-quality control data are essential to solve the problem of salinity equivalence and differentiate saline water from mineralized water.

2.5 Detection of Saline-Fresh Water Interface

Before moving to Chapter 3, where methods of detection and mapping of the saline-fresh water interface are described, it is worthwhile at this juncture to look at some previous work in this area, particularly geophysical and hydrochemical methods.

Use of direct-current resistivity methods is not new to water resources

investigations. As early as 1937, Swartz(1937) used this technique for locating fresh-water lenses in salt-water bodies on the Hawaiian Islands. Swartz (1939) also checked and found valid the Ghijben-Herzberg relationship by applying resistivity measurements in the same vicinity in 1938-1939. Since that time, little fresh-salt water interface mapping based on resistivity has been done in United States until relatively recently (Zohdy et al., 1969). However, much resistivity work on the detection of the fresh-salt water interface has continuously been done in other parts of the world (Flathe, 1970; Zohdy et al., 1974; Gorhan, 1976; and Worthington, 1977). Since the late 1960's, numerous studies in the United States have been carried out to locate contaminated waters, such as landfill leachates, mine drainage, and sewage effluent (Cartwright et al., 1968; Markel, 1973; Kelly, 1976; Klefstad et al., 1976; and U.S. Environmental Protection Agency, 1978).

Given a low hydraulic gradient, and an aquifer of almost constant thickness and composition, the apparent resistivities obtained by resistivity mapping will generally provide sufficient information for delineating the coastal zones invaded by saline water. Adams (1970) improved this mapping technique by introducing a correction procedure in order to remove the 'elevation effect' from apparent resistivity observations and called it the "modified resistivity profiling" method.

If the aquifer thickness varies over the whole investigation area then the profiling technique is better replaced by resistivity soundings. The field curves thus obtained are manually interpreted by using master and auxiliary curves in order to determine the resistivity and thickness of the aquifer. Finally, a map of the transverse resistance of a particular aquifer can be produced (Astier, 1971; and Duprat, 1972) by multiplying the aquifer thickness by its specific resistivity at each sounding station. Assuming a

minimum thickness and a minimum resistivity, an aquifer should have to be of economic interest, the corresponding minimum transverse resistance can be calculated. Hence, the isoresistance curve of a minimum value thus computed also represents the limits of a coastal aquifer which theoretically could be exploited. In order to distinguish between saline water intrusions and other 'conductors' such as intercalated clay layers, the method often used is to relate geoelectric soundings to existing borehole data or to boreholes specially drilled for this purpose.

Schröder (1970) presented a set of special 'master curves' for interpreting electrical soundings which have been obtained from coastal areas where the salinity distribution below the surface can be assumed to be in agreement with the dispersion theory. Given this condition, the 'master curves' enable a direct interpretation of the variation of the chloride content with depth.

Flathe (1963) produced five-layer master curves for the hydrogeological problems. He computed master curves in order to facilitate the interpretation of resistivity soundings obtained from a two layer aquifer i.e., an aquifer separated by an intercalated clay layer of variable thickness. A further condition for application of five-layer master curves is that the lower boundary of the aquifer must be a good electrical 'conductor', such as a saline water intrusion or a clay layer of infinite thickness.

Volker and Dijkstra, 1955; Van Dam et al., 1967; and Ginzburg, 1974, working independently in polder and delta regions aquifers of sufficiently homogeneous geological composition proposed the following geoelectric procedure for mapping saline water contaminations. Electrical soundings are carried out near all boreholes and wells which exist in the investigation area. Simultaneously, the conductivity and chloride

content of groundwater samples from the boreholes are determined. A graph can consequently be assembled by relating the chloride contents to the true aquifer resistivities as obtained from the soundings. Once such a graph is established, more geoelectrical soundings are carried out to cover the whole investigation area. Finally, a map showing the chloride distribution of groundwater can be prepared from the soundings, by converting directly true aquifer resistivities to chloride concentrations.

Recently Al-Ruwaih (1992) used a surface geoelectrical method to detect the brackish-saline water interface and delineate the extension of shallow water bearing formations in the Kuwait group. At the same time, studies of groundwater chemistry were also carried out to identify water type and range of salinity. Accordingly he made various vertical electrical soundings, using the Schlumberger configuration. The interpretation of VES lines obtained by curve matching (Orellana and Mooney, 1966) revealed four major layers. A contour map of measured apparent resistivity values/(AB/2) = 147m showed a gradual decrease of resistivity in a S-W to N-E direction.

The auxiliary point method for the approximate interpretation of resistivity soundings was extensively used before the introduction of the iterative computing method. This method was first published by Ebert (1943). Each of the branches of an apparent resistivity curve is approximated by a two-layer apparent resistivity curve. The coordinates of the cross of this two-layer curve are considered to represent the thickness and the resistivity of a fictitious layer that replaces the sequence of shallower layers. Ebert (1943) gave four graphs that should be used, respectively, for bell-type, bowl-type, ascending-type and descending type three layer cases. Orellana and Mooney (1966) published a modification of the Ebert method and combined the bowl type and

the ascending type into a common mathematical formulation. These days however, the curve matching methods described above are not widely used due to the general availability of more sophisticated forward and inverse iterative computer modelling techniques (Patra and Mallick, 1980).

The (MRT) microprocessor-controlled traversing system is effectively a resistivity imaging system, having been designed to provide information from which the distribution of subsurface resistivity in cross section along a profile can be determined. It is of particular value in areas where the strata show both lateral and vertical variation in electrical properties. The field technique involves making repeated constant-separation apparent resistivity traverses along the chosen profile, the spacing being incremented at each pass. In this way an apparent resistivity space section, or pseudosection is built up, which when contoured provides a qualitative picture of the distribution of subsurface resistivity. Where the subsurface structures are two-dimensional (2D) and some control is available, quantitative interpretation is possible. The MRT system removes many of the practical difficulties of resistivity profiling, making it possible to collect the necessary data more easily and much faster than by conventional methods (Griffiths, Turnbull and Olayinka, 1990).

In recent years, tomographic inversion of resistivity data has become an important topic, aiming to achieve more accurate delineation of subsurface structures (Noel and Walker, 1990; Shima, 1990; Daily and Owen, 1991; Noel and Xu, 1991 and Barker, 1992). However, data obtained during conventional Wenner pseudosection surveys, for example, are too sparse for tomographic processing and therefore it is necessary to develop a regime for collecting a larger set of data. The advent of resistivity meters electronically multiplexed to large electrode arrays has been a

significant recent development in the field of resistivity surveying (Griffiths and Turnbull, 1985; Van Overmeeren and Ritsema, 1988; Noel and Walker, 1990). These systems expand the choice of electrode configurations and the number of data that can be collected in a realistic time although, hitherto, their main application has been to the automation of conventional pseudosection surveys (Griffiths, Turnbull and Olayinka, 1990).

As the resistivity method is time consuming in that individual soundings may take from several hours to several days depending upon surface conditions and the required depth, inductive EM techniques have been developed in the last 20 years or so. As inductive measurements require no contact with the surface, while in resistivity measurements current has to be introduced into the ground by means of electrodes, these techniques have certain advantages.

One of the most popular electromagnetic methods for groundwater exploration and saline intrusion detection is the frequency domain low induction number conductivity mapping; this uses EM terrain conductivity meters (Fraser, 1984; and McNeill, 1980), calibrated directly in ground conductivity, such as the Geonics EM34. The main drawback of the method is its limited exploration depth (<50m) and its restriction to mapping low conductivities. Max-Min is the more traditional horizontal loop EM measuring system which measure in-phase and out-of-phase EM field responses. It is an effective system in obtaining the resistivity and thickness of the subsurface layers. Interpretation is done by computer software curve matching.

More recently the transient (or time domain) EM (TEM) sounding method has started to be used more effectively and to a depth (>50m) for detecting the fresh-salt

water interface in coastal aquifers (Gay, 1983; Stewart and Gay, 1986). Transient soundings are typically made using a square transmitter loop with a small receiver coil located at the center of the loop. The steady transmitter current produces a primary magnetic field which is directed upward inside the loop and downward outside the loop. When the transmitter current is abruptly turned off, current is induced in the ground which tries to maintain the magnetic field which was present prior to turnoff. The magnetic field produced by the induced current is called the secondary magnetic field. In practice the voltage induced in a receiver coil by the secondary magnetic field is measured. This voltage curve is called a transient. Interpretation of transient data is accomplished by curve matching (Kaufman and Keller, 1983) or computer inversion (Anderson, 1982) in much the same way as is done for DC resistivity data. The TEM method is fast becoming the up-and-coming EM method as its results particularly in complicated areas such as in deserts for the discovery of groundwater or in coastal areas for the delineation of the saline-fresh water interface, has proved to be fast and more dependable.

3. METHODS OF DETECTION AND MAPPING OF THE SALINE-FRESH WATER INTERFACE

As seen in chapter 2.5, over the years many methods have been proposed and employed to detect saline intrusions and to map the saline-fresh water interface. However, salinity of the groundwater can be directly detected through the determination of electrical conductivity and its hydro-chemistry. In the present study the techniques have been limited to the DC electrical resistivity method, the electromagnetic method and chemical method. In addition the geoelectrical data, obtained in field, have been used to compare to borehole logs and other data determined in the field or in the laboratory such as permeability, porosity and etc.

3.1 Electrical Resistivity Method

The resistivity of a porous medium is largely a function of the water content as the mineral grains are in general resistive. The conductivity of the water, its volume and the distribution through the medium are the principal parameters in determining the bulk electrical properties of the medium.

When an electrical current is passed into the ground by means of two electrodes and a potential drop measured between a second pair placed in line with them, it is possible to calculate a quantity known as the apparent resistivity from a knowledge of the magnitudes of the current and potential drop together with the electrode geometry. If the ground is homogeneous this is the true ground resistivity, but in general it is a weighted average of the resistivities of the formations through which the current passes, often referred to as 'apparent resistivity'. It is from an analysis of the variation of this

quantity with changes in electrode geometry and position that deductions about the subsurface can be made.

3.1.1 Wenner and Schlumberger Arrays

A great variety of electrode arrangements are available to measure earth resistivities. The present study has been limited to the Wenner and Schlumberger arrays, although the Wenner at some sites has made use of the Offset system (Barker, 1981).

The Wenner array is one of the most commonly used electrode arrays for determining resistivity. In it four electrodes are equally spaced along a straight line, as shown in Figure 3.1. The distance between any two adjacent electrodes is called the array spacing (a). A current I is passed between the outer electrodes A, B and the consequent potential drop ΔV measured between the two inner electrodes M, N. Apparent resistivity ρ_a is obtained by using the relationship:

$$\rho_a = 2 \pi a \frac{\Delta V}{I} \qquad 3.1$$

Many instruments while measuring the quantities ΔV and I separately usually combine them to give a ground resistance R.

The Schlumberger array also, is widely used in measuring earth resistivities. In this configuration the distance MN is small compared to the distance AB, generally smaller than AB/ 5 (see Figure 3.2). The potential gradient over the interval MN is practically equal to the electric field strength at the centre of the configuration, since

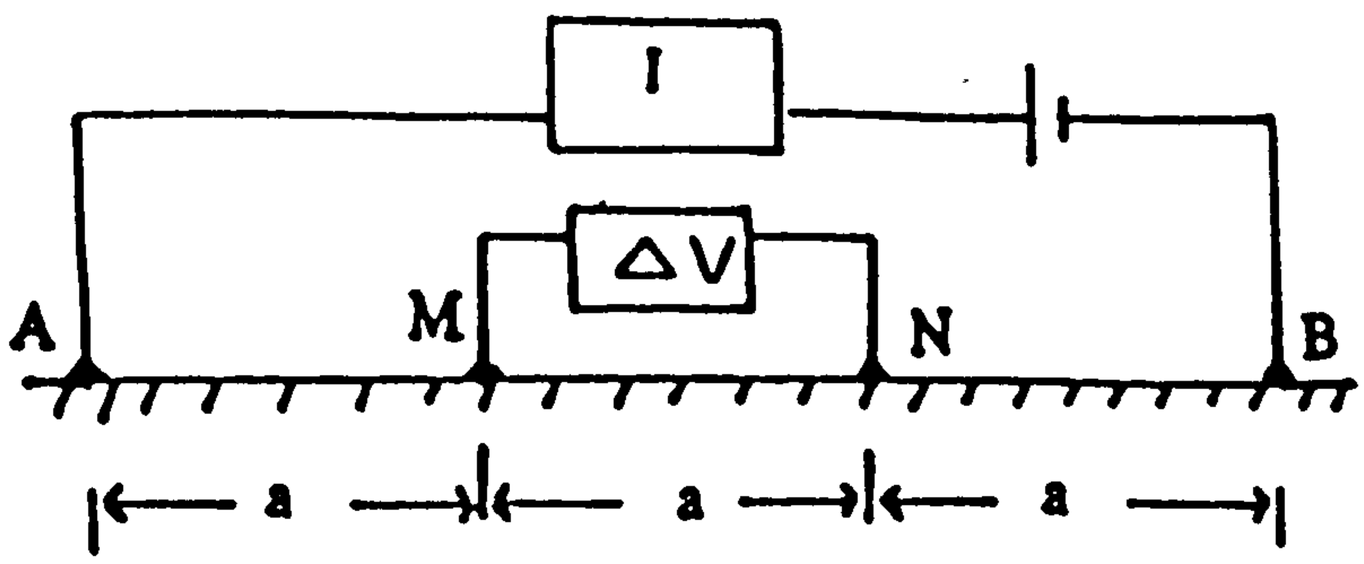

Figure 3.1

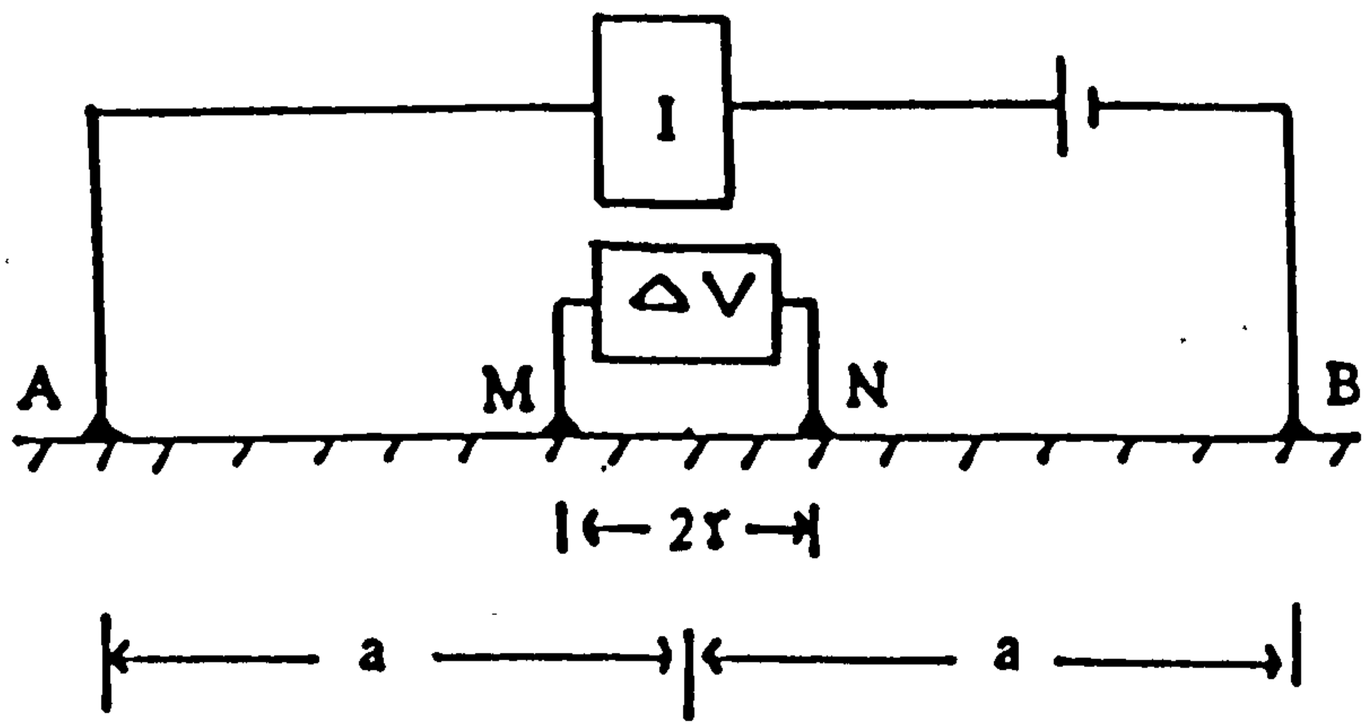

Figure 3.2

the field is nearly uniform in the neighbourhood of this point. Apparent resistivity ρ_a is measured by using the relationship:

$$\rho_a = \pi \frac{a^2 - r^2}{2r} R \qquad 3.2$$

where (a) is the spacing and taken as half the distance between the current electrodes, 2r (MN) is the distance between the potential measuring electrodes, and R is the resistance ($\Delta V/I$).

The following are the reasons for choosing Simple Wenner and Offset Wenner arrays in the present work:

a. The signal-contribution contours for the Wenner array at depth are slightly flatter than those for the Schlumberger array; it has been suggested by Milsom (1989) that the Wenner will locate flat-lying interfaces more accurately.

b. Comparing the two arrays for the same current electrode spacing the voltage differences in Wenner sounding measurements is larger as the distance between the potential electrodes is generally larger; this makes any reading error in the measured potential difference a smaller percentage for the Wenner compared to the Schlumberger. Indeed in some instances of low ground resistivity, Schlumberger becomes virtually unusable because of the frequency with which the potential electrodes have to be moved.

c. There is often a difficulty in drawing the Schlumberger curves.

d. The effects of near surface inhomogeneity may be reduced using off-setting techniques.

3.1.2 Offset Wenner system

During the first year of the present study the Offset Wenner system, developed at the University of Birmingham, was used. This has several advantages over both the Schlumberger and the conventional Wenner systems. By this system, it is possible to overcome the lateral resistivity variations, which are not detectable by other methods. Also the resistivity surveying is less time consuming as a multicore cable and fixed five electrodes array can be used for various sorts of configurations. The diagram below shows the set up used for such readings. The idea is to use five electrodes at a time and by using a switching device the configuration can be changed. The two measurements (Rd_1 and Rd_2) cancel the effect of lateral variation (Barker, 1981).

Basic array

1 2 3 4 5 Electrodes

∇ ∇ ∇ ∇ ∇

∇ ∇ ∇ ∇) Rd_1

}Rd

∇ ∇ ∇ ∇) Rd_2

All the Wenner resistances, however derived, may be converted to apparent resistivity ρ_a, using the relationship as given in equation 3.1. ABEM's battery operated resistivity meter, the Terrameter SAS 300, was used in measurements of all the vertical electric soundings taken under different arrays.

3.1.3. ABEM's Terrameter SAS 300

The ABEM's SAS Terrameter system consists of a basic unit called the Terrameter SAS 300 which is supplemented as desired with the SAS 2000 booster, for situations where the voltage and/or current need to be increased. SAS stands for Signal Averaging System, a method whereby consecutive readings are taken automatically and the results are averaged at each stage; the updated running average is presented automatically on the display. SAS results are more reliable than those obtained using single-shot systems. The Terrameter SAS 300 (basic unit) was used for all the resistivity surveys in the present study.

The Terrameter contains three main units, all housed in a single casing: the transmitter, the receiver and the microprocessor. It has the following five controls:

(i) SAS selector (also called the Cycles Selector). This 4-position selector is used to choose either the single reading mode or 4, 16, or 64 automatically averaged readings.

(ii) Voltage/resistivity range selector (also called the Range Selector).

(iii) On/Off switch. Switches power on and off.

(iv) Current Selector.

(v) Measure pushbutton. When this control is depressed, the microprocessor runs through its automatic diagnostics program and, if everything is satisfactory, starts the Terrameter measurement procedure automatically. When the measurement is complete, it returns to the standby mode with the result provided by the digital display.

The following is the procedure used for carrying out the vertical electric soundings taken under Offset and Simple Wenner arrays with the Terrameter. The instrument is positioned between the potential electrodes (M and N) and terminals P1

and P2 are connected to terminals M and N respectively. The current electrodes (A and B) are connected to terminals C1 and C2 respectively. The Range Selector is turned to the 1 ohm position, the Cycles Selector to position 4 and the Current Selector to position 20mA. The power is switched on and the Measure button is pressed. The four readings that appear successively on the display are observed. If they are nearly equal, the noise level is low and the final reading is recorded. The instrument is then switched off to conserve battery power. Some times there are negative resistance readings which could be caused by the following reasons:

(a) The current or potential electrodes have been connected with reversed polarities.

(b) The noise level may be much higher than the signal level (long distances between A and B and low current).

3.1.4. Observational Errors

3.1.4.1. Instrumental errors

The accuracy of the Terrameter is clarified by stating that a reading of 2.42 shows higher precision than a reading of 2.4, but it is not necessarily any more accurate. The overall system accuracy of the Terrameter (with or without the SAS 2000) is ± 2% of the reading.

3.1.4.2. Spacing errors (Wenner)

Any error in spacing while taking measurement of a sounding in a field causes erroneous readings of resistance there also. In equation 3.1, say there is an error of Δa in spacing, a, which brings about an error of ΔR in resistace, R. Therefore, errors in spacing, a, and resistance, R, would be $\Delta a/a$ and $\Delta R/R$ respectively. The maximum

error in product in r.m.s terms will be:

$$\delta V/V = \sqrt{(\Delta a/a)^2 + (\Delta R/R)^2} \qquad (3.1a)$$

3.1.4.3. Offset errors

(a) Observational Offset errors: Errors of observation may be computed using the tripotential relationship (Carpenter and Habberjam, 1956), which states that for any set of four electrodes it is only possible, by changing the roles of the current and potential electrodes, to measure three different resistances. For electrodes 1, 2, 4, and 5 in figure below these resistances are referred to as R_A, R_B, and R_C.

Offset Wenner	∇^C	∇^P	∇^P	∇^C	_	Rd_1
Arrangements	_	∇^C	∇^P	∇^P	∇^C	Rd_2
	∇^C	∇^P	_	∇^P	∇^C	R_A
	∇^C	∇^C	_	∇^P	∇^P	R_B
	∇^C	∇^P	_	∇^C	∇^P	R_C
Electrodes	1	2	3	4	5	

The tripotential relationship, $R_A = R_B + R_C$, must then hold for any subsurface geology and any electrode spacing. Small differences will occur, however, due to observer error. The percentage 'observational error' e_{obs} (a) may be computed from:

$$e_{obs}(a) = \frac{R_A(a) - [R_B(a) + R_C(a)]}{R_A(a)} \times 100\% \qquad (3.3)$$

The value of e_{obs} will normally vary between ± 2%. If e_{obs} is large an instrument

malfunction is indicated and the source of the error should be sought. Leakage of current from damaged cables and high contact resistances at the electrodes often causes high observational errors. Calculation of e_{obs} during the measurement of a sounding helps to achieve data of consistently high quality. A single root-mean-square (rms) observational value may be calculated for each sounding curve in a standard way and used as a means of classifying and comparing the soundings according to their quality.

(b) Lateral resistivity effect: One important advantage of the Offset sounding system is the ability to estimate the magnitude of lateral resistivity effects. This estimate is provided at any spacing, a, by the 'Offset error', e_{off} (a), defined by the following expression:

$$e_{off}(a) = \frac{R_{d1}(a) - R_{d2}(a)}{R_d(a)} \times 100\% \qquad (3.4)$$

where R_{d1} and R_{d2} are resistances measured with each of the normal Wenner arrays, the arithmetic mean of these two values providing the Offset Wenner resistance, R_d. Near-surface lateral effects cause Offset errors which change randomly in magnitude and sign with increasing electrode spacing. The Offset technique substantially reduces these effects. If e_{off} (a) is consistently greater than 20 percent and of the same sign, deeper and larger scale lateral variations, such as dipping beds and faults, are likely to be present.

3.1.5. Interpretation

The apparent resistivity/electrode separation curve obtained by vertical electric

soundings is interpreted by the use of the computer software Bossix or Offix programmes produced by Interpex Ltd. These are in fact forward and inverse modelling programmes for interpreting soundings, from a variety of electrical depth techniques including Offset Wenner soundings data. The forward modelling allows the creation of synthetic resistivity sounding curve for a number of plane layers on the assumption that each layer is laterally homogeneous. Inverse modelling is an interactive iterative process to obtain the best least squares fit to the field data. The results from the forward and/or inverse modelling are directed to a printer and/ or plotter for a print-out of the model and its parameters (for an example see Figure 3.3).

3.1.5.1. Ambiguity of Interpretation

As indicated above the resistivity technique for depth probing provides a curve showing the variation of apparent resistivity with electrode separation. With expansion of the current base about a fixed central point the current penetrates deeper into the ground so that the electrode separation at any one determination can be loosely correlated with depth. The interpretative procedure outlined above consists of matching a model of a layered earth, of various thicknesses and resistivities, to the field curve. However there is an ambiguity of interpretation, a lack of uniqueness in that the same synthetic curve (to match the field curve) can be produced by a number of different layered models. The problem is that what is being measured in the resistivity method is *transverse resistance* T (the product of the resistivity and the thickness of a bed) and *longitudinal conductance* S (the ratio of thickness to resistivity), and it is almost impossible, unless there is some external control, to differentiate between thickness and resistivity; it is highly manifested in beds whose thicknesses are small compared to

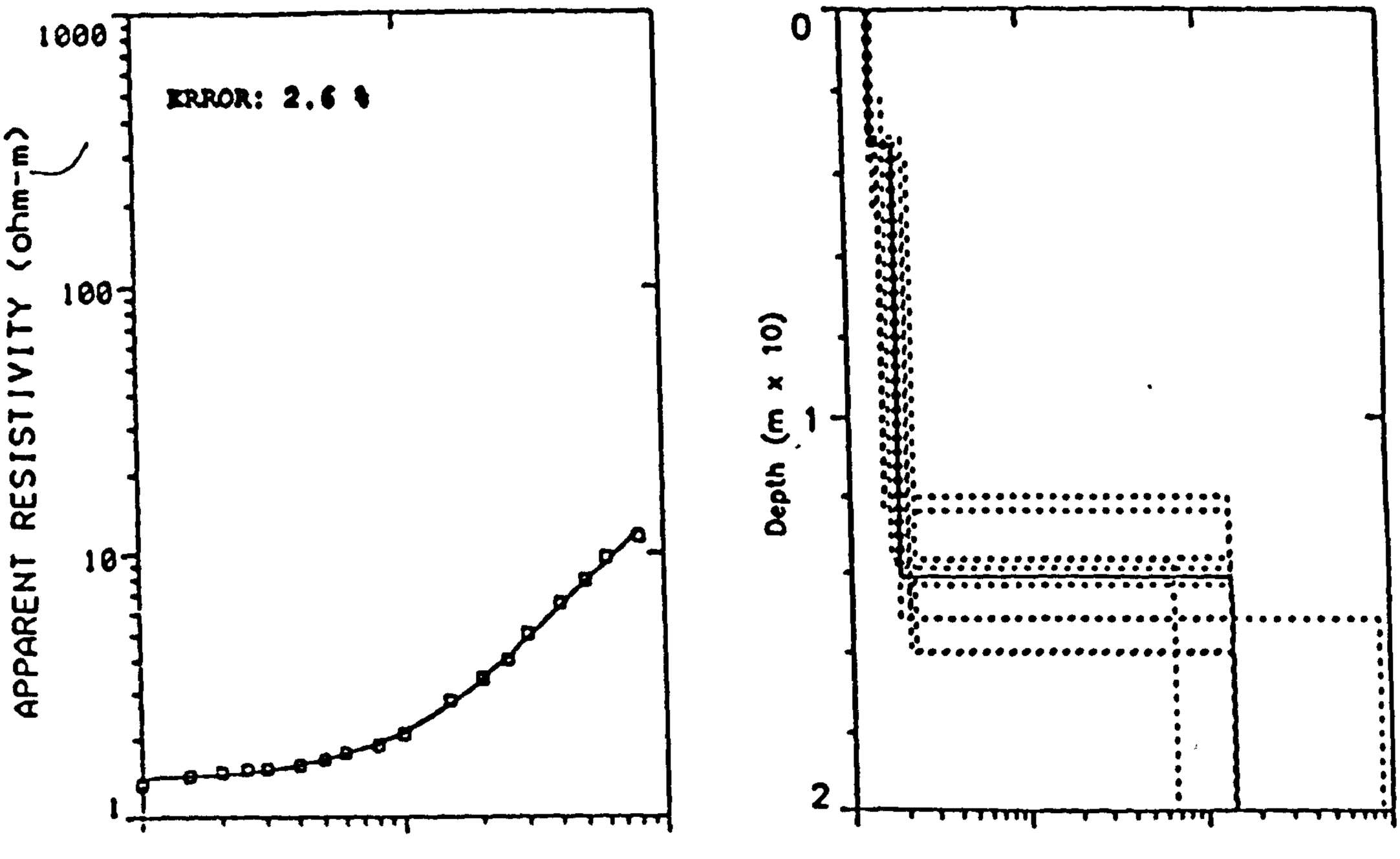

Figure 3.3. Equivalence curves along side the field curve.

their depths.

This important ambiguity has been described in terms called 'the principle of equivalence' and 'the principle of suppression'. Equivalence arises when for a particular sub-surface layer compared to the overlying layer:

(a) the resistivity is higher (or lower) than the adjacent layers.

(b) T (or S) is very large and

(c) S (or T) is very small.

On the field curve this layer cannot be distinguished from any other layer which has a different resistivity and thickness but where the product T (or the ratio S depending which is the larger) has the same value. As can be seen, two types of equivalence can occur depending on which of the parameters S or T is the larger: S-equivalence when a thin bed lies interbedded between more resistive ones, often described as the type H curve; and T-equivalence when the thin bed lies between more conductive ones, often described as the type K curve. While Maillet (1947) provides a form of solution to the problem by the construction of his 'Dar-Zarrouk' curves, in this particular exercise the range of equivalent models was reduced to the one chosen through borehole information (see Figure 3.3).

Suppression relates to a bed with a resistivity intermediate between the bed above and that below it. Such a bed, again if thin, has virtually no effect on the field curve. Even when its thickness increases to have influence on the apparent resistivity curve, this change appears to be related to changes in transverse resistance or longitudinal conductance of the enclosing beds.

3.2 Electromagnetic Method

The electromagnetic survey was carried out with the MaxMin I-8 (commonly

known as Apex MaxMin) portable instrument. This instrument is designed for water, mineral exploration and geoengineering applications. It permits the choice of eight octavely spaced operating frequencies i.e. 110, 220, 440, 880, 1760, 3520, 7040, and 14080 HZ. To arrive at the much needed parameters, the most commonly used transmitter powered operating mode, MAX 1 (also known as the horizontal loop mode) is used; it is an effective mode in obtaining the resistivity and thickness of the subsurface layers. It has advanced noise rejection procedure which results in faster and more accurate surveys.

The following is the procedure and instrumentation (see Photographic Plate 3.1) used for the MaxMin I-8 electromagnetic method survey:

a) The Receiver: The receiver is a one piece unit in which there are two coils which are solenoidal in shape and are mounted in the upper end of the tubes on each side of the console. Inside the console is the basic electronic circuitry of the system mounted on printed circuit boards. The read out meters, control switches and connectors are all mounted on the console. It is powered by four 9-volt transistor type alkaline batteries.

b) The Transmitter: It consists of three components, connected together by retractile cables. These components are the coil, the console and the battery pack with charger. The transmitting coil is an oval shaped loop with a unit at one end containing a bubble level, a cable connector and an electro-mechanical tilt sensor for ensuring horizontality. The console contains all of the electronic circuitry, read out meters, control switches and connectors. The battery pack consists of a set of rechargeable gel cells mounted in a carrying belt.

c) The Reference Cable: This links the transmitter and receiver. It contains teflon-insulated conductors electronically connected to form a twisted pair within a

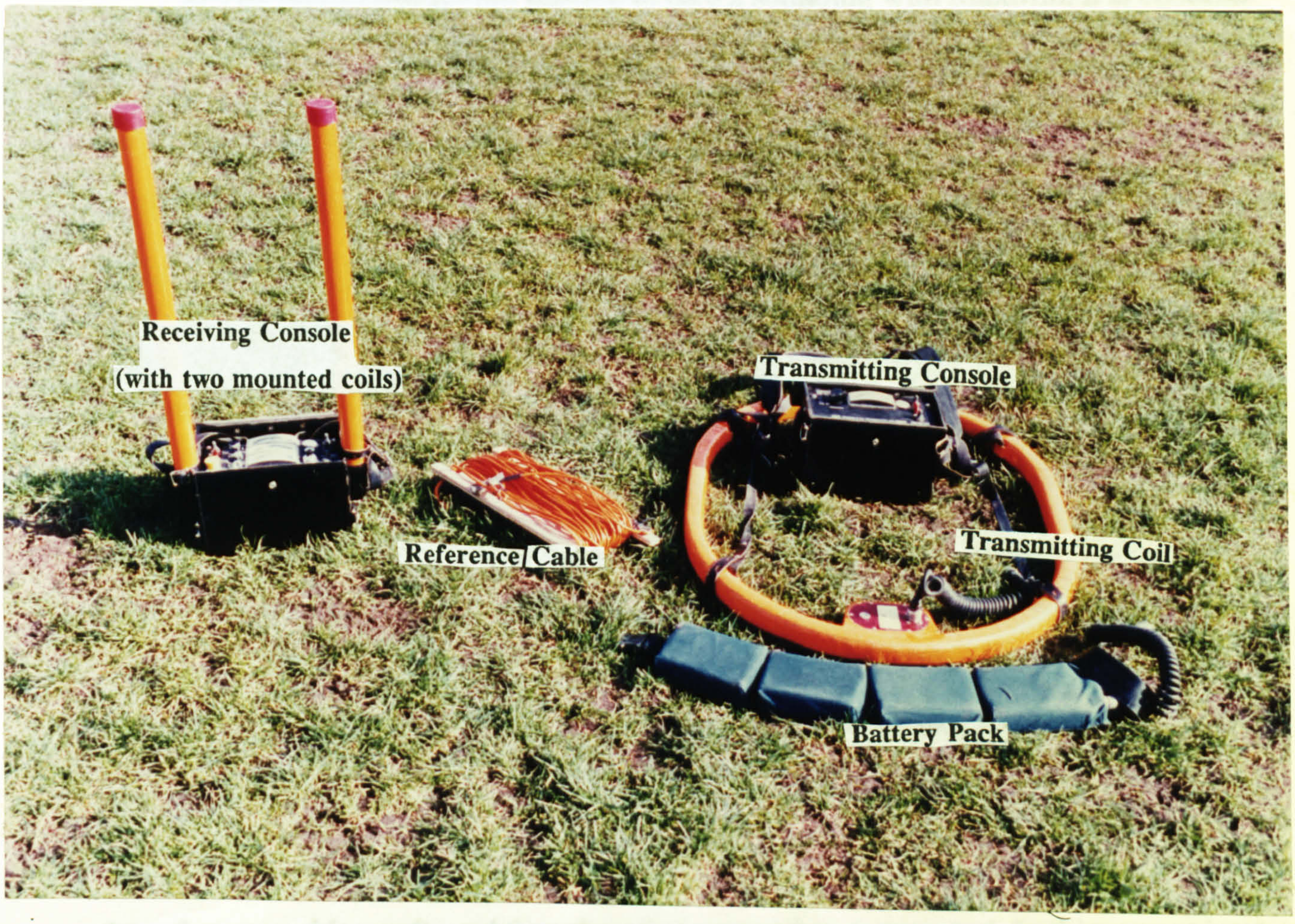

Photographic Plate 3.1

teflon jacket. It has end connectors and safety thimbles. The cable also serves as the intercom link between transmitter and receiver.

d) The Procedure: Before starting to take a sounding with MaxMin, it is checked for zero offset on the tilt meter as well as on the in-phase and out-of-phase meters; this is corrected beforehand otherwise a noticeable discrepancy is caused between the two readings for different scales i.e. that taken near the end of a given scale and its repeat value on a coarser scale. The coils while taking the readings are held horizontal using the bubble levels. To carry out a sounding 50m and 100m reference cables are used alternatively to change the depth of penetration. In either of the 50m or 100m cables the end of the cable was held over the same point at which a vertical electric sounding was previously made. In mode MAX 1 the transmitter operator stands opposite and facing the receiver operator who records the in-phase and out-of-phase readings at a fixed frequency of 110 HZ. Then by changing to other frequencies in turn, readings are recorded until all the frequencies have been used. To take a second sounding, the transmitter operator moves to take the receiver operator's position and the receiver operator moves 50 metres or 100 metres farther away (depending upon the length of the reference cable used), and then the whole procedure is repeated. In this way at least 4 soundings were recorded in the case of the 50m cable and 2 soundings if the 100m cable was used.

3.2.1. Observational Errors(EM)

(a) Errors due to loop spacing: Errors in the measurement caused by errors in the loop spacing or orientation must be considered. In the horizontal coil EM system, for a primary field:

$$H_p = -m/4\pi a^3 = c/a^3 \qquad (3.5)$$

where $m/4\pi$ is a constant c and (a) is the coil spacing, and H_p is set to 100 % for true coil spacing. If the nominal (true) coil spacing is a_n, and the actual coil spacing is a_a, then the observational error due to coil spacing is found from the following equation:

$$\text{Error} = (H_a - H_n)/H_n \qquad (3.6)$$

$$= (a_n^3 - a_a^3)/(a_a^3) \times 100\ \% \qquad (3.7)$$

(b) Errors due to orientation: Consider a case when one of the coils is misoriented from its proper position through an angle α, the ratiometer measurement will be ($\cos\alpha$) 100 %. Usually, a fairly large error in orientation of one of the coils can be tolerated; if the angle α is 8°, the error in measurement will be only about 1 percent. Serious errors can occur, however, when traversing rugged terrain with the horizontal coplanar or vertical coaxial loop arrangement. Consider the case in which both coils in a horizontal coplanar arrangements are held level, but the line connecting the coils makes an angle α with the horizontal. Equation (3.5) may be rewritten as

$$H_p = (-m/4\pi a^3)\ (3\ \text{Sin}^2\alpha - 1) \qquad (3.8)$$

The error in the measurement is (3 $\text{Sin}^2\alpha$ - 1) 100 percent. For a slope of 8°, the error is 5.8 percent (Keller and Frichknecht, 1966). When the horizontal coplanar or vertical coaxial arrangements are used in hilly terrain, it is necessary to orient the coils parallel to the slope, or to make corrections to the measurements when the inphase components is considered in interpretation.

3.2.2 Interpretation

EMIXMM is a forward and inverse modelling software computer programme, prepared by Interpex Ltd., for interpreting electromagnetic sounding data taken with the Apex MaxMin. EM sounding curves can be obtained as parametric soundings (with increasing frequency) or as geometric soundings (with increasing spacing). Using its forward modelling facility, the software can calculate synthetic curves for a model with up to ten plane layers; these curves are obtained using the method described by Patra and Mallick (1980). Results obtained are in terms of the in-phase and out-of-phase components for each frequency and coil spacing value. These data are presented as a percentage of the free space response. Graphic displays are presented as in-phase and quadrature response versus induction number or as Argand diagrams (Eadie, 1979). On the Argand diagram the in-phase component is plotted along the abscissa and the out-of-phase component of the same ratio plotted along the ordinate.

Inverse modelling produces a model which best fits the data in a least squares sense. Now when a starting model is supplied the resistivity inversion takes place (in a iterative manner) and parameters are adjusted by the use of ridge regression (mathematical calculations) Inman, (1975); and a best fit model to the data, is obtained. The results from the forward and/or inverse modelling are directed to a printer and/or plotter for a print-out of the accepted model Figure 3.3a.

3.2.2.1. Equivalence

As with VES techniques described above, one of the difficulties of data interpretation is the problem of equivalence. The following treatment on equivalence

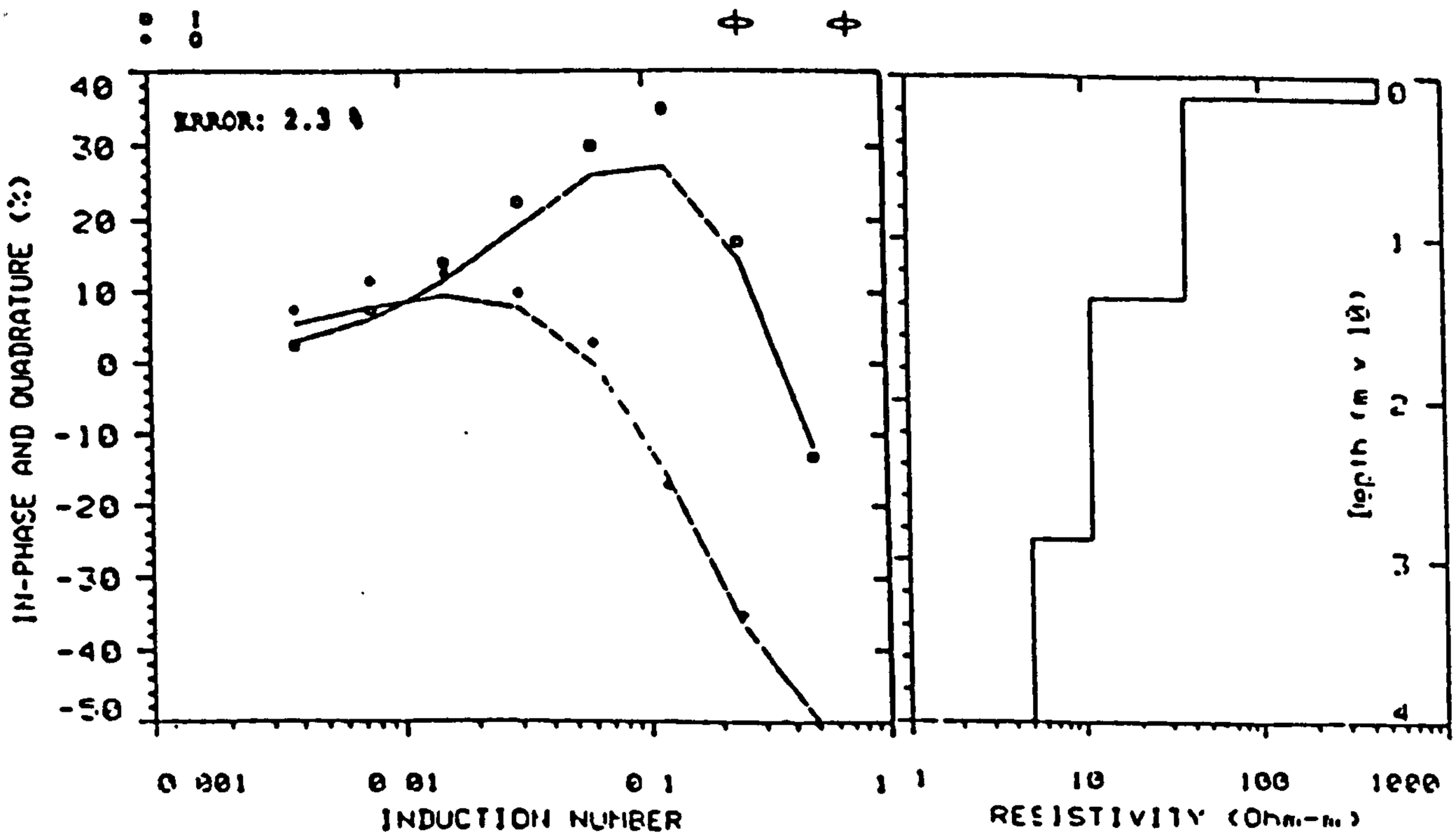

Figure 3.3a. Electromagnetic sounding curve based on field data points.

in electromagnetic sounding is based on studies of Mallick and Verma (1979).

Several H-type and K-type earth models have been considered for several source-receiver systems and separations. The horizontal coplanar loops system is better than other source-receiver orientations in the sense that the RMS difference between the responses of two equivalent models is greater for the horizontal coplanar loops system than that for other source-receiver systems. The following empirical relations for equivalence have been established. H-type earth section:

$\sqrt{h}/\rho$ = constant

K-type earth section:

$h^2\rho$ = constant

where h and ρ are the intermediate layer thickness and resistivity respectively. From the above two relations, it is obvious that it is resistivity in the H-type model and thickness in the K-type model which play a dominant role in producing equivalence.

3.3. Conductivity of groundwater

As conductivity is preferred rather its reciprocal resistivity, because the former increases with salt content, the conductivity of the groundwater samples is determined for all the water samples obtained from most of the vertical electric sounding sites. Conductivity and resistivity of water can easily be interchanged by the formula given in Equation 2.8. The conductivity of each groundwater sample so obtained is used to calculate total dissolved solids (TDS).

The following is the procedure and instrumentation used for the conductivity determination of groundwater samples: the conductivity of groundwater samples obtained from the boreholes, is determined by a conductivity meter called 'Aqua Lytic',

Figure 3.4, which automatically gives water conductivity in µSiemen/cm at a reference temperature of 25°C. The accuracy of the instrument is checked out by calibrating at 25°C prepared standard solutions of 10, 100 and 1000 mg/l NaCl. A percentage error of ± 2% was arrived at which can be considered to be negligible.

First the actual temperature of the groundwater sample is taken and then this value is set on the temperature compensation scale (2) on the instrument. The instrument is now compensated for the temperature variation of conductivity and gives a conductivity value at the reference temperature. The conductivity cell (5) is then immersed in water but, before taking the reading, the cell is agitated thoroughly ensuring that all air bubbles trapped inside the cell have escaped through the openings provided in the cell body, as any air bubbles trapped in the cell can cause erroneous readings. As the conductivity range selector (3) has a wide range of values, the proper selection of the range is made which gives a sufficiently high deflection on the meter (middle of the scale) and this value is recorded. The scale has two sets of markings: upper (0-10) and lower (0-3). The upper scale is used when the testing range selected is a multiple of 10. By multiplying the given multiples with the actual divisions obtained on upper or lower scales give the correct reading of conductivity of water in µSiemen/ cm at the reference temperature.

3.4 Determination of chloride ions in groundwater by chemical methods

Chloride in groundwater sample is most conveniently determined using (AAS) atomic absorption spectroscopy. The first step is to quantitatively precipitate silver chloride by the addition of a known amount of silver nitrate.The amount of chloride in the original sample is then known by the determination of excess silver in the solution,

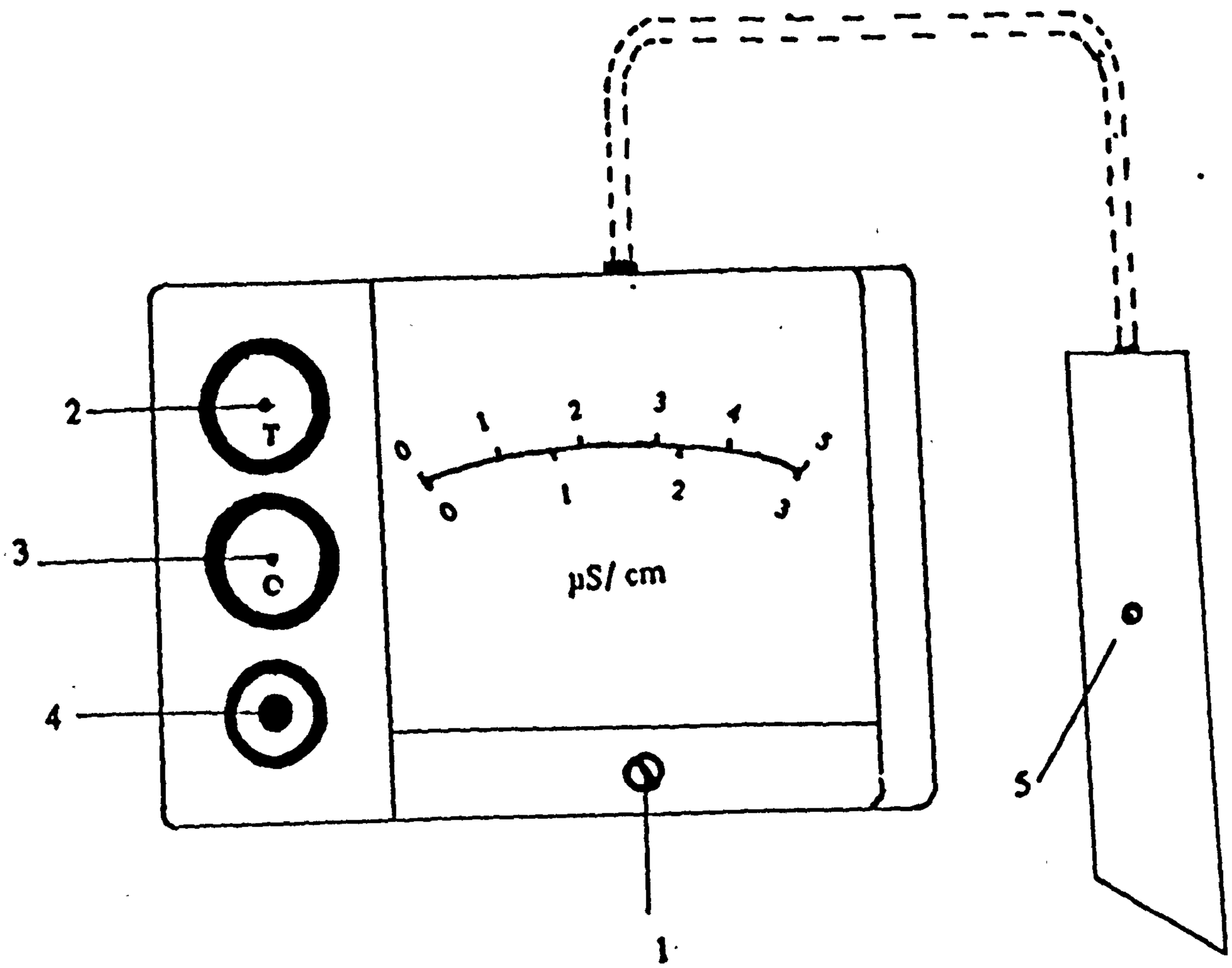

Fig. 3.4 Conductivity meter 'Aqua Lytic'.

1. Meter mechanical zero set screw.
2. Temperature compensation.
3. Conductivity range selector.
4. Press button for read out.
5. Conductivity cell.

when the precipitated silver chloride has been removed (Reichel, 1969; Truscott, 1970). The principle of AAS is that atoms in a non-emitting ground state absorb light of a characteristic wavelength. The extent of the absorption will increase as the number of atoms increases. The light source is selected so that it emits only the atomic spectrum of the element to be determined.

The following is the procedure, used in making up the solutions and carrying out the tests in the present study: an aliquot of the groundwater sample solution containing 0.5 to 5 mg of chloride was placed in a 200 ml volumetric flask. Then 20 ml of 1000 mg/l silver solution and 1 ml chloride free nitric acid are then added to the solution, and this was further made up to a volume of 1000 cc with distilled water. The solution contained 100 mg/l Ag. The mixture is allowed to stand overnight in a dark place to prevent photochemical reactions taking place. Side by side standard calibration solutions are also prepared containing 0, 1, 2.5, 5, 7.5, 10 mg/l Ag in separate standard plastic bottles. The following day replicate absorbance readings are taken of the sample and standard solutions using the atomic absorption spectrometer. Finally absorbances are compared, the concentration of excess silver calculated and the concentration of chloride in the sample obtained from:

Concentration of silver (g/l) =

$$mg/l\ \ Ag \times dilutionfactor \qquad (3.9)$$

Amount of chloride in sample solutions (g) =

$$\frac{[Ag\ formed(mg/l)\ x\ 0.329\ x\ [samplevol(ml)]}{1000} \qquad (3.10)$$

Concentration of chloride (g/l) =

$$\frac{Amount\ of\ chloride\ (mg)}{Vol\ of\ sample\ (litre)} \qquad (3.11)$$

CHAPTER 4. ELECTRICAL CONDUCTION AND FLUID FLOW ANALOGY IN POROUS MEDIA

An analogy can be explained as an agreement or correspondence in certain respects between things otherwise different. Electrical conduction in porous medium generally occurs through the fluid present and the fluid flow in a porous medium is a function of the interconnection of the pore spaces, which in an unconsolidated sediment are themselves dictated by the shape, size and distribution of the particles present. It appears therefore that an analogy does exist between the two things and hence a relationship between electrical formation factor and permeability may be expected.

Over the years this analogy has been used to predict the quantitative and qualitative properties of aquifers and other porous media. The qualitative studies are mostly related with the saline intrusions, lateral delineation of the water bearing formations, etc. The quantitative analyses are concerned with the geophysically measured formation parameters like formation factor to estimate total porosity, permeability, chemical composition of the groundwater or transmissivity, etc. (Heigold, 1979; Biella et al., 1983; Jackson et al., 1978; Lovell, 1983; and Huntley, 1986).

Archie (1942) showed a correlation between formation factor and porosity for a fully brine-saturated medium with no other conductive material being present. This relationship can be described as

$$FF = \frac{R_o}{R_w} \qquad (4.1)$$

$$FF = n^{-m} \qquad (4.2)$$

where FF is the formation factor, R_o is the bulk resistivity of the saturated formation, R_w is the resistivity of the interstitial fluid, n is the porosity and m is an empirical index.

Winsauer et al., 1952 later modified Archie's law to give

$$FF = a\, n^{-m} \qquad (4.3)$$

where a and m are empirical values peculiar to the particuliar rock under study. For their brine saturated sand data, this empirical equation produced a better fit. However it violates the boundary condition of FF = 1 at n = 100 % for values of a = 0. Although they made no direct measurement of permeability, they did examine the tortuosity of the samples, concluding that the values obtained for electrical conduction and fluid flow were not in agreement with each other.

The term formation factor can further be defined as intrinsic or true formation factor and apparent formation factor. Sand grains have a very high resistivity, so for pore fluids of high salinity (low electrical resistivity) and clay free sediment or sediment of low clay content (in other words the conductive material is almost absent), it is typically assumed that all of the electricity is conducted by the fluid through the pore space. In this case formation factor remains constant, and is known as the intrinsic or true formation factor. This concept of intrinsic formation factor has been examined

by many researchers (Patnode and Wyllie, 1950; Urish, 1981; Worthington, 1973, 1975, 1976).

The formation factor is called "apparent" if its value is calculated through overall resistivity values without correction for matrix conduction. Thus (for clay rich sediments or low salinity pore fluid) it is a property which is controlled only by structural properties of the pore fluid matrix. The relationship between true and apparent formation factor can be defined as follows (Huntley, 1986).

$$\frac{1}{FF_a} = \frac{1}{FF_1} + \frac{R_w}{R_m} \qquad (4.4)$$

where FF_a and FF_i are the apparent and intrinsic formation factor, R_m and R_w are the matrix and fluid resistivities respectively.

So far two methods are known for the correction of apparent formation factor for matrix conduction. One developed by Worthington (1973, 1975, 1976) and has only been applied to sandstones, whereas its validity is yet to be applied in loose materials. The other one has been applied in alluvium by Park and Dicky (1989), and its validity depends on a strict calibration of geophysical data with well data.

Since the development of the concept of formation factor and its relation to porosity, changes have been made to the original idea to take into account the tortuosity of the sediment. Tortuosity is not only a function of the porosity of the sediment but it also depends upon the geometry of the pores. Ideally the value of tortuosity should be measured in the laboratory for every sediment, but because of the lack of suitable

experimental technique, other methods have been developed to obtain it by relating it to measurable physical properties such as porosity, permeability or electrical formation factor.

Taking the simple capillary model and applying it to the flow of electric currents in porous media, Wyllie and Spangler (1952) produced

$$FF = \frac{1}{n}\frac{L'}{L} \qquad (4.5)$$

where L' is the length of the average pore channel and L is the length of the sample. L' is greater than L; L'/ L is the electric tortuosity. Combining this equation with Archie's law produces

$$\frac{L'}{L} = n^{-[m-1]} \qquad (4.6)$$

suggesting that the electric tortuosity depends on the value of m, and the porosity of the sample. It can be shown both theoretically (Sen et al., 1981) and empirically (e.g. Jackson et al., 1978) that formation factor is dependent only on porosity and tortuosity in sediments.

From the definition of tortuosity it is quite clear that if the effective path length and the shortest distance between two faces is the same then the tortuosity value equals 1.0, which puts a lower limit to tortuosity values. Based upon mathematical modelling Dullien (1979) and Scheidegger (1974) showed that tortuosity values lie between 1.0 and 3.0.

The experimental work of Jackson et al., 1978; Lovell 1983; and Biella et al., 1983 working independently on monogranulars and mixtures of artificial and natural sands showed that the relationship between formation factor and porosity is site specific and the numerical values of the constant, m has a wide range. Natural sands (which all obey Archie's law) has values of m in the range 1.4 to 1.6 (Archie, 1942; Atkins and Smith, 1961; Taylor Smith, 1971; Windle and Wroth, 1975). In other words m depends upon the shape of the particles while variations in grain size and the spread of particle sizes have little effect on formation factor. Figure 4.1.

4.1 Permeability and formation factor relationship

Considering that relationships between formation factor and porosity and between porosity and permeability exist, both direct and inverse relationships (empirical equations) have been developed in the literature to relate formation factor and permeability (see Figure 4.1a). Direct relationship between formation factor and permeability have been reported by many authors (e.g. Croft, 1971; Kelly, 1977; Kosinski and Kelly, 1981; and Urish, 1981).

$$k = b\, FF^{c} \tag{4.7}$$

where k is the permeability, FF is the formation factor and b and c are constants.

On the other hand inverse relationships are possible and have been shown to exist by Lovell (1983); Barker and Worthington (1973) and Biella et al (1983).

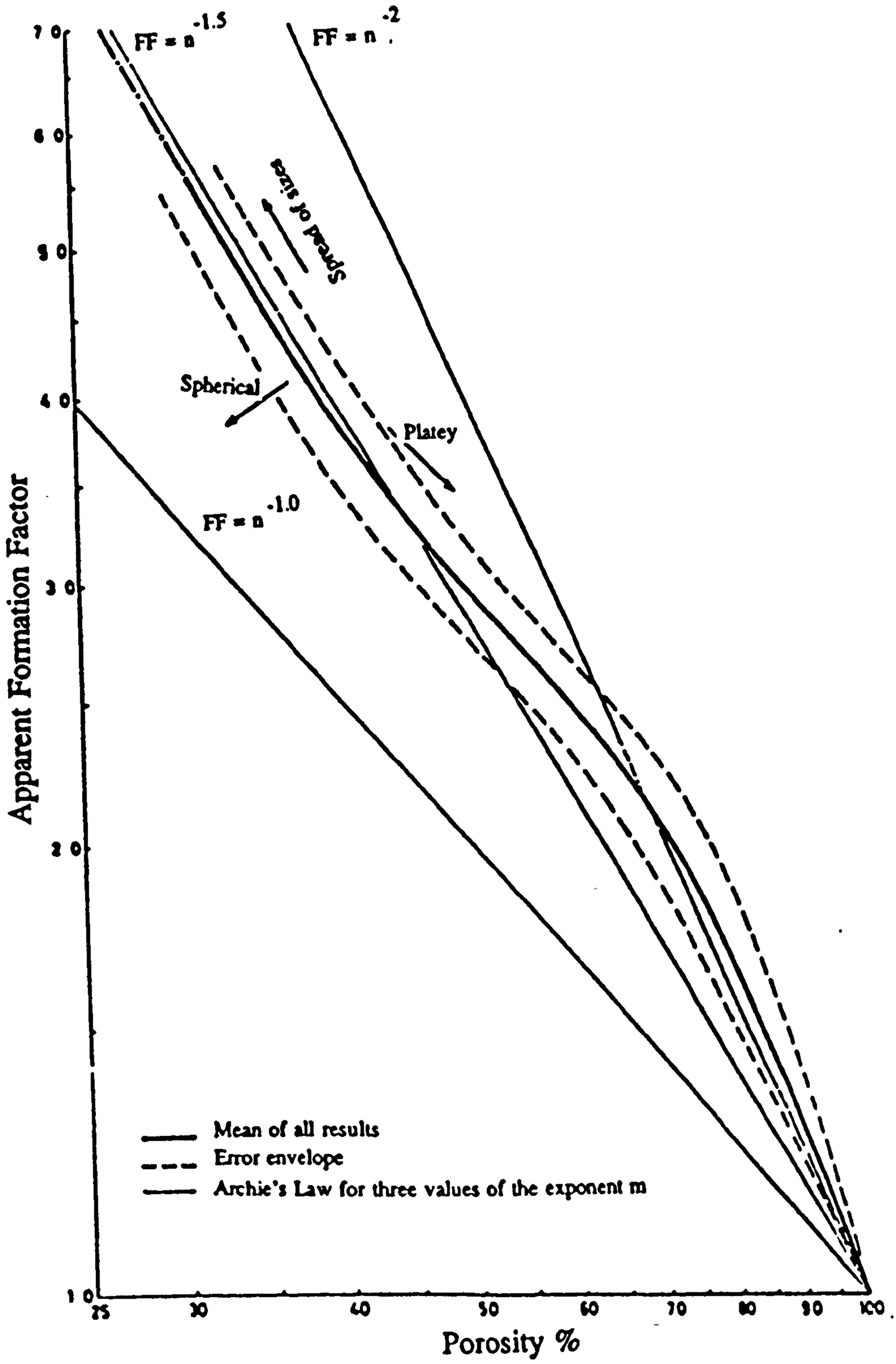

Fig. 4.1 Formation factor Vs. porosity relationship for marine sediments of different particle sizes and shapes.

(After Jackson et al., 1978).

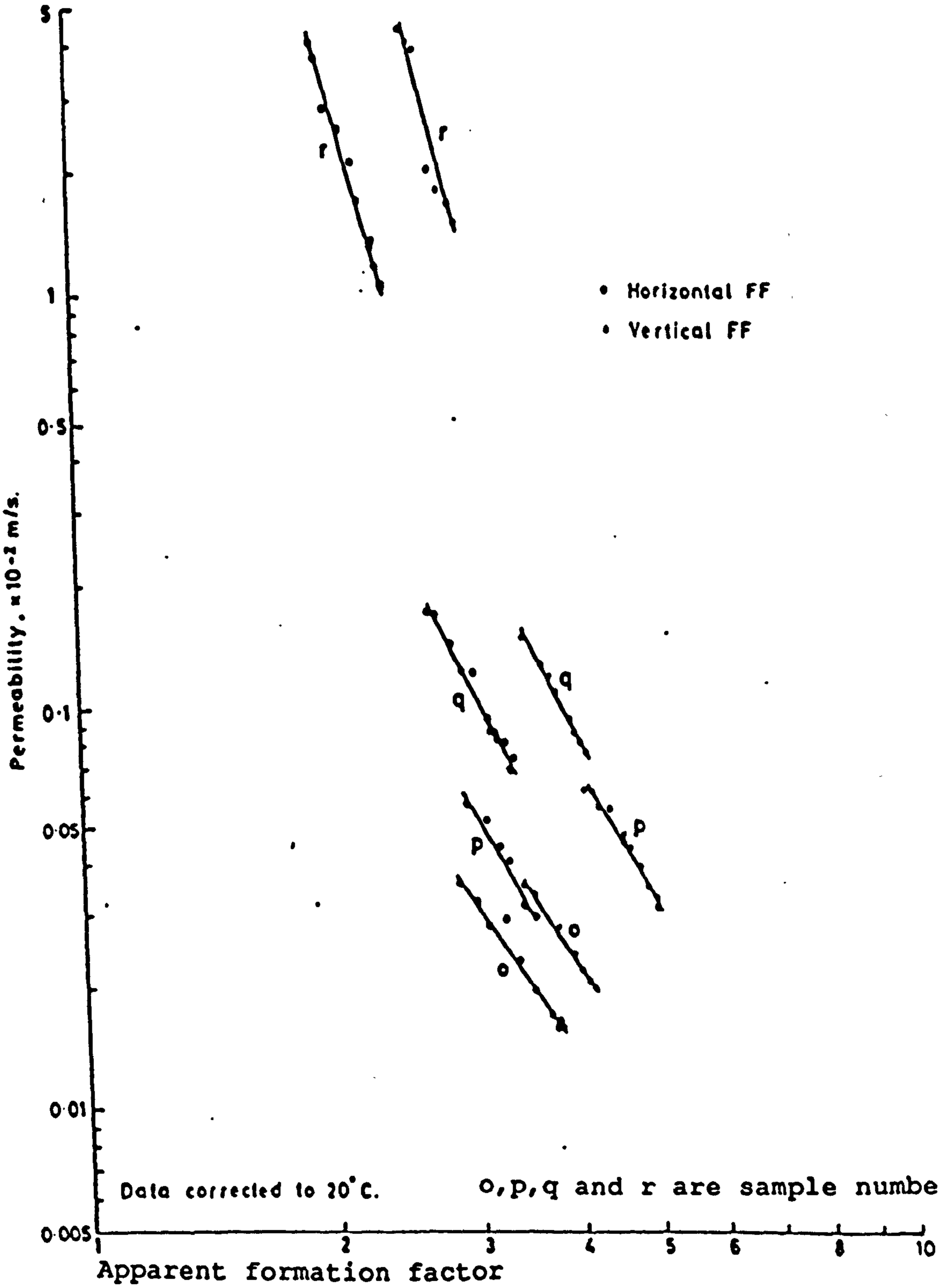

Figure 4.1a. Permeability plotted against Apparent Formation Factor for natural sand samples (after Lovell, 1983).

$$k = b\ FF^{-c} \tag{4.8}$$

where b and c are constants.

Kelly and Reiter (1984), using their theoretical model showed that a direct relation between permeability and electrical resistivity can be obtained if the average transverse resistivity rather than bulk resistivity is used in the relation. Such a situation is caused by layering in natural sediments which produces transverse isotropy, thus introducing data scatter in field relations.

4.2 Permeability and methods of its determination

The permeability of soil or a rock is a measure of its ability to transmit fluid, such as water under hydro-potential gradient (Lohman, 1972). Henry Darcy, a French civil engineer while working on the fundamental problem of the mechanics of fluid flow in sands, discovered that for sands of the same nature the flow of water was proportional to the difference in hydraulic head and inversely proportional to the length of the sand in the direction of water flow. In mathematical form Darcy's Law can be expressed as

$$k = \frac{q\,L}{h\,A} \tag{4.9}$$

where q is the rate of flow, k is the coefficient of permeability in velocity units, A is the area of cross section, h is the head loss and L is the length of the sample.

Permeability is called intrinsic permeability if in a porous permeable medium,

it is function of the material properties only, and is independent of the nature or properties of the fluid and can be expressed as

$$\phi = \eta v / \rho g i \qquad (4.10)$$

where ϕ is the intrinsic permeability, η is the viscosity, v is the velocity, ρ is the density of the fluid, i the hydraulic gradient and g is the acceleration due to gravity. It has the units of area (darcy).

Permeability is known as hydraulic conductivity, when the fluid flow is not only influenced by the material properties but also depends upon the fluid properties and can be expressed either as equation 4.9 or simply as

$$k = v / i \qquad (4.11)$$

where k has units of velocity m / sec, since the hydraulic gradient is dimensionless, v is the velocity of fluid and i is the hydraulic gradient. Table 4.1 shows a table after Lambe and Whitman, 1969; for permeability conversion.

Many methods of determining permeability in the laboratory or the field are in practice but during the present study the following methods have been used : The constant head permeameter and grain size analyses in the laboratory. The constant head test, pump test and Guelph permeameter in the field.

4.2.1 Laboratory methods

4.2.1.1 Constant head method

This method is found suitable for the determination of the permeability of

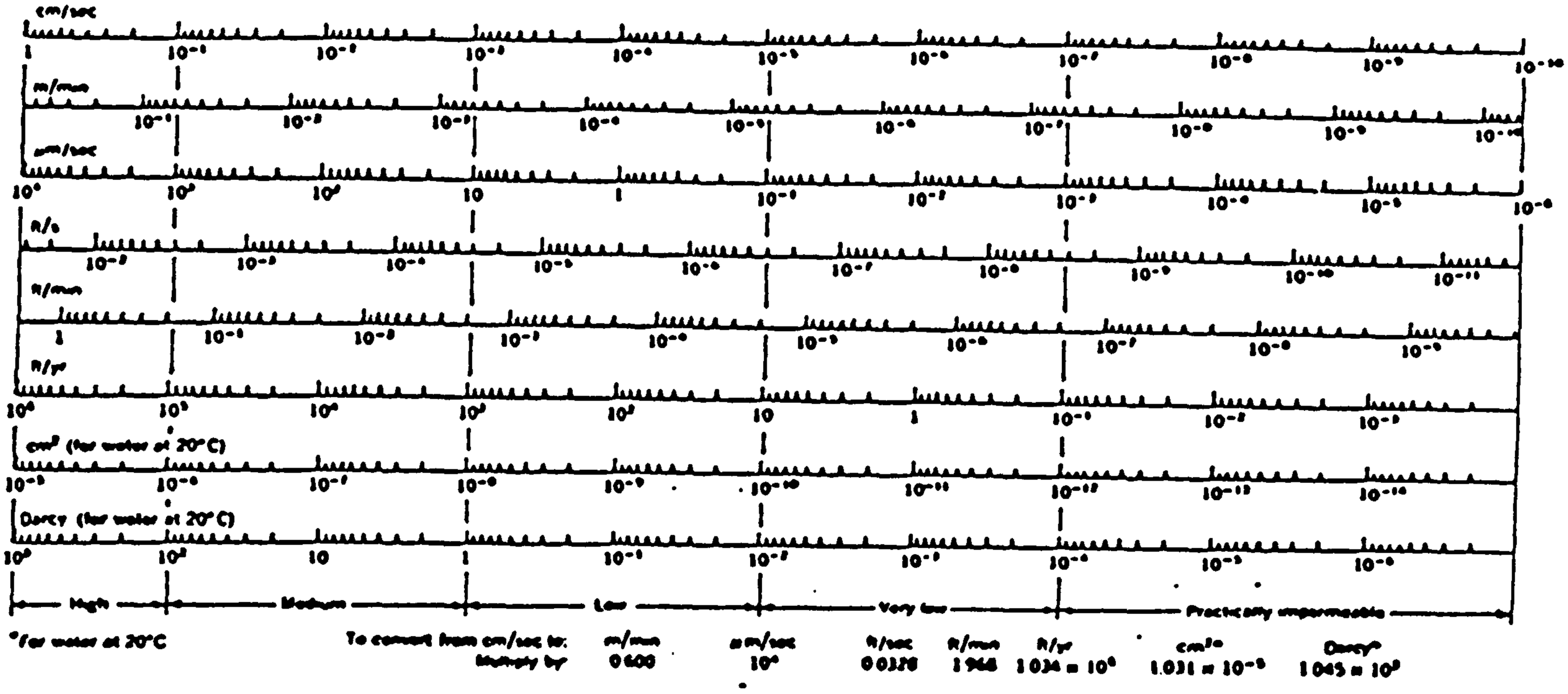

Table. 4.1 Permeability conversion chart.

(After Lambe and Whitman, 1969).

medium to coarse grained sediment. The following is the procedure and apparatus used for the test. Figure 4.2.

1) Constant head reservoir cell.

2) A permeameter cell.

3) Manometer tubes.

4) Measuring cylinder.

5) Stop watch.

The test begins by allowing distilled water to rise gradually in the cell and the manometer, taking every precaution that no air bubbles remain in the system. Then using a plastic cone filled with deaired water, fine gravel are loaded into the cell, up to the depth of about 2 cm and a wire mesh placed on the top of it. The sample is then slowly loaded into the cell with constant tapping of the cell, to get rid of any air trapped in the sample. A second wire mesh is now placed on the top of the sample and another gravel layer over the top of wire mesh. The constant head supply is now connected to the top of the cell making it ready for testing. When the hydraulic head is applied to the sample, it takes some time to reach a steady state condition. As soon as this condition is achieved, the stop watch is started and the volume of water passing through the sample during a given time interval is collected in a separate cylinder. The data collected from the test is used to determine the permeability k of the sample, using Darcy's law.

4.2.1.2 Permeability by grain size analyses

Over the years attempts by many researchers have been made to derive a quantitative relationship between the pore geometrical properties of the sediment and permeability. The outcome has been many empirical relationships between permeability and grain

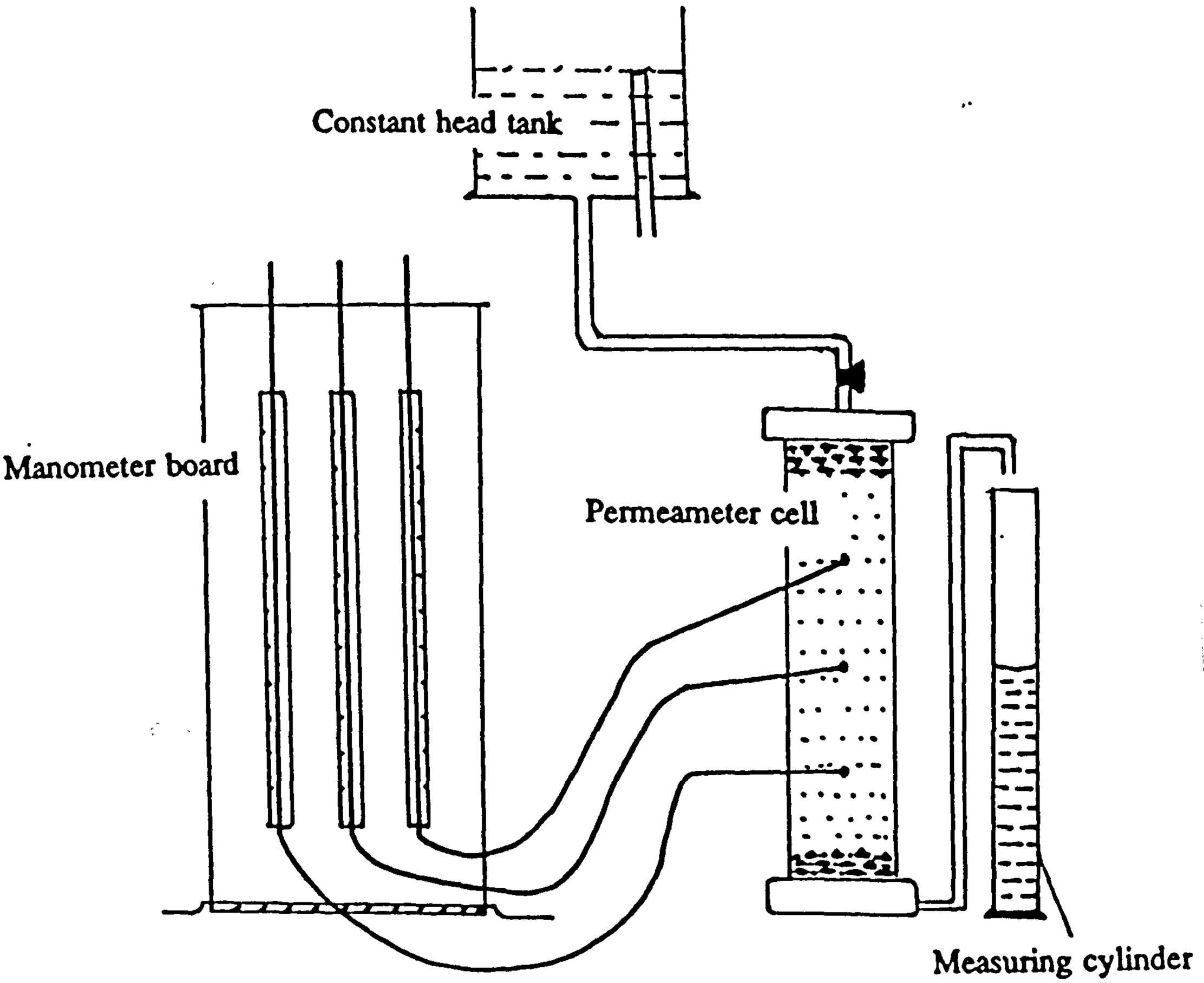

Fig. 4.2 Constant head apparatus.

size distribution and pore geometry.

Hazen's (1892) formula has been a widely used method to obtain permeability from effective grain size using equation

$$k = c\, d_{10}^2 \quad cm/s \tag{4.12}$$

where d_{10} is the grain size at which 10 percent of the material is of smaller grains. c is a constant with a value ranging between 90-120 (Solymer and Ilobachie, 1986).

Slichter (1899) proposed another form of such a relationship for uniform sands

$$k = \frac{771}{c} d^2 \quad cm/s \tag{4.13}$$

the parameter c in this equation being a function of the porosity of sediment.

Terzaghi (1925) extended Slichter's (1899) relationship to include non-uniform sand of variable grain shapes by using

$$k = \frac{c}{\eta} \left[\frac{N-0.13}{3\sqrt{(1-N)}}\right] d_{10}^2 \tag{4.14}$$

Relating relative resistance to porosity through a parameter f(N), Rose (1950) gave a formula for permeability determination,

$$k = \frac{gd^2}{1000\eta} \quad \frac{1}{f(N)} \quad cm/s \tag{4.15}$$

where η is the viscosity of fluid, and f(N) can be obtained from the following relationship, where N is the porosity of the sediments.

$$f(N) = 1.115\ (1-N)\ \frac{(1-N)^2+0.018}{N^{1.5}} \qquad (4.16)$$

Carman, 1939; Scheidegger, 1974; Dullien, 1975; working independently related permeability to pore geometry in order to get more appropriate results. Mathematical models which correlate permeability to pore geometry take into account tortuosity.

The Kozeny-Carman equation was originally proposed by Kozeny (1927) as an extension of Poiseuille's equation for fluid flow through capillary tubes. It was later modified by Carman (1939) and since then it has been widely used to obtain permeability in all sorts of porous medium.

$$k = \{D^2\ n^3\ \mu\ C\} / \{\eta\ (1-n)^2\ \} \qquad (4.17)$$

where k is the permeability coefficient in velocity units, D is the mean grain diameter, n is the fractional porosity, μ is the unit weight of fluid, C is the grain shape tortuosity factor and η is the fluid viscosity.

4.2.2 Field permeability tests

A critical review of most of the field methods is given by Bouwer (1978); Lohman (1972) and Solymer and Iloabachie (1986). For the present study field methods were limited to the use of the in-situ constant head test, the Guelph permeameter and the pumping test.

4.2.2.1 In-situ constant head test

The in-situ constant head test has been found to be more appropriate and less time consuming particularly in coarser sediments. In the present study it has been carried out in the borehole excavated and installed with a screen for such tests. Figure 4.3. It comprises of 3 sections:

1) A borehole with 100 mm dia casing pipe to have a flow of water in and out.

2) A bowser (water tanker) to supply water with 50 mm dia pipe into the borehole.

3) A water pump attached to a flow meter in order to record flow-out rate of water.

In the in-situ constant head test, using the 50 mm dia pipe the rate of inflow of water is adjusted into the main bore hole until a constant head achieved; water is then pumped out using another 50 mm dia pipe , and once an equilibrium with flow of water in, and therefore out, of the borehole is reached, the readings of the flow rate of water are recorded. The constant water level in the borehole was also recorded. There are numerous methods of calculating permeability from the results of such tests, however in the present case the following formula (Hvorslev, 1951) is used to calculate it:

$$k = \frac{q}{FH_c} \qquad (4.18)$$

where k is the permeability, q is the rate of flow of water, F is in-take factor see (Figure 4.3), and H_c is the constant head.

4.2.2.2 Guelph permeameter test

The Guelph permeameter is an in-hole recently developed constant head permeameter. The method involves measuring the steady-state rate of water recharge into unsaturated soil from a cylindrical well hole, in which a constant depth (head) of water is maintained Reynold et al., 1986. It comprises of four sections (Figure 4.4):

1) Tripod Assembly: This consists of a Tripod Base with moveable Tripod Bushing and 3 detachable Tripod legs; when united this section acts as the base for the whole system.

2) Support Tube And Lower Air Tube Fittings: Through these fittings water is conducted from the reservoir assembly into the well hole also maintaining a constant head in the well hole.

3) Reservoir Assembly: This provides a means of storing water and measuring the out-flow rate while the permeameter is in use.

4) Well Head Scale And Upper Air Tube Fittings: An air tube coupling connects the upper air tube to the middle air tube. The upper tube serves as an extension to facilitate setting the well head after the well head scale is put in place.

As the Guelph permeameter test was carried out in medium to coarse grained sediments, the permeameter after its assembly was set on its combination reservoir system as per its working instructions. The permeameter was filled with water and placed in the prepared well hole, and then the following standardized procedure was followed. A 5 cm well head was established by slowly raising the air inlet tube. The rate of fall of the water level was also observed and recorded from the graduated

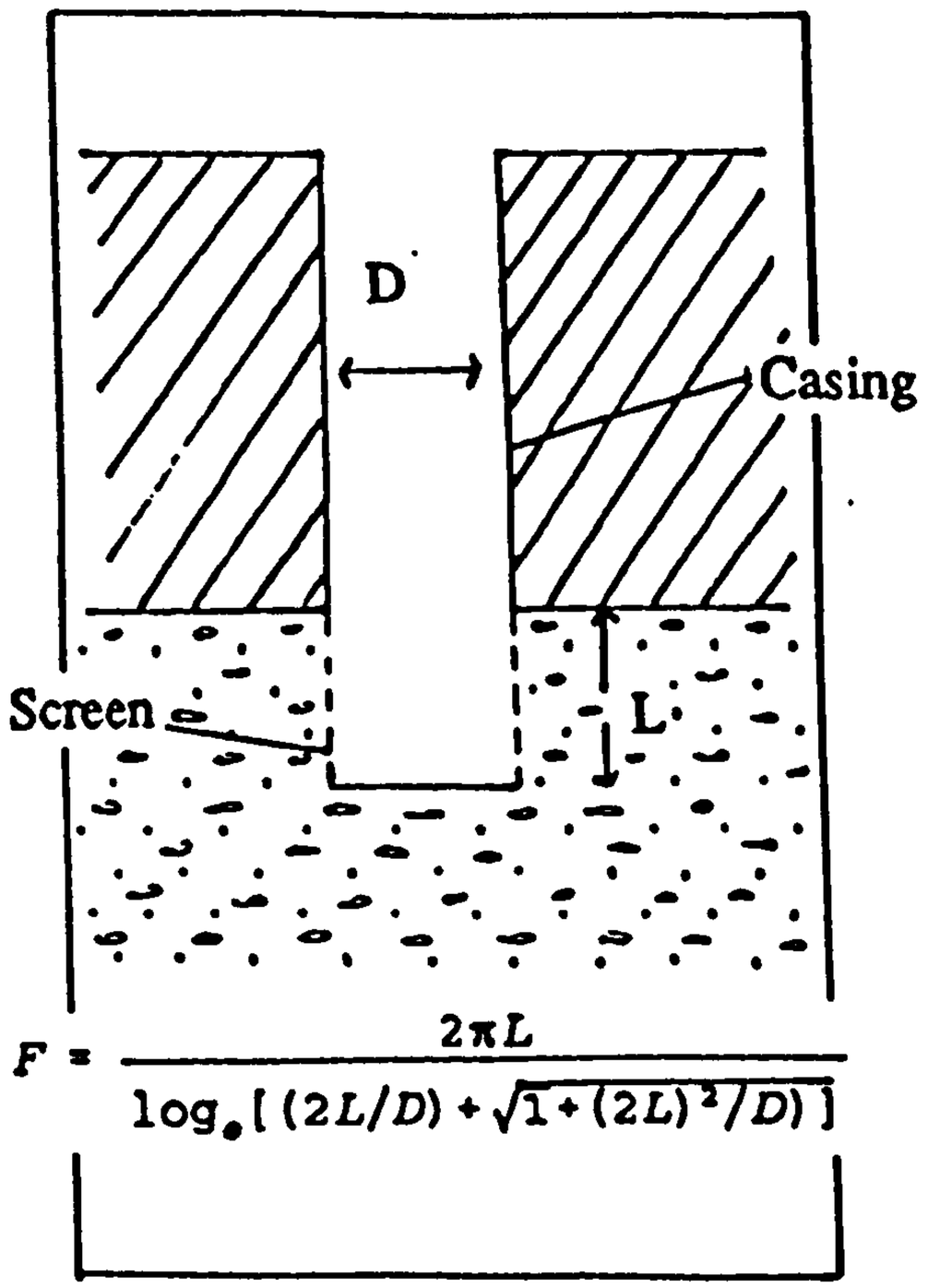

$$F = \frac{2\pi L}{\log_e\left[(2L/D) + \sqrt{1 + (2L)^2/D}\right]}$$

Fig. 4.3 In situ Constant head test.

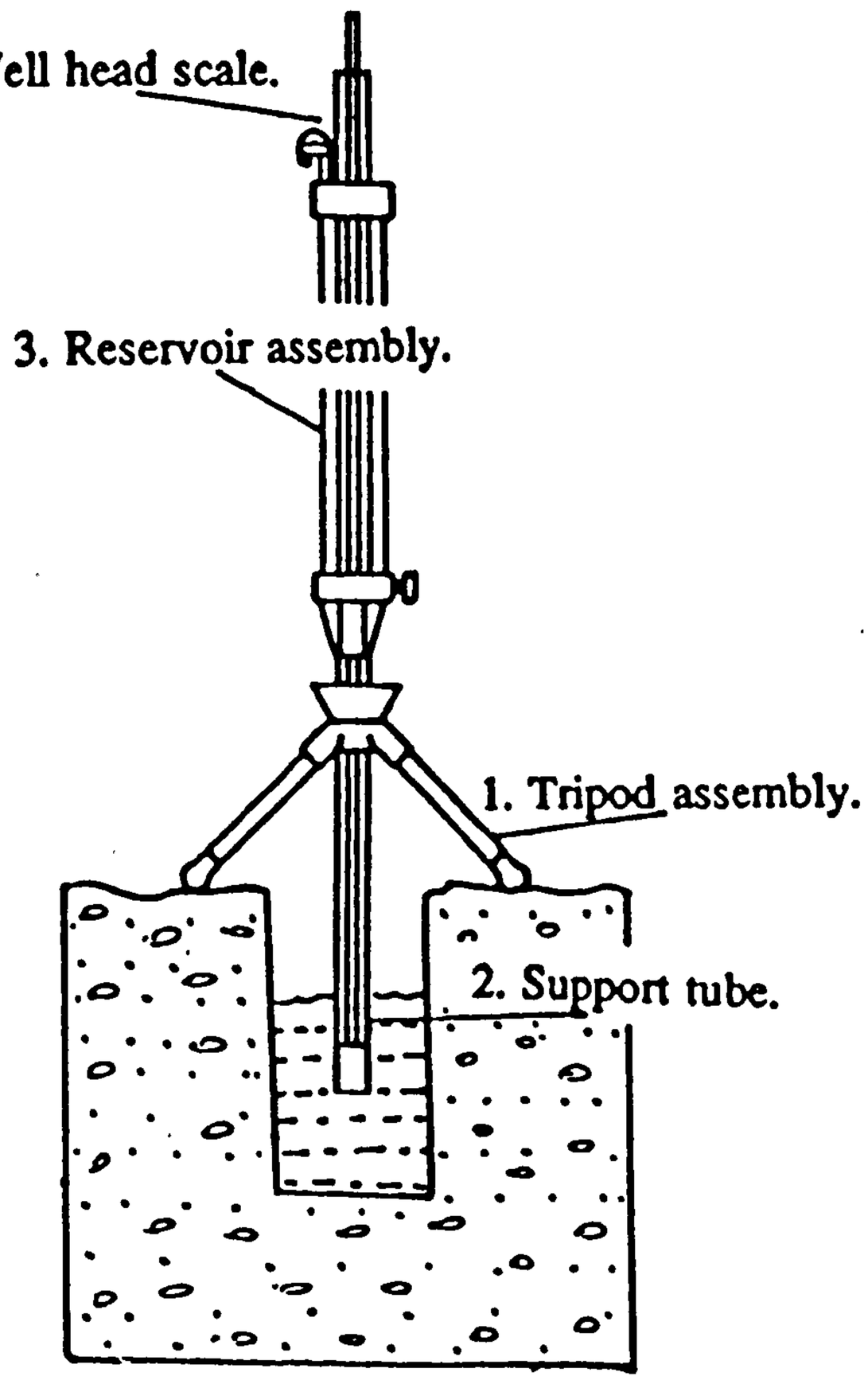

Fig. 4.4.Guelph permeameter.

reservoir. After these measurements, a further well head of 10 cm was created and the measurement process repeated. The results were recorded on a prescribed data sheet and the permeability calculated by using the following formula.

$$k = (0.0041)\ (X)\ (R_2) - (0.0054)\ (X)\ (R_1) \quad cm/s \qquad (4.19)$$

where x is the combined reservoir constant having a value of 35.39 cm^2, R_1 is the steady state rate of flow at the 5cm head and R_2 is the steady state rate of flow at the 10 cm head.

4.2.2.3 Field pumping test

Field pumping tests are appropriate to soils or rocks with high permeabilities. These are generally carried out by pumping water out of a borehole at a known constant rate and observing the drawdown of the water table in a series of other boreholes known as observation wells (piezometers) set out radially from the pumped hole. From these observations, the drawdown curve can be plotted and the permeability calculated.

In the present study, the following procedure was adopted to conduct the pumping test. A main borehole (discharging well) and 4 piezometers making two lines of wells perpendicular to each other were drilled to about 7 m at the Aber College Farm site (See pumping test Plan Figure 4.6.a and a Photographic plate 4.6.b.). Piezometers were located at varying distances from the centrally-installed well. The discharging well and the piezometers are cased with 100 mm diameter pipe so that a submersible pump could be inserted easily in the base. In the discharging well a 3 m

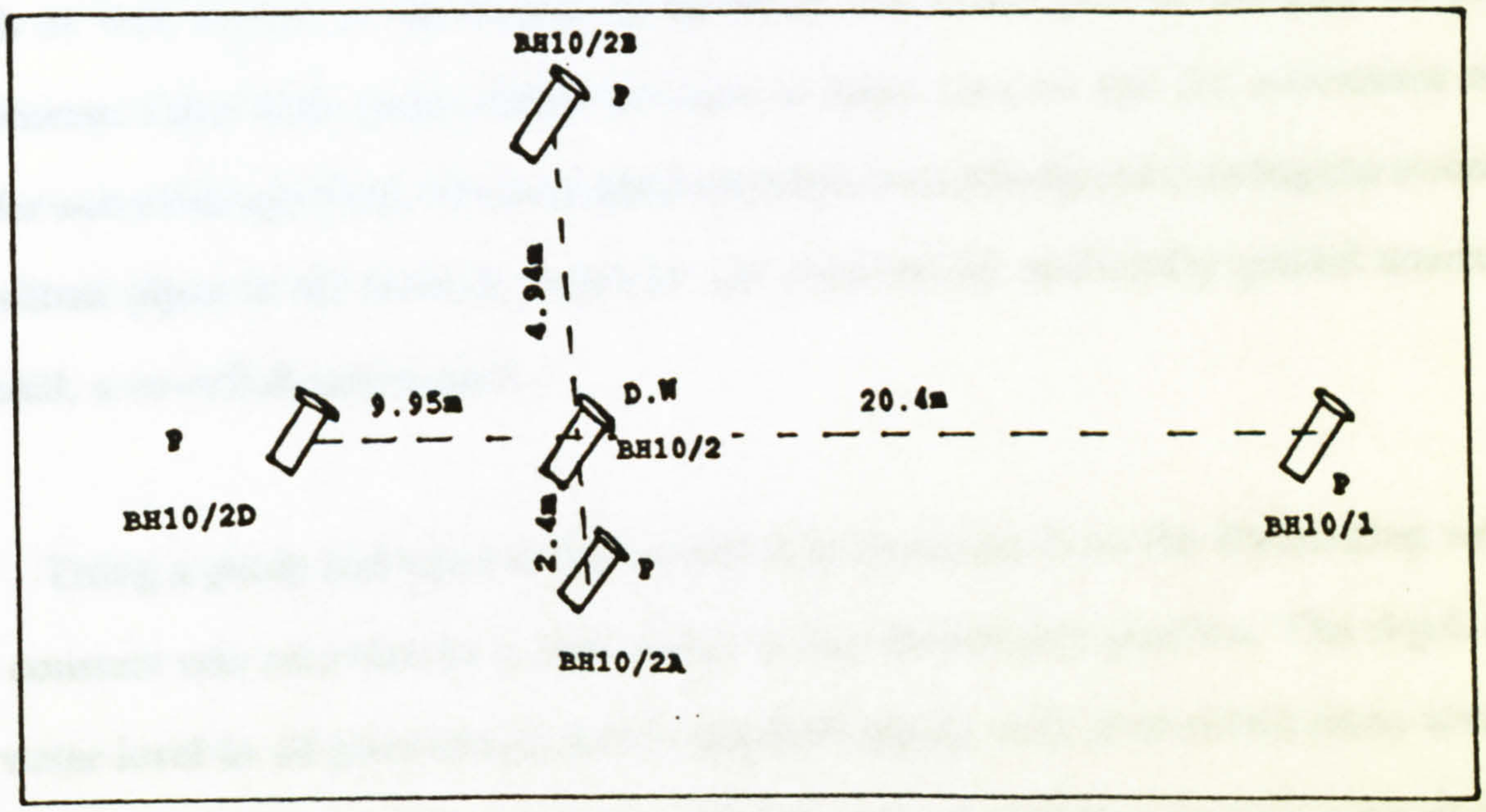

Figure 4.6.a Pumping test Plan.

Photograhic Plate 4.6.b Showing a discharging well and piezometers.
D.W = Discharging well, P = Piezometer.

length of well screen at the bottom is installed, the lower part of the pipe of the piezometers have been made slitted in order to have easy to and fro movement of aquifer water through them. The formation material immediately surrounding the screen and slitted pipes in all holes is removed and replaced by artificially graded coarser material, a so-called gravel pack.

Using a pump and a power unit, water is pumped out from the discharging well at a constant rate recorded by a flow meter in the discharging pipeline. The depth to the water level in all piezometers and in the discharging well is recorded many times during the course of the test. As the water levels drop fast during the first hour of the test, readings are taken at frequent intervals on a printed form, with the time between readings being gradually increased as pumping continues. These tests are repeated a few times on various days. For a confined aquifer, using the observed data the permeability is calculated as

$$k = \frac{Q}{2\pi D(s_1 - s_2)} \ln\frac{r_2}{r_1} \qquad (4.20)$$

where Q is the well discharge in m^3 / day, k is the hydraulic conductivity, D is the thickness of the aquifer, r_1 and r_2 are the respective distances of the piezometers from the pumped well in meters and s_1 and s_2 are the respective elevations of the water levels in the piezometers in metres.

4.3 Porosity

All porous media contain pores and spaces which are surrounded by the solid

material. The ratio of the volume of these pore spaces to the total volume of the sample is a dimensionless quantity known as porosity, which can be given as a percentage or as a fraction. The porosity of naturally-occurring sediments may range widely depending upon the geological history, depositional patterns, and the imposed conditions.

4.3.1 Method of determination of porosity

The choice of the method used for porosity determination depends upon the nature of the material. Several methods have been described in many standard text books (Dullien, 1979; Scheidegger, 1974; Bourbie et al., 1987).

The most convenient and widely used laboratory method is by putting the sample into a mould of known volume and drying it in the oven. After measuring the specific gravity of the grains in the laboratory the porosity is determined by using the following equations.

$$V_s = W_s / G_s \gamma_w \qquad (4.21)$$

$$V_v = V_t - V_s \qquad (4.22)$$

$$N = V_v / V_t \qquad (4.23)$$

where V_s is the volume of the solids, γ_w is the unit weight of water, G_s is the specific gravity of the grains, V_v is the volume of the voids, V_t is the total volume and N is the porosity of the sediment.

This porosity is representative of the maximum packing of the sediment and may not be equivalent to the insitu value.

CHAPTER 5. CORRELATION OF FORMATION RESISTIVITIES TO CHLORIDE CONCENTRATION

A measurement of fluid conductivity cannot resolve the type of dissolved solids. It is, however, common to relate electrical conductivity to an equivalent chloride concentration (Kwader, 1986). This relation can be used as an indicator of total dissolved solids for sea water, but it is not valid when a significant part of the dissolved solids are concentrated with anions other than chlorides. To derive more quantitative information about concentration of dissolved solids, an attempt has been made to correlate formation resistivities measured through direct resistivity methods to chloride concentration.

First, water samples from 31 boreholes were collected and chemically analysed for chloride anions. The electrical conductivity for all the samples were determined and it ranged from 240 to about 10000 µmhos/cm at 25° C. Table 5.1 enlists all the details of the data obtained from the boreholes and with analysis carried thereon. Generally, the total dissolved solids in ground water increase as water moves towards the beach area, where T.D.S range from 1082 to about 6387 mg/l.

The relation between chloride concentration and water conductivity on samples from boreholes was investigated. The data obtained from Aber College farm , Malltraeth area, and Morfa Bychan area, are summarized in Figure 5.1. Each dot represents one sample. The correlation coefficient is equal to 0.998. Some scatter of the data is due to difference in the concentration of chlorides in the groundwater from place to place. Figure 5.1 has been constructed with chloride values expressed in mg/l and conductivity in µmhos/cm. Figures 5.2 and 5.3 show a very little scatter observed in the

Borehole No.	Conductivity (μmhos/cm) at 25° C	Estimated fluid resistivity (Ω.m)	Measured aquifer resistivity (Ω.m)	Total dissolved solids (ppm)	Chloride concentration (ppm)
AB.10/2D.T	240	42	157	154	58
AB.10/2.T	290	35	110	185	70
AB.10/1.T	500	20	54	320	131
AB.10/1.B	1180	8.5	31	755	330
MB.VES1	421	24	95	270	103
MB.VES2	502	20	85	322	129
MB.VES3	530	19	87	340	136
MB.VES4	518	19	86	332	129
MB.VES5	600	17	55	484	180
MB.VES8	588	17	69	376	152
MB.VES9	582	18	76	360	146
MB.VES10	584	18	78	361	138
MBVES6J"	1800	6	12	1152	488
MBVES6I"	9980	1	2	6387	2870
MBVES6B	6200	1.8	4	3968	1742
MBVES6A	5100	2	5	3264	1436
MT.20B	350	29	84	224	66
MT.20A	390	26	70	250	76
MT.22C	600	16	60	385	150
MT.20F	480	21	72	307	101
MT.20E	422	24	99	270	81
MT.22A	686	15	53	439	209
MT.21C	660	15	54	423	200
MT.23D	900	12	40	578	244
MT.23B	950	10	35	608	252
MT.1B	3200	3.2	6	2048	880
MT.9B	1690	6.4	14	1082	465
MT.4A	5480	2	4	3507	1402
MT.3B	6600	1.5	3	4224	1820
MT.6B	4922	2.1	4	3150	1450
MT.12C	9910	1	1	6342	2732
MT22B	914	11	45	584	233

AB = Aber College Farm, MT= Malltraeth, MB= Morfa Bychan.

Table 5.1 Chemical analyses of ground water samples for chloride ions.

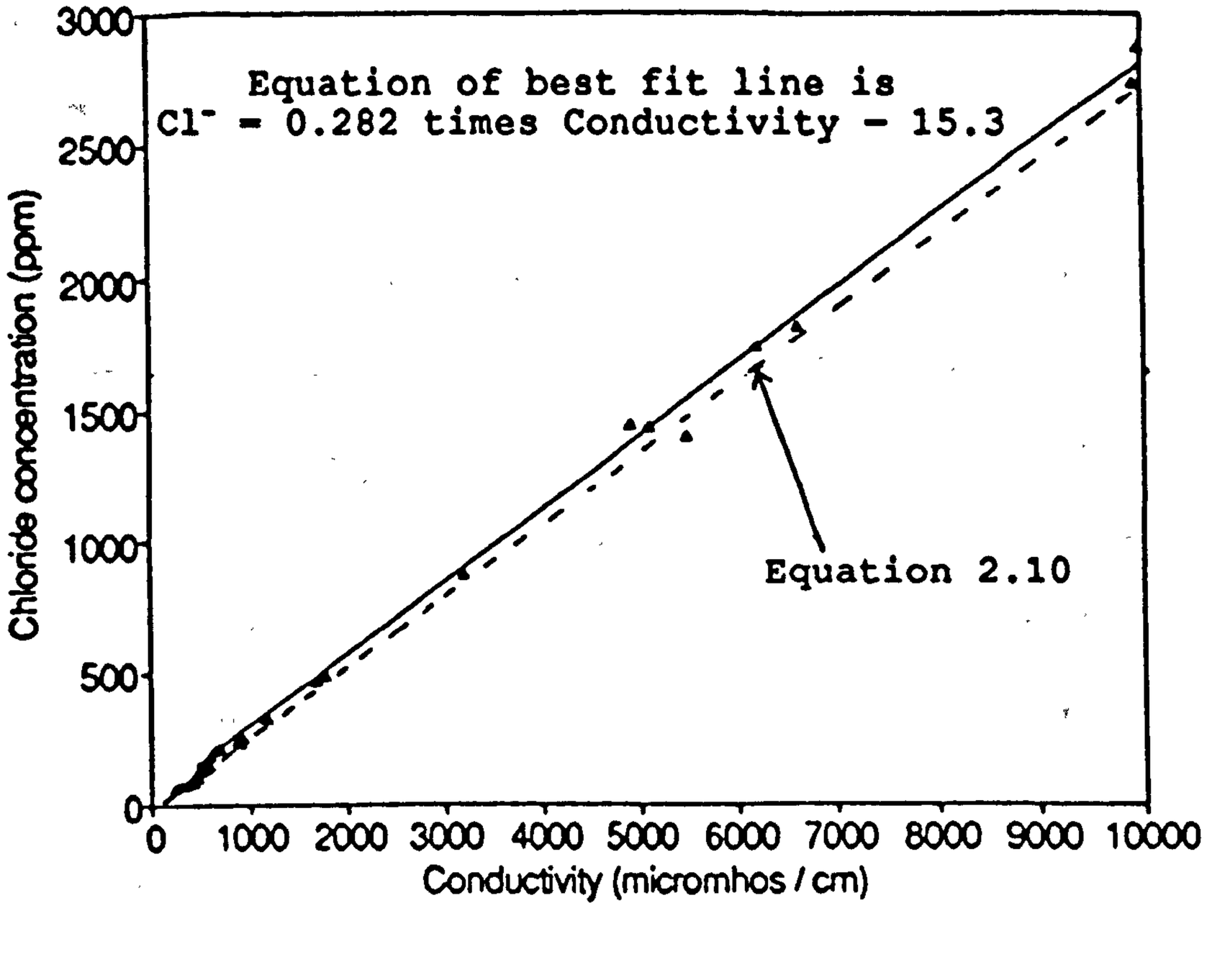

Fig. 5.1. Relation measured between Chloride concentration and fluid conductivity on water samples from different areas.

ground water samples from the Malltraeth and Morfa Bychan aquifers. The correlation coefficient is 0.998 and 0.999 for Malltraeth and Morfa Bychan aquifers respectively. Seawater samples collected from the Malltraeth, Morfa Bychan and Aber College farm area, were analysed for chlorides in the laboratory, and gave results as 26800 ppm, 24545 ppm and 26169 ppm respectively.

On the basis of Figures 5.2 and 5.3, 500 ppm chloride concentration correspond to a fluid conductivity of about 1900 µmhos/cm or a fluid resistivity of about 5 ohm-m, and 250 ppm chloride concentration correspond to a fluid conductivity of about 950 µmhos/cm or a fluid resistivity of about 10 ohm-m. This is not far away from the information summarized by Kwader (1986), who has put 500 ppm chloride concentration corresponding to a fluid resistivity value of 6 ohm-m and 250 ppm chloride concentration to a fluid resistivity of 9 ohm-m. Here specially 500 ppm chloride concentration has been selected because boreholes/wells that reach chloride concentration of 500 ppm are considered to be significantly intruded with seawater (Goswami, 1968; Mills et al., 1988; Hoekstra et al., 1990), and is taken as a basis for the fresh-salt water interface. In the present study on the other side 250 ppm chloride concentration, which also correspond to a measured bulk resistivity value of 35 ohm-m (Table 5.1), is selected as the basis of a mixing zone (transition zone). This value is in more agreement to Mills and Ryder (1977); Jacob, (1980); and Stewart et al., (1982), who have put the lower limit of the mixing zone between 200-250 ppm chloride concentration than Goswami (1968) who puts the lower limit at 300 ppm chloride concentration.

In surface electrical methods, formation resistivities rather than fluid resistivities are measured (see Van Dam et al., 1967). In the present study to correlate formation

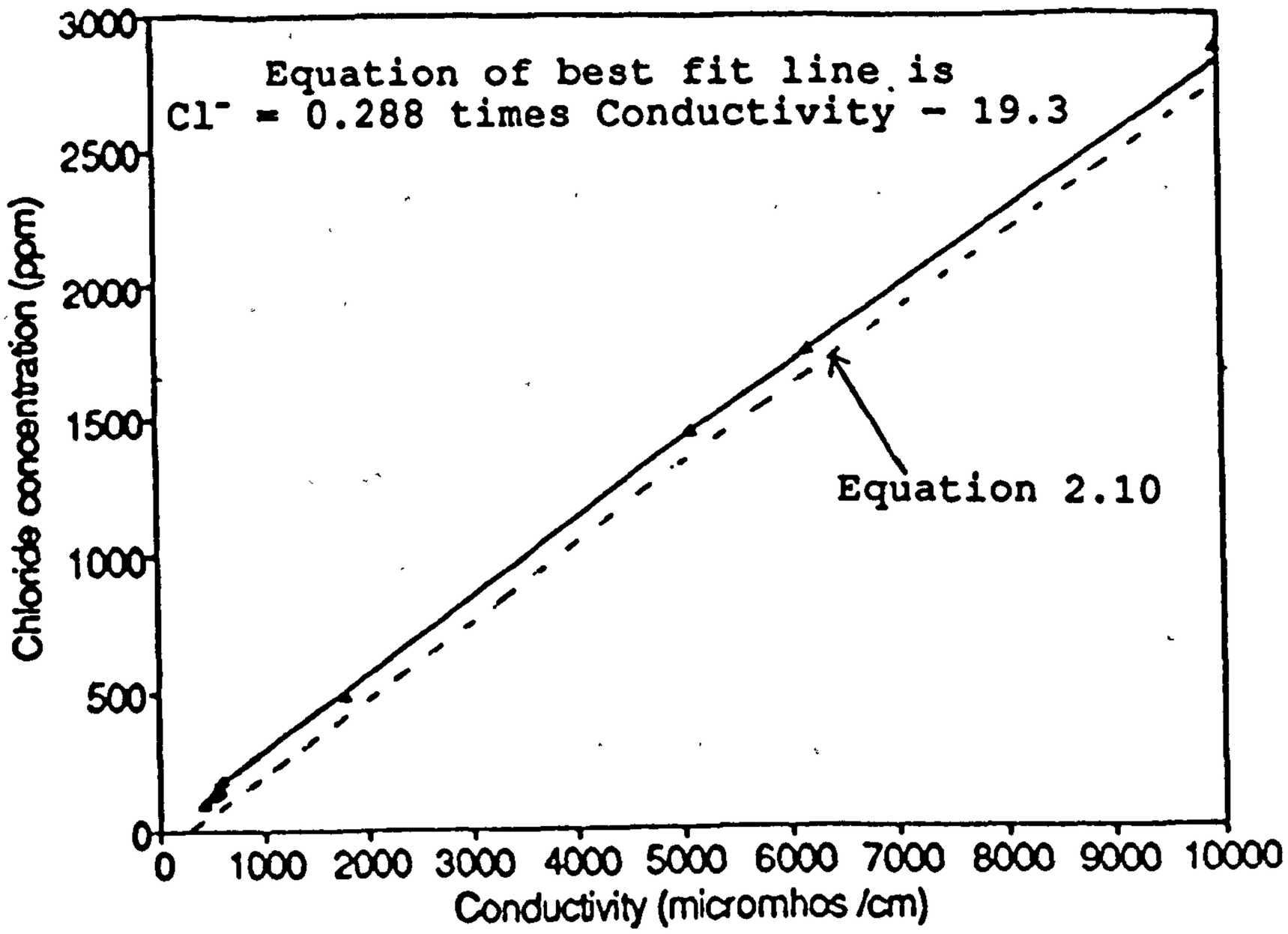

Fig. 5.2 Relation measured between Chloride concentration and fluid conductivity on water samples from Morfa Bychan area.

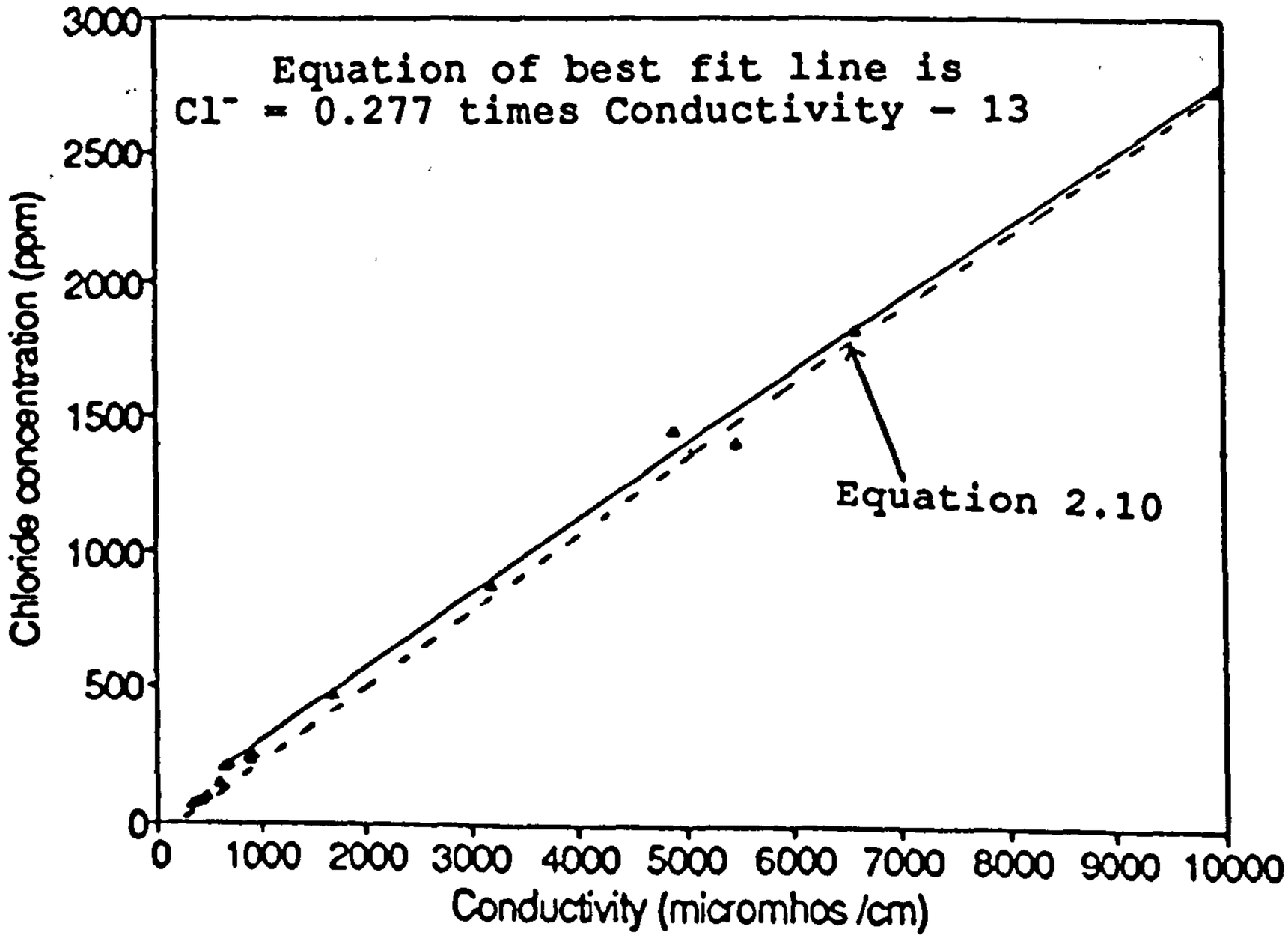

Fig. 5.3 Relation measured between Chloride concentration and fluid conductivity on water samples from Malltraeth area.

resistivities to chloride concentration the following approach has been made: The resistivity measurements were carried out in the vicinity of all the 31 boreholes at Aber college farm, Malltraeth, and Morfa Bychan sites; where ground water samples were also collected. The results of the interpretation of measurements are compared with the chloride concentration data of ground water samples obtained from certain depths in the boreholes. This correlation is hindered by (1) the availability of a relatively limited number of boreholes at which resistivity soundings have been made, and (2) the inconsistent quality of the interpreted formation resistivity obtained from the resistivity sounding results. By carefully selecting resistivity sounding results of good quality, and representative of the regional hydrologic regime, some six data points were available for the Malltraeth aquifer. These data points are shown in Figure 5.4. This figure is used for converting the aquifer resistivity into the chloride concentration of the ground water in sand deposits at the location of measurement. On the basis of this figure, an aquifer resistivity of about 7 ohm-m is expected to correspond to a chloride concentration of 500 ppm. This value is nearly in agreement with the work of Mills et al., (1988) and Hoekstra et al., (1990) who have shown it to correspond to a bulk resistivity of 8 ohm-m. And a value of 7 ohm-m would also be consistent with the data of Guo (1986) for sand aquifers in China.

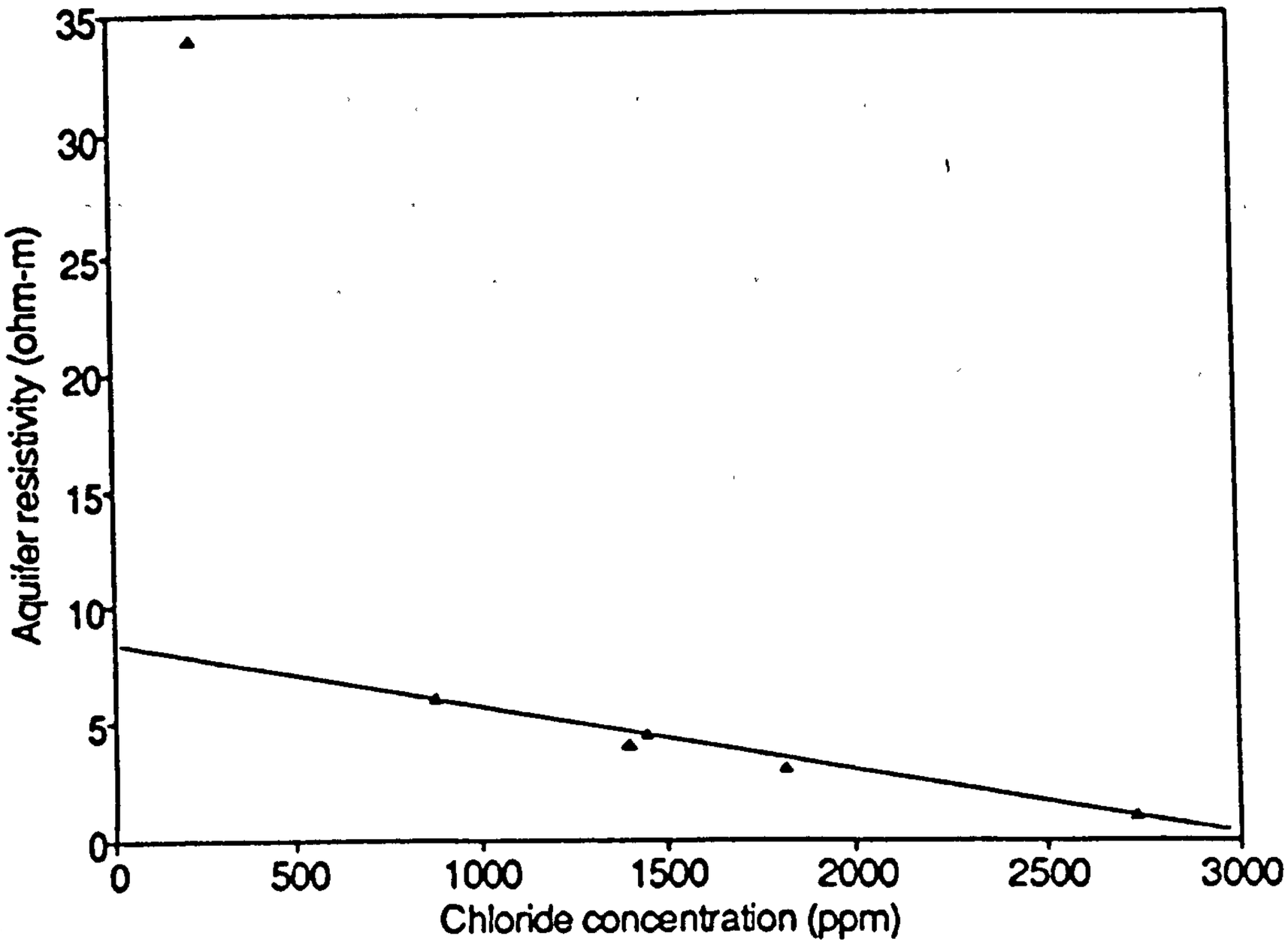

Fig. 5.4 Relation between Chloride concentration and aquifer resistivity in selected borewells.

CHAPTER 6. CASE HISTORY 1. ABER COLLEGE FARM AREA

6.1 Introduction and Geology of the Area

The site of investigation, the College Farm area at Aber, is situated on the coast at the outfall point of the Aber river near Llanfairfechan in Gwynedd (Fig. 6.1). This area occurs between two known geological sections, the Glan-y-mor-isaf section which lies to the southwest, and the Llanfairfechan section and is exposed on the A55 North Wales Coast Road, which lies to the northeast. It is a generally flat area although there are a few places of gentle undulations. The Aber-Dinlle, a major fault passes some distance away from the study area. The Aber river passes through the centre of the study area.

According to the published data regarding the Glan-y-mor-isaf section (Hart and Pointon, 1982), from the interpreted Quaternary stratigraphy of the A55 North Wales Coast Road at Llanfairfechan (based on borehole logs collected for their construction, and the borehole data obtained in this study after sinking boreholes by the manual percussion method in the study area), the lithological units in the area can be divided into two major groups: (a) the Holocene (less than 10,000 years old); and (b) the Pleistocene (more than 10,000 years old) Table 6.1.a.

a. The Holocene:

1. Surface fill.

2. Sand and Gravel. The gravel is generally clast-supported with interstitial fine to coarse sand. General lack of fines but occasional occurrence of silt or silty clay. Pebbles and cobbles are rare. The depositional environment is fluvial.

3. Clays and Silts. Bluish to grey coloured silts, clayey silts, and silty clays.

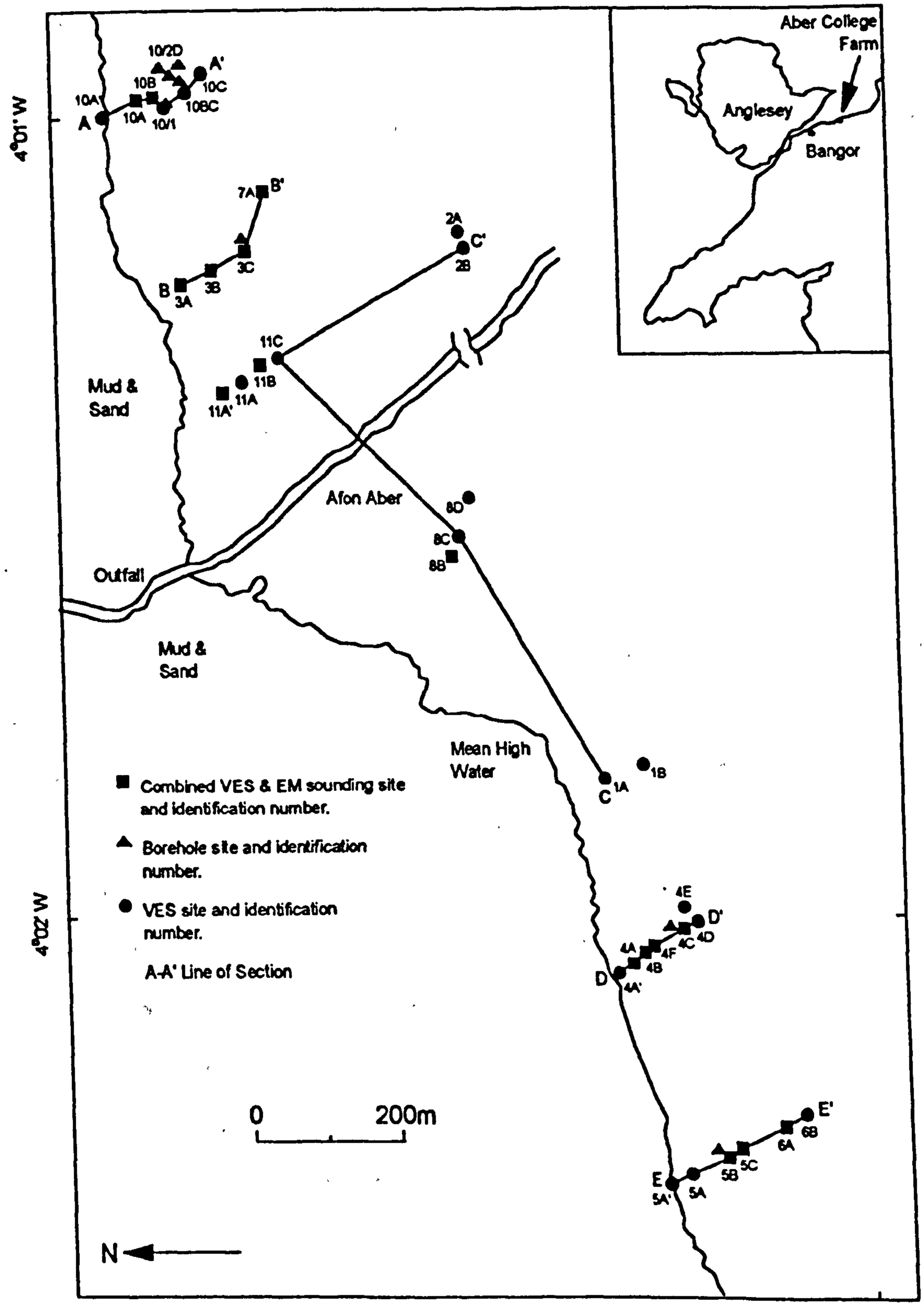

Fig. 6.1. Map showing location of study area, Aber College Farm, Gwynedd

Occasional sand and gravel beds. No cobbles or boulders. Depositional environment is marine, possibly fluvial if associated with unit 2.

4. Peat. Brown to black in colour. The depositional enviroment is terrestrial. The base of the peat forms the junction between the lower Holocene and the upper Pleistocene deposits.

b. The Pleistocene:

1. Sand and Gravels. In this unit there is an abundance of pebbles and cobbles and occasional boulders are found. Clays or clayey silt lenses are found. Depositional environment is fluvial.

2. Irish Sea Till. Red-brown diamicton (poorly sorted gravel-sand-mud admixture) with frequent and occasional thick gravel intra-beds. The diamicton is matrix-supported but contains abundant coarse clasts of cobble and boulder grade, and is typically highly over consolidated. The associated gravels are clast-supported. The diamicton is most likely to be till deposited in contact with ice. Its depositional environment is associated with ice moving southwards down the Irish Sea Basin. The gravels are glaciofluvial in origin, deposited by meltwater streams either in front of the glacier (proglacial), or within (englacial), above (supraglacial) or beneath (subglacial) the ice. They may be channelised into the underlying diamicton (proglacial), deposited in isolated mounds (crevasse-fillings) or form sinuous upstanding ridges (eskers). This till characteristically contains far less coarse material (sand, gravel, cobbles and boulders) than the Welsh Till, it can therefore be classified as a 'typical' to 'matrix-dominated till'.

3. Welsh Till. Grey diamicton (till) with frequent and occasionally thick gravel intra-beds. The diamicton is matrix-supported but contains very abundant coarse clasts

of cobble and boulder grade, and is typically highly overconsolidated. The associated gravels are clast-supported, depleted in fines, and contain a greater percentage of cobbles and boulders than the diamicton. Its depositional environment is in a variety of glacial subenvironments but all associated with ice moving northwards out from the Snowdonian mountains. Very large boulders are more common in the Welsh Till than in the Irish Sea Till because of the proximity of highly resistant bedrock as source material.

The geological and hydrogeological information in the study area was obtained from auger boreholes which revealed the presence of a confined upper aquifer consisting of unconsolidated fine to coarse-grained sand and gravel extending from 2 to 7 meters, intercalated with one or two thin soft clay and peat lenses. This is underlain by a bed of impervious glacial till of varying thickness composed of boulders, cobbles, sand and mud admixture and forms the base of the upper aquifer. Geophysical data provided information regarding the presence of a lower aquifer lying below the glacial till.

The results of mechanical analyses of granular samples obtained during sinking of the auger holes in the study area are tabulated (Table 6.1.b). It can be seen from this table that there is predominance of finer fractions of glacial outwash sediments towards the top of the upper aquifer. Coarse material occupies the bottom of the aquifer.

Due to the presence of 50 % granular material at the surface, the aquifer is partially recharged from percolation of rain water falling on the surface of the ground. As there is a heavy annual rainfall in the area for example 878mm in 1991 and 1220mm in 1992, most of the rainfall infiltrates into the underlying glacial outwash

Era	Epoch /Age	Lithological units
Quaternary	Holocene (< 10,000 years BP)	Surface Fill Fluvial Sand & Gravel Marine Clays & Silts Peat
	Pleistocene (> 10,000 years BP)	Fluvial Gravels Irish Sea Till Welsh Till Irish Sea Till

Table 6.1.a. Lithology with geological age of the sediments, Aber college farm.

Depth Range 0 - 1.5 m		
Size Content	**Minimum**	**Maximum**
Gravel	10 %	15 %
Sand	46 %	56%
Silt & Clay	26 %	44 %
Depth Range 1.6 - 7.2 m		
Size Content	**Minimum**	**Maximum**
Gravel	15 %	55 %
Sand	44 %	84 %
Silt & Clay	1 %	2 %
Parameter	**Minimum**	**Maximum**
Porosity	23 %	37 %
Rainfall (mm)	878 (year 1991)	1220 (1992)

Table 6.1.b. General characteristics of the alluvium.

sediments to replenish the groundwater storage. The water table gradient in the area is towards the sea: The groundwater from the aquifer moves out into the sea; within the tidal zone the fresh groundwater is underlain by a body of saline water.

In glaciated regions, reports of studies in Illinois (Buhle and Brueckman, 1964; Foster and Buhle, 1951, McGinnis and Kempton, 1961), Missouri (Frohlich, 1973; Frohlich, 1974; Meidav, 1960), and Rhode Island (Allen et al., 1963) indicate some of the difficulties encountered in glacial materials. For example Liesch (1969) noted, based on work in Minnesota, that

" Aquifers in glacial deposits are characteristically lenticular, sinuous and discontinuous. Past experience has demonstrated that the assumption cannot be made that a well drilled in the vicinity of a successful producing well in such aquifers will be equally successful." We might therefore expect that the aquifer at College Farm is laterally inhomogeneous.

6.2 Detection/Mapping of the saline-fresh water interface using Geophysical Methods and Hydrochemistry

Thirty-four vertical electric soundings were made at selected sites (Figure 6.1) with the ABEM Terrameter resistivity meter. Simple Wenner and Offset Wenner arrays were used for this study. Soundings were made up to maximum electrode spacings ranging from 40 m to 80 m for the simple Wenner array and 32 m to 64 m for the Offset Wenner array. Physical obstructions such as metal fences which divides the whole farm area into smaller units, made it impossible to utilize large electrode spacings.

Sixteen electromagnetic soundings were also made at the selected centres of the sites where previously vertical electric soundings were made (Fig. 6.1), using MaxMin I-8 portable equipment. Suitable survey sites are limited compared to the vertical electric soundings because of: buried gas pipelines, railroad tracks, and mostly the metal fences which cause erroneous readings.

Nearby wells often provide additional subsurface information (such as layer thickness and nature of material). To imitate such information, the thicknesses of some layers individually and combinedly can be fixed in inversion and the remaining parameters determined. Parameter-resolution improvement has previously been observed using this technique (Sandberg and Jagel, 1988).

As all necessary precautions were taken while laying out any line for measuring a vertical electric sounding, whether for Simple Wenner array or Offset Wenner array, the calculated maximum error comes out to be ± 2.2 % for the Simple Wenner (using Equation 3.1a); and for the Offset array worked out to be ± 1.55 % (using Equation 3.3). The observational error due to EM loop spacing worked out to be ±3 %. The magnitude of these errors seem to produce insignificant effect on the results of the measurements.

Figure 6.2a shows an example of a comparision of field data to a mathematically fitted curve at site 10B. Lithologic information from an adjacent borehole 10/2 was used to constrain the layer thickness in the VES interpretation. First the 3rd layer consisting of sand and gravel (being the upper aquifer) was found to be conductive and 5.2 meters thick. The higher resistive layers either side of layer 3 means that ambiguity of interpretation due to equivalence would be a problem unless there was some external control. It was found convenient to divide this layer into two on the basis of the

borehole log, providing a more complex seven layer model which was not resolved by the sounding curve. The inversion process then kept the known layer thickness constant whilst the other parameters were varied to produce a best fitting curve. To solve the S-equivalence problem the equivalence option of the program was utilised. This gave the best possible model along with the other close fitting models which are shown alongside the field curve (see Figure 6.2a). The details of the minimum and maximum bounds of the equivalence results obtained are listed in Appendix Table 6A. By this process the fit of the model curves to the VES data is improved considerably compared to direct inversion of the sounding data. Table 6.2 shows all the interpreted and adjusted results of all the soundings in the study area. Table 6.3 shows the comparision of the geological drill log in borehole 10/2 and the interpreted results of the VES and EM soundings done near the borehole at site 10B.

The complex model of seven layers thus obtained by using vertical electric sounding at the same site was then fed into the computer software EMIX-MM programme for further inversion calculations. As the curve model was found to be producing equivalence, and moreover to solve the S-equivalence problem , the EMIX-MM equivalence program was also started which gave a model in good agreement with the VES model with the minimum percentage of fitting error (Figure 6.2b). The equivalence models are given alongside the Figure 6.2b. And the details of the minimum and the maximum bounds of the equivalence results given in Appendix Table 6B.

Appendix Figures 6C, 6D, 6E, and 6F (see appendices) are more examples of the comparision of field data to mathematically-fitted curves and these have also been interpreted by adjustments and making use of the borehole data obtained in the vicinity

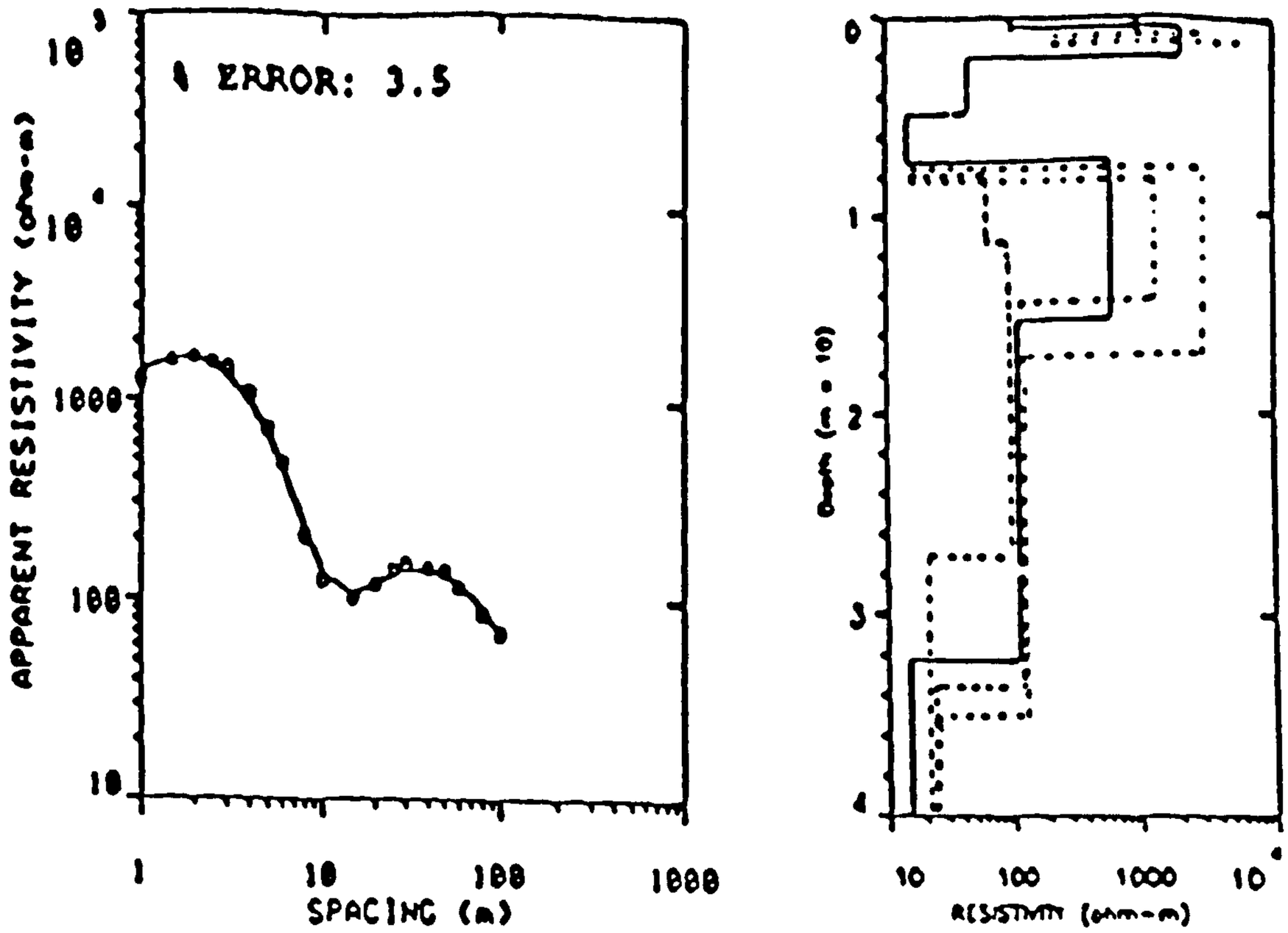

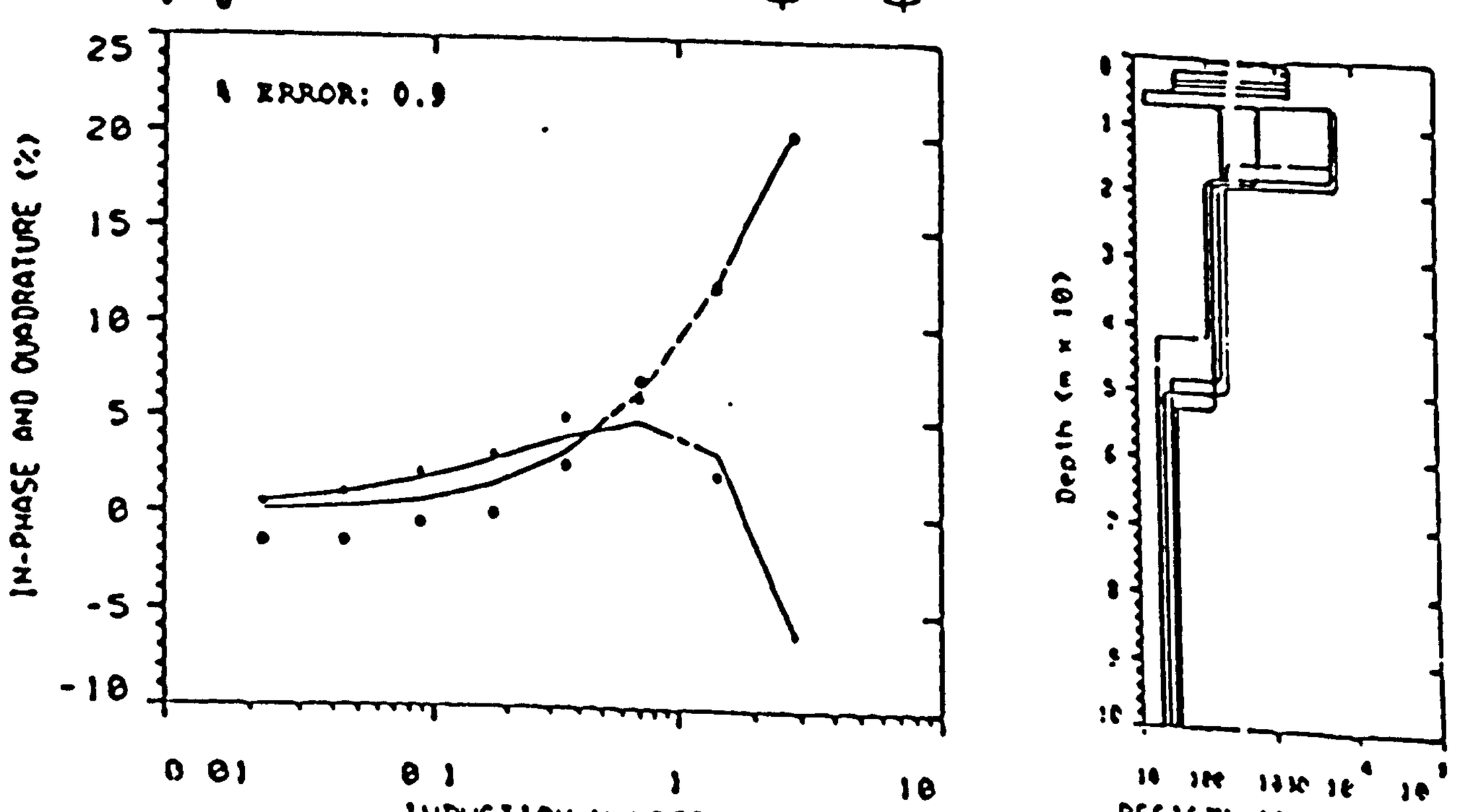

Fig. 6.2. Vertical electric sounding curve (a) and electromagnetic sounding curve (b) at site 10B based on field data points.

Stn	L1		L2		L3		L4		L5		L6		L7
	Ω.m	m	Ω.m	m	Ω.m	m	Ω.m	m	Ω.m	m	Ω.m	m	Ω.m
10A'	2.6	0.4	15	0.4	267	12.8	89	8.9	1	-	-	-	-
10A	400	1	56	0.4	14	1	209	18	102	20.5	11	-	-
10B	100	0.5	2090	1.5	45	2.8	15	2.4	614	8	111	17	15
BH10/1	100	0.5	1248	1.5	54	2.8	31	2.4	364	9	112	16	25
10BC	14	0.8	160	4.3	286	11.3	141	11	31	-	-	-	-
10C	24	0.5	157	2.3	98	4.2	247	10	148	26	31	-	-
3A	1851	1.7	109	1.6	34	0.5	317	7	99	7.7	21	-	-
3B	509	1.1	119	1	41	0.7	462	6.9	94	9.7	33	-	-
3C	207	0.7	111	1.3	419	3.6	145	24.3	46	-	-	-	-
7A	550	0.5	1614	1.7	139	1.7	301	8	118	17.9	61	-	-
1A	218	0.9	270	12.5	156	19	35	-	-	-	-	-	-
1B	117	0.1	795	2.4	236	15	169	12	69	-	-	-	-
8B	100	2	164	1.3	280	7.8	86	19.7	35	-	-	-	-
8C	120	0.2	1219	0.4	124	1.6	277	7.3	88	22.5	35	-	-
8D	260	0.3	349	1	57	3	282	9.3	117	21	60	-	-
11A'	2457	0.2	5056	0.8	164	23	30	-	-	-	-	-	-
11A	2011	0.7	335	3.4	161	36.6	33	-	-	-	-	-	-
11B	208	0.9	89	1.5	475	4.4	140	39.3	33	-	-	-	-
11C	588	1.5	142	1.5	524	4.3	140	38.8	76	-	-	-	-
2A	1276	0.4	594	0.4	1530	8	117	-	-	-	-	-	-
2B	1109	0.3	546	0.8	2010	3.7	548	12	60	-	-	-	-
4A'	2.8	0.9	24	0.9	309	11.5	107	10.2	1	-	-	-	-
4A	175	0.4	904	1.4	160	1	35	0.3	407	5	126	16.5	18
4B	448	0.3	8220	0.8	151	2.1	62	0.5	524	4.9	155	14.6	37
4F	151	0.5	219	0.3	140	0.6	837	5.1	120	23.4	44	-	-
4C	1024	0.6	203	0.7	2106	1.9	172	26.1	47	-	-	-	-
4D	160	0.7	50	3.7	2726	1.4	90	21.6	44	-	-	-	-
4E	160	1	788	4.6	141	8.2	217	5	135	13	44	-	-
5A'	3	0.2	31	2.4	443	11.4	83	13	1	-	-	-	-
5A	100	0.5	270	0.4	38	3	121	36	19	-	-	-	-
5B	67	0.3	31	4.4	130	37.9	19	-	-	-	-	-	-
5C	34	0.7	54	10	125	35	41	-	-	-	-	-	-
6A	47	0.7	32	6.8	117	22	52	-	-	-	-	-	-
6B	67	0.4	33	9	149	15.7	52	-	-	-	-	-	-

Table 6.2. Multilayer Sounding Results.

Stn = Station, L1 = Layer Number,

Ω.m = Resistivity, m = Thickness.

La-yer Nu-mber	VES Sounding Resisti-vity in ohm.m	VES Sounding Thickne-ss in (m)	EM Sounding Resisti-vity in ohm.m	EM Sounding Thickne-ss in - (m)	Geological Drill Log
1	100	0.5	101	0.5	Silty and clayey soil with fine sand & gravel (1m depth).
2	2090	1.5	1593	1.5	Coarse sand and gravel (1.9 m - depth).
3	45	2.8	40	2.8	Thin lenses of peat & clay.Sandy silt with gravel saturated with water (4.6m - depth).
4	15	2.4	15	2.4	Sandy silt with gravel saturated with contaminated water (depth 7m). E.o.h.
5	614	8	550	10	Boulders,gr-avel,sand & mud admixture (correlated data)
6	111	17	126	15.5	Gravel & sand saturated with water (correalated data)
7	15	-	20	-	Gravel & sand saturated with contaminated water (correlated data)

Table 6.3. Vertical electric and electromagnetic soundings data 10B with geologic log near borehole 10/2, Aber college farm.

of these soundings.

The construction of geoelectric sections is an intermediate stage in the preparation of various contour and isopach maps. A geoelectric section A-A′ drawn perpendicular to the coast and across various sites of VES and EM soundings as well as borehole sites BH10/1 and BH10/2D in the area (map Figure 6.1) is shown in Figure 6.7. The interpreted results of soundings is given in Table 6.2., and the comparision of the geological drill logs and the interpreted results of the soundings near boreholes is given in Tables 6.3 & 6.4. Arrows at the top of the cross section show VES or VES & EM combined sounding locations. From correlation with nearby commercial borehole logs to the North-East, the geoelectric section A-A′ shows that there are two aquifers in the area, an upper aquifer and a lower aquifer, separated by impervious glacial till with resistivities ranging from 209 ohm.m to 614 ohm.m. In the upper and lower aquifers a change in the salinity is easily detected through observation of the change in the bulk resistivity of the aquifers. Variations in the surface layer resistivity (4.6 ohm.m) along the coast indicate that the sediments are saturated with saline water through to mixing zone sediments caused by wave and tidal action. The gradual increase of resistivities inland in the upper aquifer from 15 ohm.m to 157 ohm.m and in the lower aquifer from 89 ohm.m (with 1 ohm.m below it) to 148 ohm.m (with 31 ohm.m below it) relates to a gradual inland decrease in the concentration of dissolved solids in the groundwater. In the upper aquifer the mixing zone is separated from fresh water by the bulk resistivity range from 31 ohm.m (inland) to the 15 ohm.m (coast) with chlorides ranging from 250 ppm to much higher values. In the lower aquifer, the mixing zone is shown in the figure separated by a dotted line with bulk resistivities range from 31 ohm.m (inland) to 8 ohm.m (coast) with chlorides between 250-500 ppm. The saline water in the lower aquifer is shown with bulk resistivities between 1

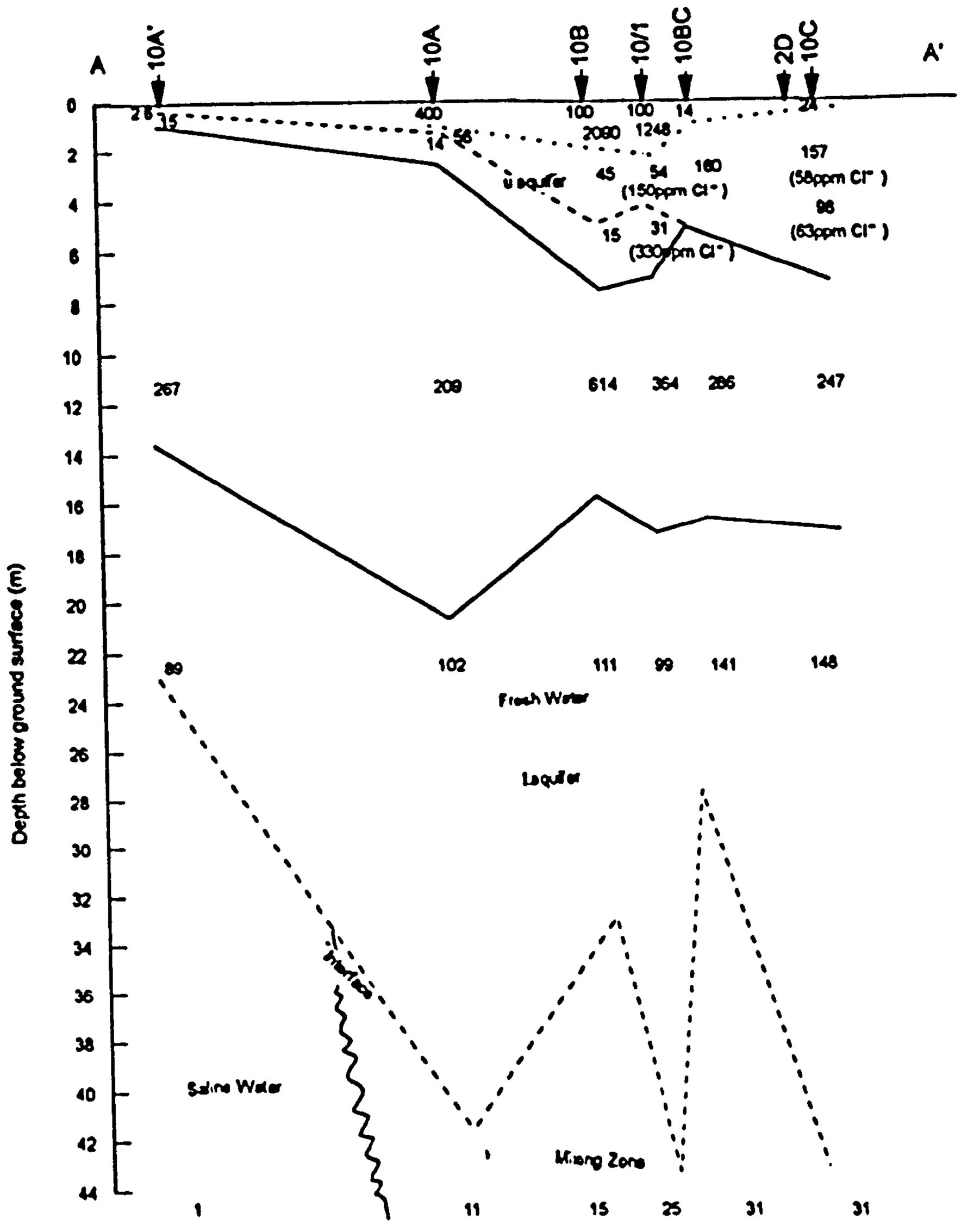

Fig. 6.7. Geoelectric section A-A' derived from vertical electric and electromagnetic soundings.
Resistivities in ohm-m.
Scale: Hor: 1:1000, Vert: 1:200.

Layer Number	VES Sounding Resistivity in ohm.m	VES Sounding Thickness in (m)	VES Sounding (Depth-in m)	Geological Drill Log
1	24	0.5	0.5	Laminated silty clay with fine sand
2	157	2.3	2.8	Fine sand with gravel & cobbles.
3	98	4.2	7	Sand & gravel(with-water).E.o.h.
4	247	10	17	Boulders, gravel,sand & mud admixture (correlated-data)
5	148	26	43	Sand & gravel (with water) correlated-data.
6	31	-	-	Sand & gravel(with-contaminated water) correlated-data.

Table 6.4. Vertical electric and electromagnetic soundings interpreted data 10C with geologic log near bore hole 10/2D, Aber college farm.

ohm.m (coast) to less than 11 ohm.m (up to 7 ohm.m) inland with chlorides more than 500 ppm.

A second geoelectric section B-B′ Figure 6.8, drawn across various sites of VES or VES & EM combined soundings and a borehole location is shown in area map Figure 6.1. Arrows at the top of the cross section show VES or VES & EM combined sounding locations. Appendix Figure 6C shows an example of a comparision of field data to a mathematically fitted curve at site 3C. The interpreted results of the soundings is given in Table 6.2, and the comparision of the geological drill log and the interpreted results of the soundings near the borehole given in Table 6.5. As in A-A′ the geoelectric section B-B′ shows that there are two aquifers, an upper aquifer and a lower aquifer separated by an impervious layer of glacial till with bulk resistivities ranging from 301 ohm.m to 467 ohm.m. The upper aquifer has a small mixing zone with bulk resistivity of 34 ohm.m and chlorides about 250 ppm. The bulk resistivities in the upper aquifer increase inland from 109 ohm.m to 139 ohm.m. The lower aquifer has a mixing zone with bulk resistivities ranging from 21 ohm.m (coast) to 33 ohm.m (inland) with chlorides more than 250 ppm. Bulk resistivities of the lower aquifer increase from 99 ohm.m (with 21 ohm.m below it) to 118 ohm.m (with 61 ohm.m below it) which relates to a gradual decrease in the concentration of dissolved solids in the groundwater inland.

A third geoelectric section C-C′ Figure 6.9, parallel to the coast line is drawn across the Aber River (see area map Figure 6.1). Appendix Figure 6D shows an example of a comparision of field data to a mathematically fitted curve at site 2B. The interpreted results of the soundings are given in Table 6.2. This cross section shows two aquifers the upper one and the lower aquifer separated again by impervious glacial

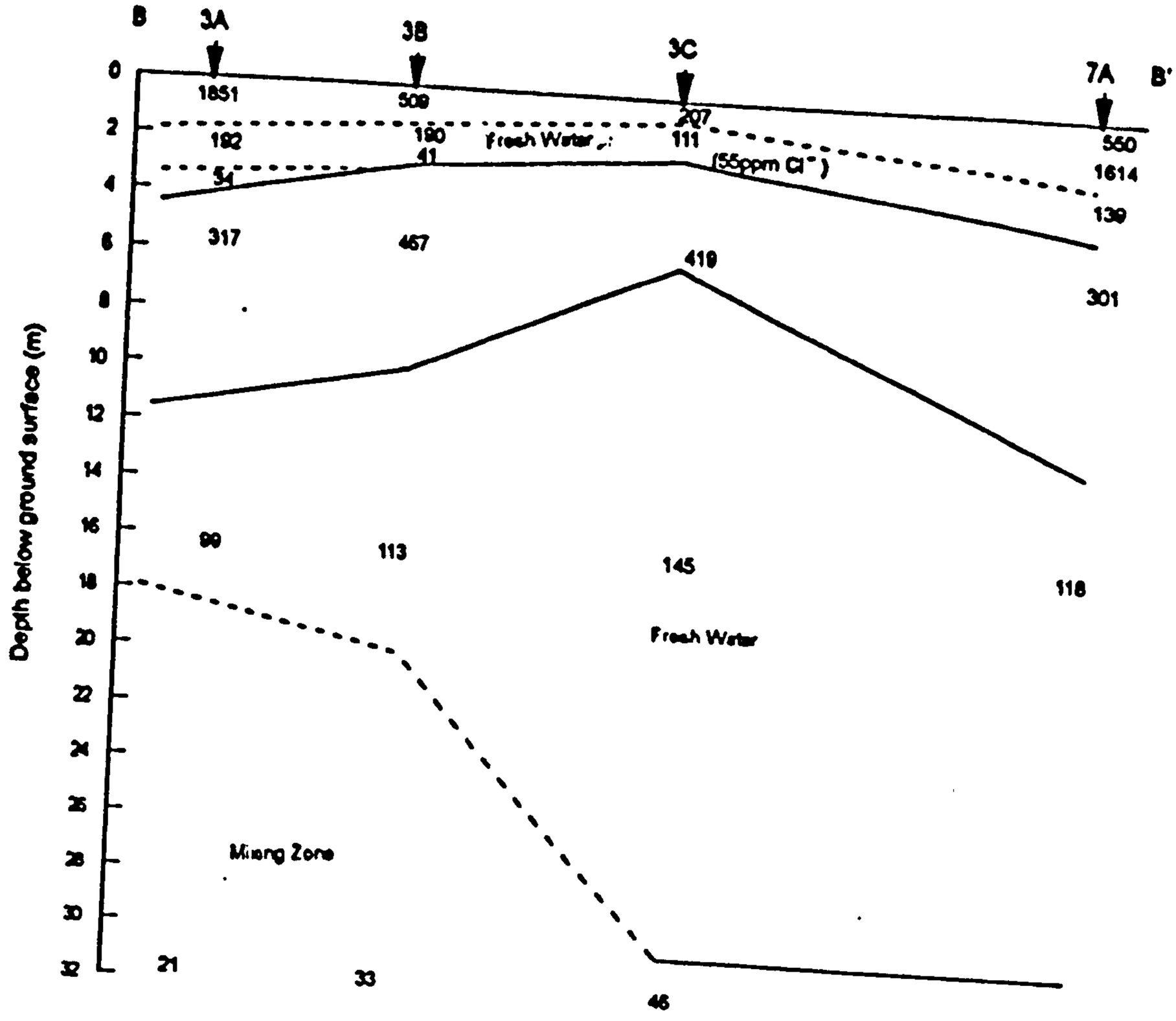

Fig 6 8. Geoelectric section B-B' derived from vertical electric and electromagnetic soundings.
Resistivities in ohm-m.
Scale: Hor: 1:1000, Vert: 1:200.

Layer Number	VES Sounding Resistivity in ohm.m	VES Sounding Thickness in (m)	EM Sounding Resistivity in ohm.m	EM Sounding Thickness in (m)	Geological Drill Log
1	207	0.7	210	0.6	Sandy silty soil with gravel
2	111	1.3	114	1.3	Fine sand with silt (with-water).W.T at 0.8m & E.o.h 3.2m.
3	419	3.6	409	3.6	Boulders,sand gravel & mud admixture(correlated data).
4	145	24.3	138	22.4	Sand & gravel with water (correlated data).
5	46	-	52	-	Gravel & sand with contaminated water (correlated data).

Table 6.5. Vertical electric and electromagnetic soundings interpreted data 3C with geologic log near bore hole 3C, Aber college farm.

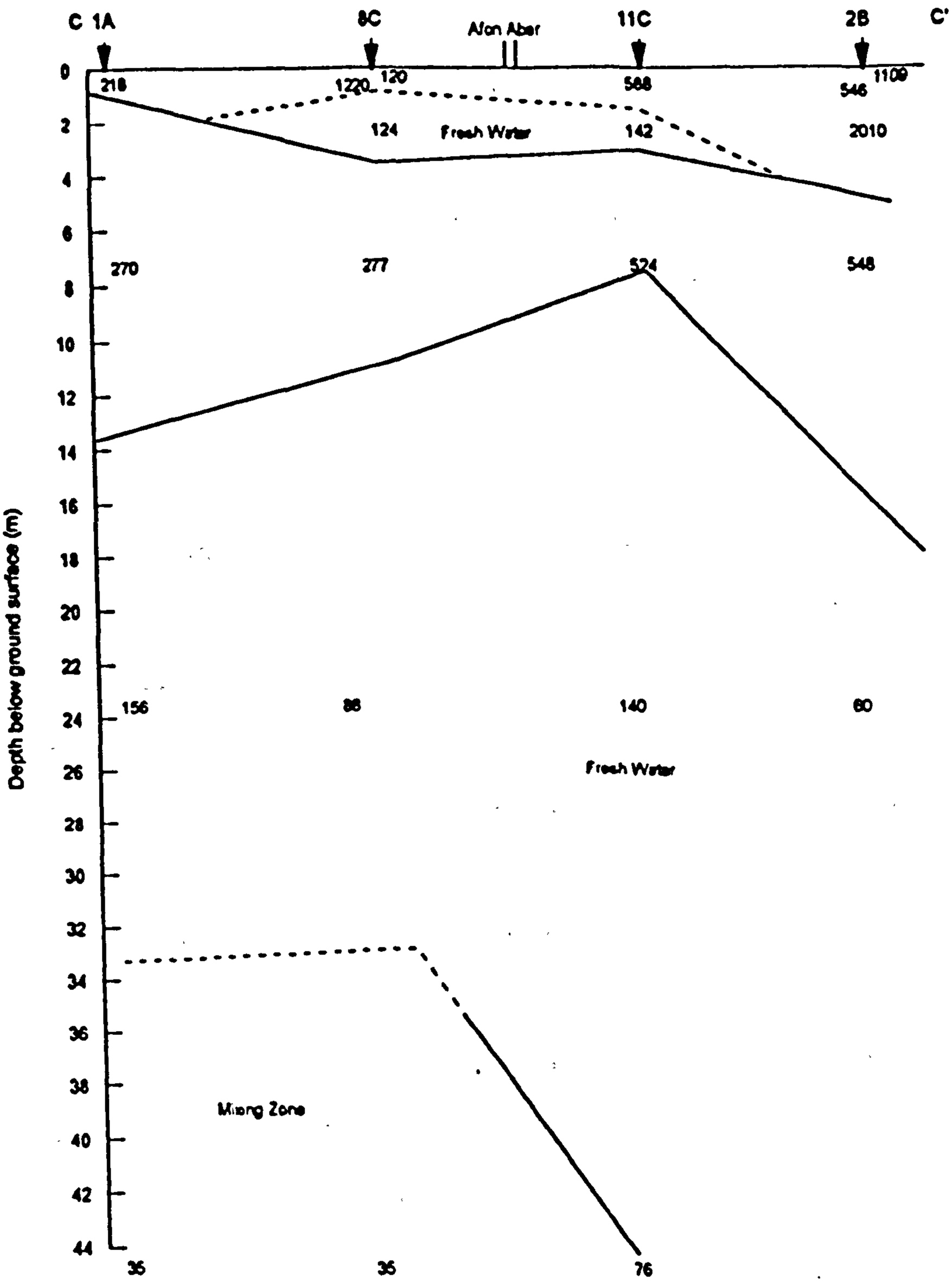

Fig. 6.9. Geoelectric section C-C' derived from vertical electric and electromagnetic soundings.
Resistivities in ohm-m.
Scale: Hor: 1:6666, Vert: 1:200.

till with a bulk resistivities ranging from 270 ohm.m to 548 ohm.m. The upper aquifer is saturated with fresh water with bulk resistivities from 124 ohm.m to 142 ohm.m and spread around the Aber river. The lower aquifer has the greatest thickness near the vicinity of the Aber river and such a thick aquifer is not encountered in any other part of this study area which suggests that the old channel course perhaps was in the north of the present course. The lower aquifer has a very small mixing zone with bulk resistivity 35 ohm.m and chlorides about 250 ppm; there is also an absence of saline water which suggests that presumably the inflow of more fresh water from the river prevented the saline intrusion from the sea.

A fourth geoelectric section D-D′ Figure 6.10, drawn perpendicular to the coast and across various sites of soundings and a borehole is shown in the area map Figure 6.1. Appendix Figure 6E shows an example of a comparision of field data to a mathematically fitted curve at site 4C. The interpreted results of soundings are given in Table 6.2., and a comparision between the geological drill log and the interpreted results of soundings is given in Table 6.6. In this cross section one of the two peculiar features is the abrupt omission of glacial till half way from the coast to inland along the section line. This omission of glacial till suggests that possibly this is because of the faulting in the region. The other peculiar feature is the presence of two aquifers upper and lower up to midway of the section separated by glacial till and then, due to the omission of glacial till there is a single aquifer inland. The variation in surface layer resistivity along the coast indicate sediments saturated with highly saline water through to mixing zone sediments. The mixing zone's bulk resistivities in the small area of the upper aquifer range from 24 ohm.m to 35 ohm.m. The main aquifer has bulk resistivities which range from 107 ohm.m (with 1 ohm.m below it) near the coast to 147 ohm.m (with 47 ohm.m below it) inland. The mixing zone in the main aquifer has

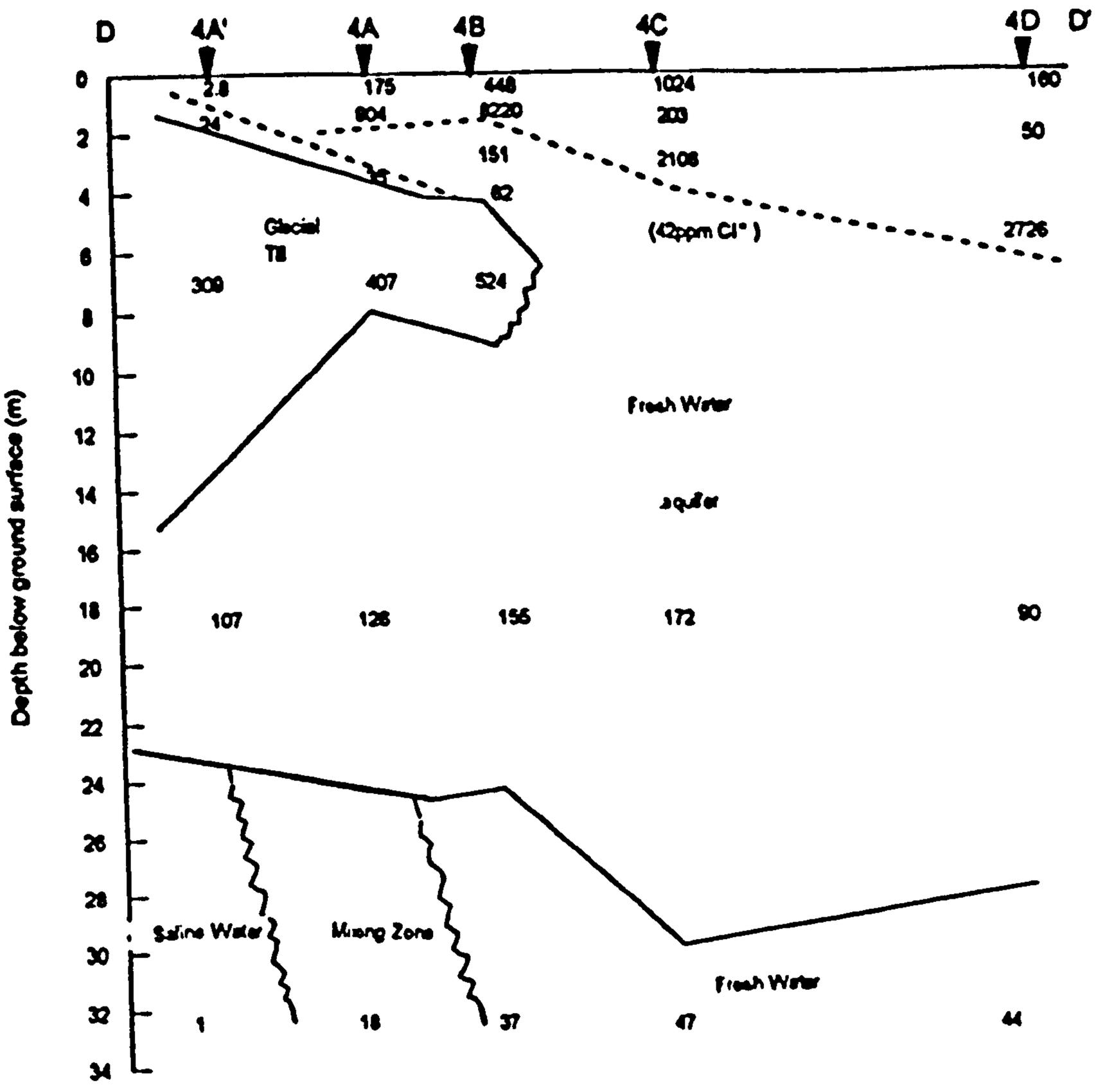

Fig 6.10. Geoelectric section D-D' derived from vertical electric and electromagnetic soundings.
Resistivities in ohm-m.
Scale: Hor: 1:750, Vert: 1:200.

Layer Number	VES Sounding Resistivity in ohm.m	VES Sounding Thickness in (m)	EM Sounding Resistivity in ohm.m	EM Sounding Thickness in (m)	Geological Drill Log
1	1024	0.6	771	0.8	Sandy silt soil with gravel.
2	203	0.7	986	0.4	Sand with some gravel
3	2106	1.9	3581	2.2	Coarse sand & gravel.
4	172	26.1	93	24.8	Sand & gravel. Water after 4.0m (E.o.h at 4.5m).
5	47	-	65	-	Sand & gravel with contaminated water (correlated data).

Table 6.6. Vertical electric and electromagnetic soundings interpreted data 4C with geologic log near bore hole 4C, Aber college farm.

bulk resistivities ranging from 8 ohm.m to 35 ohm.m with chlorides ranging from 250-500ppm. The saline water has bulk resistivities from 1 ohm.m to less than 18 ohm.m (up to 7 ohm.m) with chlorides more than 500 ppm.

A fifth and the final geoelectric section E-E′ Figure 6.11, is perpendicular to the coast line and crosses various soundings sites plus a borehole (see area map Figure 6.1). Appendix Figure 6F shows an example of a comparision of field data to a mathematically fitted curve at site 5B. The interpreted results of soundings given in Table 6.2., and a comparision of geological drill log and interpreted results of soundings is given in Table 6.7. In this cross section there are three peculiar features. The first feature is the presence of glacial till only up to the coast, with its omission further inland suggesting that as this part of the area is adjacent to geologic section D-D′, it possibly suffered due to the same faulting in the region. The second feature is the continued presence of clay as an upper layer saturated with water, thus forming an aquitard. Its presence is evident from the behaviour of bulk resistivities showing little or modest change throughout the layer; its presence is also confirmed by the geological drill log. The third feature is the presence of a single aquifer only with bulk resistivities ranging from 83 ohm.m to 149 ohm.m. It has a mixing zone at the bottom with bulk resistivities ranging from 8 ohm.m to 35 ohm.m with chlorides ranging from 250-500 ppm. The saline water has bulk resistivities ranging from 1 ohm.m to less than 19 ohm.m (up to 7 ohm.m) with chlorides more than 500 ppm.

The last stage of the detection of saline-fresh water interface is the construction of saline-fresh water interface contour maps in order to detect the extent to which saline water has intruded inland. All the geoelectric sections previously discussed have been used in the construction of these maps of the study area. The maps Figures 6.12 and

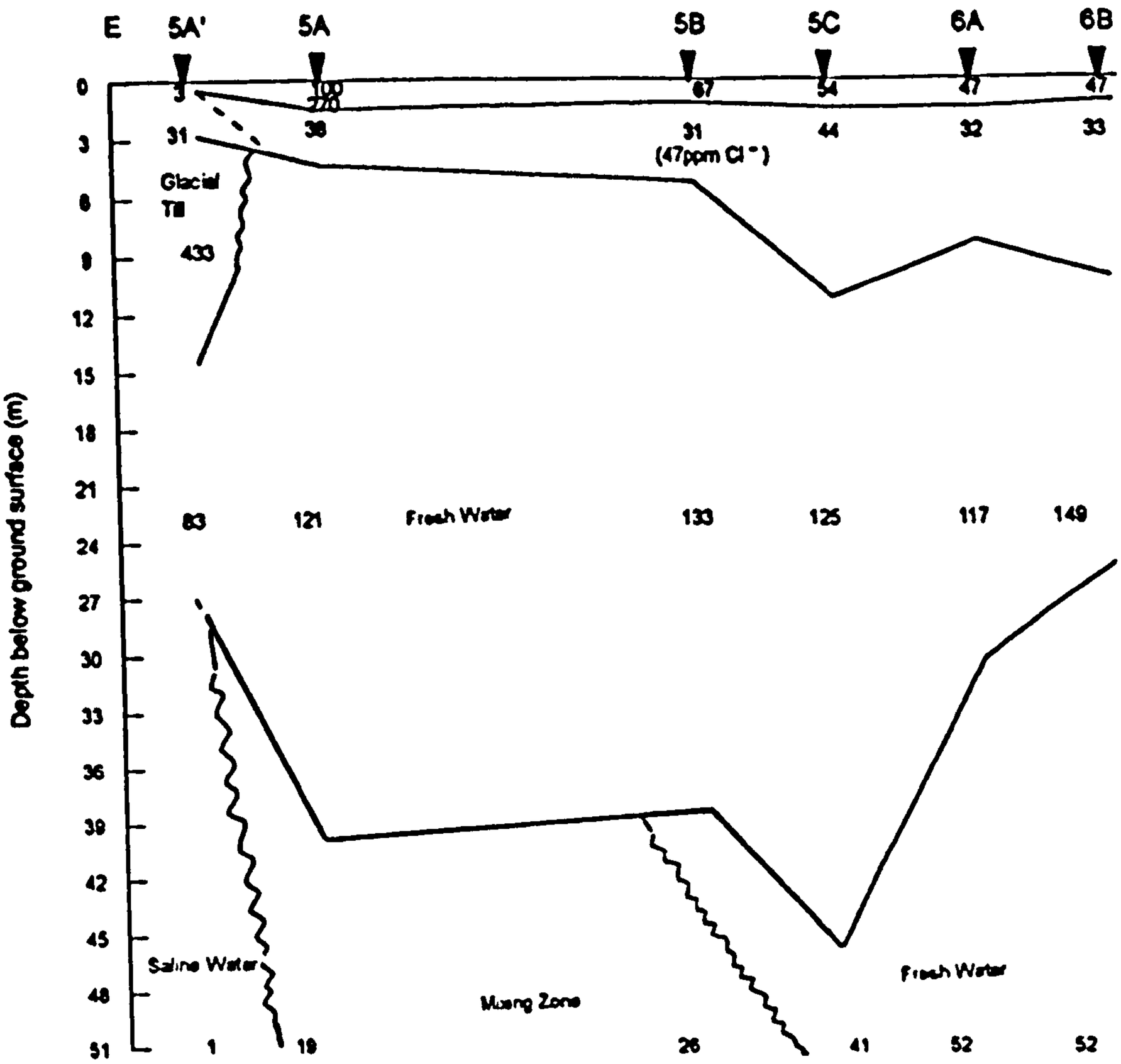

Fig 6.11. Geoelectric section E-E' derived from vertical electric and electromagnetic soundings.
Resistivities in ohm-m.
Scale: Hor: 1:1000, Vert: 1:300.

Layer Number	VES sounding Resistivity in ohm.m	VES Sounding Thickness in (m)	EM Sounding Resistivity in ohm.m	EM Sounding Thickness in (m)	Geological Drill Log
1	67	0.3	67	0.3	Silty sandy clay with pebbles.
2	31	4.4	31	4.4	Silty clay with water at 1.0m & E.o.h 3.5m.
3	130	37.9	116	36.3	Sand & gravel with water (correlated data).
4	19	-	29	-	Sand & gravel with contaminated water (correlated data).

Table 6.7. Vertical electric and electromagnetic soundings interpreted data 5B with geologic log near bore hole 5B, Aber college farm.

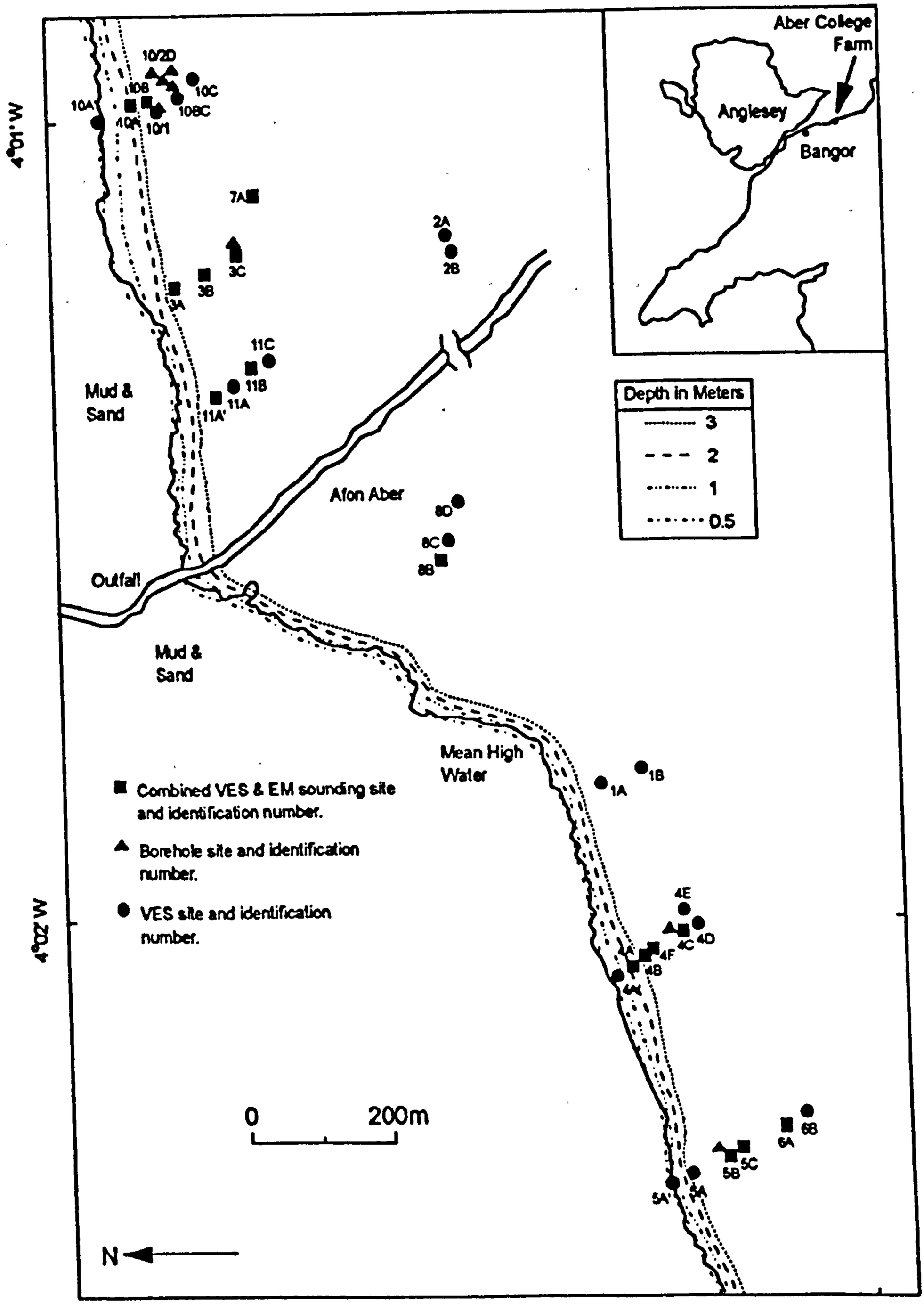

Fig. 6.12. Depth to a bulk resistivity of less than 35 ohm-meters (or more than 250ppm chloride concentration) Upper aquifer, Aber College Farm.

6.13 show the extent of the contamination zones with bulk resistivities less than 35 ohm.m and chlorides 250 - 500 ppm (for an approximation definition of these values see chapter 5). Contour map Figure 6.12 further shows that the contamination of fresh water with saline water in the upper aquifer appears to occur along a 100 m wide coastal strip. Near the coast it is found at a depth of 0.5 m, whereas inland it is found at a depth of 3m. Contour map Figure 6.13 shows that the contamination of fresh water with saline water in the lower aquifer is comparatively quite widespread and it appears to occur along a 300 m wide coastal strip. Near the coast it is found at a depth of 20 m, whereas deeper inland it is found at a depth of about 50 m. The saline groundwater is approximately defined by 7 ohm.m and chlorides more than 500 ppm (see chapter 5). Figure 6.14, is a contour map drawn showing the zone of saline water. Saline groundwater appears to occur along 100 m wide coastal strip. Near the coast line it is found at a depth of 22 m and inland at the greater depth of 34 m. The source of the saline water appears to be sea water. The wave and tidal mechanisms are thought to cause mixing of sea water with fresh water. However the heavy rainfall in the area which infiltrates underground prevents the sea water from deep penetration inland.

6.3 Effect of Spring Tides on Interface

Figure 6.15 A′-A has been drawn along geoelectric section line A-A′ and shows what the area looks like at high water spring tide , after taking into account the ground surface levelling at the site. The new section A′-A has also been extended towards the mean low water level. Mean high water (M.H.W.), sea level (S.L.), water table (W.T), upper aquifer, lower aquifer along with mixing zones (M.Z.) and fresh-saline water interface have also been shown in the section. The impervious glacial till layer has been shown to separate the two aquifers. It is evident from Figure 6.15 that the fresh water

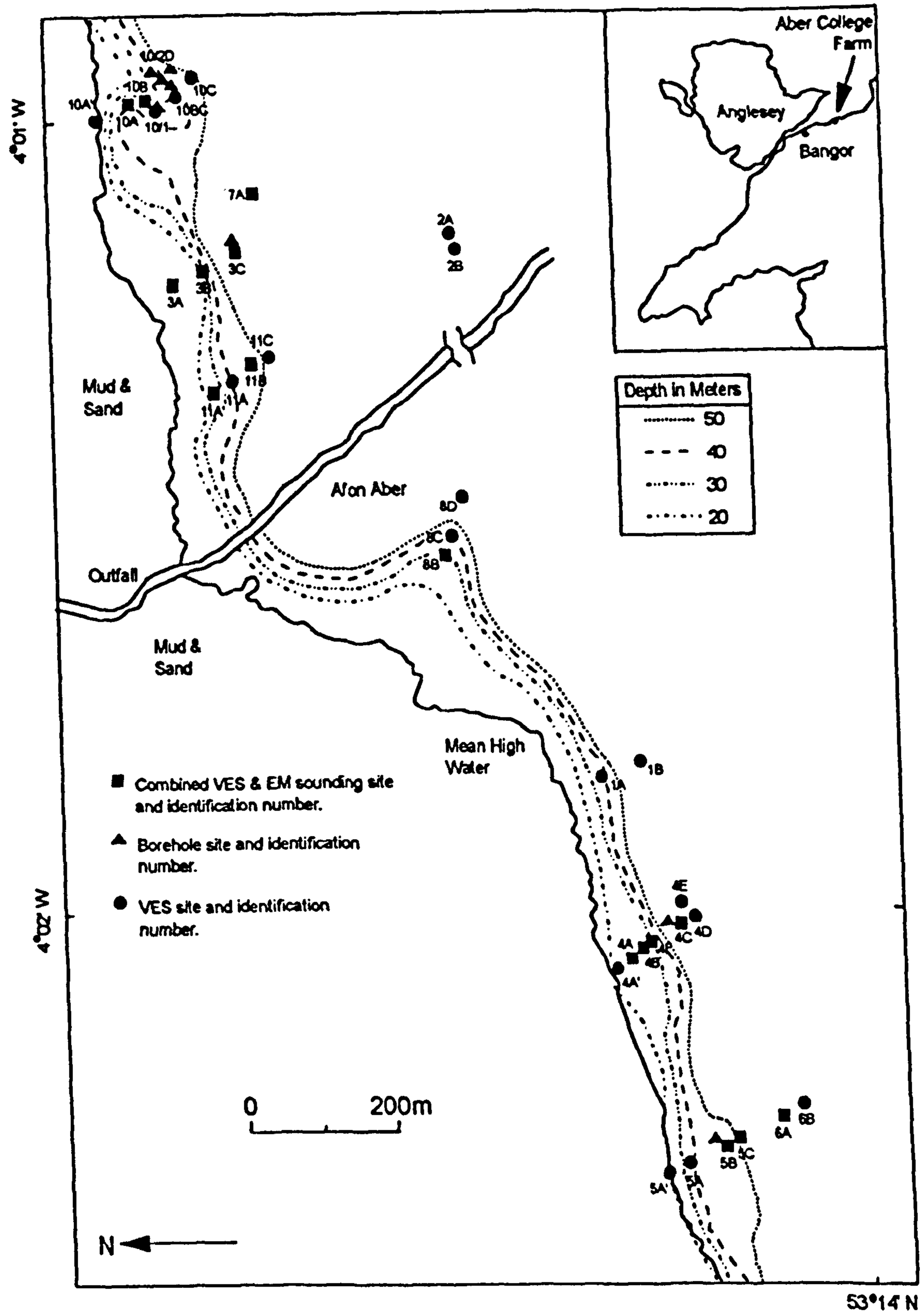

Fig. 6.13. Depth to a bulk resistivity of less than 35 ohm-meters (or more than 250ppm chloride concentration) Aber College Farm.

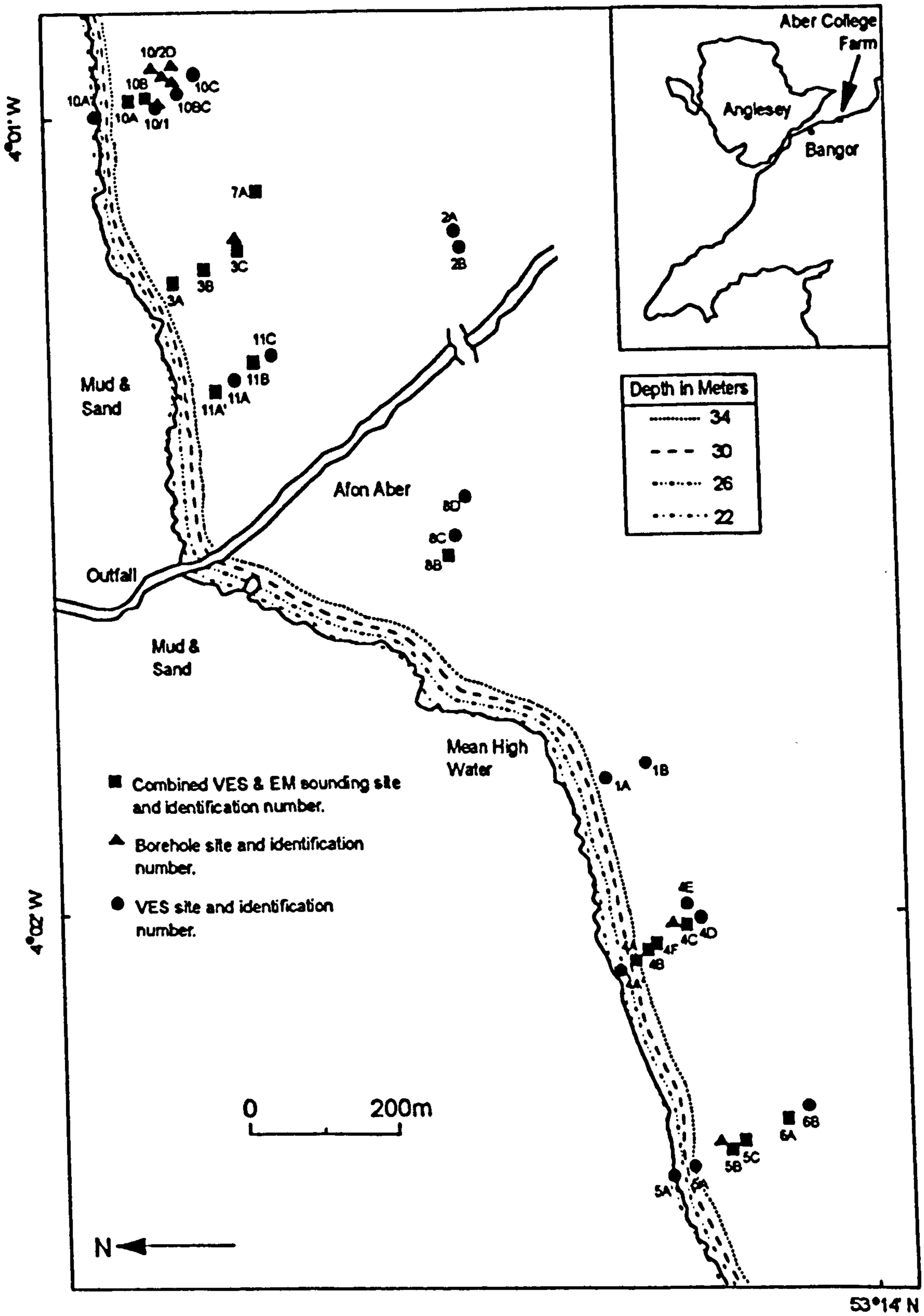

Fig. 6.14. Depth to a bulk resistivity of less than 7 ohm-meters (or more than 500ppm chloride concentration) Aber College Farm

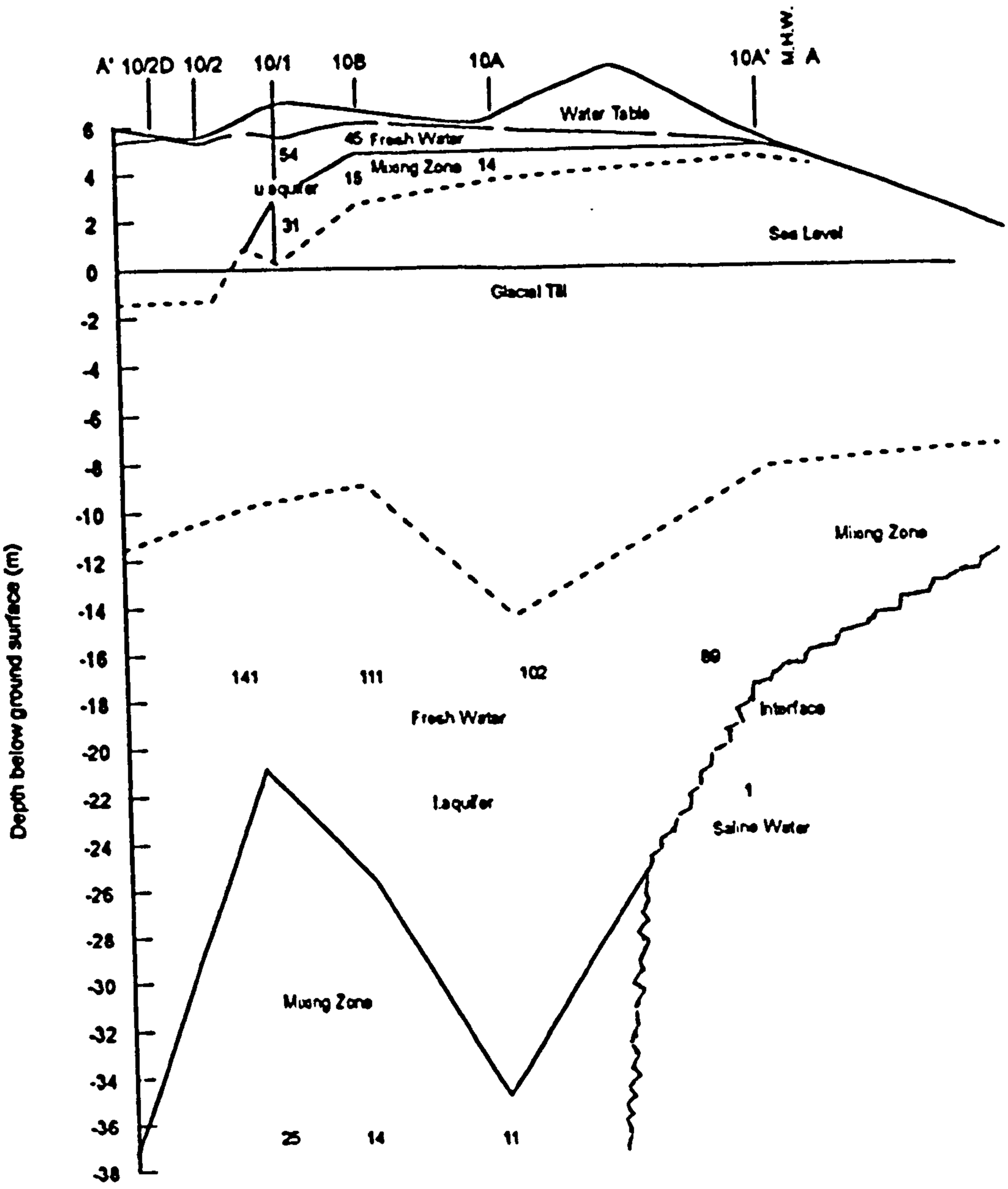

Fig 6.15. Saline and fresh water interface along line A-A'.
Scale: Hor: 1:1000, Vert: 1:200.

gradient is towards the sea. In the lower aquifer, the mixing zone separates fresh water from saline water. As the section has been extended further and interface represents in figure through broken-dotted line , it has been shown that how the picture of the area would look like towards the mean low water level such as beyond the limits of section A′-A.

To observe the actual effect of spring tide on the ground water level, a portable Water Level Recorder (Model IH89/103), Photograph Plate 6.1, was installed over the borehole 10/1 with an arrangement to record on a chart drum the effect of the spring tide on ground water level over a twenty-four hour period. Simultaneously it was also arranged to take water samples every hour from the depth of borehole starting at 0800 to 1600 hours; these were analysed in the laboratory and the results shown in Table 6.8. Figure 6.16. is a xeroxed copy of the recorded chart showing the tidal effect causing fluctuations in the ground water level for 24 hours. Subsequently a graph, Figure 6.17., was drawn taking into account the chart data and the actual ground water table rise and fall data recorded during day time high-tide cycle (Table 6.9).

The study of Figures 6.16 & 6.17 show that the maximum groundwater level does not reach the spring tide maximum (at 11.58 hours) simultaneous with it: there is a time lag of about one quarter of an hour. Further the water level remains high for about an hour and then falls rapidly to the original level. Overall it takes three and half hours from rise to fall of water level due to the tidal effect. It further appears that the low spring tide has no effect on water level. Herzberg (1901) recognized rise and fall of water levels due to tidal effects and further found that the response lagged three to four hours behind the tide.

Photographic Plate 6.1 Showing portable Water Level Recorder at work over a borehole.

Time (Hours)	Salinity (Cl^- ppm)
8.o	325
9.0	327
10.0	326
11.0	330
12.0	351
13.0	355
14.0	355
15.0	347
16.0	334

Table 6.8. Summary of salinity change in ground water due to the tidal effect.

Time (hours)	Rise of Water Table (m) (Tidal Effect)
8.00	.01
9.00	.01
10.15	.005
11.00	.235
12.00	.385
12.25	.39
12.75	.39
13.00	.31
13.45	.01
15.00	.01

Table 6.9. Summary of rise and fall of water level due to the tidal effect.

WATER LEVEL GAUGE RECORD

Aber College Farm (B.H. 10/1) RIVER

Figure 6.16

AT

DATE 26.9.92 to 27.9.92 (10.05 pm to 15.45 pm)

27.9.92

L.W. - 7.42 a.m. = 1.08 m depth ground surface.

H.W. - 12.35 pm = 0.69 m depth " "

High Tide on 27.9.92 @ 11.58 a.m. (10.0m)

High Tide on 26.9.92 @ 11.34 pm (10.1m)

26.9.92

L.W. @ 5.45 pm = 1.10 m depth.

Figure 6.16

Low Tide 27.9.92 (6.32 a.m.)

Low Tide 26.9.92 (17.59)

Out

In

(26.9.92)

HRS 1 2 3 4 5 6 7 8 9 10 11 12 13 14 15 16 17 18 19 20 21 22 23HOL 24

TER LEVEL SCALE IN FEET

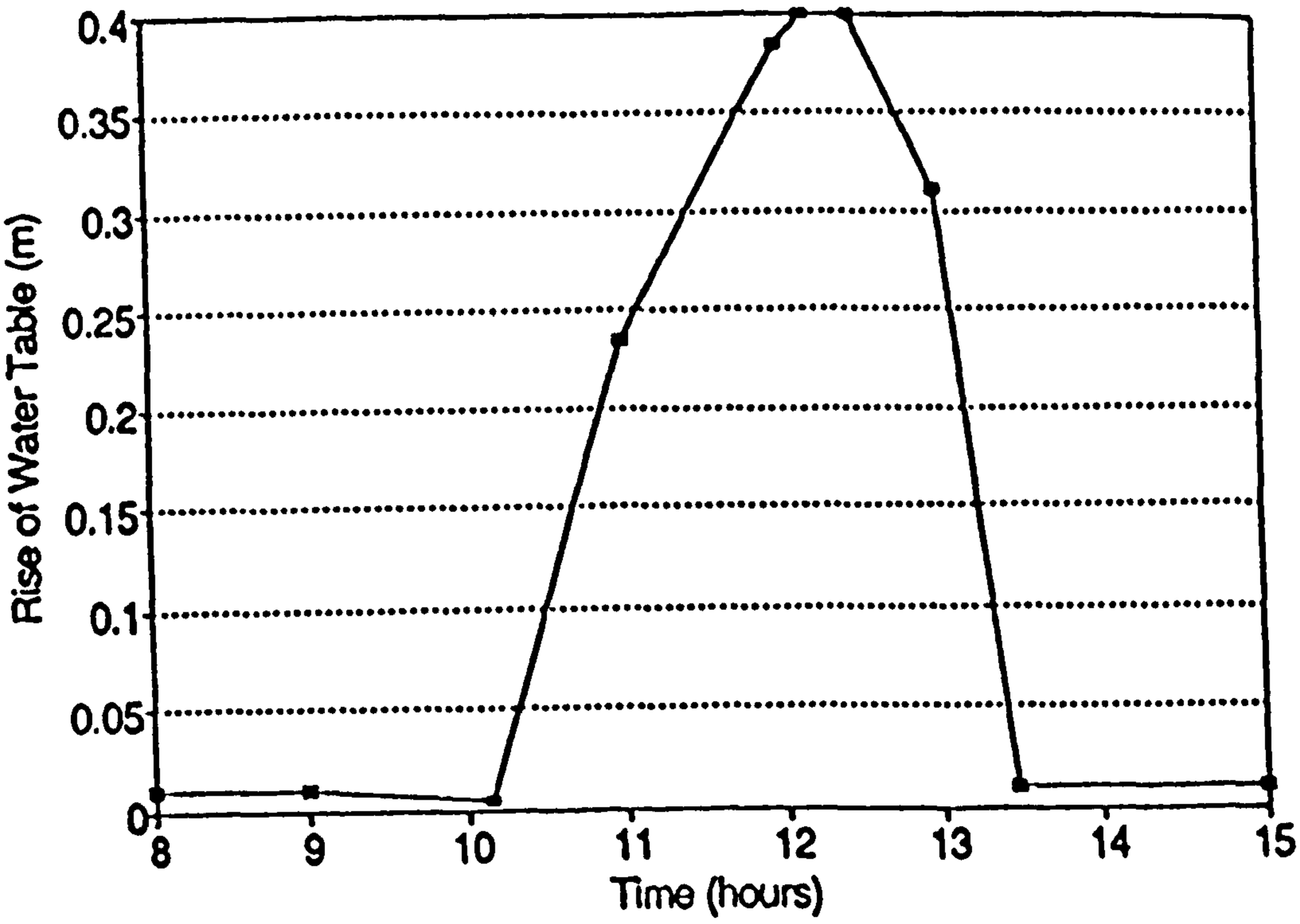

Figure 6.17 Graph showing rise and fall of groundwater level due to the tidal effect.

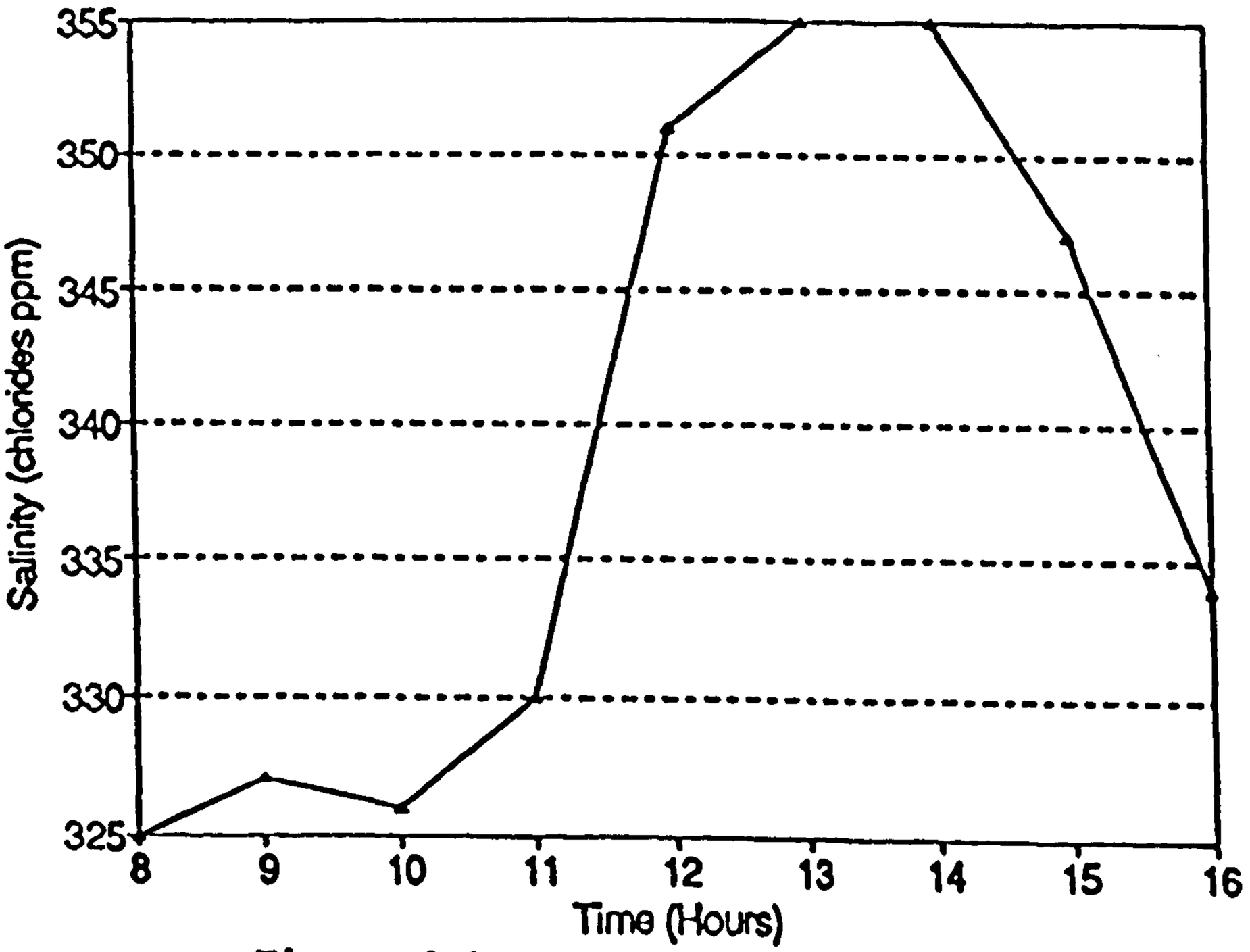

Figure 6.18 Graph showing a salinity change in groundwater every hour due to the tidal effect.

A comparision between rise and fall of water level shown on Figure 6.17. with salinity change in ground water is shown on Figure 6.18. It is evident that the salinity (Cl^- 325 ppm) of ground water becomes greater with the high tide but returns to the original state with a considerable time lag as compared to the rise and fall of water level. For instance when water level reaches its peak high value at 12.15 hours, the salinity is still short of its high concentration value (Cl^- 355 ppm), when the level starts falling; at 13.00 hours salinity appears to reach its peak value. When the water level reaches its original low level at 13.45 hours, salinity appears to still remain at its peak value. It further seems that it would have to take another hour for salinity to reach its original state.

The results show that the effect of rise and fall of spring tide on the water table is almost simultaneous but on the salinity there is a greater time lag, salinity almost taking double the time from rise to fall to its original state as compared to the effect on the ground water levels.

A final test was carried out using a geophysical method to assess the tidal effect on the ground water level and saline-fresh water interface. Five vertical electric soundings using a simple Wenner array with spacing up to 80 m, were made near the site of borehole 10/1 on the day of a spring tide maximum. These soundings were measured at a interval of one hour, such as sounding 10/1 S_1 closed at 10.30 hours, 10/1 S_2 closed at 11.30 hours, 10/1 S_3 at 12.30 hours, 10/1 S_4 at 13.30 hours and 10/1 S_5 at 14.30 hours. Spring high tide was at 11.58 hours.

It is evident from the interpreted results of VES soundings, Table 6.10, that resistivities/thicknesses of upper aquifer (fresh water and mixing zone) show a trend

* Resistivity
** Thickness

VES10/1 S_1 Time 10.30 hours	VES10/1 S_2 Time 11.30 hours	VES10/1 S_3 Time 12.30 hours	VES10/1S_4 Time 13.30 hours	VES10/1S_5 Time 14.30 hours
* Ω.m. ** m	* Ω.m. ** m	* Ω.m. ** m	* Ω.m. ** m	* Ω.m. ** m
1267- 2.4	1495- 2.2	1742- 2.1	1245-2.4	1098-2.5
59- 1.5	78- 1.8	91- 2	57- 2.1	55- 1.8
31- 2.8	34- 2.8	25- 2.9	30- 2.6	32- 2.6
364- 9.9	230- 9.9	438- 9.9	286- 10	230- 10
113- 26.2	168- 26.4	132- 26.2	165-26.1	181-26.3
48-	57-	18-	41-	51-

Table 6.10. Summary of change in Resistivities/ Thicknesses of different layers due to fluctuations in water level caused by tidal effect.

of rise and fall around the timings of rise and fall of ground water level due to the tidal effect.

Figure 6.20, showing models based on the interpreted five soundings, gives a clear comparative picture of fluctuations of resistivity / thickness of both aquifers with the change in ground water level. Sounding model 10/1 S_3, made at closing time 12.30 hours, shows nearly an agreement with the peak water level which was at 12.15 hours (see Figure 6.17). Total thickness of upper aquifer (fresh water and mixing zone) Table 6.10 clearly shows fluctuations with the change of water level and it also tallies with changes in high water level. The bulk resistivity of lower layer (mixing zone) which also fluctuate every hour and reaches 18 ohm.m its lowest value at 12.30 hours, further agrees with the change of saline intrusion because of tides. Thus this test confirms that tides do affect the saline-fresh water interface and geophysical methods provide a suitable tool to obtain information about any changes in the development or alteration of an interface with time.

6.4 Effect on Interface due to the Pumping

Pumping tests were carried out at the Aber college farm site using a discharging well and four piezometers which were installed for this purpose (see chapter 4). The screen of the pumped well was installed over the three metres of the water bearing layer (upper aquifer) and piezometers at distances of 2.4, 4.94, 9.95, and 20.4 metres with a depth of about 7 metres.

For a pumping test the following assumptions and conditions should be satisfied:

(i) The aquifer is confined.

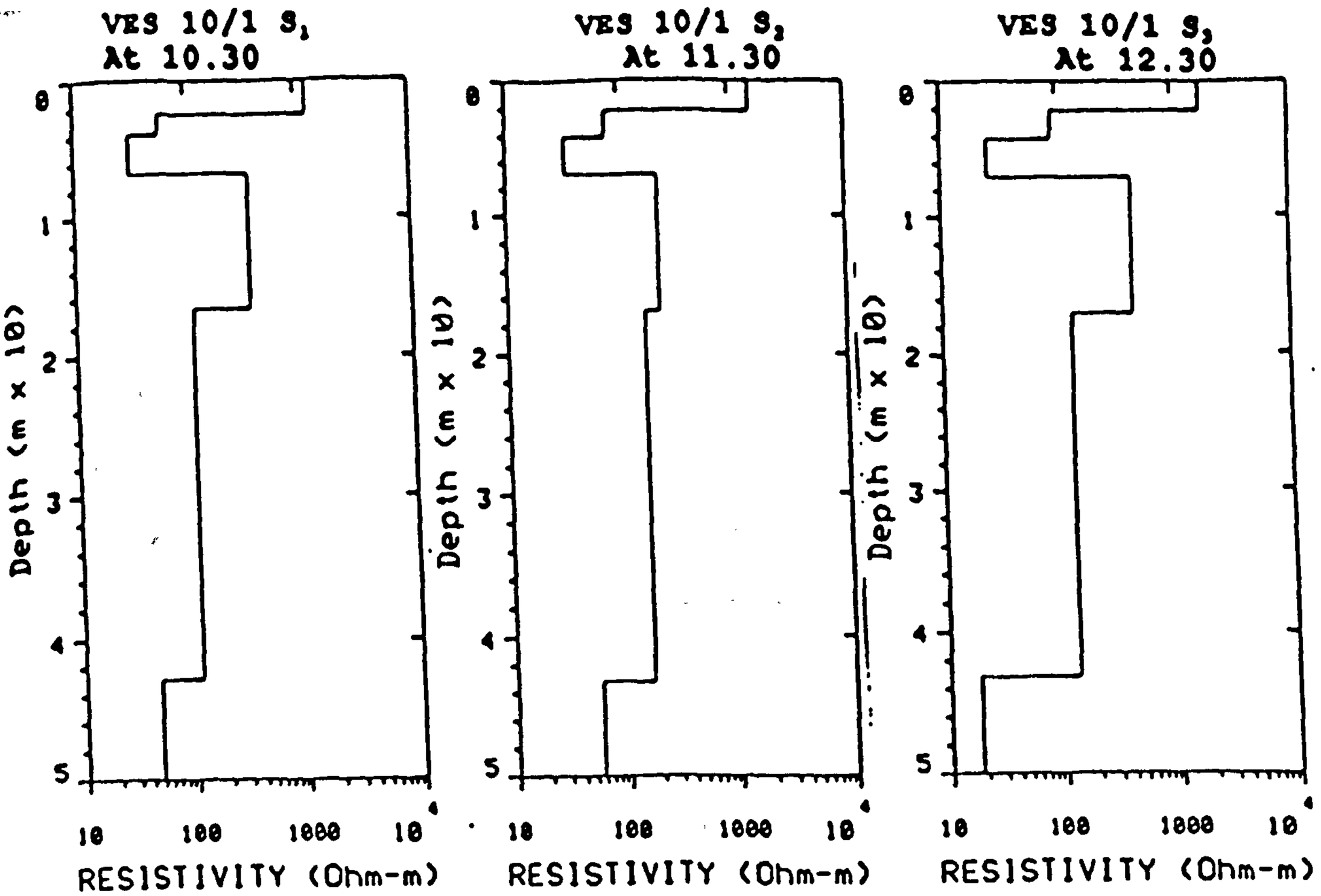

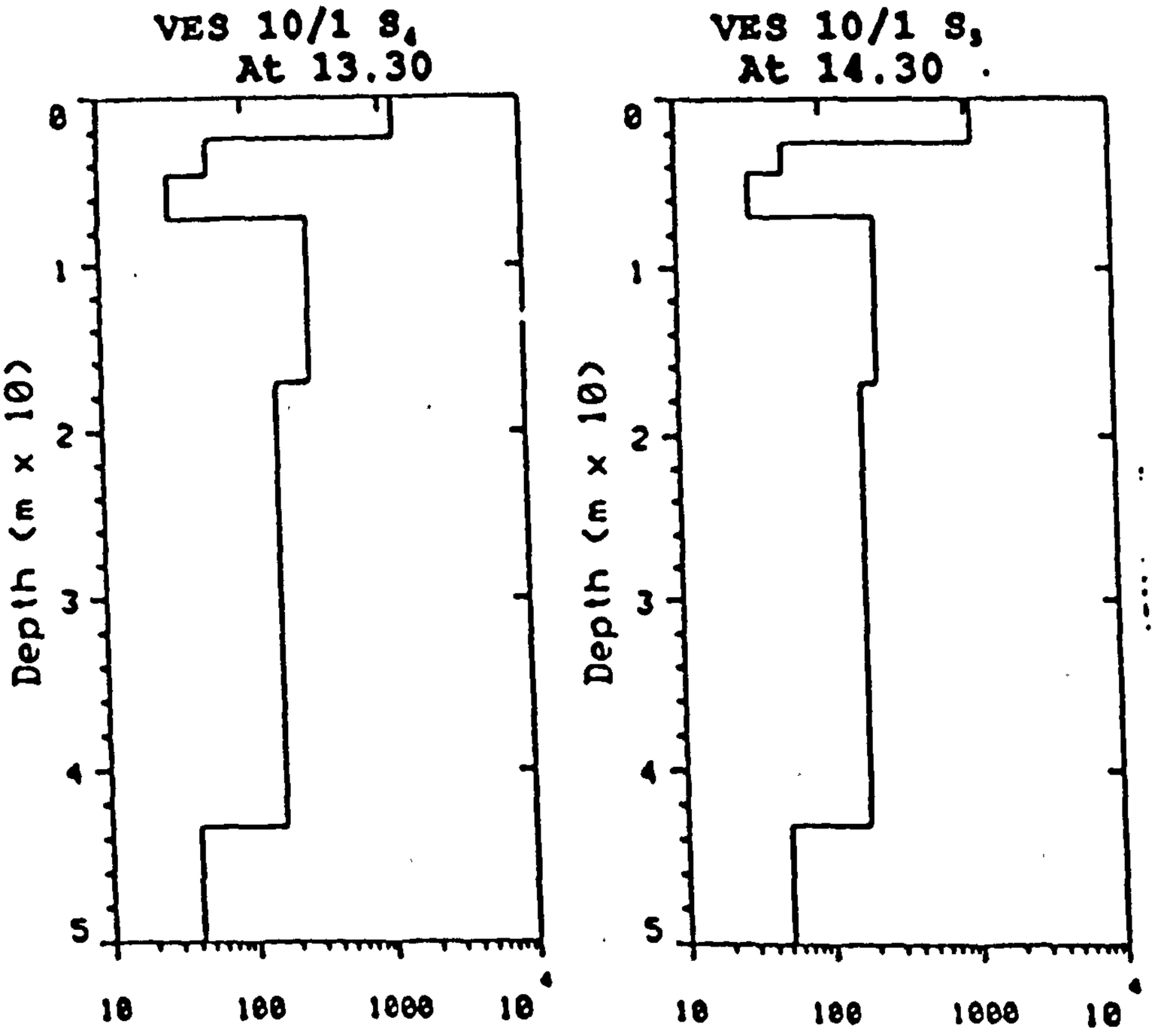

Figure 6.20. Comparative models showing change in Resistivities/Thicknesses of different layers due to fluctuations in water level caused by tidal effect.

(ii) Flow to the well is in steady state.

Thiem (1906) was one of the first to utilize two or more piezometers to determine the hydraulic conductivity of an aquifer. The Thiem method will be used to analyze data from the pumping test. Table 6.11.a. gives the drawdown after pumping for nearly 30 minutes with a constant discharge rate Q = 120.96 m^3/day and the flow had reached a steady state. The numerical values of the respective steady state drawdown (s_1) 0.25m and (s_2) 0.16m in the piezometers (r_1) 2.4m and (r_2) 4.94 metres away from the pumped well are substituted into the Thiem equation (see equation 4.20). The same procedure is followed using other combinations of piezometers. In addition one of the piezometers is used as a second discharging well for further tests. The results of pump tests are given in Table 6.11.b.

Before carrying out the pump test, water samples from the depth of the pumped wells and piezometers were also collected for salinity testing. The same procedure was repeated immediately after the the test. The results are given in Table 6.11.c.

It is evident from the salinity test carried out on the samples from the pumped wells and piezometers, that the pumping causes a considerable increase of salinity. The results further show that a pumping well particularly near a coast could cause upconing as is evident from the sudden jump in salinity to Cl^- 367 ppm from an original Cl^- 328 ppm, a value which is comparatively even higher than what the spring tide water could cause (Cl^- 355 ppm, see Figure 6.18).

Piezometer	10/2A	10/2B	10/1	10/2D
Drawdown in metres	0.25 m	0.16 m	0.05 m	0.11 m

Table 6.11.a. Drawdown in the piezometers 7 metres below ground surface 30 min. pumping, pumping test Aber college farm.

r_1 (m)	r_2 (m)	s_1 (m)	s_2 (m)	Transmissivity KD m^2 /day
2.4	4.94	0.25	0.16	154
9.95	20.4	0.11	0.05	228 (Mean 191)

Table 6.11.b. Transmissivity of the upper-aquifer Aber college farm.

Pumped well (P.W) / Piezometer	Salinity (Cl^- ppm) Before test	Salinity (Cl^- ppm) After test
10 / 1 (P.W & P) (Nearest to coast)	328	367
10 / 2 (P.W)	75	95
10 / 2A (P)	72	83
10 / 2B (P)	76	82
10 / 2D (P)	61	63

Table 6.11.c. Results of salinity change before and after pumping test Aber college farm.

6.5 Permeability of the sediments

The pumping test was also used to arrive at the determination of permeability of the upper aquifer sediments. Other methods such as the constant head test in the field and grain size and constant head permeameter tests in the laboratory, were also used to calculate the permeability of the sediments from the same aquifer. Table 6.12 summarizes permeability values measured or calculated by the different methods.

The analogy between electrical conduction and fluid flow in porous media has been used to quantitatively predict transmissivity, porosity and permeability from electrical formation factor (Heigold, 1979; Biella et al., 1983; Jackson et al., 1978; Lovell, 1983; and Huntley, 1986). The transmissivity mean value of 191 m^2/day Table 6.11.b., when it is divided by the electrical aquifer thickness (4.4 metres) gives a permeability value of 5×10^{-4} m/sec (see Table 6.13). The value of permeability thus obtained is nearer to the measured values rather than the calculated values.

At borehole 10/1 the value of the resistivity of the porous medium, (R_o) = 54 ohm-m, and that of the resistivity of the fluid, (R_w) = 20 ohm-m, was used to determine the value of the electrical formation factor. This value was used in the formation factor-permeability log-log plot (Lovell, 1983) to estimate the value of the permeability as given in Table 6.12. All the permeability values obtained by the different methods (Table 6.12) are the mean average values. For the laboratory-determined values the range of variation was limited to within a quarter of a magnitude, whereas the field-determined values had a slightly higher variation range of about half of a magnitude.

An approach has been made to relate electrical measurements directly to transmissivity. By definition then, we should expect a relation between transmissivity and the product of aquifer apparent formation factor, an average fluid resistivity, and aquifer thickness. This product may be considered a normalized transverse resistance (Kosinski et al., 1981). It is closely related to the aquifer transverse resistance. Table 6.13 gives a value of normalized transverse resistance of 171 $\Omega.m^2$ for the upper aquifer.

The transmissivity and permeability values obtained for the upper aquifer prove to be moderate values and do not come in the category of high values as defined by Howard (1987). Water bearing sediments with such transmissivity and permeability values could be classed in a category which minimizes the rate of landward advance of the saline intrusion.

6.6 Porosity Estimated from Geoelectric data

An approach to estimating porosity from geoelectric data for the upper sediments composed of sands and gravel, involves the use of the well known Archie equation for unconsolidated sands (Atkins and Smith, 1961; Taylor Smith, 1971; Windle and Wroth, 1975; and Doveton, 1986).

Using the equation $FF = R_o/R_w = n^{-m}$ (already given in chapter 4),where FF is the formation factor, n is the porosity, R_o is the bulk formation resistivity derived from vertical electric sounding field curves, and R_w is the fluid resistivity estimated from borehole water samples and taking m equal to 1.2 for natural sand and gravel (the value used by Doveton, (1986) for the similar type of sediment) it is possible to obtain a

Methods	Permeability (m/s)
1. Pumping test	7.4×10^{-4}
2. Constant head (Field test)	7.6×10^{-4}
3. Constant head (Lab. test)	1.7×10^{-3}
4. Grain size (Hazen's-formula)	2.7×10^{-3}
5. Grain size (Kozeny-Carman)	7.7×10^{-4}
6. By using electrical formation factor	1.6×10^{-3}

Table 6.12. Shows a list of the permeability values measured or calculated by different methods.

* Fresh water (upper aquifer)
** Mixed water (upper aquifer)

Resistivity of Aquifer (Ω.m)	Aquifer Thickness (m)	Estimated Permeability (m/sec)	Estimated Normalized Transverse Resistance ($\Omega.m^2$)
54* 31**	1.5* 2.9**	5×10^{-4}	171

Table 6.13. Estimated value of permeability and the Normalized transverse resistance by relating with electrical measurements.

value for porosity from electrical data. Applying the equation to the results of the interpretation for geoelectric stations boreholes 10/1, 10/2, and 10/2D and the resistivity measurements of fluid obtained from boreholes (which were 20, 35, and 42 ohm.m) yield porosity values which range from 0.33 to 0.43. The lower end of the range (0.33 was obtained for borehole 10/2D) probably represents porosity of a relatively clean clastic unit. These values are slightly higher than the values 0.23 to 0.37 determined in the laboratory on the actual sediment (see Table 6.1.b).

The porosity estimates obtained from geoelectric data fall within a range of values reasonable for a sand and gravel aquifer. These estimates also agree and fall within the range of 0.25 to 0.43 determined by Ayers (1988) using seismic data and an empirical relationship between bulk density and compressional velocity. The geophysically-derived porosities are generally higher than values obtained during the course of other hydrogeologic studies of the lower Platte Valley (Marlette, 1952; Ferris, 1967; and GMI, 1987).

6.7 Deviation from the Ghijben-Herzberg Relationship

The fresh water head at three places such as VES 10A′, VES 4A′, and VES 5A′, ranged from 3.65 to 4.35 metres above mean sea level. The Ghijben-Herzberg relationship calls for a 40 to 1 ratio of the depth of interface to the height of water table above sea level. If the head in the fresh water body (between 3.65 to 4.35 metres) were in balance with a stabilized salt water body then the fresh saline water contact would occur between 146-174 metres below mean sea level. But at Aber college farm coast area this contact zone was found to occur within 17.45 to 21.45 metres below mean sea level. The value thus obtained shows deviation from the Ghijben-Herzberg

relationship.

6.8 Discussion

The contour maps Figures 6.12 and 6.13 show the extent of the contamination zones with salinity 250-500 ppm chlorides in upper and lower aquifers. In the upper aquifer the contamination is restricted to a 100 metres wide coastal strip and has spread to a depth of 3 metres inland, whereas in the lower aquifer it has spread to about a 300 metres wide strip and to a depth of 50 metres inland.

The saline water (Figure 6.14) with salinity of more than 500 ppm chlorides has spread to a 100 metres wide coastal strip and a depth of 34 metres inland. Looking at the strip around the Aber river in Figures 6.12, 6.13 and 6.14, it is evident that the area surrounding the river is least affected either by contamination or extensive salinity as compared to other areas along the coastal area. This suggests that probably continuous fresh water infiltration from the Aber river prevented the saline intrusion in this section of the area. As there is heavy rainfall in the area, and most of the rain water infiltrates underground, with little or no withdrawal of groundwater, this has kept the gradient of fresh water towards the sea and in turn has restricted the saline water to a considerable depth.

The moderate values of measured permeability and transmissivity is an important reason for minimizing the rate of landward advance of the intruding saline water, as Howard (1987) has shown.

The transmissivity of aquifer sediments obtained through pumping test when

divided by electrical aquifer thickness gives an estimated value of permeability (Tables 6.11.b and 6.13) this value appears to be quite near to that obtained by direct measurement. This shows that a geophysically-measured parameter of a formation could be a reliable source in determining permeability from transmissivity.

It has further been observed in the study area that spring tides do affect the salinity of groundwater but the similar effect brought about by pumping is more injurious than tides: the salinity increase in groundwater brought about by pumping reaches a chlorides value of 367 ppm which is slightly higher than the value brought about by tides (chlorides 355 ppm), particularly when pumping has taken place near a coast.

Vertical electric soundings made every hour near the coast has clearly demonstrated (Figure 6.20 and Table 6.10) that the geophysical method has proved to be a good tool to record fluctuations in groundwater level caused by the rise and fall of tides.

Geoelectric data formed the basis for estimating the bulk porosity of the aquifer by applying the well known Archie equation. A range of porosity values acceptable for fluvial sand and gravel was obtained.

A deviation from the theoretical 'Ghijben-Herzberg relationship' has been observed at the Aber college coastal area. Jacob and Schmorak, (1960) observed that any deviation in 'Ghijben Herzberg relationship' is due to the following facts:

(1) The contact between the fresh-saline water is not abrupt but is in the form of a zone of mixing (zone of brackish water) with a gradation from fresh to salt water.

(2) Both the fresh and saline water bodies are not stagnant as assumed by the Ghijben-Herzberg relationship. A downward component (caused by recharge through precipitation) exist in the fresh water zone. The fresh water is in continuous state of motion as is evidenced by the seepage surfaces above sea level in the beach area. The existence of such surfaces is not considered in the Ghijben-Herzberg relationship nor is there any provision for the escape of fresh water below the sea level (Wiest, 1965).

CHAPTER 7. CASE HISTORY 2. MALLTRAETH AREA

7.1. Introduction and Geology of the area

Marsh and sands, translated as the 'sodden sands', form a large flat bottomed valley in the southern portion of Anglesey (location map Figure 7.1). Geological formations ranging from Precambrian to Recent in age are found on the island and coupled with the great age range of the formations is an astonishing structural complexity.

The oldest rocks are micaschists of the Precambrian in age, which lie on the south eastern side of the Berw fault which forms one edge of the depression containing Malltraeth marsh and sands (Edwards, W., 1904; Embleton, C., 1964; Greenly, E., 1919). Lying against this fault and underlying the floor of the marsh are limestones, sandstones, red beds, and coal measures of Carboniferous age. Lying unconformably beneath the Carboniferous rocks are green schists and some minor tuffs of the Precambrian. The harder Precambrian metamorphosed rocks have proved more resistant to erosion, forming the higher ground on either side of the valley. While the softer Carboniferous formations have been weathered down to form the valley floor.

The Quaternary deposits of Anglesey are mostly seen covering the floor of the depression forming Malltraeth marsh and sands. While boulder clay is on both sides of the valley, it is not clear whether it exists beneath the alluvium or if it was eroded prior to the deposition of the alluvium.

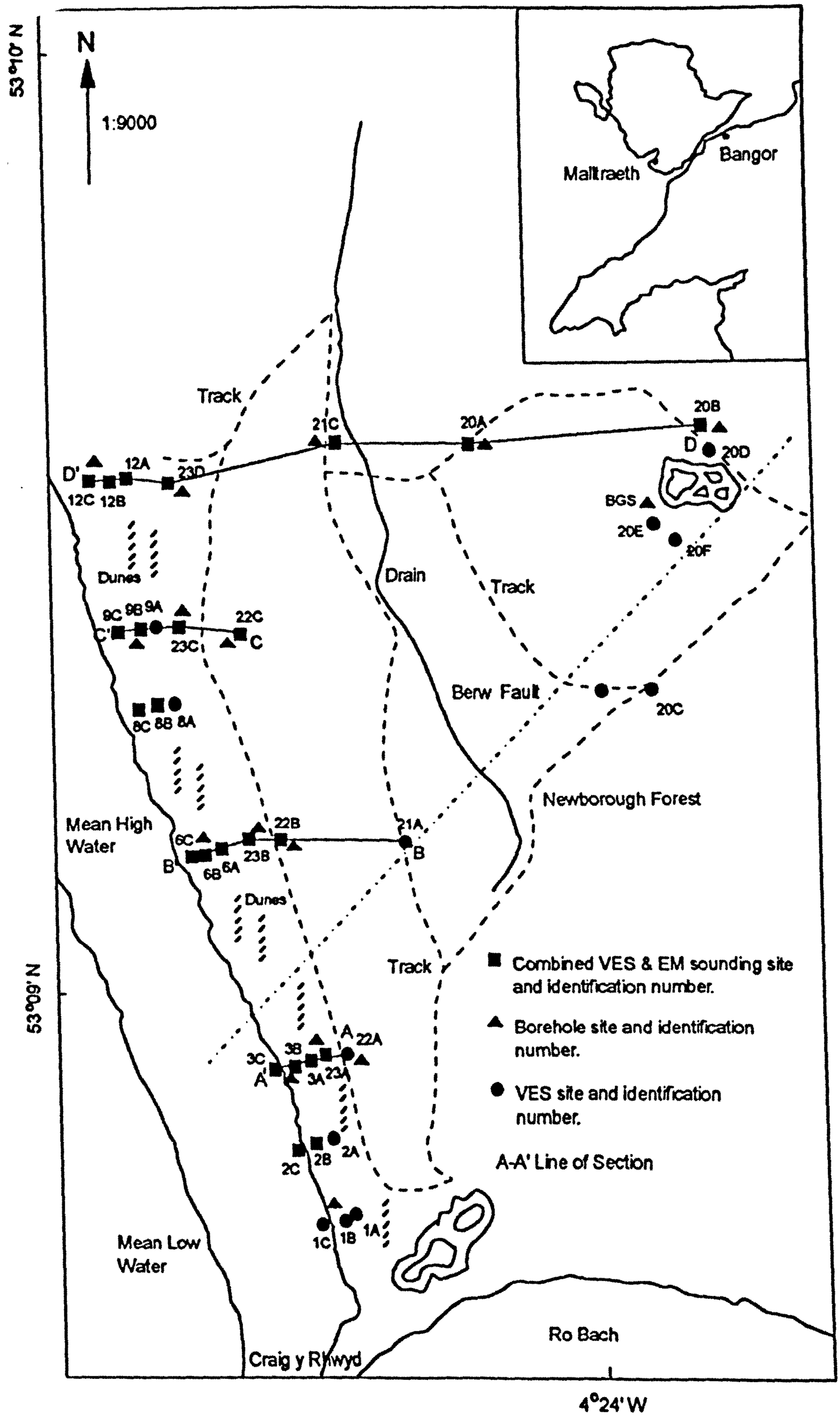

Fig. 7.1. Map showing location of the study area, Malltraeth.

The Newborough forest site which forms a part of the Malltraeth area is separated from Malltraeth beach by very high and broadly spread dune sands, lying parallel to the Malltraeth beach Figure 7.1. This site comprises a sand body of some 20 metres in thickness overlying boulder clay with bedrock at about 30 metres depth. Extensive in-situ testing has been carried out in the past to correlate the geophysical and geotechnical properties of the site. The geology of the area has been revealed by many boreholes drilled near the pond (Table 7.1.a), at this site by the British Geological Survey (Cratchley et al 1982; Davis, 1982; Al-Azzawi, 1986). The sand body is composed of fine to medium grained sand which has a medium to high sphericity (Davis, 1975).

The geological and hydrogeological information in the study area was obtained from hand auger boreholes and British Geological Survey boreholes which revealed the presence of an unconfined aquifer consisting of unconsolidated fine to medium grained sand, extending from the surface down to depths of about 20 metres in the Newborough forest area and about 55 metres in the Malltraeth beach dunes area. This is underlain by a bed of boulder clay forming the base of the aquifer. This aquifer is in direct contact with the sea all along the beach.

The results of mechanical analyses of granular samples obtained during sinking of the hand auger boreholes in the study area are tabulated below Table 7.1.b. It can be seen from this table that there is predominance of finer fractions of sand towards the top of the aquifer and gradually the sand gets coarser towards greater depth. Due to the predominance of granular material at the surface, the aquifer is recharged from direct percolation of rainwater falling on the sand dunes. It could be well understood that the most of the rainwater infiltrates into the underlying alluvial sand to replenish the

Lithology	Depth (m)
Dry sand	0.8
Saturated sand	15.5
Sand, gravel and cobbles	22.5
Boulder clay	30-60 (resistivity interpreted findings)
Bed rocks	

Table 7.1.a. Geological drill log (British Geological Survey) Newborough forest, near VES 20E, Malltraeth.

a. Parameter	Minimum value	Maximum value
1. Porosity	0.39%	0.43%
2. Rainfall (m.m)	725 (year 1991)	952 (1992)
b.Grain content	Minimum value	Maximum value
Percentage of sand (2m depth)	98	100
Percentage of silt and clay (2m - depth)	0.1	2

Table 7.1.b. General characteristics of the alluvium.

groundwater storage. The water table gradient in the area is towards the sea i.e. the groundwater from the phreatic aquifer moves out into the sea and within the tidal zone in the beach area the fresh groundwater is underlain by a body of saline water.

7.2. Detection/Mapping of the Saline-fresh water Interface using Geophysical Methods and Hydrochemistry

Thirty seven vertical electric soundings were made at selected sites (Figure 7.1) with the ABEM Terrameter. Simple Wenner and Offset Wenner arrays were used for this area. Soundings were made up to maximum electrode spacings ranging from 80 to 150 metres for the simple Wenner array and 64 to 128 metres for the Offset Wenner array. In the Newborough forest section of the Malltraeth area, physical obstructions such as the concentration of trees and various zig-zag tracks made it impossible to utilize large electrode spacings.

Twenty four electromagnetic soundings were also made at the selected centres of the sites where previously vertical electric soundings were made, using MaxMin I-8 portable equipment (Figure 7.1). Suitable survey sites are limited compared to the vertical electric soundings because regularly standing bull-dozers, trucks, trollies and many other metallic objects lying in the Newborough forest section of the study area cause erroneous readings.

In Malltraeth, particularly over the dunes, the EM observational error due to coil misorientation, using Equation 3.8, was worked out to be only ± 0.1 %. The maximum possible error for the Simple Wenner array was calculated to be $\pm$ 2.6 % . The multilayer sounding results for all the soundings carried in the area are given in Table

7.2. Figure 7.2 shows an example of VES and EM field data (obtained at site 3C) interpreted with computer software together with the range of equivalence models available for the same data. The model of the VES sounding (7.2.a) has good agreement with the model of EM sounding (7.2.b). The equivalence bounds of DC resistivity sounding or EM sounding results at site 3C are given in Appendix Table 7G and 7H respectively. Table 7.3 shows the comparision of the geological drill log in the hand-augered hole at site 3C with the B.G.S drilled log in the area same compared to the interpreted results of the VES and EM soundings carried out near the site 3C.

The construction of geoelectric sections is an intermediate stage in the preparation of various contour and isopach maps. A geoelectric section A-A′ (Figure 7.3), drawn perpendicular to the coast line and across various sites of the VES and EM soundings such as 22A, 23A, 3A, 3B, and 3C as well as hand-augered holes (see area map Fig. 7.1). From the correlation, the geoelectric section A-A′ shows that there is a phreatic aquifer with impervious boulder clay below it having resistivities from 2 ohm-m (coast) to 10 ohm-m (inland), and bed rock at the bottom with resistivities ranging from 142 ohm-m to 295 ohm-m. The phreatic aquifer has saline water with resistivities from 1.4 ohm-m (coast) to 7 ohm-m (inland) with more than 500 ppm chloride concentration (the saline-fresh water interface shown through a curved line separates saline water from mixed water). The gradual increase of resistivities inland relates to a gradual decrease in the concentration of dissolved solids in the ground water inland. An important feature in the section (Figure 7.3) is evident that the mixing zone with resistivities from 8 ohm-m to 35 ohm-m (or chloride concentration between 250-500 ppm) starts immediately below site 3A and then abruptly ends as the thickness of sand in the aquifer layer below the sand dune increases. This indicates that as the sand dune at the top intercepts almost all the considerably high rainfall (see Table 7.1) diluting

VES number	Layer number1 R (Ω.m)	Th m	Layer number2 R (Ω.m)	Th m	Layer number3 R (Ω.m)	Th m	Layer number4 R (Ω.m)	Th m	Layer number5 R (Ω.m)	Th m
1A	248	1.8	25	5.7	1.6	7	131		-	
1B	60	.5	6	3	1.4	7.5	587		-	
1C	1.2	2.5	1	5.3	700		-		-	
2B	35	.6	6.4	4.6	2	5.7	30		-	
2A	246	1.9	29	9.2	3.7	11.4	29		-	
2C	1.2	3.4	.9	4.4	150		-		-	
3A	79	.6	8	6.8	3	11.8	28		-	
3B	28	.3	3	5.7	2.5	9.1	55		-	
3C	1.4	3.3	2	10.7	142		-		-	
4A	82	.8	4	7	3	10.5	25		-	
6A	386	1	30	3.8	13	10.1	9		-	
6B	36	1	4	8	12	14.5	18		-	
6C	23	.4	1.2	12	9	6.5	32		-	
9A	93	.2	1859	.6	43	12	12	35.6	11	
9B	236	.7	14	7.2	5.4	33	13.5		-	
9C	1.6	7.6	4	31.7	172		-		-	
12A	467	1.4	35	12.9	13	22	6		-	
12B	652	.8	19	11.4	5.4	18	6		-	
12C	1	2.5	4	13.5	6		-		-	
23A	1300	1.7	257	4.3	64	51	10		-	
23B	850	2	391	1.5	35	38.9	15		-	
23C	1785	.9	628	5.4	63	26.7	23		-	
23D	2575	.9	40	16	12.4	16	42		-	
22A	2054	1.1	53	15.8	295		-		-	
22B	625	1.2	45	33.4	61		-		-	
22C	653	.6	60	32.5	15		-		-	
20A	1350	1.1	70	29.2	19		-		-	
20B	812	1.6	84	21.4	20	6.2	56		-	
20C	1205	.7	59	19	19		-		-	
20D	2016	1.4	141	21	79		-		-	
20E	1430	1.6	99	20.4	31		-		-	
20F	1796	1.5	72	20	32		-		-	
21A	1826	.7	3150	2.2	118	29	177		-	
21C	1210	.7	54	27.8	20		-		-	

Table 7.2. Multilayer sounding results.
R = Resistivity, Th = Thickness.

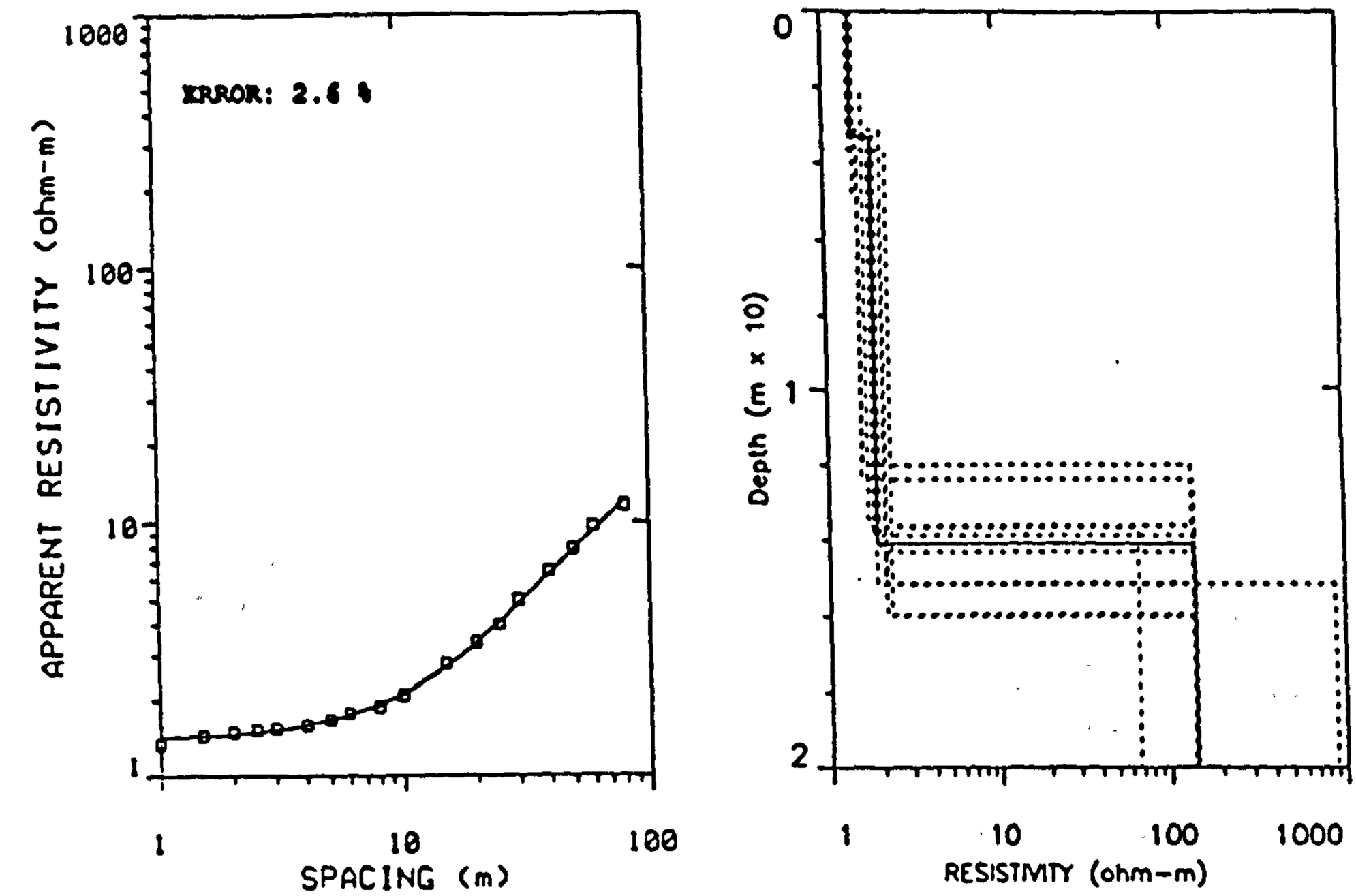

.a.

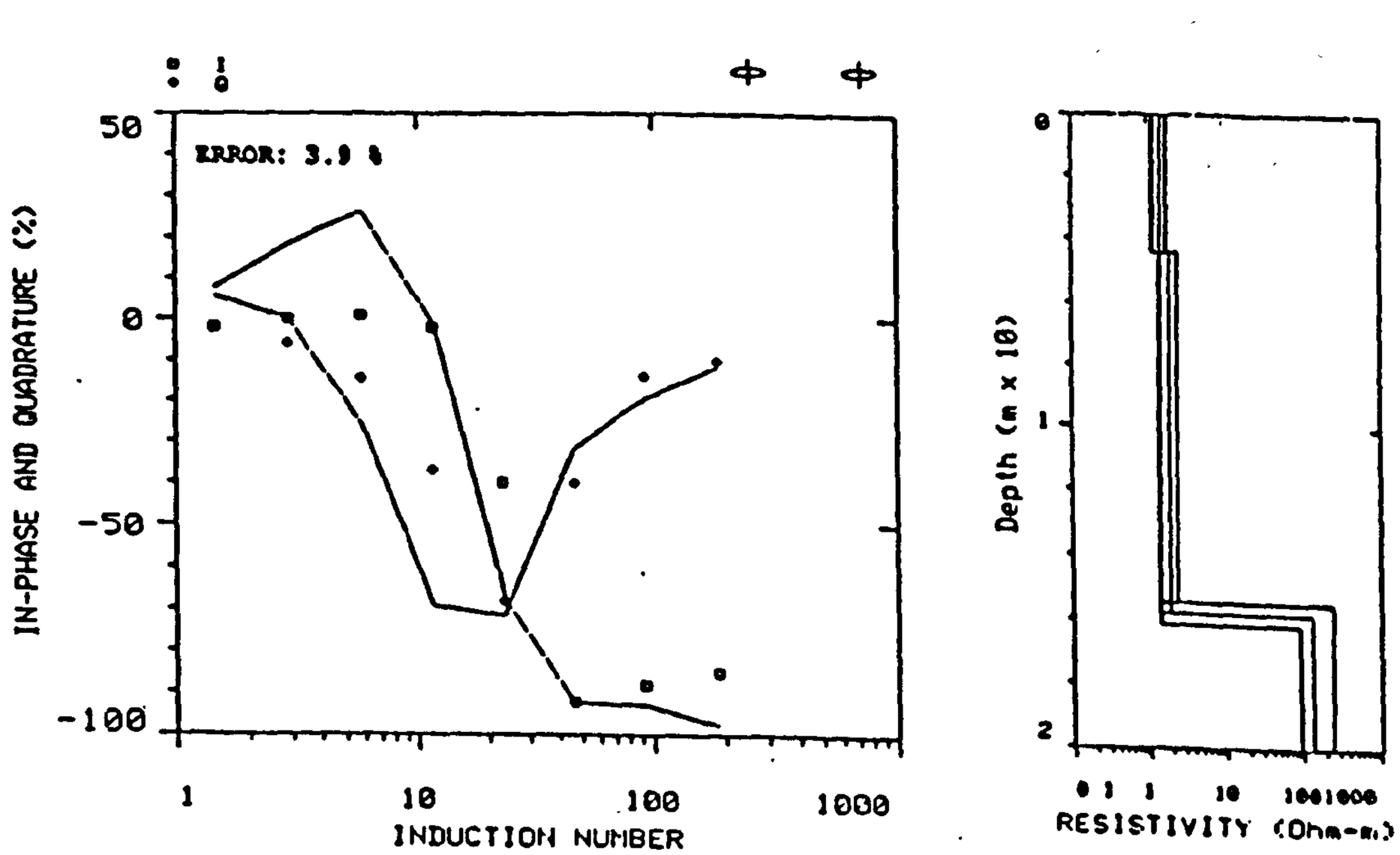

.b.

Fig. 7.2. Vertical electric sounding curve (a) and electromagnetic sounding curve (b) at site (3C) based on field data points, alongside their equivalence curves.

Layer No.	VES sounding R(ohm-m)	Th(m)	EM sounding ohm-m	m	Geological drill log
1	1.4	3.3	1	4.4	Fine to medium sand.Depth 0.5m. W.T 0.2m.
2	2	10.7	2	11.4	Saturated sand, B.G.S. logs. Refer Table 7.1.a.
3	142		142		-

Table 7.3. Vertical electric and electromagnetic soundings 3C interpreted data with geologic log, Malltraeth.

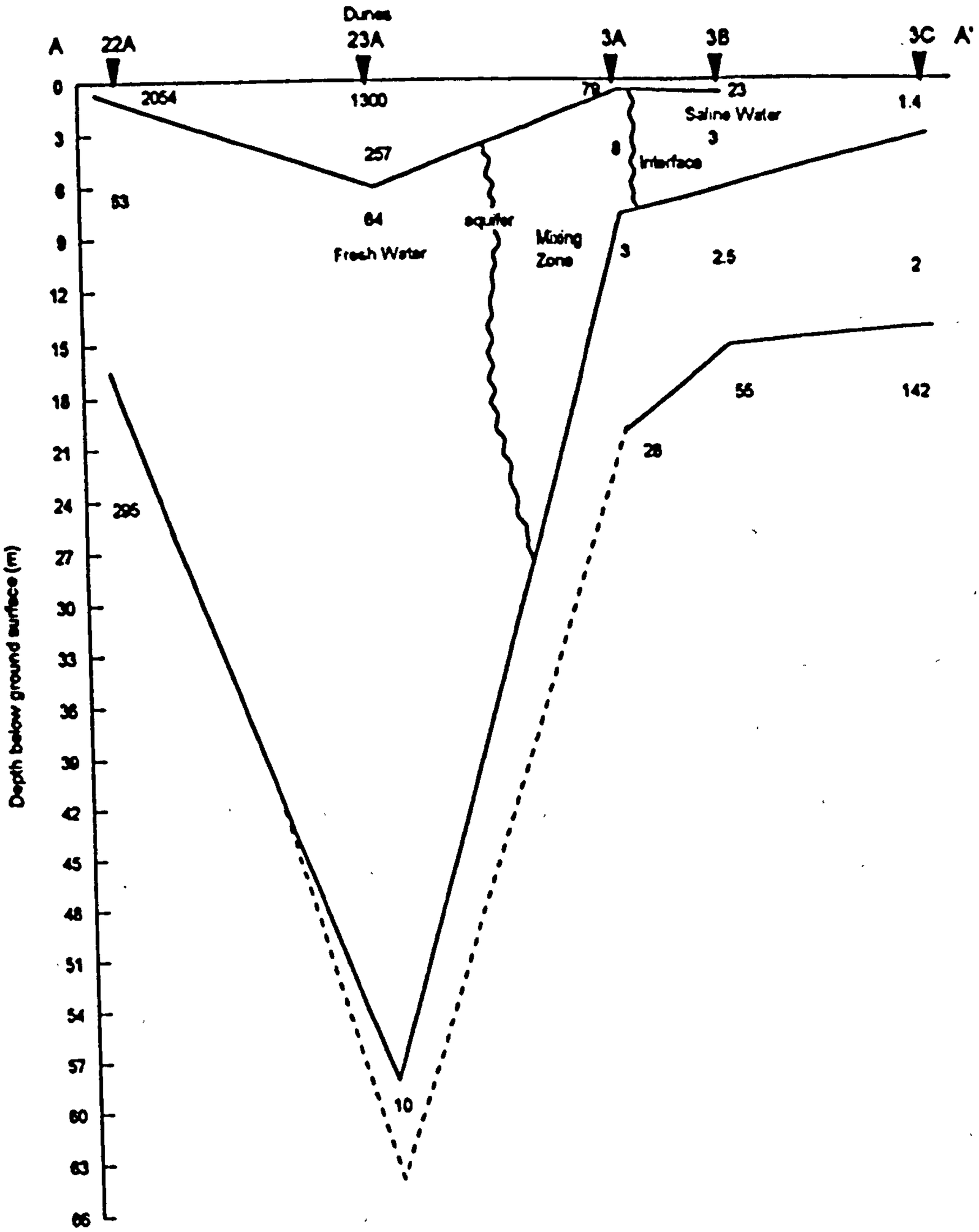

Fig. 7.3. Geoelectric section A-A' derived from vertical electric and electromagnetic soundings.
Resistivities in ohm-m.
Scale: Hor. 1:500, Vert 1:300.

rapidly the saline water, it halts further flow inland of the saline water. The boulder clay layer below the aquifer is indicated by a slight increase in resistivities from coast to inland. Figure 7.3.a has been drawn along geoelectric section line A-A′ and shows what the area looks like at high water spring tide, after taking into account the ground surface levelling at the site. The section has been extended towards mean low water level. Sea level (S.L), water table (W.T), saline interface with saline water, mixing water zone and fresh water zone have been clearly shown. It is evident from Figure 7.3.a that the fresh water gradient is towards the sea.

Another very typical feature in the section (Figure 7.3) is shown by the behaviour of resistivities inland from the coast in the lowest bedrock layer: near to the coast the resistivity of bed rock has a high value of 142 ohm-m, decreases abruptly inland and then suddenly increases to 295 ohm-m. This is clearly suggestive that the beds are not horizontal the decrease in the middle order resistivities being caused by dip with particularly soft rocks being sandwiched by hard rocks at the two extreme ends. This is further suggestive of faulting in the area. Figure 7.4.a, a sketch section drawn across marsh and sands showing the solid geology , greatly exaggerated in the vertical (from Greenly, 1919), and Figure 7.4.b solid geology map of the area agrees well with this suggestion. The boulder clay layer is seen to be missing below VES site 22A, which suggests that it was eroded prior to the deposition of the alluvium.

A second geoelectric section B-B′ (Figure 7.5) drawn across various sites of VES or VES and EM soundings and hand-augered holes is shown in area map Figure 7.1. Arrows at the top of the cross section show VES or VES and EM combined sounding locations. The interpreted results of all the soundings along this section is given in Table 7.2. Figure 7.6 shows an example of a VES curve (a) and EM sounding

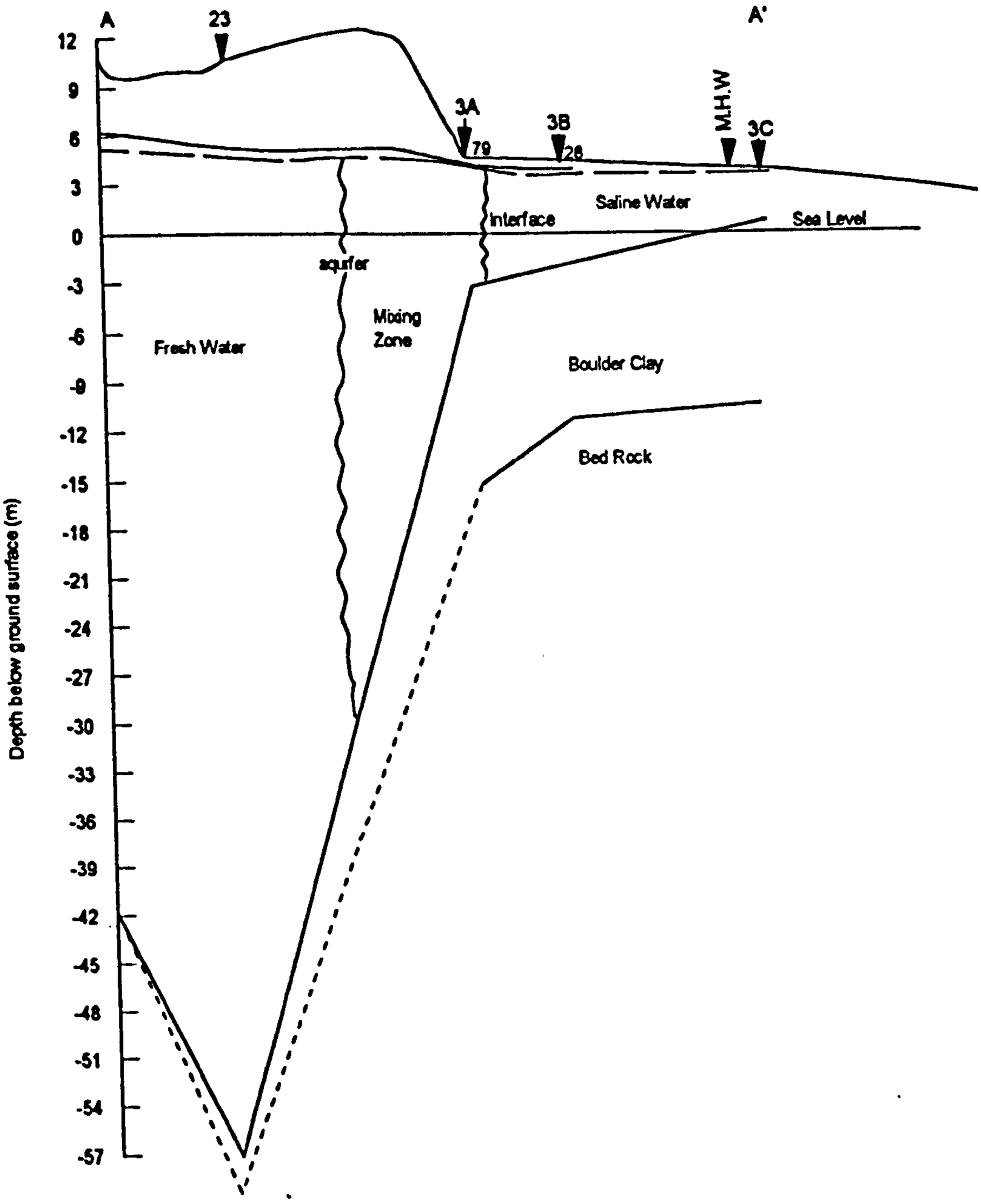

Fig. 7.3.a. Saline and fresh water interface along line A-A'

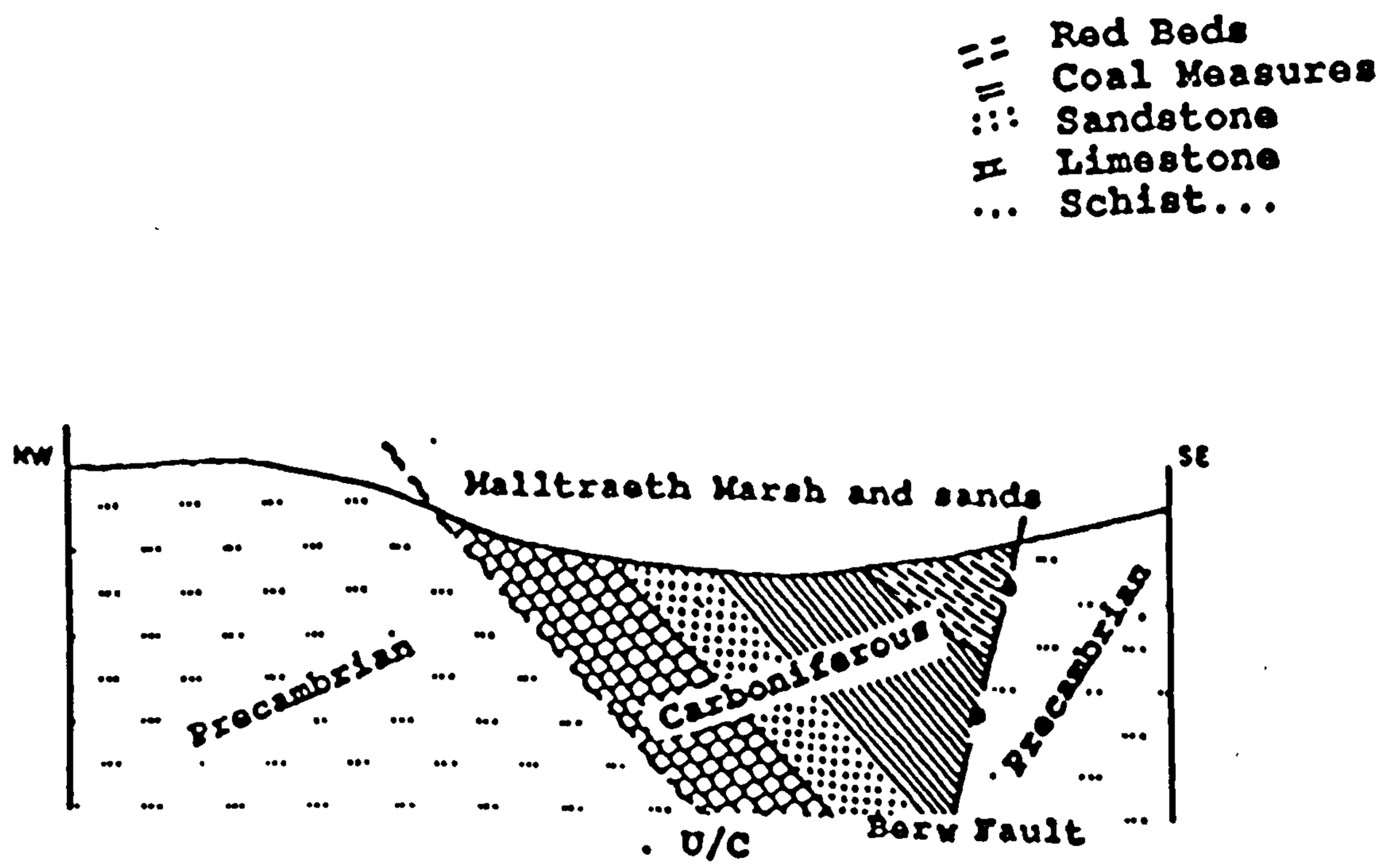

Figure 7.4.a Sketch section across Malltraeth Marsh and Sands showing the solid geology. Greatly exaggerated in the vertical (from Greenly, 1919).

1km

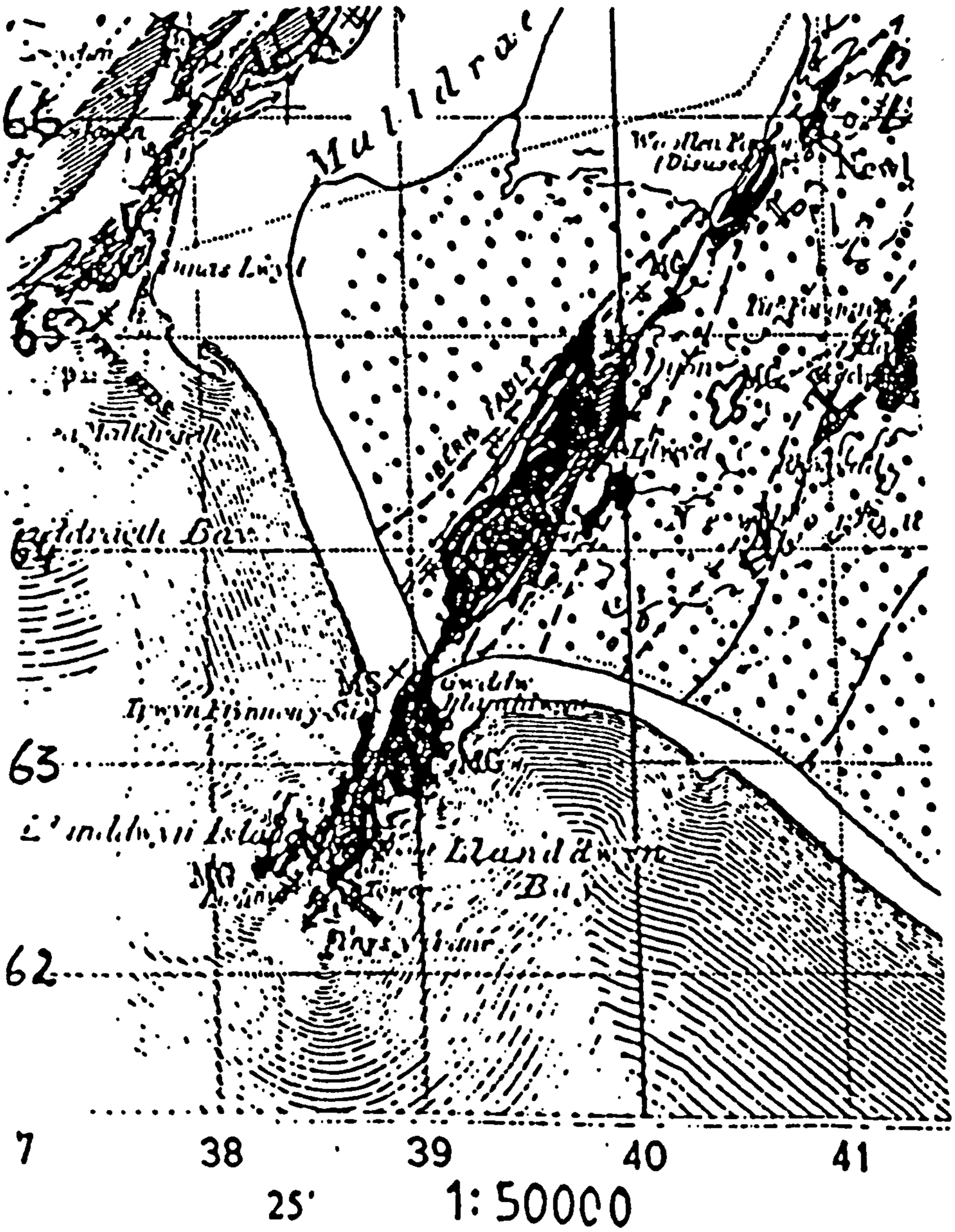

Figure 7.4.b. Solid geology map, Malltraeth.

Note: There is some confusion about the name of Berw fault. Berw is the real name of the fault named after a place in the area, and Bern is an old misprint needs correction.

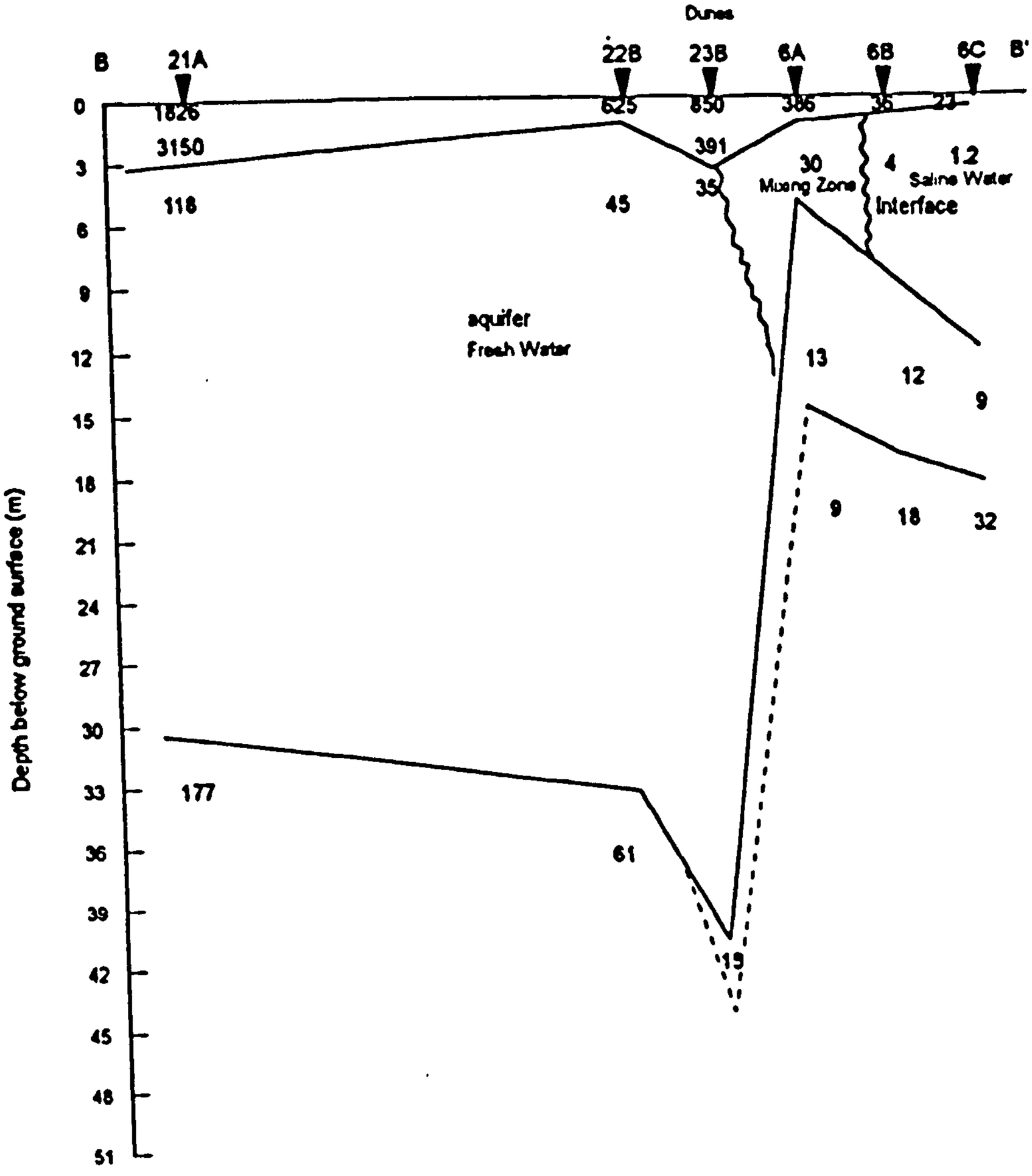

Fig 7.5. Geoelectric section B-B' derived from vertical electric and electromagnetic soundings.
Resistivities in ohm-m.
Scale: Hor. 1:2000, Vert. 1:300.

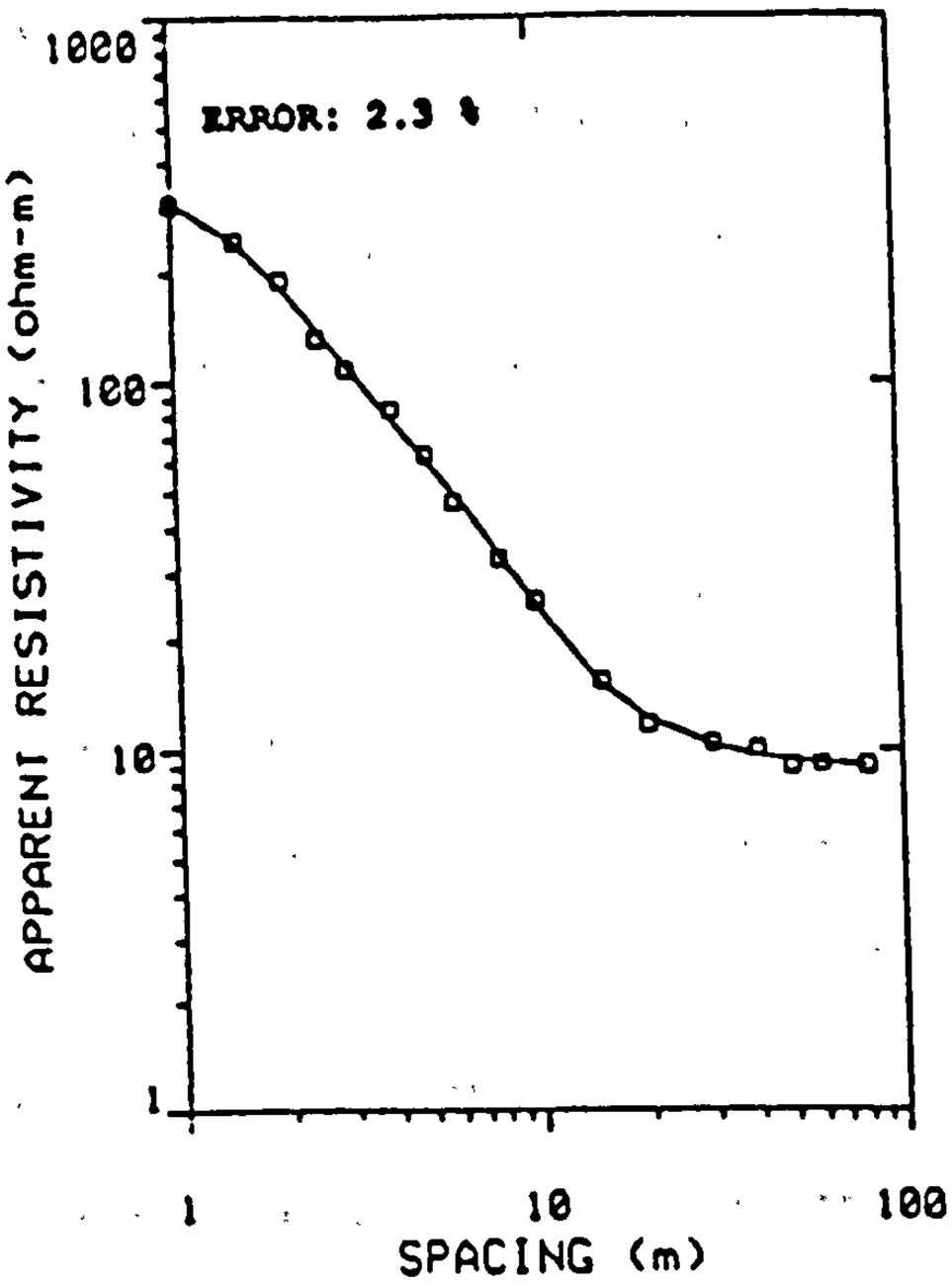

.a.

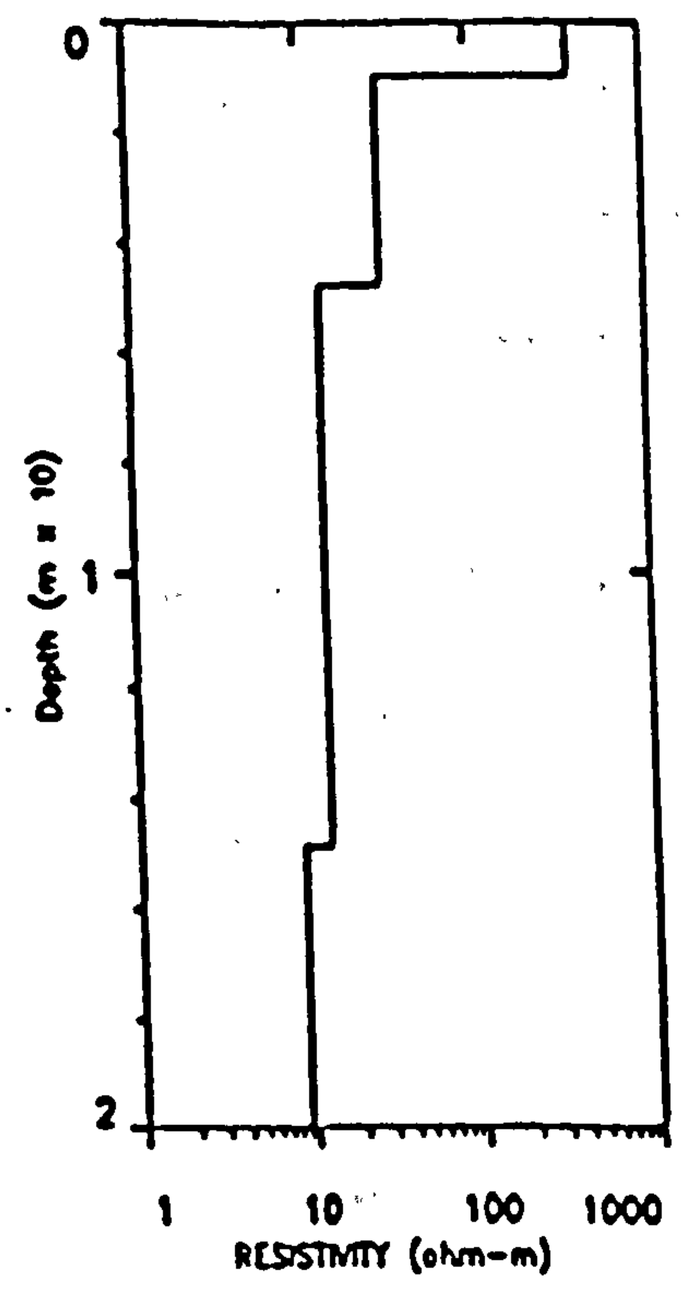

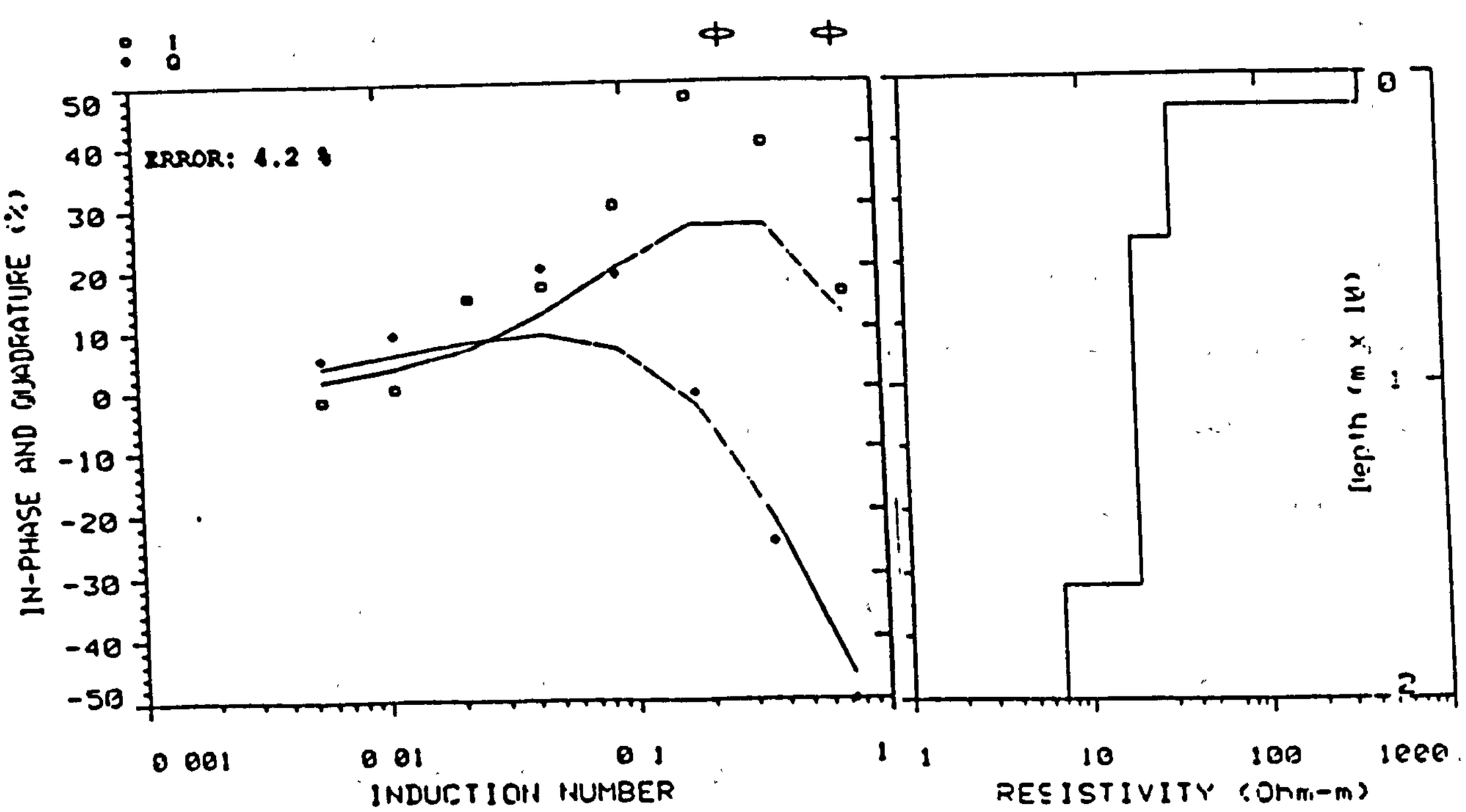

.b.

Fig. 7.6. Vertical electric sounding curve (a) and electromagnetic sounding curve (b) at site (6A) based on field data points.

curve (b) at site 6A; Table 7.4 shows the interpreted soundings with a geologic log. This section shows that there is one aquifer consisting of a sand layer. Its saline water zone ranges from 1.2 ohm.m at the coast to 7 ohm.m inland (with more than 500 ppm chloride concentration) and interface separates (shown through a curved line in the section Figure 7.5) the saline water from the mixing zone. The mixed water zone is separated (through another curved line in the same section) from fresh water and ranges from 8 ohm.m to 35 ohm.m (chloride concentration between 250-500 ppm). It is evident in the section that rainfall on the extensive sand dunes is the possible cause of recharging the aquifer with excessive fresh water thus halting the inland flow of the saline intrusion. The sand aquifer has a boulder clay layer below it showing a gradual increase in resistivities from 9 ohm.m at the coast to 15 ohm.m inland. This layer appears to be missing well inland (below sites 22A and 21A), presumably being eroded before the deposition of alluvium. Solid rock forms the lowest layer in the section; the abrupt lowering of resistivities in the middle of the section repeats the evidence that soft dipping rocks are sandwiched in the middle by hard rock lying at the extreme ends.

A third geoelectric section C-C′ Figure 7.7, drawn perpendicular to the coast and across various sites of soundings and hand-augered holes is shown in the area map Figure 7.1. The interpreted results of all soundings are given in Table 7.2. Figure 7.8 shows an example of a VES curve (a) and EM sounding curve (b) at site 9B. Table 7.5 gives the interpreted VES and EM soundings for site 9B in comparision with the geologic log. This section shows that there is one aquifer consisting of a sand layer. Its saline water zone ranges from 1.6 ohm.m at the coast to 7 ohm.m inland (with more than 500 ppm chloride concentration) and interface separates (shown through a curved line in section Fig. 7.7) the saline water from mixed water zone. The mixed water zone ranges between 8 ohm.m to 35 ohm.m (with chloride concentration between 250-500

Layer No.	VES sounding R(ohm-m)	Th(m)	EM sounding ohm-m	m	Geologic drill log
1	386	1	381	1	Fine to medium sand. Depth 1.4m. W.T 0.9m.
2	30	3.8	32	4.3	Saturated sand, B.G.S logs. Refer Table 7.1.a.
3	13	10.1	19	11.1	-
4	9		7		-

Table 7.4. Vertical electric and electromagnetic soundings 6A interpreted data with geologic log, Malltraeth.

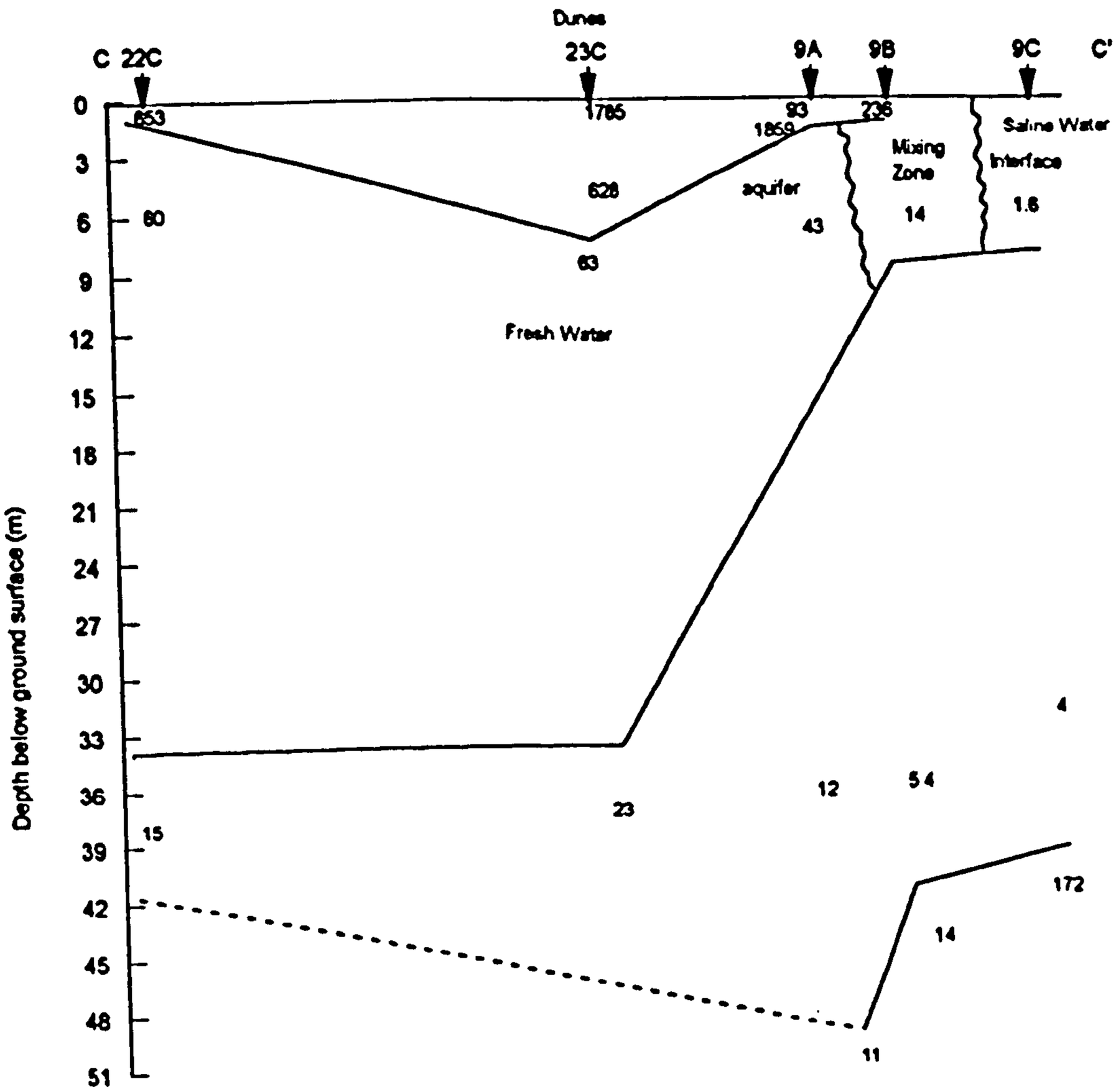

Fig 7.7. Geoelectric section C-C' derived from vertical electric and electromagnetic soundings.
Resistivities in ohm-m.
Scale: Hor. 1:750, Vert: 1:300.

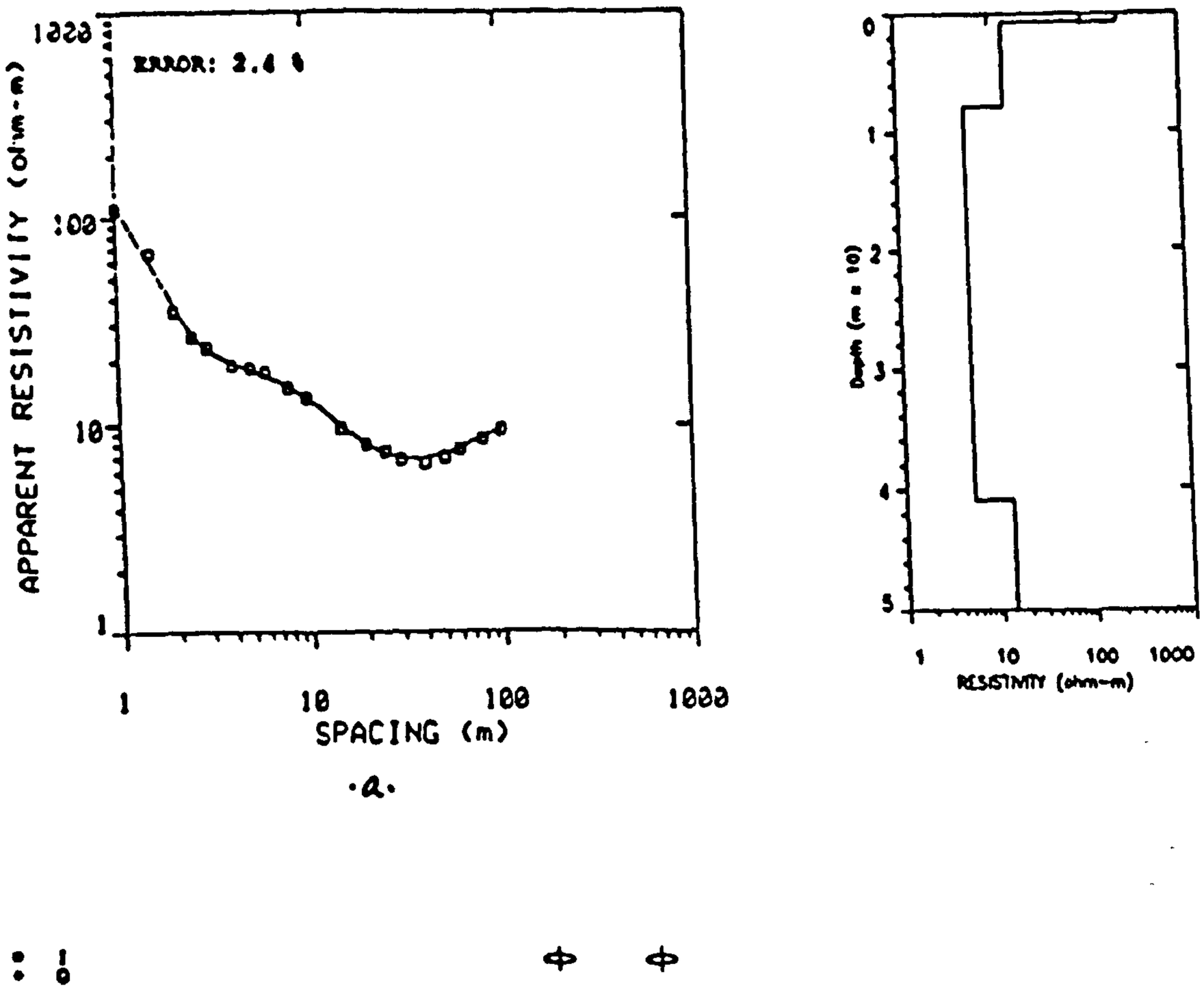

.a.

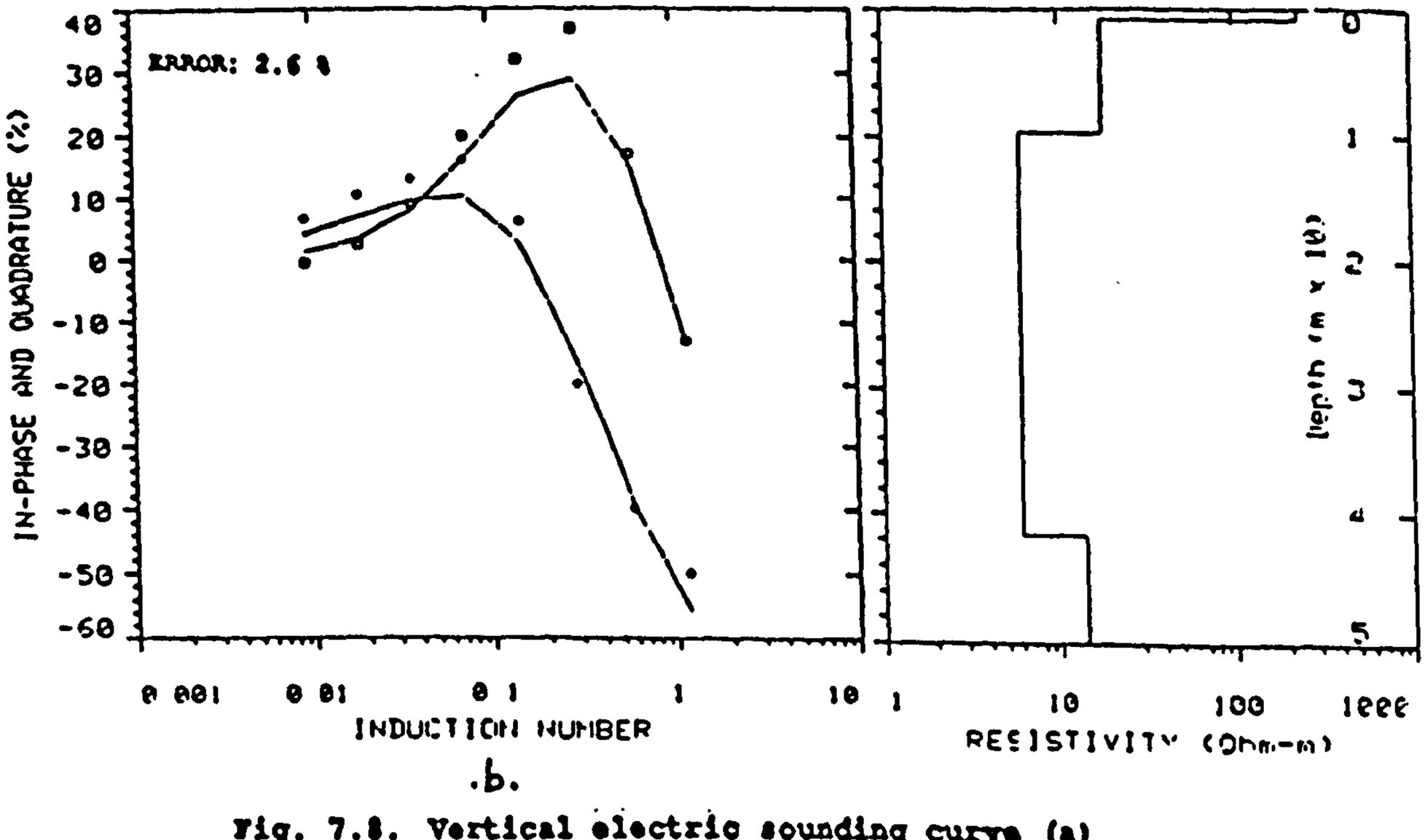

.b.

Fig. 7.8. Vertical electric sounding curve (a) and electromagnetic sounding curve (b) at site (9B) based on field data points.

Layer No.	VES soundings R(ohm-m)	Th(m)	EM soundings ohm-m	m	Geologic drill log
1	236	0.7	237	0.8	Fine to medium sand.depth 1.1m. W.T. 0.5m.
2	14	7.2	18	8.9	Saturated sand, B.G.S. logs. Refer Table 7.1.a.
3	5.4	33	6	32	-
4	13.5		14		-

Table 7.5. Vertical electric and electromagnetic soundings 9B interpreted data with geologic log, Malltraeth.

ppm); a second curved line separates mixed water zone from fresh water. It is evident in the section that sand dunes are the barrier for further inland inflow of the saline intrusion because the dunes provide lot of fresh water recharge to the groundwater and thus maintain the fresh water gradient towards the sea. Impervious boulder clay forms the next lower layer to the aquifer. The dipping bed rocks form the lowest layer, soft rocks being sandwiched by the hard rocks at the extreme ends, as in the previous section.

A fourth and the final geoelectric section D-D′ (Fig 7.9) is the longest section and drawn from the coast to deep inside the Newborough forest. The interpreted results of all soundings are given in Table 7.2. Figure 7.10 shows the example of a VES curve (a) and an EM sounding curve (b) at site 12A. Table 7.6 gives the VES and EM soundings for site 12A compared to the geologic log. This section shows that there is one aquifer consisting of a sand layer. This section has been drawn with a horizontal scale of 1:7500. It is evident in the section that the saline zone has a resistivity range from 1 ohm.m at the coast (with more than 500 ppm chloride concentration) to 7 ohm.m inland and interface (shown through a curved line in the section Figure 7.9) separates saline water from mixed water zone. The mixed water zone has range of resistivities from 8 ohm.m to 35 ohm.m inland (with chloride concentration between 250-500 ppm). It appears yet again that the sand dunes play a major role in preventing saline water from penetrating further inland, absorbing almost all the rainwater and providing recharge to the groundwater to maintain a fresh water gradient towards the sea. Boulder clay with resistivities ranging from 4 ohm-m to 20 ohm-m is immediately below the sand aquifer. At the bottom lies bed rock with resistivities ranging from 6 ohm.m to 56 ohm-m; presumably representing dipping soft rocks to hard rocks. A very interesting feature is also observed in this section. As this section covers a great length

Layer No.	VES sounding R(ohm-m)	Th(m)	EM sounding ohm-m	m	Geologic drill log
1	467	1.4	459	1.3	Fine to medium sand. Depth 1.7m. W.T 1.3m.
2	35	12.9	37	12.4	Saturated sand, B.G.S logs. Refer Table 7.1.a.
3	13	22	11	16.2	-
4	6		5		-

Table 7.6. Vertical electric and electromagnetic soundings 12A interpreted data with geologic log, Malltraeth.

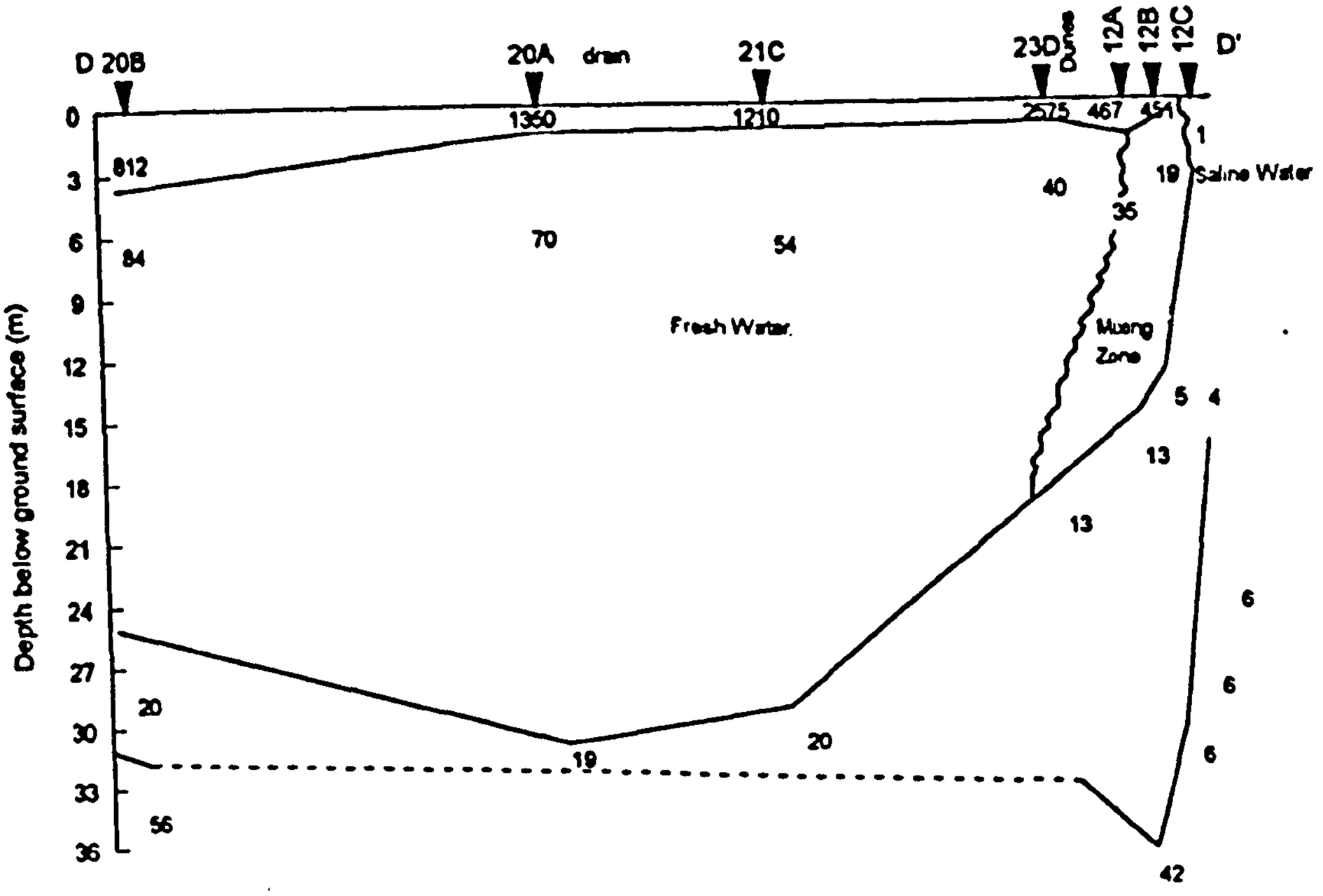

Fig. 7.9. Geoelectric section D-D' derived from vertical electric and electromagnetic soundings.
Resistivities in ohm-m.
Scale: Hor: 1:7500, Vert: 1:300.

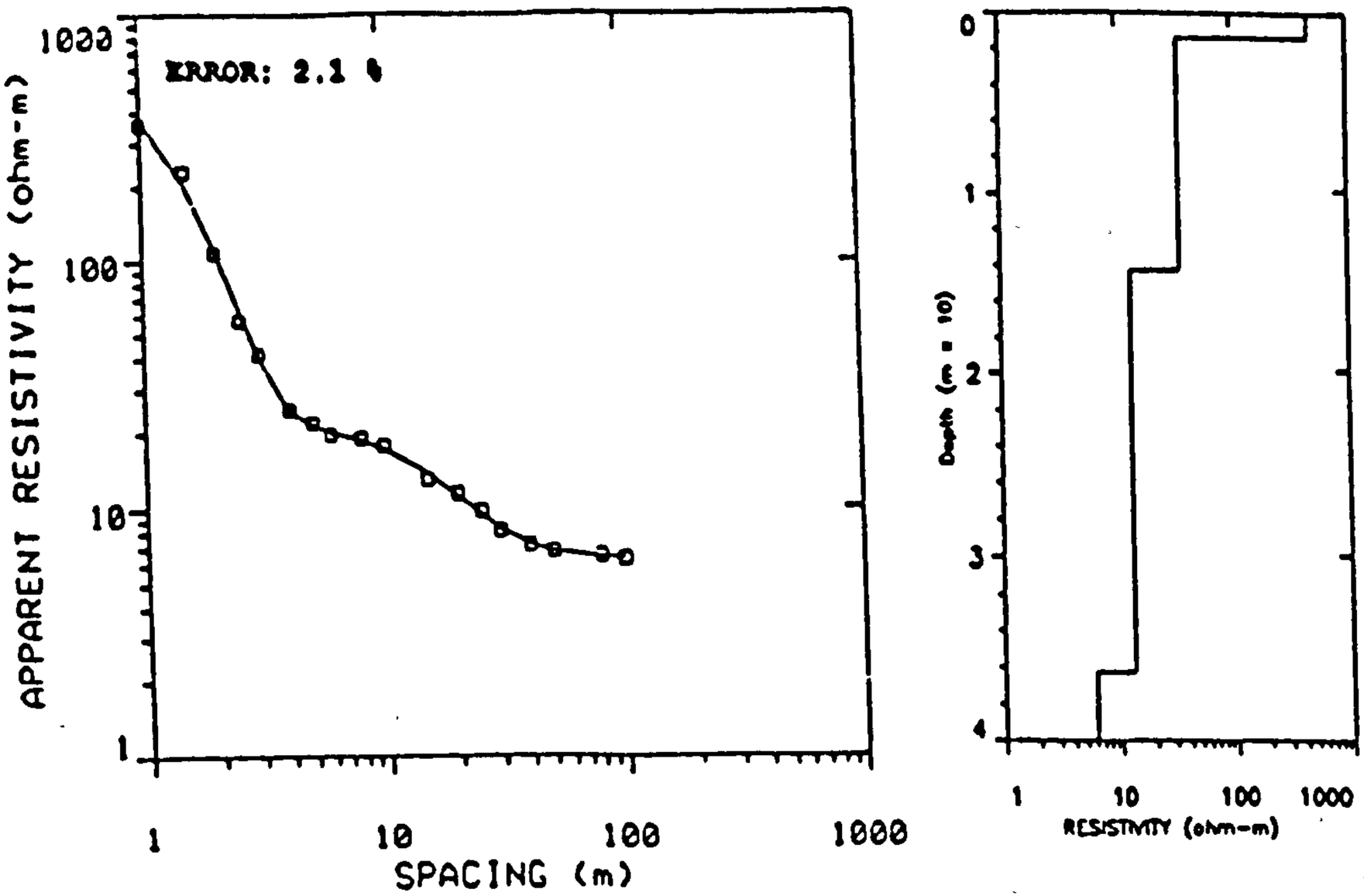

·a·

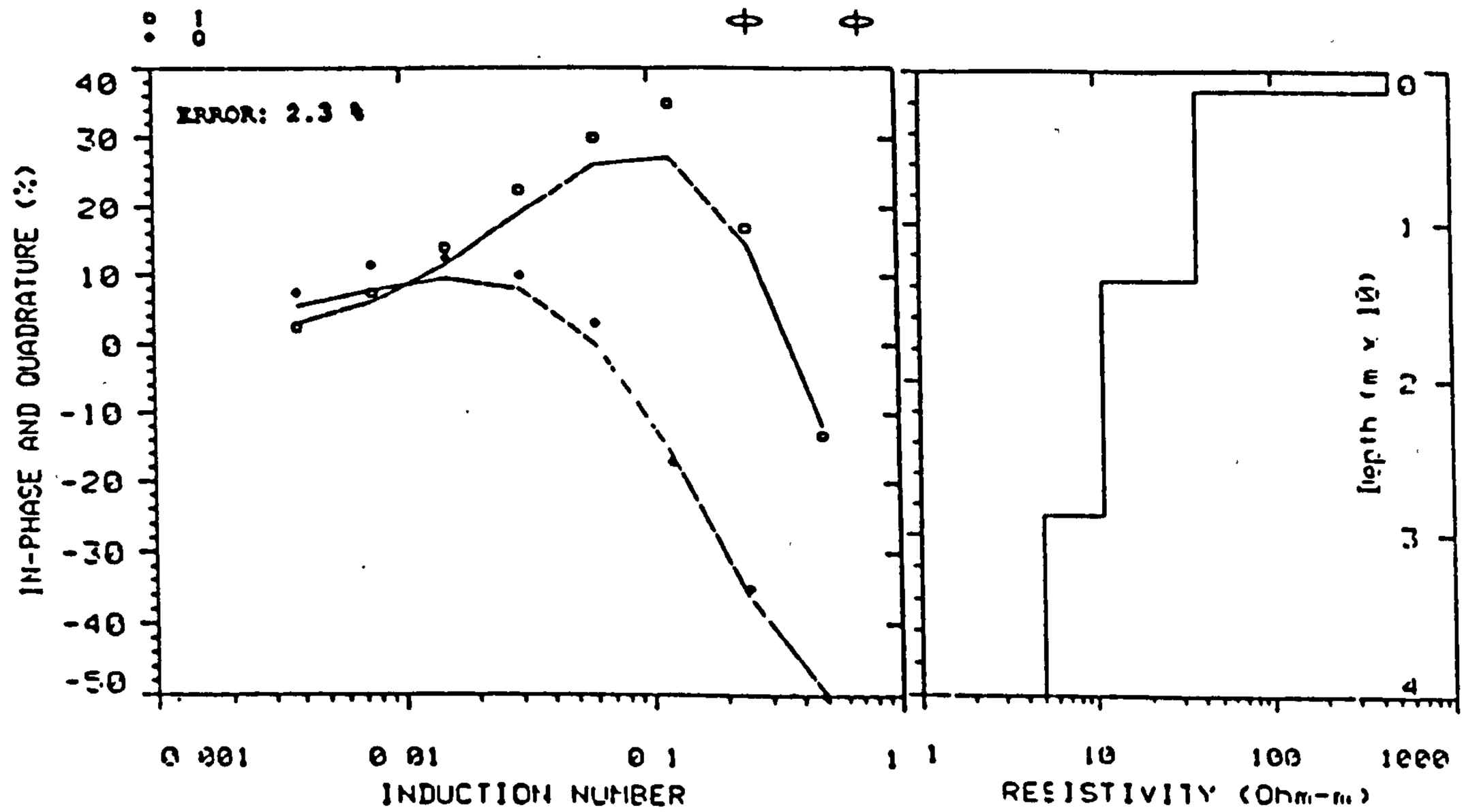

·b.

Fig. 7.10. Vertical electric sounding curve (a) and electromagnetic sounding curve (b) at site (12A) based on field data points.

in the Newborough forest behind the coastal dunes, it appears that the thickness of the sand layer, particularly below VES sites 20A and 21C, enlarges behind the dunes with the clay layer thinning down. A very narrow drain also passes in the area near the site 20A in the section. This suggests the possibility that this area might be an old route of the Cefni River which presently flows further west of this site.

The last stage in the mapping of the saline-fresh water interface is the construction of interface contour maps in order to detect the extent to which the saline water has intruded inland. All the geoelectric sections pertaining to the Malltraeth area have been used in the construction of these maps of the study area. The map, Figure 7.11 shows the extent of the mixed water zone with bulk resistivities less than 35 ohm.m and chloride concentration between 250-500 ppm. Figure 7.11 further shows that the contamination of fresh water with saline water in the aquifer appears to occur along a 70-150 metres wide coastal strip. Near the coast it is found at a depth of 5m, whereas deep inland it is found at a depth of about 10-40 metres.

The saline water is approximately defined by 7 ohm.m with chlorides more than 500 ppm. Figure 7.12, is a contour map drawn showing the zone of saline water. Saline groundwater appears to occur along a 30-60 metres wide coastal strip. Near the coast line it is found at a depth of 2-12 metres and inland at the depth of 6-8 metres.

The source of the saline water appears to be sea water. The wave action and the tides in the sea water is thought to cause mixing of sea water with fresh water. However the heavy rainfall in the area which infiltrates underground prevents sea water from deep penetration inland.

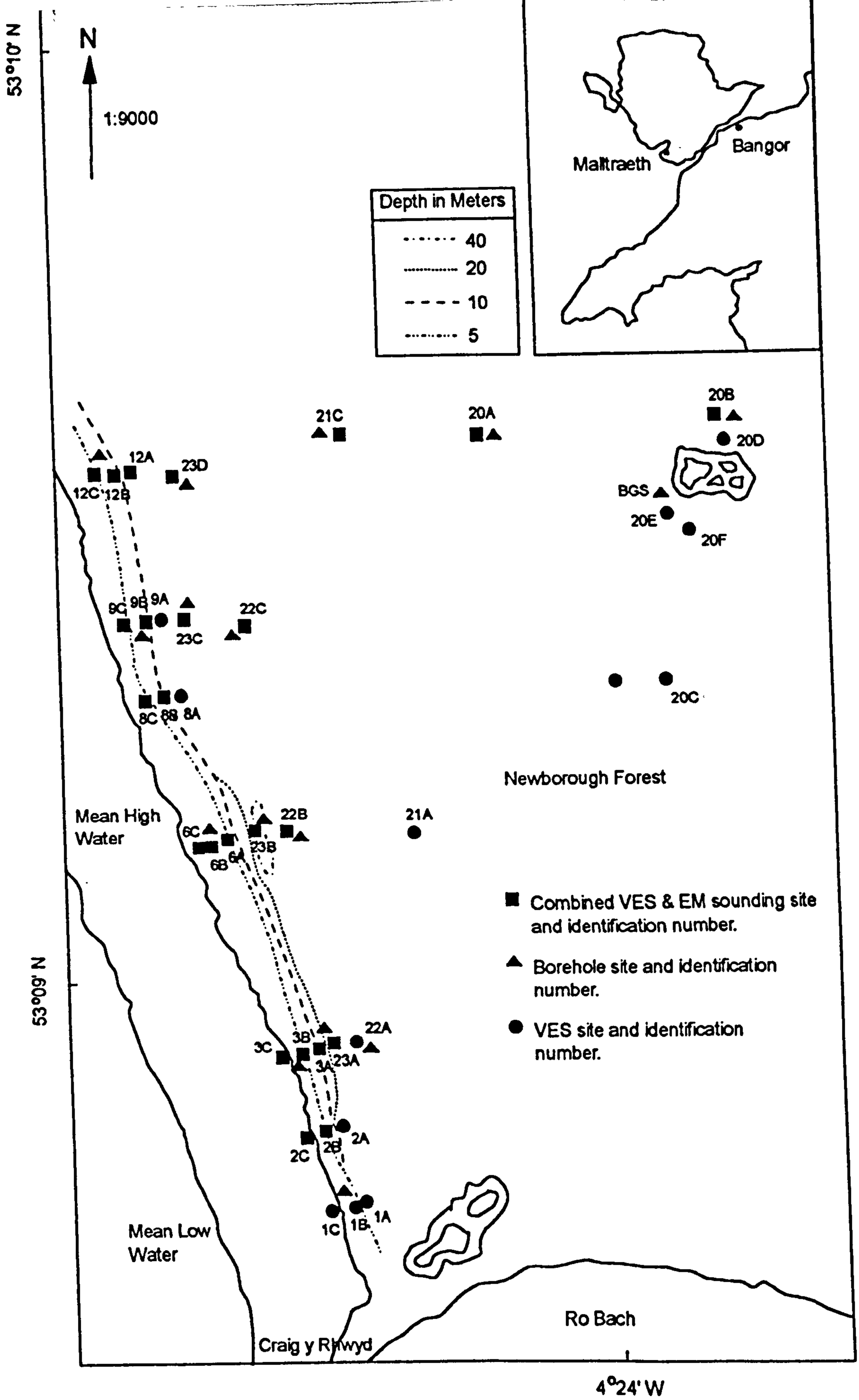

Fig. 7.11. Depth to the bulk resistivity of less than 35 ohm-meters (or more than 250ppm chloride concentration), Malltraeth.

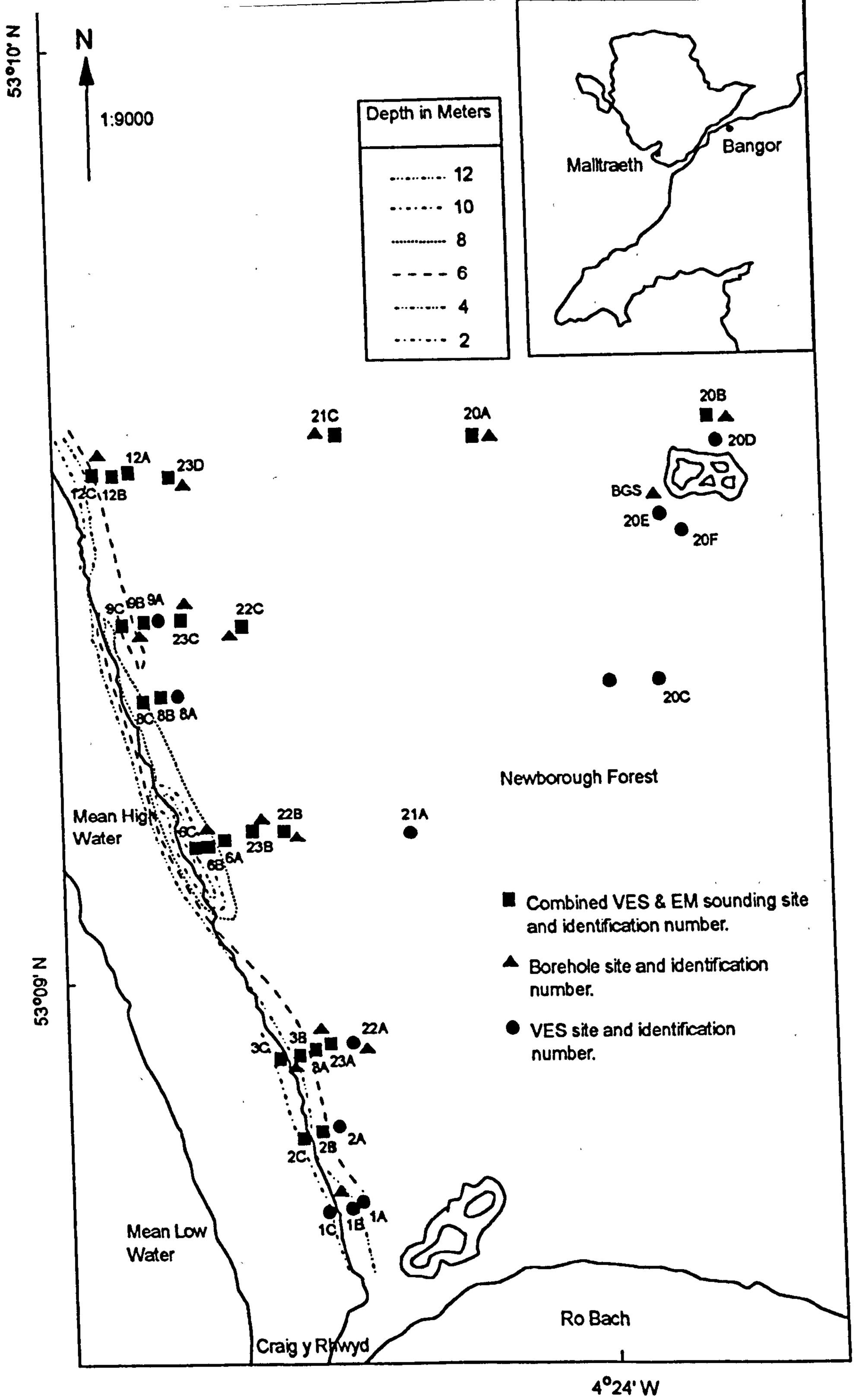

Fig. 7.12. Depth to the bulk resistivity of less than 7 ohm-meters (or more than 500ppm chloride concentration), Malltraeth.

7.3. VES versus EM soundings on dry sand (Dunes)

During the field study in the Malltraeth sand dunes, it was observed that the EM soundings fail to pin-point exactly the depth of the conductive layer, such as the saturated sand layer (aquifer), as compared to the vertical electric soundings. Table 7.7 gives comparative interpreted results of VES and EM soundings carried out at sites 23A, 23B, and 23C, all in the sand dunes. Actual water table levels were also found out at the time of measuring the soundings. However by inserting the actual water table and borehole log data into the interpretive computer program and constraining the program through the known thicknesses of dry upper layers a good fit was obtained Table 7.7a.

7.4 Permeability of sediments and saline intrusion

Permeability of sediments at various sites in the Malltraeth area were determined in the field using the Guelph permeameter and by grain size and constant head permeameter tests in the laboratory. At the auger borehole and VES site 20E, using the value of the resistivity of the porous medium, (R_o) = 99 ohm-m, and that of the resistivity of the fluid, (R_w) = 24 ohm-m, the value of the electrical formation factor was determined. This value was used in the formation factor-permeability log-log plot (Lovell, 1983) to estimate the value of the permeability as given in Table 7.8. The Table 7.8 also summarizes permeability values measured or calculated by different methods. There is very good agreement between the various methods of assessing permeability.

The permeability values obtained for the aquifer in the Malltraeth area prove to

Layer No.	Site 23A		Site 23B		Site 23C	
	VES R / Th	EM R/Th	VES R/Th	EM R/Th	VES R/Th	EM R/Th
1	1300/1.7	1395/2.8	850/2	921/3.3	1785/0.9	1748/3.5
2	257/4.3	325/6.7	391/1.5	415/3.7	628/5.4	712/8
3	64/51	87/44	35/38.9	56/41	63/26.7	89/25.5
4	10/	15/11	15/	18/12	23/	20/13.8
5		85/		76/		88/
W.T. at 5.4m.			W.T at 4.2m.		W.T at 5.8m.	

Table 7.7. Comparative interpreted results of the VES and EM soundings shown with respect to the actual water table depth in sand dunes, Malltraeth.

Site 23A		Site 23B		Site 23C	
VES ohm-m/m	EM ohm-m/m	VES ohm-m/m	EM ohm-m/m	VES ohm-m/m	EM ohm-m/m
1276/1.7	1467/2.4	892/2	2539/2.2	1664/1	2002/2
296/3.7	386/3	293/2.2	3064/2	643/4.8	7050/3.8
63/74	87/48	55/48	56/74	85/16	91/16
12/-	25/8	12/-	24/12	27/-	21/22
-	98/-	-	142/-	-	62/-

Table 7.7a. Comparative re-interpreted results of the VES and the EM soundings, when watertable depth parameters are fixed while inverse modelling program on computer is allowed.

Methods	Permeability (m/sec) min.	max.
1. By Guelph permeameter (field test)	1.1×10^{-4}	5.6×10^{-4}
2. Constant head permeameter (laboratory test)	1.8×10^{-4}	4.1×10^{-4}
3. Grain size (Hazen's formula)	3.7×10^{-4}	5.2×10^{-4}
4. Grain size (Kozeny-Carman)	2.2×10^{-4}	5.1×10^{-4}
5. By using electrical formation factor.	2.2×10^{-4}	

Table 7.8. Shows a list of the permeability values measured or calculated by different methods.

be moderate values and do not come in the category of high values. Water bearing sediments with such permeability values could be classed in a category which minimizes the rate of landward advance of the saline intrusion.

7.5 Discussion

The contour map Figure 7.11 shows the extent of the mixed water zone with salinity of chlorides concentration between 250-500 ppm in the Malltraeth unconfined sand aquifer. In the aquifer the contamination is restricted to a 70-150 metres wide coastal strip. Near the coast it is found at a depth of about 10-40 metres. It is also evident that towards the north (estuarine sediments) of the study area the contamination seems less wide spread as compared to the opposite direction. The saline water, Figure 7.12, with salinity of chlorides concentration of more than 500 ppm appears to occur along a 30-60 metres wide coastal strip. Near the coast line it is found at a depth of 2-12 metres and inland at a depth of 6-8 metres. The saline water also seems to be less wide spread towards the north (estuarine sediments) of the study area as compared to the opposite direction. This is presumably because the sediments are getting finer towards the estuary as the silt/clay content increases. As a consequence permeability decreases which results in the decrease of the saline intrusion.

It is shown in the area that the wide-spread and highly elevated sand dunes act as a catchment area for most of the heavy rainfall and allows infiltration to replenish the groundwater. This continuous recharge of fresh water maintains a fresh water gradient towards the sea and consequently halts the inflow of sea water inland. D'Andrimont (1903) observed that water flows in a dune aquifer toward the sea rapidly enough to prevent sea water infiltration. Hubbert (1940) concluded that the continuous

flow of fresh water to the ocean must be balanced by sufficient recharge to maintain a state of equilibrium between the fresh-salt water bodies. In this study area both conditions are met as there is a continuous flow of fresh water towards the sea and a sufficient recharge to the aquifer from continuous rainfall in the surroundings and particularly on the tops of the dunes.

The permeability values obtained for the sediments in the area are of such moderate values that this feature is another important reason in minimizing the rate of landward advance of the intruding saline water, as Howard (1987) has shown.

It has also been observed that the water table depth and borehole log data are essential in the interpretation of EM soundings as comparable to VES soundings, particularly for the data over the dunes in order to get the best possible computer fit to the data.

In this area the geophysical methods have also demonstrated the provision of information about dipping bed rocks, as well as giving data regarding soft rock sandwiched between hard rock at two ends. This observation in the study area is well supported by Greenly (1919).

It is also shown that the Cefni River possibly had a channel in the past behind the dunes and parallel to the drain shown in the area map, Figure 7.1. The Cefni River's present route is further westward.

CHAPTER 8. CASE HISTORY 3. MORFA BYCHAN AREA

8.1. Introduction and Geology of the area

Morfa Bychan is a small coastal town about 2.5 miles away from Porthmadog, between Criccieth and Porthmadog, and on the northern extremity of Cardigan Bay (location map Figure 8.1). The site is relatively flat, with an average elevation of + 4.50 metres O.D and is bounded to the east and south by sand dunes of the Afon Glaslyn estuary. The site is further bounded to the north and west by low lying relatively marshy ground and drained by open ditches. As per British Regional Geology, North Wales, the site consists of granular material mostly sand, gravels, etc., with intrusive igneous rocks at the base; ground water levels are thought to be high.

The geological and hydrogeological information in the Morfa Bychan area has been obtained from hand-augered boreholes and particularly from the Welsh Water Authority (WWA) borehole logs (Table 8.1.a); these reveal the presence of an unconfined aquifer consisting of unconsolidated fine to medium-grained sand. This is underlain by a layer of boulder clay and then bed rock forming the base of the aquifer, but at some places it is underlain directly by the bed rock. The aquifer is in direct contact with the sea all along the coast.

The results of the mechanical analyses of granular samples obtained during the sinking of the hand auger holes in the Morfa Bychan area are tabulated (see Table 8.1.b). The table shows that there is a predominance of fine to medium grained sand in the aquifer. Due to the dominance of granular material at the ground surface, the aquifer gets recharged from direct percolation of rain water falling on the surface and

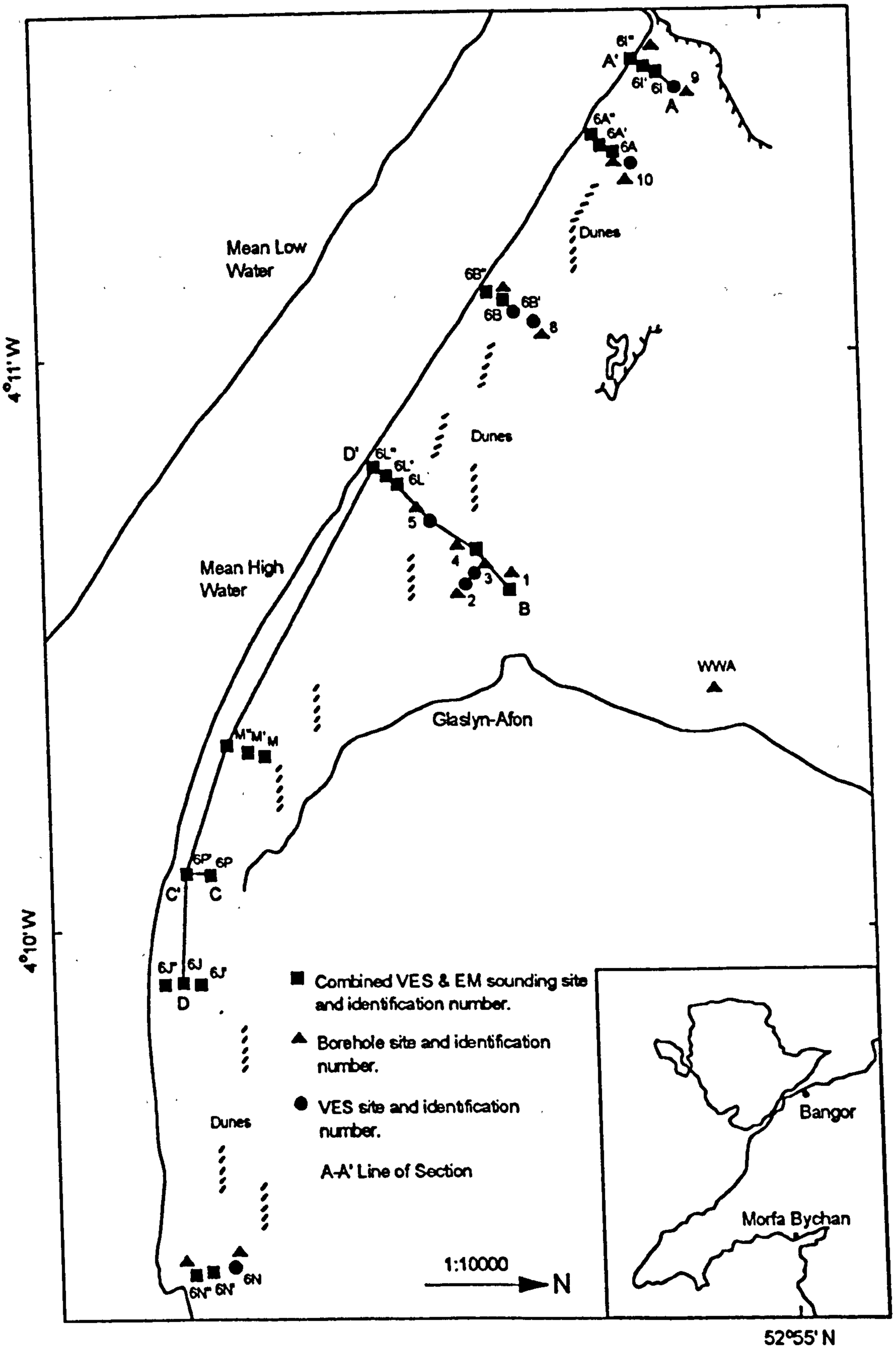

Fig. 8.1. Map showing location of the study area, Morfa Bychan.

Lithology	Depth (m)
Medium sand	0.5
Medium sand with some gravel	2.7
Medium sand	22 Borehole No. 7, Morfa Bychan (Welsh Water Authority).

Table 8.1.a. Geological drill log (Welsh Water-Authority), Morfa Bychan area.

Parameter	Minimum Value	Maximum Value
Porosity	0.40 %	0.45 %
Rainfall	832mm (1991)	1015mm (1992)
Grain Size Content	Minimum Value	Maximum Value
Percentage of sand (depth 1.2m) Fine sand more than medium sand.	98.7	99.6
Percentage of silt and clay (depth 1.2 m)	0.3	1.3

Table 8.1.b. General characteristics of the alluvium.

particularly on the sand dunes. As seen in other areas, most of the rain water infiltrates into the underlying alluvial sand and recharges the aquifer. The water table gradient in the area is towards the sea i.e. the groundwater from the phreatic aquifer moves out into the sea and within the tidal zone in the beach area fresh groundwater is underlain by saline water.

8.2 Detection/Mapping of the Saline-Fresh water Interface using the Geophysical Methods and Hydrochemistry

Thirty-one vertical electric soundings (VES) were made at selected sites (Figure 8.1) using the ABEM Terrameter. Simple Wenner and Offset Wenner arrays were used for this study. Readings were made up to maximum electrode spacings ranging from 80 to 150 metres, using the simple Wenner array, and from 64 to 128 metres for the Offset Wenner.

Twenty-three electromagnetic soundings were also made at selected centres of the sites where previously vertical resistivity soundings were made, using MaxMin I-8 portable equipment (Figure 8.1). Suitable survey sites were limited, compared to the resistivity soundings because of metallic fences, electric poles, etc., which cause erroneous readings.

The interpretive results for all the soundings carried out in the area are given in Table 8.2. Figure 8.2 shows an example of the field data obtained from VES and EM soundings at site 61 together with mathematically fitted curves via the software models alongside their equivalence. The shape of the curves indicate that the current has passed through three geoelectric layers. The model of VES sounding (8.2a) has good

VES number	Layer number1 R (Ω.m)	Th m	Layer number2 R (Ω.m)	Th m	Layer number3 R (Ω.m)	Th m	Layer number4 R (Ω.m)	Th m	Layer number5 R (Ω.m)	Th m
VES 1	950	.5	95	13.7	36	5.9	147		-	
VES 2	211	.4	76	19.6	35		-		-	
VES 3	250	.7	89	21	33		-		-	
VES 4	254	.3	86	20.4	32		-		-	
VES 5	1079	.5	55	17.6	11		-		-	
VES 8	758	.5	69	10.8	132		-		-	
VES 9	895	1.5	76	21.3	400		-		-	
VES10	836	1.2	78	8.9	114		-		-	
6I	7	1.2	32	15	149		-		-	
6I′	4	1.9	12	7.5	55		-		-	
6I″	2	4.9	7	3.5	55		-		-	
6A′	6	1.6	56	11.7	52		-		-	
6A	5	4.6	35	6.7	49		-		-	
6A″	3	5.3	14.7	5.7	49		-		-	
6B′	9	1.1	40	10.4	55		-		-	
6B	4	3.7	29	10.5	48		-		-	
6B″	3	2.9	8.5	6.1	47		-		-	
6L	529	.2	3	5	49	6.7	6		-	
6L′	3	4.2	44	5.1	3	25.1	12		-	
6L″	2.5	4.6	22	3.7	3	27.3	10		-	
6P	92	5.5	20	18.7	3	22	8		-	
6P′	11	1.2	90	2.3	9	17.7	3	25	6	
6J′	2026	.4	41	19.6	2	23.2	39		-	
6J″	12	3.7	36	12.3	1.6	27.2	34		-	
6J	7.2	4	11	16.2	1.4	34.4	30		-	
6M	610	0.6	33	16	3	-	-		-	
6M′	114	0.2	6	3	59	7	1		-	
6M″	2.5	3	12	17	1.4		-		-	
6N	1154	2.3	117	21.4	14		-		-	
6N′	402	1.6	61	18	3	27.3	57		-	
6N″	2	3.4	7	13.4	3	30.4	52		-	

Table 8.2. Multilayer sounding results.
R = Resistivity, Th = Thickness.

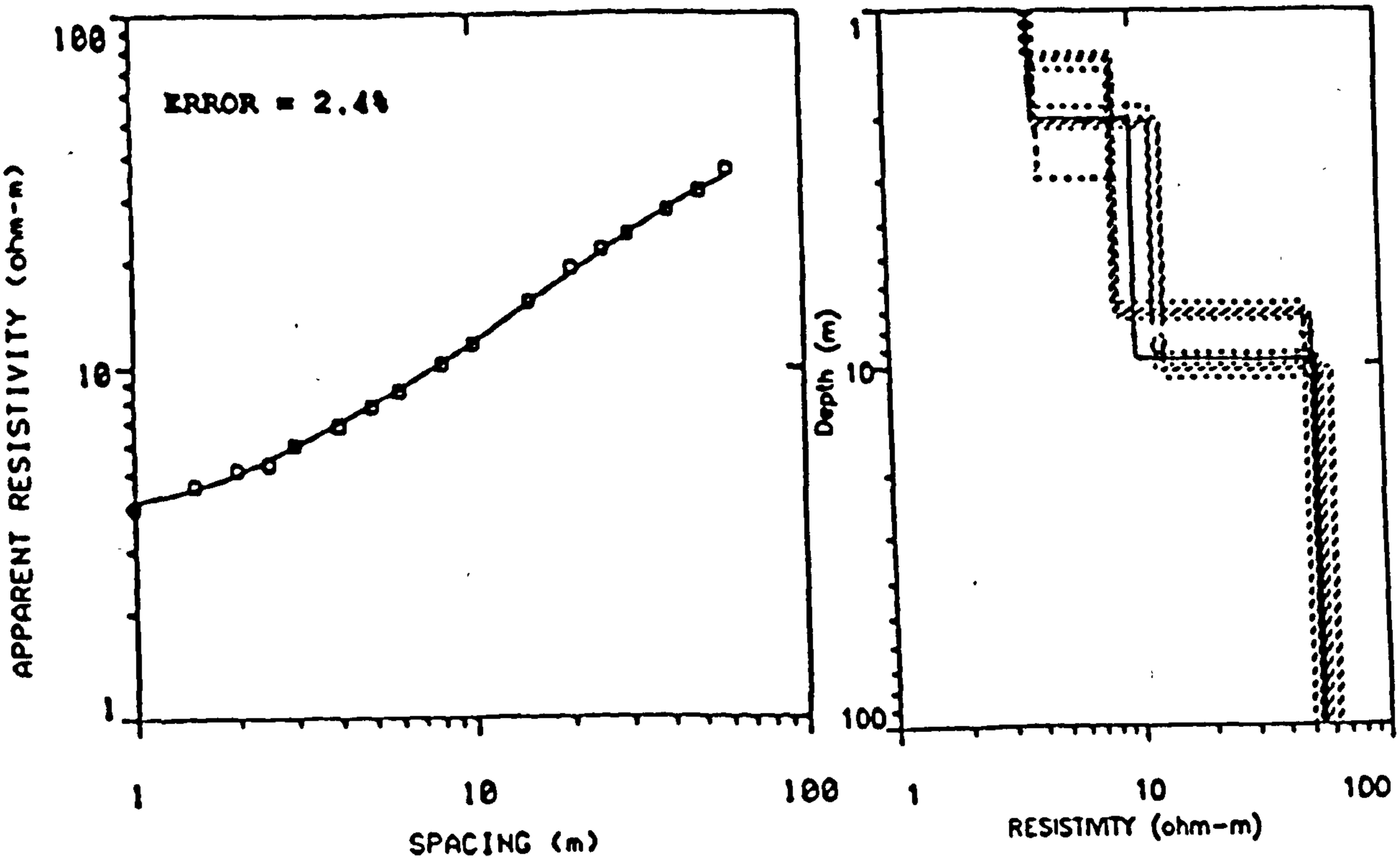

(a)

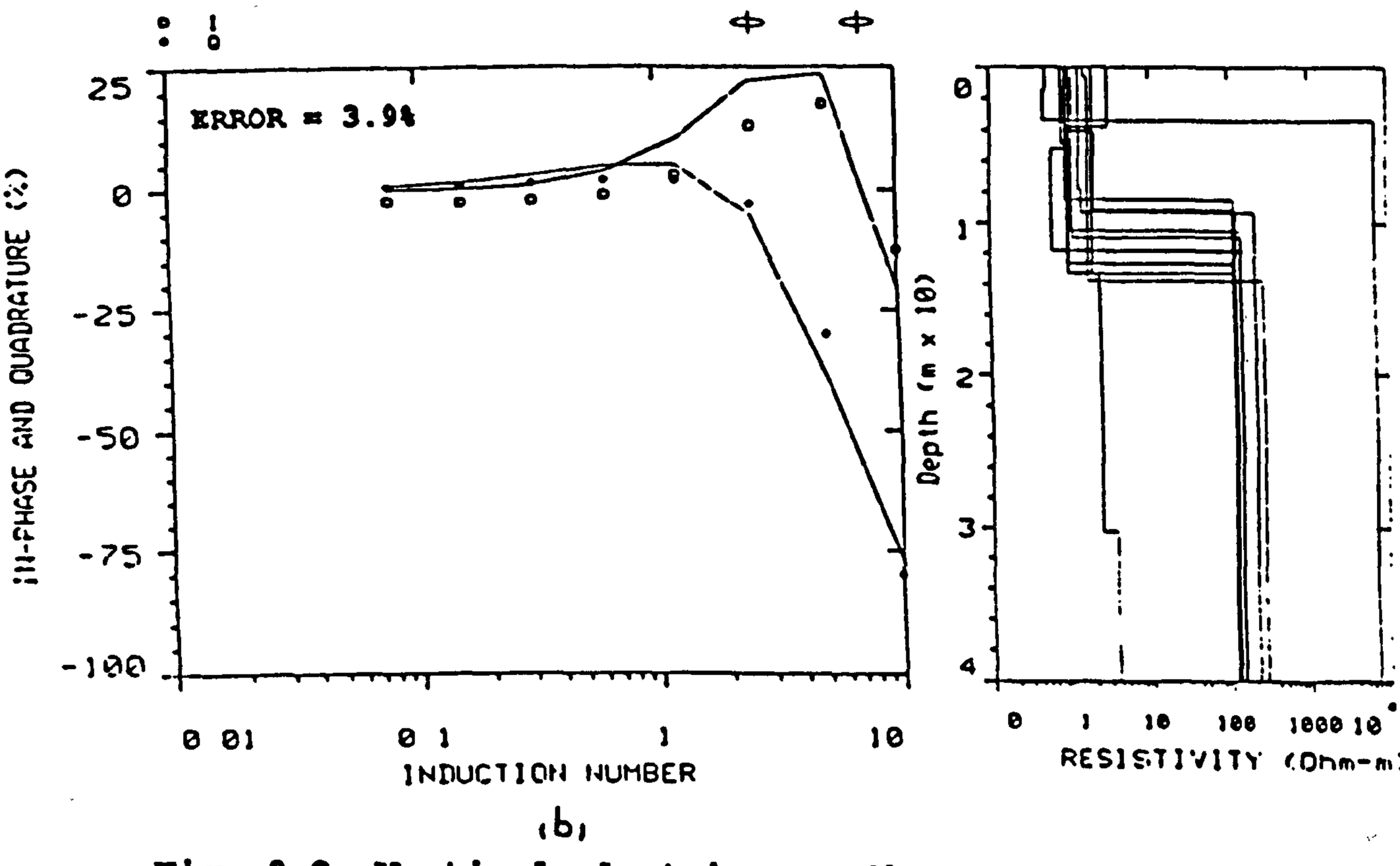

(b)

Fig. 8.2. Vertical electric sounding curve (a) and electromagnetic sounding curve (b) at site (6I′) based on field data points, alongside their equivalence curves.

agreement with the model of EM sounding (8.2b). The equivalence bounds of DC resistivity sounding or EM sounding results at site 6I' are given in Appendix Table 8I and 8J respectively. Table 8.3 shows the comparision of the geological drill log in the hand augered hole at site 6I′ and the Welsh Water Authority drilled log in the area (see area map Figure 8.1) with the interpreted results of the VES and EM soundings carried out at the same site.

The construction of geoelectric sections is an intermediate stage in the preparation of various contour maps. A geoelectric section A-A′, drawn perpendicular to the coast line and across various sites of VES and EM soundings such as VES 9, 6I, 6I′ and 6I", as well as hand augered holes is shown in Figure 8.3 (see area map Figure 8.1). Arrows at top of the cross section shows VES or VES and EM combined sounding locations. Section A-A′ shows that there is a unconfined aquifer with resistivities ranging from 2 ohm.m (and 7 ohm.m below it) at the coast to 895 ohm.m (and 76 ohm.m below it) inland. The bedrock below the aquifer layer has resistivities ranging from 55 ohm-m (coast) to 400 ohm-m (inland). The unconfined aquifer has saline water (demarcated by curved line) with resistivities ranging from 2 ohm-m (coast) to 7 ohm-m (inland) with chloride concentration more than 500 ppm. In the beach area, the saline water (in the topmost layer), presumably formed by tidal and wave action appears to rest on the mixing zone. The saline fresh water interface separates saline water from the mixing zone. The mixing zone has resistivities ranging from 8 ohm-m to 35 ohm-m with chlorides concentration between 250-500 ppm. Another curved line drawn in the Figure 8.3., shows the mixing zone separated from fresh water. The saline water zone and the mixing zone abruptly end at the seaward foot of the sand dunes, which suggests that the large amount of fresh water regularly received by the aquifer from rainwater prevents the saline water from penetrating

Layer No.	VES Sounding R(ohm.m)	Th(m)	EM Sounding R(ohm.m)	Th(m)	Geological Drill Log
1	4	1.9	7	2.4	Fine to medium sand.W.T 0.3m. Depth 0.5m.
2	12	7.5	10	9	Saturated sand some gravel, WWA borehole log, Table 8.1a.
3	55		618		-

Table 8.3. Vertical electric and electromagnetic soundings 6I interpreted data with geological log, Morfa Bychan area.

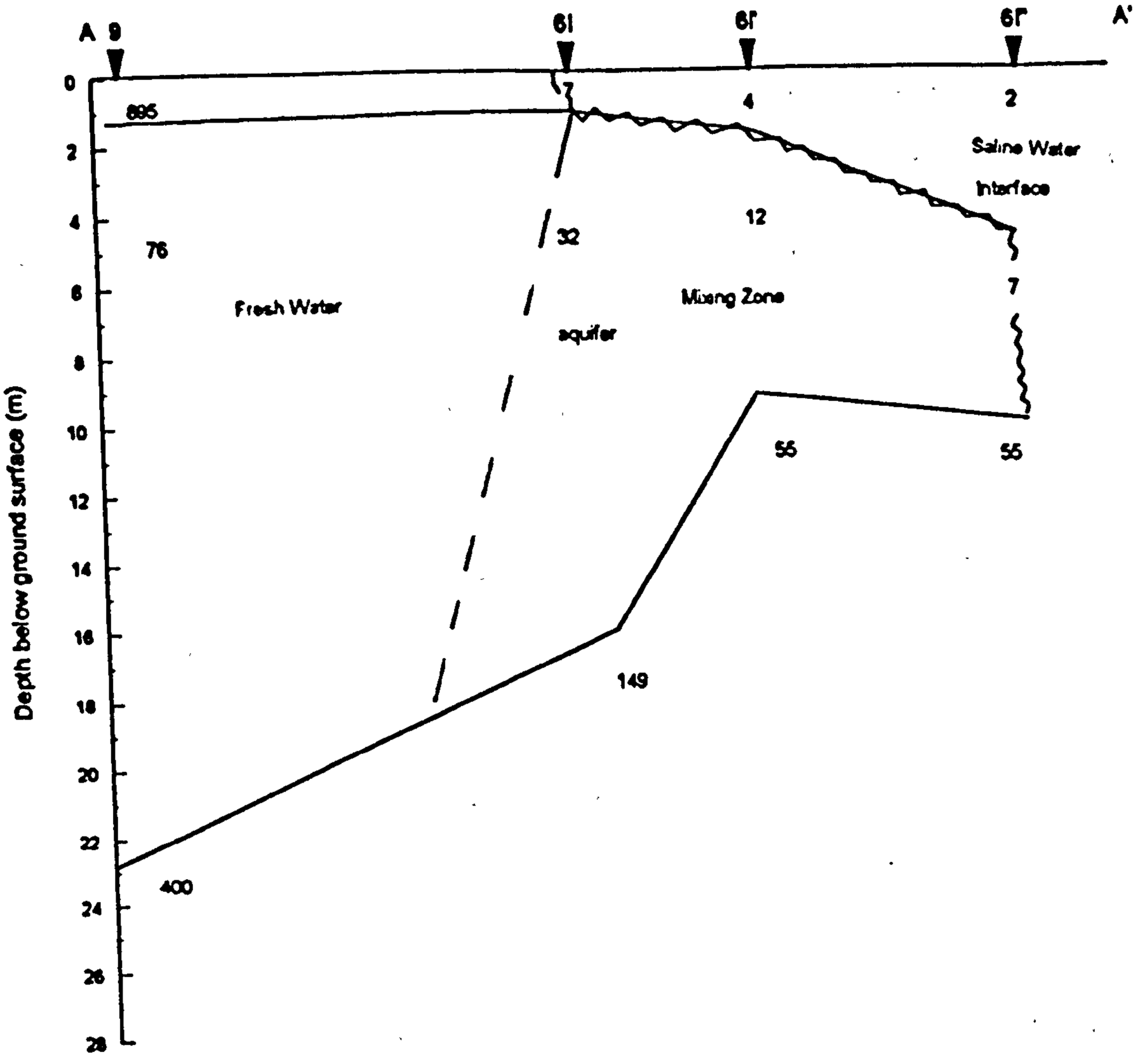

Fig. 8.3. Geoelectric section A-A' derived from vertical electric and electromagnetic soundings.
Resistivities in ohm-m.
Scale: Hor: 1:750, Vert: 1:200.

further inland. Figure 8.3.a shows the section A-A′ has been drawn after incorporating the surface levelling measurements in the values of Figure 8.3. It is evident from the Figure 8.3.a that the fresh water gradient is towards the sea.

Figure 8.5 shows a second geoelectric section B-D′ drawn perpendicular to the coast across various sites of VES or VES and EM soundings and hand augered holes (see Figure 8.1). The arrows at the top of the cross section show VES or VES and EM combined sounding locations. The interpreted results of all the soundings along this section is given in Table 8.2. Figure 8.4 shows (a) the VES curve and (b) EM sounding curve at site VES 1. Table 8.4 gives the interpreted VES and EM soundings at VES 1 compared to each other and to the geologic log. This section shows that there is one aquifer consisting of the sand layer. The saline water lying at the top, and presumably formed because of tidal and wave action, has resistivities ranging from 2.5 ohm.m to 3 ohm.m with chloride concentration more than 500 ppm. The interface separates saline water from the mixing zone. The mixing zone has resistivities ranging from 22 ohm.m to 35 ohm.m with chloride concentration 250 ppm or much higher values. A broken line drawn in the section shows the mixing zone separated from fresh water. It is evident in Figure 8.5 that fresh water begins right at the seaward foot of the dune, showing clearly again that the precipitation on the dune sand is playing an important role in preventing the saline water from intruding deep inland. A layer of boulder clay lies below the aquifer with resistivities changing slightly from 3 ohm-m (coast) to 36 ohm.m (inland). The base of this section appears to be bedrock with resistivities ranging from 10 ohm-m (coast) to 147 ohm-m (inland).

A third geoelectric section C-C′ (Figure 8.7) drawn perpendicular to the coast and across two soundings 6P and 6P′ and hand-augered holes (see Figure 8.1). The

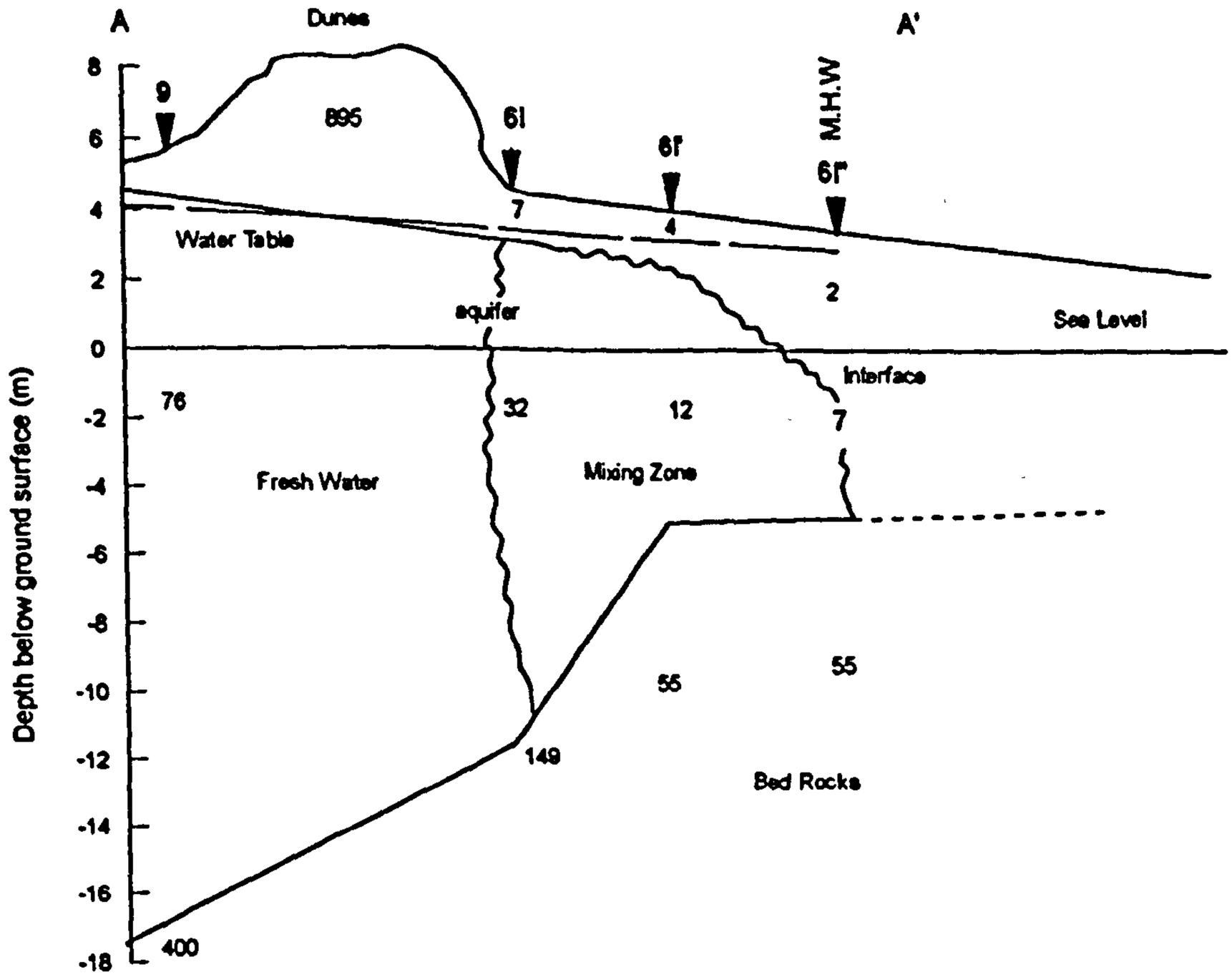

Fig. 8.3.a. Saline and fresh water interface along line A-A'

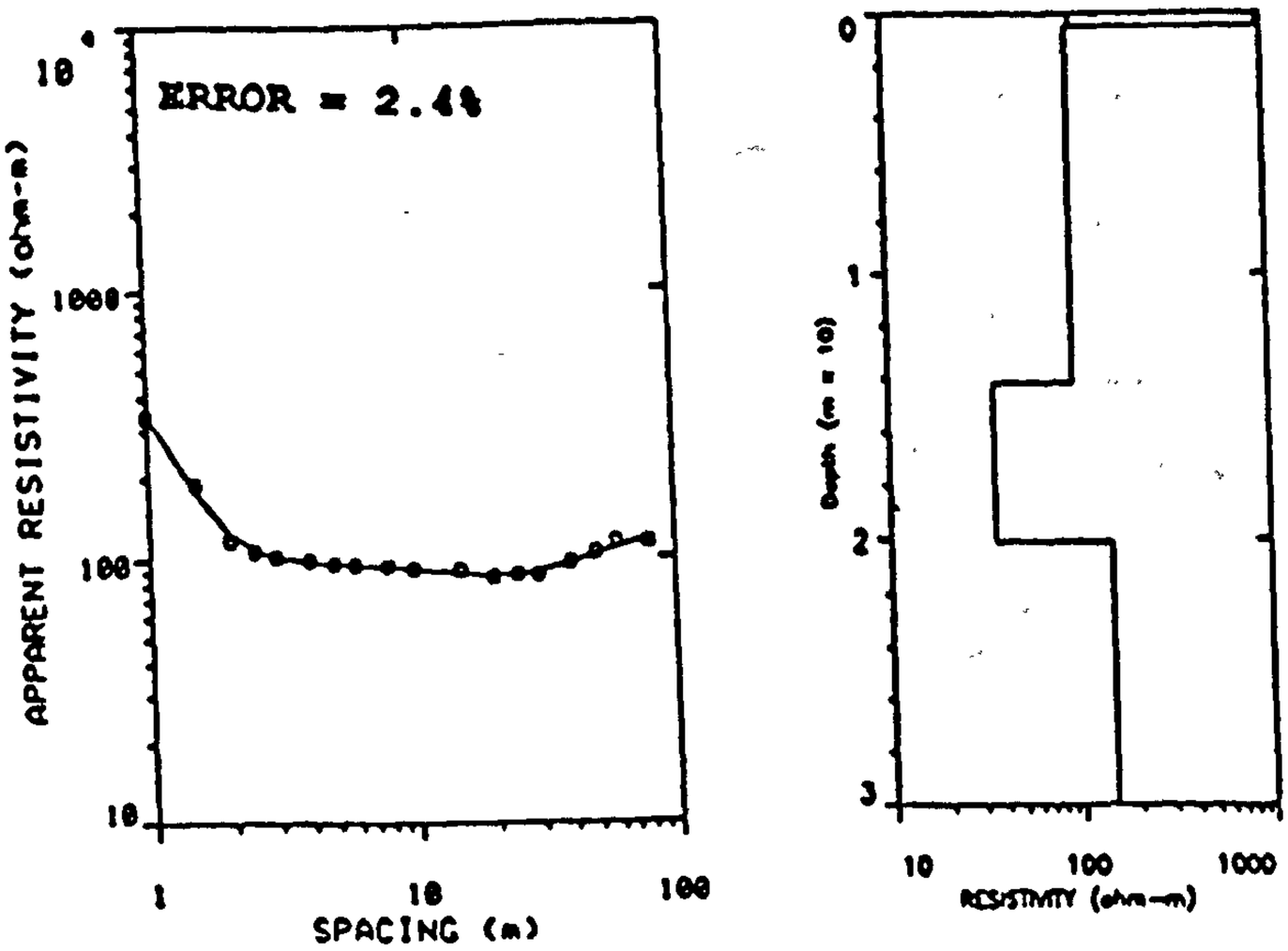

(a)

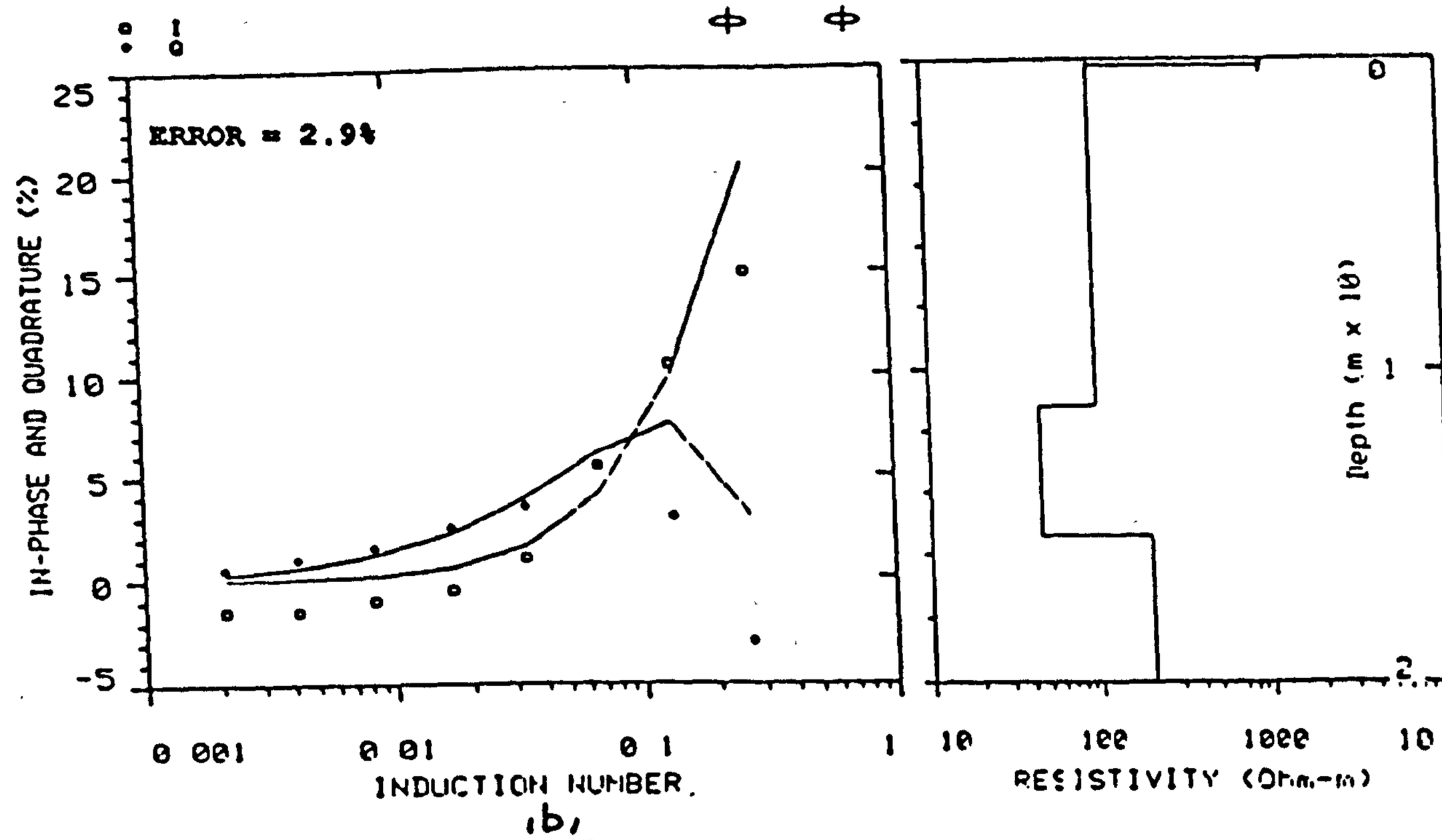

(b)

Figure 8.4. Vertical electric sounding curve (a) and electromagnetic sounding curve (b) at site VES 1 based on field data points.

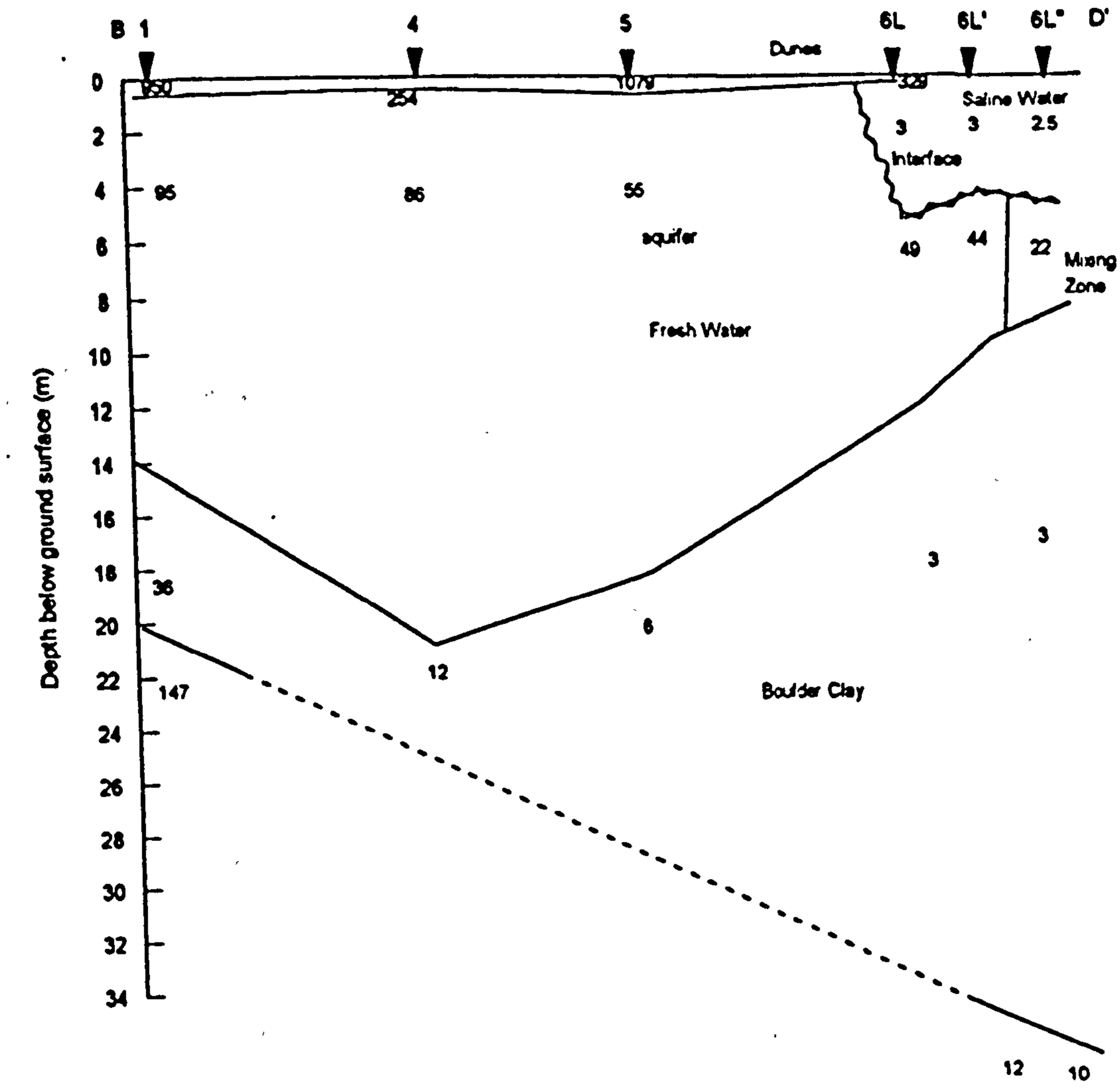

Fig. 8.5. Geoelectric section B-D' derived from vertical electric and electromagnetic soundings.
Resistivities in ohm-m.
Scale: Hor: 1:2000, Vert: 1:200.

Layer No.	VES Sounding R(ohm.m)	Th(m)	KM Sounding R(ohm.m)	Th(m)	Geological Drill Log
1	950	0.5	1041	0.2	Medium to fine sand.W.T 1.2m. Depth 1.5m.
2	95	13.7	99	11	Saturated sand some gravel, WWA borehole log. Table 8.1a.
3	36	5.9	45	4.2	-
4	147		200		-

Table 8.4. Vertical electric and electromagnetic soundings VES 1 interpreted data with geological log, Morfa Bychan area.

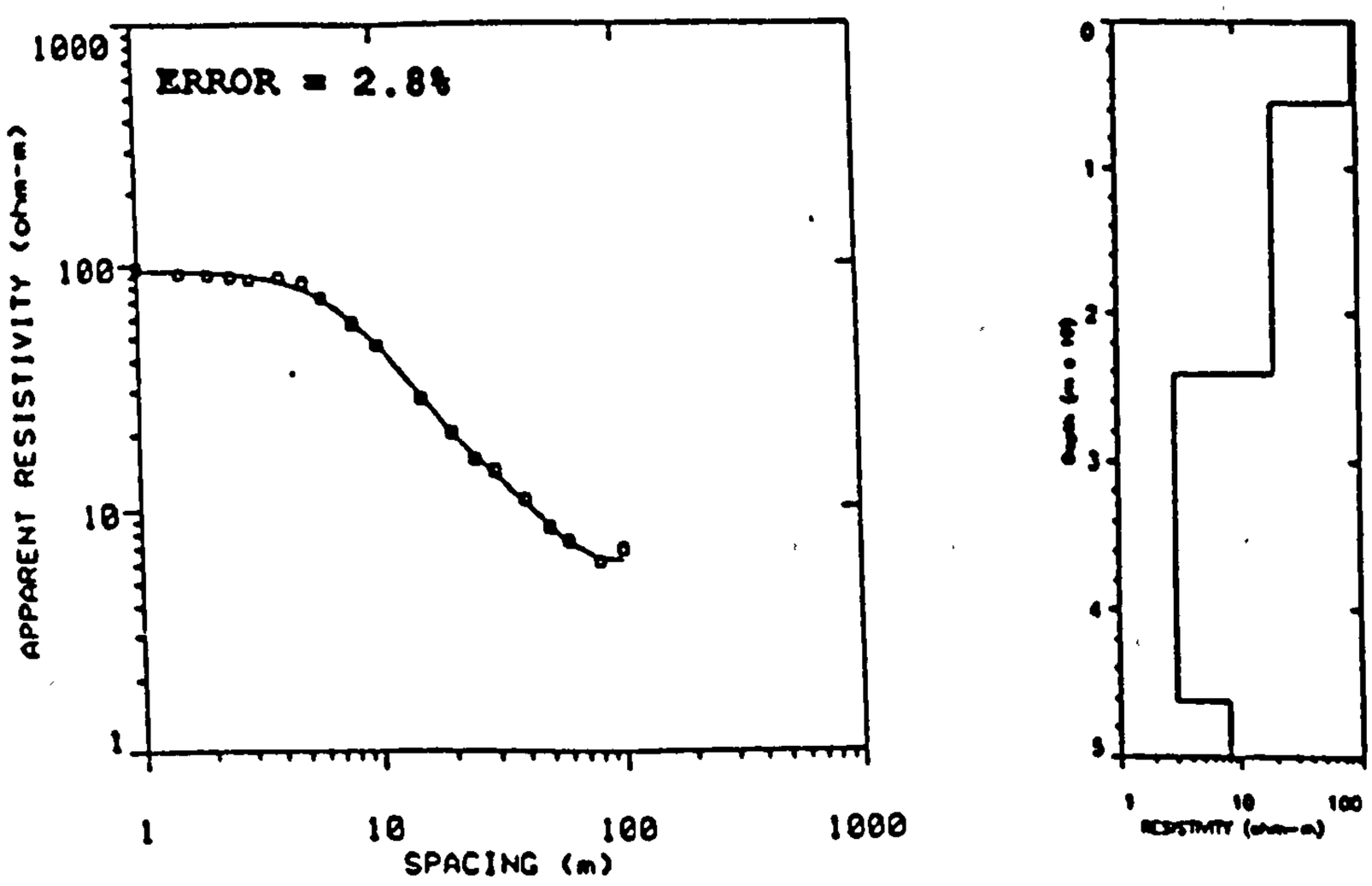

(a)

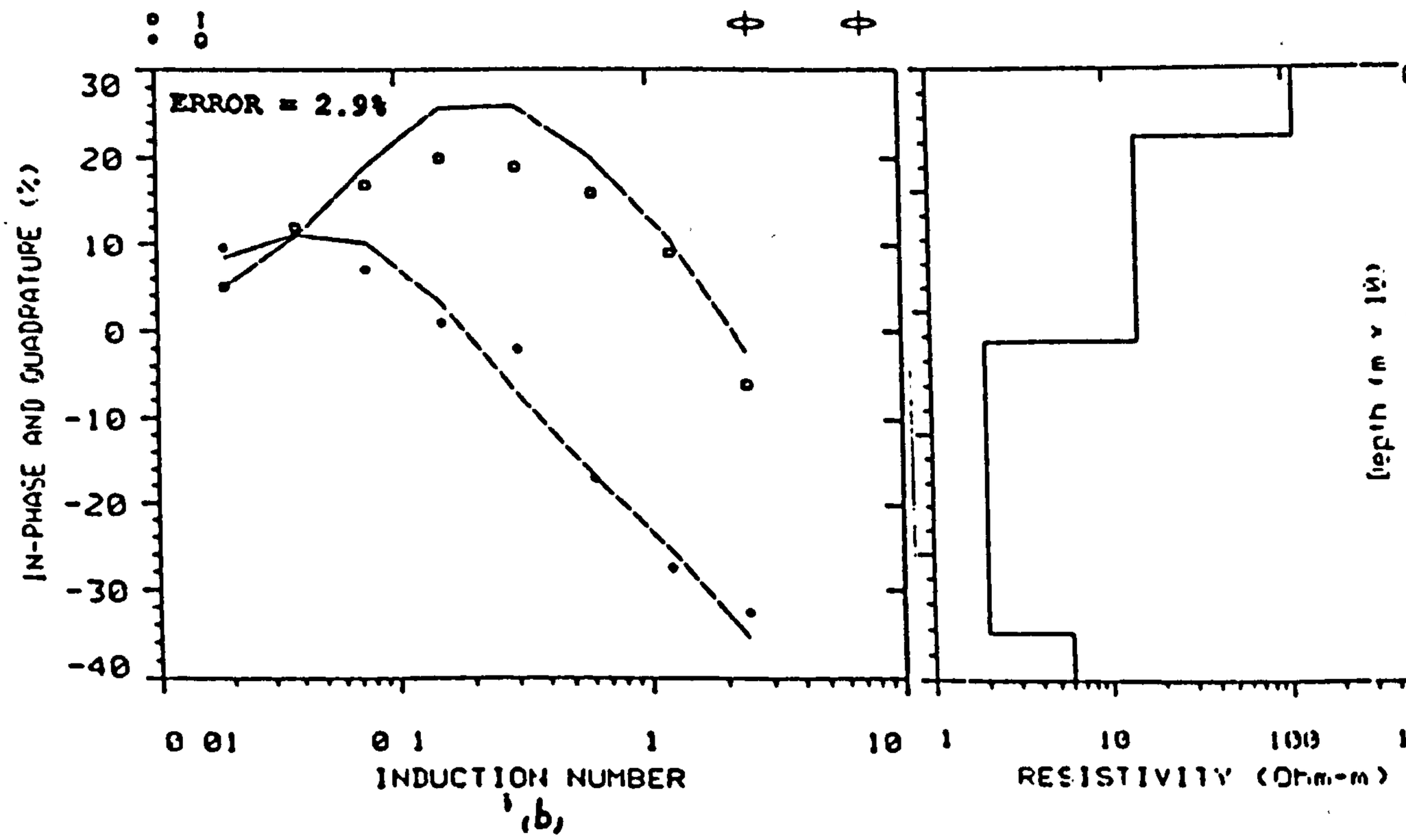

(b)

Figure 8.6. Vertical electric sounding curve (a) and electromagnetic sounding curve (b) at site 6P based on field data points.

interpreted results of soundings are given in Table 8.2. Figure 8.6 shows (a) the VES sounding curve and (b) the EM sounding curve at site 6P. Table 8.5 gives the interpreted comparative VES and EM soundings 6P with the geologic log. As before this section shows that there is one aquifer consisting of a sand layer. However there is a peculiar feature in this section in that very fresh water, with resistivities 90 ohm.m and greater, is found in the surface layer at sounding site 6P whereas at sounding site 6P′ the fresh water is sandwiched between two mixing zones. As this site is at the end point of Afon Glaslyn it is possible that a lot of fresh water is regularly infiltrated into the aquifer at this site. The mixing zone in the top layer at site 6P′ is presumably formed by tidal and wave action. The second mixing zone below the fresh water has resistivities between 9 to 20 ohm.m with the chloride concentration having values higher than 250 ppm. Below this is a boulder clay layer with a resistivity 3 ohm.m. Bedrock with resistivities ranging from 6 to 8 ohm.m defines the base of the section. It is worthwhile mentioning here that from the Welsh Water Authority drill logs, sand down to a depth of 22 metres is found. However in this study the interpreted results of the VES and EM soundings measured near the coast would seem to indicate that boulder clay lies between the sand and bedrock. It may well be that as the WWA borehole is well inland the clay is a transient feature.

A fourth and final geoelectric section D-D′ (Figure 8.8) is the longest in the study area, drawn parallel to the coast and across sounding sites 6J", 6P′, 6M" and 6L". This section shows a single aquifer consisting of a sand layer. It is evident in the section that saline water with resistivity 2.5 ohm.m and chlorides more than 500 ppm, presumably formed by tidal and wave action, is overlying a mixing zone. At sounding site 6P′ very fresh water (more than 2 metres of aquifer thickness) in the south of Afon Glaslyn lie below mixing zone. This shows an hydraulicly unstable situation where

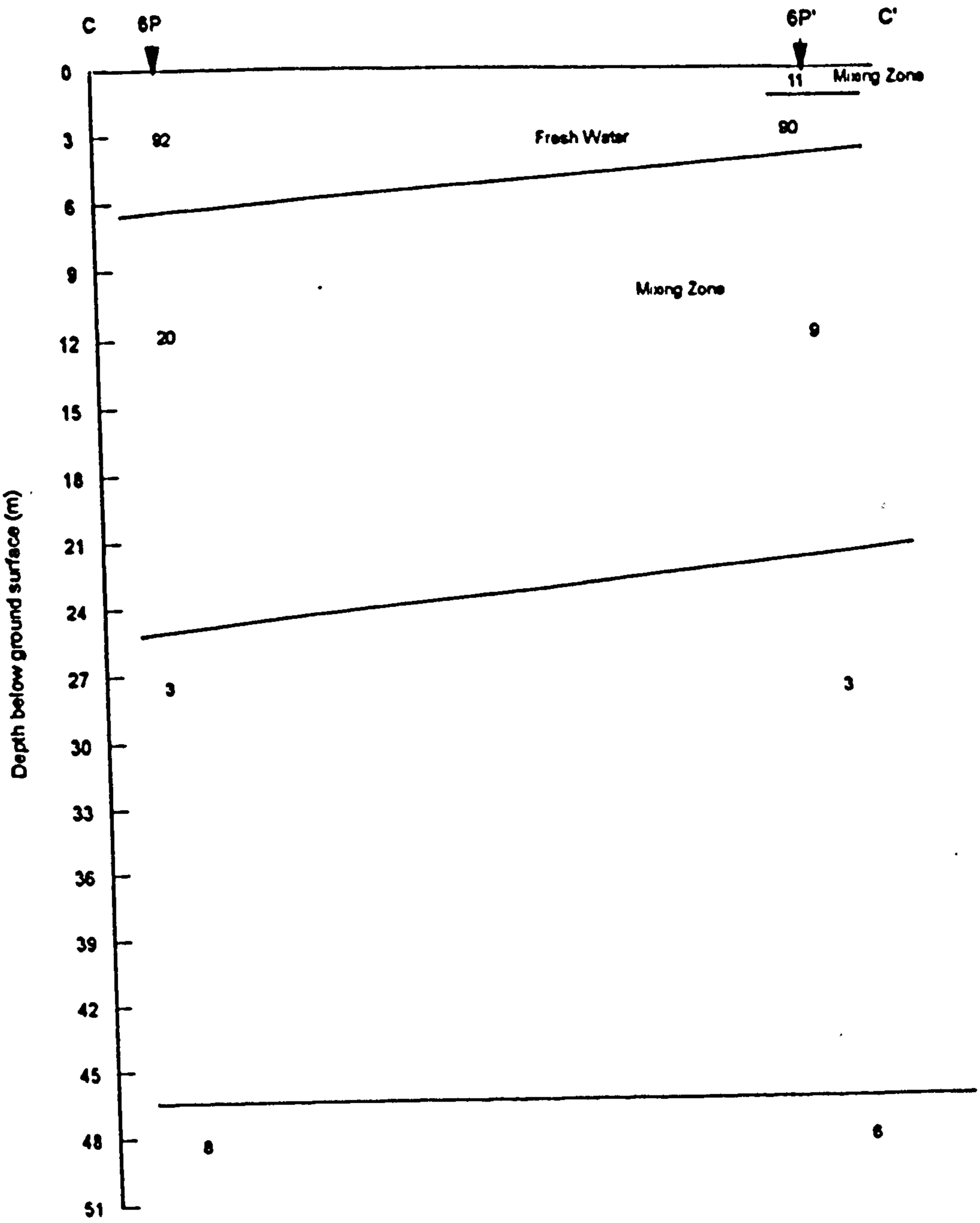

Fig. 8.7. Geoelectric section C-C' derived from vertical electric and electromagnetic soundings.
Resistivities in ohm-m.
Scale: Hor: 1:400, Vert: 1:300.

Layer No.	VES Sounding R(ohm.m)	Th(m)	EM Sounding R(ohm.m)	Th(m)	Geological Drill Log
1	92	5.5	114	5.5	Fine to medium sand. W.T 0.8m. Depth 1.0m.
2	20	18.7	15	16.9	saturated sand some gravel, WWA borehole log. Table 8.1a.
3	3	22	2	23.9	-
4	8		6		-

Table 8.5. vertical electric and electromagnetic soundings 6P interpreted data with geological log, Morfa Bychan area.

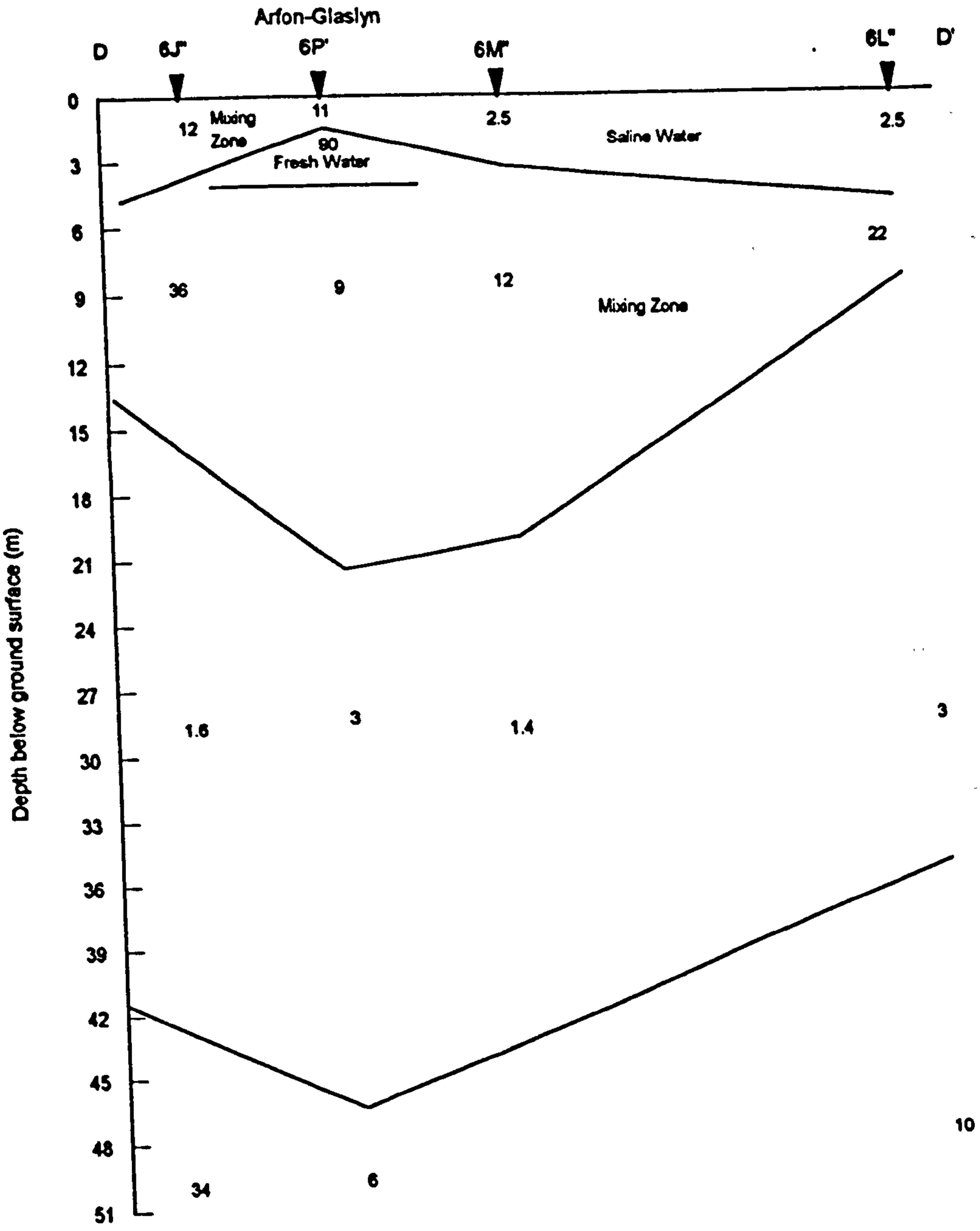

Fig. 8.8. Geoelectric section D-D' derived from vertical electric and electromagnetic soundings.
Resistivities in ohm-m.
Scale: Hor: 1:10000, Vert: 1:300.

either the mixing zone or the saline water overlies fresh water. Consequently further encroachment of seawater is to be expected. The mixing zone below the fresh water zone has resistivities ranging from 9 to 35 ohm-m and chlorides between 250-500 ppm. The other very important feature appears to be that the Afon Glaslyn in its present coarse seems not to have deviated from its original coarse. Below the mixing zone appears to be boulder clay with resistivities ranging from 1.4 to 3 ohm-m. Finally there is the bedrock with resistivities from 6 to 34 ohm-m.

The last stage of the definition of the saline-fresh water interface is the construction of interface contour maps to detect the extent to which the saline water has intruded inland. All the geoelectric sections have been used in the construction of these maps. The map Figure 8.9 shows the extent of the mixing water zone with bulk resistivity less than 35 ohm-m and chlorides between 250-500 ppm. The map further shows that the contamination of fresh water with saline water in the aquifer appears to occur along a 50-150 metres wide coastal strip. Near the coast it is found at a depth of 5 metres, whereas inland it is found at a depth of 20 metres excepting at one site south of Afon Glaslyn where it is found at the greater depth of 25 metres. The reason quite obviously is the regular infiltration of fresh water underground which in turn pushes down any intrusion of sea water.

Saline water is approximately defined by 7 ohm-m with chlorides more than 500 ppm. Figure 8.10 is a contour map drawn showing the zone of saline water; this appears to occur along a 40-100 metres wide coastal strip. Near the coast line it is found at a depth of 2 metres and inland 8 to 16 metres. It is evident from the map that south of the Afon Glaslyn the saline water zone is very narrow and pushed towards the coast as compared to other coastal parts clearly related to the infiltration of fresh water

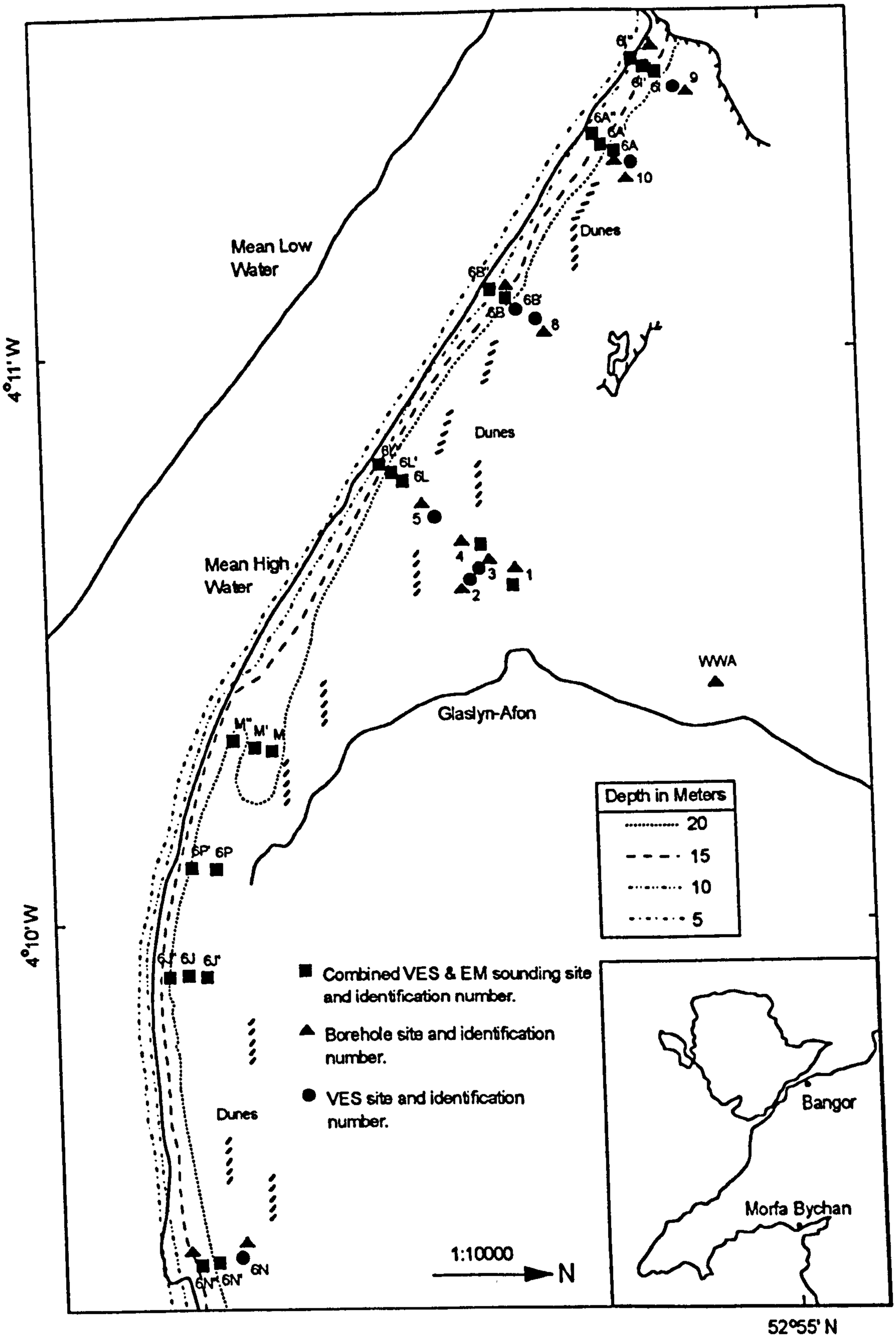

Fig. 8.9. Depth to the bulk resistivity of les than 35 ohm-meters (or more than 250ppm chloride concentration), Morfa Bychan.

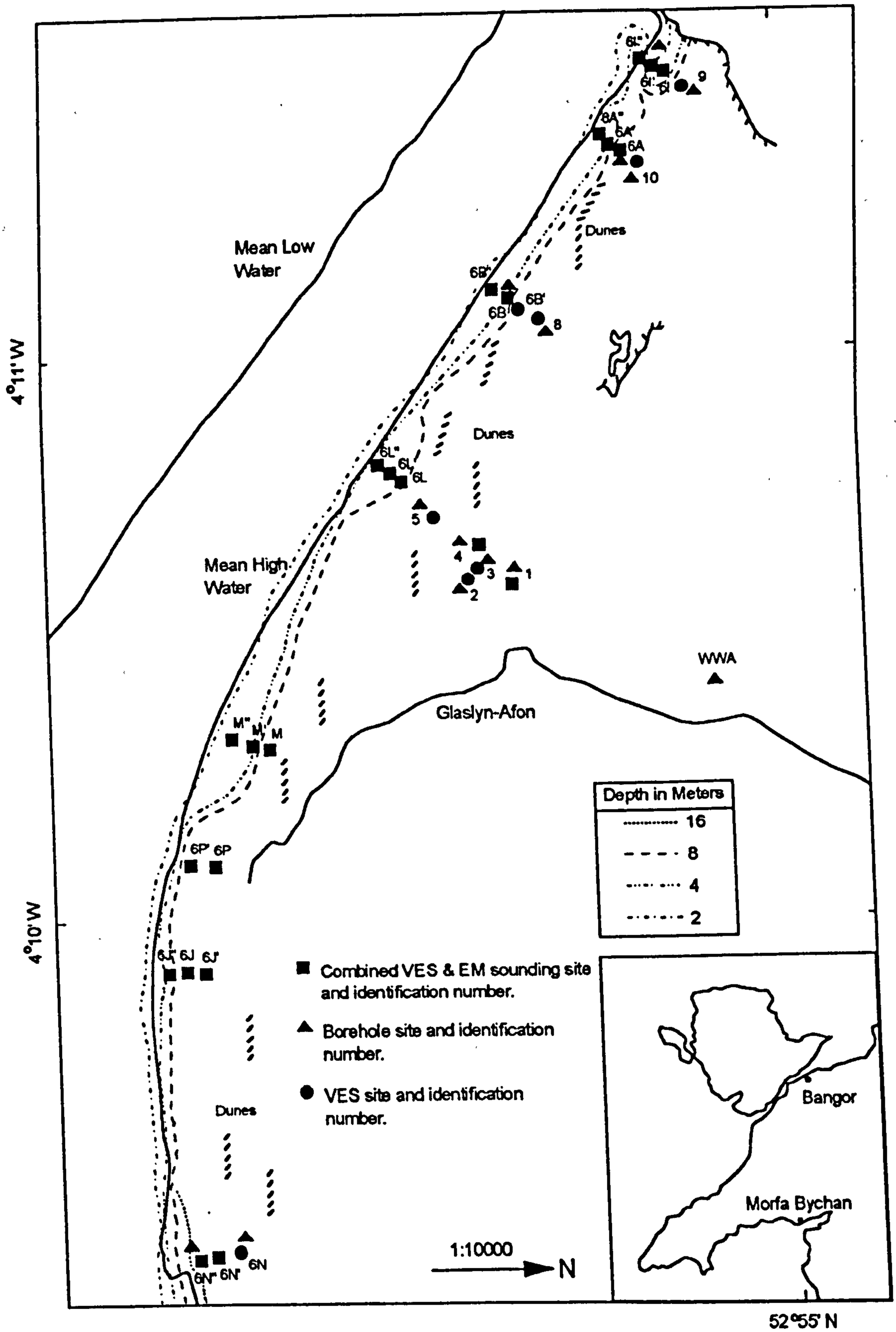

Fig. 8.10. Depth to a bulk resistivity of less than 7 ohm-meters (or more than 500ppm chloride concentration) Morfa Bychan.

underground which prevents the advancement of the saline intrusion inland. Sand dunes behind the beach simultaneously act as barriers also, while behaving as a catchment area for the interception of rain water which infiltrates rapidly to the aquifer and assisting the fresh water in restricting the advance of the saline intrusion inland.

8.3 Permeability of sediments and saline intrusions

The permeability of sediments at various sites in the Morfa Bychan area were determined in the field using the Guelph permeameter and in the laboratory by grain size and constant head permeameter tests. At auger borehole and VES site 1, using the value of the resistivity of the porous medium, (R_o) = 95 ohm-m, and that of the resistivity of the fluid, (R_w) = 24 ohm-m, the value of the electrical formation factor was determined. This value was used in the formation factor-permeability log-log plot (Lovell, 1983) to estimate the value of the permeability as given in Table 8.6. This table also summarizes permeability values measured or calculated by different methods. There is some considerable consistency between the methods. Another Table 8.6a shows the in-situ permeability tests carried further inland (see Map 8.1) by the Welsh Water Authorty. These results were obtained at different depths and it is clear that there is a difference of two magnitudes even at the same depth when the method of testing changes.

The permeability values obtained for the aquifer in the Morfa Bychan area prove to be more moderate values and do not come into the category of high values. Water bearing sediments with such permeability values could be classed in a category which minimizes the rate of landward advance of the saline intrusion.

Methods	Permeability (m/sec) min.	max.
1. By Guelph permeameter (field test)	7.5×10^{-5}	1.0×10^{-4}
2. Constant head permeameter (laboratory test)	1.0×10^{-4}	3.2×10^{-4}
3. Grain size (Hazen's formula)	1.1×10^{-4}	3.6×10^{-4}
4. Grain size (Kozeny-Carman)	1.2×10^{-4}	2.9×10^{-4}
5. By using electrical formation factor.	2.4×10^{-4}	

Table 8.6. Shows a list of the permeability values measured or calculated by different methods.

Borehole No.	Test Depth (m)	Falling/Rising Head Test	m/sec
7	1.61	Falling	1.0×10^{-6}
	8.0	Falling	1.2×10^{-7}
	8.0	Rising	2.0×10^{-5}

Table 8.6a. In-situ permeability tests by the Welsh Water Authority.

8.4 Discussion

It is observed that the continuous supply of fresh water in Afon Glaslyn from upstream, restricts the saline intrusion to a greater depth as well as to the narrowest strip as compared to the coastal area surrounding the Afon Glaslyn. Sand dunes in the area also prevent the inland advance of the saline intrusion as the heavy rainfall is quickly infiltrated towards the sea, which helps in maintaining the fresh water gradient towards the sea, as D'Andrimont (1903) and Hubbert (1940) have shown.

The permeability values are more of moderate magnitude and thus this is another important reason in minimizing the rate of landward advance of intruding saline water, as Howard (1987) has shown.

It is also observed that the Afon Glaslyn's present course still lies along its old route and there has been no deviation with the passage of time.

CHAPTER 9. GENERAL DISCUSSION

The principal aims of this project were to consider the use of geophysical electrical techniques to detect and map saline intrusions into groundwater and to examine the various parameters affecting such use, the ultimate aim being to use such techniques to examine similar problems in Pakistan. To achieve these aims three coastal/estuarine sites were chosen: the College Farm at Aber; the Cefni estuary at Malltraeth on the Isle of Anglesey; and the beach area at Morfa Bychan at the northernly edge of Tremadog Bay. Several features emerged from this investigation:

1) General characteristics of the three sites investigated

The College Farm area at Aber, is situated on the coast at the outfall point of the Aber river near Llanfairfechan in Gwynedd (Figure 6.1). The Aber river passes through the centre of the study area. The lithology comprises surface fill, sand and gravel, silts and clays, peat, Irish sea till and Welsh till. There is a major fault scarp passing some distance away from the study area. The investigation identifies two aquifers upper and lower in the area separated by glacial till and they are both in direct contact with the sea all along the coast. The bed-rock seems to lie quite deep in the area as the soundings could not pinpoint them even down to the depth of about 45 metres. Average rainfall per year in years 1991 and 1992 was 1050mm. Using Cooper et al (1964) Equation, an approximate rate of flow of the fresh water to the coast is estimated to be 50 m^3/day/m.

The Malltraeth area forms a large flat bottomed valley in the southern portion of Anglesey (Figure 7.1). The study area lies at the mouth of the Cefni river. The

Newborough forest site which forms a part of the Malltraeth area is separated from Malltraeth beach by very high and broadly spread dune sands, lying parallel to the Malltraeth beach. This site consists of a sand body of some 20 metres in thickness overlying boulder clay with bed-rock at about 15-30 metres depth. A major dislocation the 'Berw' fault runs across the area. The experimental data shows a single unconfined aquifer in the area which is in direct contact with the sea all along the coast. Average rainfall per year in years 1991 and 1992 was 850mm. An approximate rate of flow of the fresh water to the coast comes out to be 12 m^3/day/m.

Morfa Bychan is a coastal area lying about 2.5 miles to the west of Porthmadog and on the northern extremity of Cardigan Bay (Figure 8.1). The area is bounded to the east and south by coastal sand dunes and to the north and west by low lying relatively marshy ground drained by open ditches. The small river Afon Glaslyn flows through the area. The site consists of granular material mostly sand, minor gravel, boulder clay with intrusive igneous rocks at the base. As at Morfa Bychan there is a single unconfined aquifer in the area which is in direct contact with the sea all along the coast. Average rainfall per year in years 1991 and 1992 was 925mm. An approximate rate of flow of the fresh water to the coast comes out to be 5 m^3/day/m.

The saline intrusion in all 3 sites was identified as a sea water intrusion on the basis of chloride/bicarbonate ratio.

2) Effects of rivers, dunes and rain recharge on saline intrusion

From the data of the three case studies (chapters 6,7 and 8) it is observed that the high rainfall in these areas keep the natural flow in the rivers continuously going and these, along with the dunes in the area receiving abundant rainfall, maintain the gradient of fresh water towards sea water (see Figures 6.15, 7.3a, and 8.3a). Refer to

estimated rates of flow at these sites (above). The contour maps of the three areas drawn, show that the regions surrounding rivers in these areas are the least affected from saline intrusion as compared to other regions in the same areas. This effect is similar to that described by Hagemeyer (1988) who, while working on the Cross Florida Barge Canal, has shown the effect of canal fresh water preventing the intrusion of sea water. This is particularly exemplified in the Morfa Bychan area (Figures 8.7 and 8.8) where recharge from the Afon Glaslyn has prevented seawater intruding very deep inland, particularly the area surrounding the river bed, and has created a mixing zone almost 20 metres in thickness.

3) Effects of Glacial till on saline intrusion

The Aber College Farm site has two aquifers separated by glacial till. The glacial till layer protects the fresh water underneath from exchange by density currents. The Holocene formations above this glacial till layer consist of sand saturated with contaminated water and a top layer of fresh groundwater. This situation agrees well with the geophysical survey carried south-west of the polder, west of Alkamaar, Netherlands as shown by Van Dam and Meulenkamp, (1967).

The role of glacial till is quite evident in the area shown in Figures 6.10 and 6.11 where glacial till is missing in the most of the area. These data further elaborate that the glacial till's existence near the coast acts as a barrier to prevent the intrusion of seawater inland which results in a very thick fresh water zone inland safe from the effects of saline intrusion. Such a natural barrier indicates a way forward-by constructing artificial barriers-to prevent invasion of sea waters in coastal and estuarine areas.

4) Possible effects of faulting on saline intrusion

At the Aber site it has been observed that the glacial till separates two aquifers but this glacial till is found missing in some parts of the area (Figures 6.10 and 6.11). This omission of the glacial till could be attributed to the Aber-Dinlle faulting in the area, as a Quaternary fault scarp passes quite near to the study area; it is possible that this faulting could be the cause of merging two aquifers into one in that part of the study area.

In the Malltraeth area, Figures 7.3 and 7.5 show a typical V-type structure which suggests that, because of movement or erosion along the Berw fault plane, there has been an uneven deposition of sediments at that point. It possibly marks the line of the fault 'Berw'.

5) The extent of saline intrusion as a function of permeability

An aquifer is a geological formation containing water and which has a structure permitting appreciable water to move through it, both for abstraction and recharge purposes.

Coastal aquifers come in contact with the ocean at or seaward of the coastline and here, under natural conditions, fresh groundwater is discharged into the ocean. Saline intrusion results when with increased demands for groundwater in many coastal areas, where the seaward flow of groundwater has been decreased or even reversed, seawater enters the aquifer and penetrates inland. By lowering the water table in unconfined aquifers, or the piezometric surface in confined aquifers, the natural gradient sloping downward toward the ocean is reduced or reversed. Because two fluids of different densities are involved, a boundary surface, or interface, is formed wherever

the fluids are in contact.

Groundwater in its natural state is invariably moving. This movement is governed by established hydraulic principles. It has been shown that the rate of groundwater movement is governed by the permeability of the aquifer and the hydraulic gradient. 4.72×10^{-6} m/sec is taken as low and 2.3×10^{-2} m/sec as high permeability values (Todd, 1980). Natural flows are modified, by pumping wells, or steeper water tables or drains to produce higher velocities.

Transmissivity (191 m^2/day) and permeability (ranging between 3.2×10^{-4} m/sec to 1.3×10^{-3} m/sec) values determined in the field as well as in the laboratory prove to be moderate and these greatly add towards retarding the saline intrusion front from moving further inland. Howard (1987) has shown that the sediment with low to moderate permeability or transmissivity minimizes the landward movement of saline intrusions. This study at Aber College farm, Malltraeth and Morfa Bychan substantiates these findings.

In the Malltraeth area, it was further observed that the saline water also seemed to have been less wide spread towards the north (estuarine sediments) of the study area as compared to the opposite direction. This is presumably because the sediments are getting finer towards the estuary as silt/clay content is increasing as compared to sand; this results in permeability decreasing and a consequent decrease of saline intrusion.

6) The effect of tides and borehole pumping on the position of the saline interface

Field measurements at Miami (Cooper et al., 1964) and experimental studies (Cahill, 1967) have shown the landward movement of the saline water body where tidal action is the predominant mixing mechanism. Goswami (1968) observed that because of tides, particularly spring tides, a considerable shift of the saline/fresh water interface

occurs.

Meinzer (1945) warned of over pumping in coastal aquifers on the basis of field observations and predicted a continuous encroachment of salt water. Hem (1959) observed that pumping inland will reduce the head of the fresh water and, because head changes are transmitted rapidly through the system, the flow of fresh water seaward will be decreased; in fact the head may decline enough to stop entirely the seaward flow of fresh water past the interface. With the decreased fresh water flow the system will be unstable and salt water will invade the aquifer. Diersch et al., (1984), and Schmorak & Mercado, (1969) have shown that pumping a well in fresh water underlain by salt water can cause the salt water front to rise locally below the well (also called upconing) in response to the pressure depression around the well.

The geophysically-measured observations at Aber during spring tides clearly demonstrated that tides do affect the interface (see Figure 6.20). Results of the various VES soundings made on the site showed that the resistivity and thickness of the two aquifers in the area changed as the groundwater level, along with its resistivity, altered with the simultaneous rise and fall of the spring tide. Salinity changes in the groundwater before and after the rise of the spring tide further confirmed that tides do affect the interface.

Pumping tests carried out at the Aber (see Table 6.11c) showed that the salinity of groundwater near the coast changed significantly after pumping. The salinity change caused by pumping was found to be greater than that created by the spring tides.

7) The deviation from the theoretical "Ghijben-Herzberg Relationship"

The Ghijben-Herzberg Relationship calls for a 40 to 1 ratio between the depth of the interface and the height of water table above mean sea level. But at Aber this

contact zone was found to occur within 17.45 to 21.45 metres below mean sea level, which if the Ghijben-Herzberg Relationship held should be at 146-174 metres.

A deviation from the theoretical "Ghijben-Herzberg Relationship" has been observed (Jacob and Schmorak, 1960) and seems to have been caused by the following:

a) The contact between the fresh and saline water is not abrupt but is in the form of a zone of mixing (transition zone) with a gradation from fresh to salt water.

b) Both the fresh and saline water body are not stagnant as assumed by the Ghijben-Herzberg Relationship. A downward component (caused by recharge through precipitation) exists in the fresh water zone. The fresh water is in continuous state of motion as is evidenced by seepage surfaces above the sea level in the beach area. The existence of such surfaces is not considered in the Ghijben-Herzberg Relationship, nor there is any provision for the escape of fresh water below the sea level (Wiest, 1965). Such a situation exists at Aber Farm.

The reasons given by Lusczynski and Swarzenski, (1962), for the occurrence of a broad zone of diffusion in the Magothy formation in Long Island, New York, also holds good at Aber. The irregular shape and thickness of the zone of mixing might have been caused as a result of the combination of several factors:

i) Opposing flow directions in adjacent bodies of fresh and saline groundwater.

ii) Effects of movements of water within the aquifer having variable pore geometry (this has also been observed by Rumer and Harleman, 1963).

iii) Fluctuations in fresh water discharge to the seawater due to the changes in the groundwater recharge through precipitation and the variations of gradient in fresh and saline groundwater caused by oceanic tides.

iv) Molecular diffusion.

The observations made at Aber indicate that all these factors are involved in the

occurrence and shape of the zone of mixing in contrast to the ideal Ghijben-Herzberg Relationship.

8) The usefulness of geophysical probing

Much resistivity work on the detection of the fresh-saline water interface has been carried out in different parts of the world (Flathe, 1970; Kelly, 1976; Zohdy et al 1974; Gorhan, 1976; Klefstad et al 1976; and Worthington, 1977). Some investigators have used frequency domain, low induction number conductivity mapping for groundwater exploration and the detection of saline intrusions using EM conductivity meters (Fraser, 1984; and McNeill, 1980a). Elsewhere Volker and Dijkstra (1955), Van Dam and Meulenkamp, (1967) and Ginzburg (1974) working independently in polder and delta regions followed standard geoelectric procedures for mapping saline water contamination: electrical soundings are carried out near all boreholes and wells existing in the investigation area and simultaneously the conductivity and chloride content of groundwater samples from the boreholes determined. A graph can then be assembled by relating the chloride contents to the true aquifer resistivities as obtained from the soundings. Finally a map showing the chloride distribution of groundwater can be prepared, by converting directly true aquifer resistivities to chloride concentrations.

In the present study, an attempt has been made to combine resistivity and electromagnetic techniques for each of the three areas to compare these to the geological log data determined from drill holes and auger holes. It was observed that out of the two methods used the EM soundings failed to pinpoint exactly in the sand dunes the correct depth of the conductive saturated layer (aquifer). However by inserting the actual water table depth parameters and borehole log data into the interpretive computer program and constraining the program through the known

thicknesses (dry upper layers) a good fit was obtained (Chapter 7). The Offset Wenner system which, although it has many advantages over the simple Wenner, when it is used on the beach, simultaneously working on dry sand sites and near to mean high water sites, it usually gave erroneous readings presumably due to the contact resistance.

In the Malltraeth area, the electrical methods have also demonstrated the provision of information about dipping bed rocks, as well as giving data regarding soft rock sandwiched between hard rock at two ends. This observation in the study area supports the conclusion of Greenly (1919). Clearly, then, geophysical electrical observations not only can define boundaries between saline and fresh water but the resistivities determined in the interpretation procedure can also give some indication of the level of contamination, of some importance in potability/irrigation considerations (see below). Importantly, if any wells or boreholes exist, and samples of water are available for direct salinity measurements, it is then possible to calculate the electrical formation factor of the aquifer. The observations made at Aber, Malltraeth and Morfa Bychan illustrate that the formation factor, through the use of empirical curves (Jackson et al., 1978; Lovell, 1983 and Barker & Worthington, 1973), can be used to give a good measure of of both porosity and permeability of the aquifer (see Tables 7.8 and 8.6). In particular the permeability calculated through formation factor considerations fit well within a range of values obtained by various methods and varies by no more than half a magnitude from the most extremes. This is of considerable significance in calculating the hydrological characteristics of any water bearing medium without recourse to expensive pumping tests which need only, then, to be carried out as a last resort.

9) The mixing water zone

Wentworth (1951) has shown that a sharp interfacial boundary between fresh and saline water does not occur in field conditions: instead a brackish transition zone separates the two fluids developed by unsteady displacements of the interface by external influences such as tides and pumping wells. Cooper (1959) described how the movements of fresh and salt water along a contact zone tend to produce a diffusion zone of mixing rather than a sharp interface.

In an area where no other source of saline contamination exists, high chloride concentrations in groundwater can be considered rather definite proof of seawater contamination (Hem, 1959). A measurement of fluid conductivity alone cannot resolve the type of dissolved solids. It is, however, common to relate electrical conductivity to an equivalent chloride concentration (Kwader, 1986).

To derive more quantitative information about concentration of dissolved solids, an attempt has been made to correlate formation resistivities measured through direct resistivity methods to chloride concentrations (chapter 5). An aquifer with a mixing water zone has been defined to correspond to bulk resistivities ranging from 8 ohm-m to 35 ohm-m and with chlorides from 250 ppm to 500 ppm. The lower limit here agrees more with Mills and Ryder, (1977); Jacob, (1980); and Stewart et al., (1982), who have put it between 200 - 250 ppm, than that of Goswami who has put the lower limit at 300 ppm chloride concentration. Further Goswami puts the mixing zone range between 300 to 500 ppm chloride concentration.

Mixing zones in general result in suppressed 'layers' in resistivity interpretation. In the Aber area where fresh water slumps in resistivity values from high to as low as 1 ohm-m in the lower aquifer region along the coast (see Figures 6.7, 6.10 and 6.11). In contrast in the Morfa Bychan area where recharge from Afon Glaslyn occurs and

gives a 20 metres thick mixing zone.

Saline and mixing zones seem to cross lithological boundaries as seen in the Malltraeth and the Morfa Bychan areas where bed rocks show variable low resistivities because their pore spaces seem filled with saline water.

An aquifer with saline water has been defined to correspond to a bulk resistivity of 7 ohm-m or less and with a chloride concentration 500 ppm or more. This value more or less agrees with the work of Mills et al., (1988); and Hoekstra et al., (1990), who have shown it to correspond to a bulk resistivity of 8 ohm.m (and with 500 ppm chloride concentration). A value of 7 ohm.m would also be consistent with the data of Guo (1986) for sand aquifers in China.

10) Application to salinity problems in Pakistan

The general importance of this investigation to a study of the salinity build-up in irrigated areas of Pakistan cannot be over-emphasized. Permanent monitoring by electrical equipment could give a picture of the alteration in salinity of groundwater which could lead to formulating a policy for the eradication of the salinity build-up (such as by the use of fresh water recharge).

For example in areas where saline water (upper aquifer) is already being extracted an extensive geophysical survey could provide an additional data and if fresh water aquifers (at lower depths) are present, those could also be extracted alongside the upper saline water in order that their joint use would prevent the spread of salinity on the ground surface side by side lowering the water table level.

CHAPTER 10. CONCLUSIONS

The intrusion of saline water into fresh groundwater is the most common cause of pollution. Such intrusion can occur in a variety of ways from the invasion of sea water in coastal and estuarine zones to evaporation in enclosed water areas and the effects of irrigation in semi-arid zones, such as in regions of Pakistan. This study has been directed towards the examination of geophysical electrical techniques for determining the extent of saline intrusion and other hydrological parameters of the sub-surface medium with the ultimate aim of transferring such techniques to a Pakistan situation. The conclusions are:

1) Electrical resistivity depth probing (VES), electromagnetic soundings (EM) and chemical tests on groundwater samples obtained from boreholes indicate the existence of a saline-fresh water interface and a zone of mixing at three coastal/estuarine study areas.

2) The extent of saline intrusion is a function of permeability and the volume of fresh water (either from rainfall or river flow or both) available to prevent inland movement; it is also a function of the availability of any natural barriers such as glacial till and bed rock.

3) The position of the saline interface is considerably affected by spring tides but it is also modified by borehole pumping which can create upconing of saline water.

4) In the areas chosen there is a wide deviation from the theoretical "Ghijben-Herzberg Relationship", the depth of the saline interface being much less than that

calculated from the relationship. This is largely because the contact between fresh and saline waters is not abrupt - there being a mixing zone - and both fresh and saline waters are mobile, not stagnant as required by the relationship.

5) Geophysical observations provide a dependable means for the detection and mapping of a saline intrusion. They also provide acceptable values of porosity and permeability as well as valuable information concerning the interrelation between permeability and transmissivity of an aquifer.

6) A bulk resistivity of 7 ohm.m or less and chloride concentration of 500 ppm or more defined saline groundwater, and the zone of mixing water (transition zone) was defined by resistivities ranging between 8 ohm.m to 35 ohm.m with chlorides between 250 ppm to 500 ppm. As indicated in (3) the boundaries vary considerably with the tide (particularly spring tides), including an unsteady fresh water flow pattern and the permeability of the aquifer.

7) In Pakistan's severe waterlogging and salinity conditions, the geophysical methods could play a pivotal role in the detection of the severity of the problem beforehand in order to take precautions in halting the twin menace.

REFERENCES

Adams, W.M. (1970). An electrical resistivity profile in Hawaii with noval elevation correction. *Geophysical Prospecting*, v. (8) supplement to N. 4., p. 728-737.

Al- Azzawi, M. (1986). Shear wave propagation characteristics in anisotropic sediment. Ph.d thesis, University of Wales.

Allen, W.B., Hahn, G.W. and Tuttle, C.R. (1963). Geohydrological data for the Upper Pawcatuck River Basin, Rhode Island. *Rhode Island Geological Bulletin 13.*

Al-Ruwaih, F.M. (1992). The feasibility of the resistivity sounding method for detecting the brackish/saline water interface in Kuwait. *Journal of University of Kuwait (Science) 19.*

Anderson, W.L. (1982). Nonlinear least-squares inversion of transient soundings for a central induction loop system (program NLSTCI). Open-File Report 84-1129. *U.S. Geological Survey*, Denver, CO.

Archie, G.E. (1942). The electrical resistivity log as an aid in determining some reservoir characteristics. *Petroleum Technology, Technical Report 1422*, American Institute of Mining and Metallurigical Engineering., p. 54-62.

Astier, J.L. (1971). Geophysique Appliquee a l'hydrogeologie. *Masson & Cie.*, Editeurs, Paris., p. 277.

Atkins, E.R. and Smith, G.H. (1961). The significance of particle shape in formation factor-porosity relationships. *J. Petrol. Tech.*, v. 13., p. 285-291.

Ayers, J.F. (1988). Application of geophysical techniques in the study of an alluvial aquifer. *Proceedings of the 2nd National Outdoor Action Conference.* Las Vegas, NV. v. II., p. 801-824.

Badon Ghijben, W. (1888-1889). Nota in Verband met de Voorgenomen Put boring Nabij Amsterdam, Tijds. *K. Inst. Ing.*, The Hague., p. 21.

Barker, R.D. (1981). The Offset system of electrical resistivity sounding and its use with a multicore cable. *Geophysical Prospecting.*, v. 29, p. 128-143.

Barker, R.D and Worthington, P.F. (1973). Some hydrogeophysical properties of the Bunter sandstone of northwest England. *Geoexploration.*, v. 11., p. 151-170.

Barker, R.D. (1992). A simple alogorithm for electrical imaging of the subsurface. *First Break*, 10, p. 53-62.

Bear, J. (1972). Dynamics of Fluids in Porous Media. *American Elsevier*, New York., p. 764.

Bear, J. and Dagan, G. (1964). Moving interface in coastal aquifers. *Jour. Hydraulics Div., Amer. Soc. Civil Engrs.*, v. 90, no. HY 4., p. 193-216.

Bhattacharya, P.K. and Patra, H.P. (1968). Direct current geoelectric sounding. *Elsevier Publ. Co.*, Amsterdam. p. 135.

Biella, G., Lozej, A. and Tabacco, I. (1983). Experimental study of some hydrogeophysical properties of unconsolidated porous media. *Ground Water.*, 21 (6)., p. 741-751.

Bourbie, T., Coussy, O. and Zinszner, B. (1987). Acoustics of Porous media. *Editions Technip*, Paris.

Bouwer, H. (1978). Groundwater Hydrology. *McGraw-Hill*, Inc., ISBN 0-07-006715-5., p. 480.

Braithwaite, F. (1855). On the infiltration of salt water into the springs of wells under London & Liverpool. *Proc. Inst. Civil Engrs.*, v. 14., p. 507-523.

British Regional Geology, H.M. Stationary Office, 3rd Edition, (1961).

Brown, R.H. and Parker, G.G. (1945). Salt water encroachment in limestone and Silver Bluff, Miami, Florida. *Econ. Geol.*, v. 40, no. 4., p. 235-262.

Brown, J.S. (1925). A study of coastal groundwater with special reference to Connecticut, U.S. *Geological Survey Water Supply Paper 537.*, p. 101.

Buhle, M.B. and Brueckman, J.E. (1964). Electrical earth resistivity surveying in Illinois. *Illinois State Geological Survey Circular 376.*

Cahill, J.M. (1967). Hydraulic sand-model study of the cyclic flow of salt water in a coastal aquifer, U.S. *Geological Survey Prof.*, Paper 575-B., p. 240-244.

Carman, P.C. (1939). Permeability of saturated sands, soils and clays. *J. Agricultural Science.*, 29(2)., p. 262-273.

Carpenter, E.W., and Habberjam, G.M. (1956). A tripotential method of resistivity

prospecting. *Geophysics.*, 21., p. 455-469.

Cartwright, K. and McComas, M.R. (1968). Geophysical surveys in the vicinity of sanitary landfills in northeastern Illinois. *Ground Water.*, v. 6, no.5., p. 23-30.

Charmonman, S. (1965). A solution of the pattern of fresh water flow in an unconfined coastal aquifer. *Jour. Geophysical Reseach.*, v. 70., p. 2813-2819.

Collins, M.A. and Gelhar, L.W. (1971). Seawater intrusion in layered aquifers. *Water Resources Research.*, v. 7., p. 971-979.

Cooper, H.H., Jr., Kohout, F.A., Henry, H.R. and Glover, R.E. (1964). Seawater in coastal aquifers. U.S. *Geological Survey Water Supply Paper 1613-C.*, p. C12 - C32.

Cooper, H.H. (1959). A hypothesis concerning the dynamic balance of fresh water and salt water in a coastal aquifer. *Jour. of Geophysical Research*, v. 64, N.4., p. 461-467.

Cratchley, R.C., Davis, A.M. and Taylor Smith, D. (1982). Enhancement of the role of geophysics in marine geotechnical investigations. *Oceanology Int.* - 82 Conf. Paper. Brighton, England.

Croft, M.G. (1971). A method of calculating permeability from elastic logs. U.S. *Geological Survey Pros. Paper 750--B.*, p. 265-269.

D'Andrimont, R. (1902). Notes sur l'hydrologie du littoral belge. *Soc. Geol. Belg. Au.*, Liege., v. 29., p. 129-144.

D'Andrimont, R. (1905). Note preliminaire sur une nouvelle methode pour etudier experimentalement l'allure des neppes aquifers dans les terrains permeables en petit. *Soc. Geol. Belg. Au.*, Liege, v. 32., p. 115-120.

Daily, W. and Owen, E. (1991). Cross-borehole resistivity tomography. *Geophysics*, 56., p. 1228-1235.

Darcy, H. (1856). Les fontaines publiques de la ville de Dyon. v. Dalmont, Paris., p. 647.

Davis, A.M. (1975). Beach morphology and porosity. M.Sc thesis, University of Wales.

Davis, S.N. and DeWiest, R.J.M. (1966). Hydrogeology. *John Wiley and Sons*, New York., 463 p.

Diersch, H.J., Prochnow, D. and Thiele, M. (1984). Finite element analysis of dispersion affected salt water upconing below a pumping well. *Appl. Math. Modelling.*, v. 8., p. 305-

312.

Dobrin, M.B. (1976). Introduction to Geophysical Prospecting. New York, *McGraw Hill Book Co.*, p. 339-361.

Doveton, J.H. (1986). Log Analysis of subsurface Geology. *John Wiley and Sons, Inc.*, New York., p. 273.

Dullien, F.A. (1975a). Prediction of tortuosity factor from pore structure data. *J. AICHE.*, 21(4)., p. 820-822.

Dullien, F.A. (1979). Porous media fluid transport and pore structure. *Academic Press*, London.

Duprat (1972). Examples d'Application de Traitements Automatiques a l'Interpretation de Sondages Electriques. *Communication presentee au 34 eme Congres de l'E.A.E.G. a*, Paris., p. 19.

Eadie, T. (1979). Stratified earth interpretation using standard horizontal loop EM data. *Research in Applied Geophysics*, No. 9, University of Toronto, Toronto, Ontario, Canada.

Ebert, A. (1943). Grundlagen zur Auswertung geoelektrischer Tiefenmessungen en. Beitr. Angew. *Geophys.* 10: 1-17.

Edwards, W. (1904). The glacial Geology of Anglesey, Liverpool. *Geological Soc., Proceedings.*, v. 10., p. 26-37.

Embleton, C. (1964). A Deglaciation of Arfon and southern Anglesey and the origin of the Menai Straits. *Geological Association Proceedings.*, v. 75., p. 407-429.

Ferris, J.G. (1967). Cyclic water-level fluctuations as a basis for determining aquifer transmissivity. In Methods of Determining Permeability, Transmissivity and Drawdown. *U.S. Geol. Surv. Water-Supply Pap.*, p. 1536-I.

Flathe, H. (1955). Possibilities and limitations in applying geoelectrical methods to hydrogeological problems in coastal areas of northwest Germany. *Geophysical Prospecting.*, v. 3, no. 2., p. 95-110.

Flathe, H. (1963). Five layer master curves for the hydrogeological interpretation of geoelectrical resistivity measurements above a two story aquifer. *Geophysical Prospecting.*, v. 11, No. 4., p. 471-508.

Flathe, H. (1970). Interpretation of geoelectrical resistivity measurements for solving

hydrogeological problems. In Morley, L.P., ed., *Mining and Ground Water Geophysics*, 1967. Geological Survey of Canada, *Economic Geology Report, no. 26*, p. 580-597.

Flathe, H. (1976). The role of a geologic concept in geophysical research work for solving hydrogeological problems. *Geoexploration.*, v. 14, no. 3/4., p. 195-206.

Foster, M.D. (1942). Chemistry of groundwater in Hydrogeology. (O.E. Meinzer, ed.), *McGraw-Hill*, New York., p. 646-655.

Foster, J.S. and Buhle, M.B. (1951). An integrated geophysical investigation of aquifers in glacial drift near Champaign-Urbana, Illinois. *Economic Geology.*, v. 46, no. 4., p. 367-397.

Fraser, D.C. (1984). Airborne mapping of water resouces with DIGHEM systems. *Dighem Surv. and Processing*, Inc., Mississauga, Ontario.

Freeze, R.A. and Cherry, J.A. (1979). Groundwater. *Prentice Hall*, Inc., Englewood Cliffs, N.J., p. 604.

Frohlich, R.K. (1973). Detection of fresh water aquifers in the glacial deposits of the north western Missouri by geoelectrical methods. *Water Resources Bulletin.*, v. 9, no. 4, p. 723-734.

Frohlich, R.K. (1974). Combined geoelectrical and drill-hole investigations for detecting fresh water aquifers in north western Missouri. *Geophysics.*, v. 39, no. 3., p. 340-352.

Gay, M.C. (1983). Evaluation of transient electromagnetic soundings for deep detection of salt water interfaces. Unpublished M.S. thesis, University of South Florida, Tampa. p. 93.

Gizburg, A. (1974). Resistivity surveying. *Geophysical Surveys.*, v. 1, no. 3., p. 325-355.

Glassstone, S. (1946). Textbook of physical chemistry, 2nd ed., *D. Van Nostrand*, p. 1320.

Groundwater Management, Inc. (1987). City of Lincoln, Nebraska, modelling study. *Consultant report to City of Lincoln.*

Gorhan, H.L. (1976). The determination of the saline/fresh water interface by resistivity soundings. *Bull of the Assn. of England Geol.*, 13, p. 163-175.

Goswami, A.B. (1968). A study of salt water encroachment in the coastal aquifer at Digha, Midnapore district, West Bengal, India. *Bull. Int. Assoc. Sci. Hydrol.*, 13(3)., p. 77-87.

Greenly, E. (1919). The Geology of Anglesey., vol. 1 and 2, pub. *HMSO*.

Griffiths, D.H. and Turnbull, J. (1985). A multi-electrode array for resistivity surveying. *First Break*, 3(7)., p. 16-20.

Griffiths, D.H.; Turnbull, J. and Olayinka, K. (1990). Two-dimensional resistivity mapping with a computer-controlled array. *First Break*, 8(4)., p.121-129.

Guo, Y.A. (1986). Estimation of TDS in sand aquifer water through resistivity log. *Ground Water.*, v. 24, no. 5., p. 598-600.

Hagemeyer, R.T. (1988). Resistivity study of the lower Withlacooche River-Cross-Florida Barge Canal Complex. M.Sc. thesis, University of south Florida, Tampa.

Hagemeyer, R.T. and Stewart, M. (1990). Resistivity investigation of salt water intrusion near a major sea level canal. *Geotechnical and Environmental Geophysics.*, v. II., p. 67-77.

Hantush, M.S. (1968). Unsteady movement of fresh water in thick unconfined saline aquifers. *Bull. Int. Assoc. Sci. Hydrol.*, 13(2)., p. 40-60.

Harris, W.H. (1967). Stratification of fresh and salt water on barrier islands as a result of differences in sediment permeability. *Water Resources Research.*, v. 3., p. 89-97.

Hazen, A. (1892). Experiments upon the purification of sewage and water at the Lawrence Experimental Station, Nov. 1, 1899 to Dec. 31, 1891. *Massachusetts State Board of Health, 23rd Annual Report.*, p. 425-600.

Heigold, P.C. (1979). Aquifer Transmissibility from Surficial Electrical Methods. *Ground Water.*, v. 17, no. 4., p. 338-345.

Hem, J.D. (1959). Study and interpretation of the chemical characteristics of Natural Water. *USGS Water Supply Paper.*, p. 314.

Hem, J.D. (1970). Study and interpretation of the chemical characteristics of Natural Waters. *USGS Water Supply Paper.*, 1473, p. 1-363.

Henry, H.R. (1964). Interface between salt water to fresh water in coastal aquifers. U.S. *Geological Survey Water Supply Paper 161306*, p. 29-35.

Herzberg, B. (1901). Die Wasserversorgung einiger Nordsee bader. *Jour. Gasbeleuchtung und Wasserversorgung*, Munich., v. 44, p. 815-819, 842-844.

Hoekstra, P., and Blohm, M.W. (1990). Case histories of time domain electromagnetic soundings in environmental geophysics. *Geotechnical and Environmental Geophysics.*, v. II., p. 1-15.

Howard, K.W.F. (1987). Benificial aspects of sea-water intrusion. *Ground Water*, v. 25., no. 4., p. 398-406.

Hubbert, M.K. (1940). The theory of groundwater motion. *Jour. Geol.*, v. 48., p. 785-944.

Huntley, D. (1986). Relation between permeability and Elect. resistivity in granular aquifers. *Ground Water.*, v. 24, no. 4., p. 466-474.

Hvorslev, M.J. (1951). Time lag and soil permeability in groundwater observations. *Water-Way Experiment Station*, Bulletin no. 36, U.S. Army Corps of Engineers, Vicksburg.

Inman, J.R. (1975). Resistivity inversion with ridge regression. *Geophysics.*, 40., p. 798-817.

Isaacs, J.D. and Bascom, W.N. (1949). Water table elevations in some Pacific coast beaches. *Trans. Amer. Geophys. Union.*, v. 30., p. 293-294.

Jacob, C.E. (1950). Flow of groundwater in Engineering Hydraulics. (H. Rouse, ed.), *John Wiley and Sons.*, p. 321-386.

Jacob, M. and Schmorak, S. (1960). Salt water encroachment in the coastal planes of Israel-IUGG Comm. of subterranean waters. *Sc. Pub.*, no. 52., p. 408-421.

Jacob, P. (1980). Some aspects of the hydrogeology of coastal collier county. In., (P.J. Gleason, ed.), water oil and geology of Collier, Lee and Hendry Counties, *Miami Geological Society.*, p. 21-26.

Jackson, P., Taylor Smith, D. and Stanford, P.N. (1978). Resistivity-porosity-particle shape relationship for marine sediment. *Geophysics.*, 43., p. 1250-1268.

Kashef, A.I. (1968a). Dispersion and diffusion in porous media salt water mounds in coastal aquifers. *Water Resouces Research Institute at Raleigh* (sponsored by the office of Water Resouces Research, Washington .D.C.), Final Report no. 11., p. 1-280.

Kashef, A.I. (1968b). Fresh salt water interface in coastal groundwater basins. *Memories, Association Internationale Des Hydrogeologiques*, Tome VII, Reunion d'Istanbul (proceedings of the International Assoc. of Hydrogeologists), 8., p. 369-375.

Kaufman, A.A. and Keller, G.V. (1983). Frequency and transient soundings. *Elsevier Science Publ.* Co., Inc.

Keller, G.V. and Frischknecht, F.C. (1966). Electrical methods in Geophysical Prospecting. *Pergamon Press*, New York., p. 90-197.

Kelly, W.E. (1976). Geoelectric sounding for delineating groundwater contamination. *Ground Water.*, v. 14., p. 6-10.

Kelly, W.E. (1977). Geoelectrical sounding for estimating aquifer hydraulic conductivity. *Ground Water.*, v. 15., p. 420-424.

Kelly, W.E. and Reiter, P.F. (1984). Influence of anisotrophy relation between electrical and hydraulic properties of aquifers. *Jour. Hydrology.*, 74., p. 311-321.

Klefstad, G., Sandlein, L.V.A. and Palmquist, R.C. (1976). Limitations of the electrical resistivity method in landfill investigations. *Ground Water.*, v. 13, no. 5., p. 418-427.

Kosinski, W.K. and Kelly, S.F. (1981). Geoelectric soundings for predicting aquifer properties. *Ground Water.*, v. 19, no. 2., p. 163-171.

Kozeny, J. (1927). Uber Kapillare Leitung des Wassers in Boden, Ber. *Wien Akad.*, 136 A., p. 271.

Krul, W.F.J.M. and Liefrinck, F.A. (1946). Recent groundwater investigations in the Netherlands. *Elsevier Publishing Co.*, New York., 78 p.

Kunetz, G. (1966). Principles of direct current resistivity prospecting. *Gebruder Borntrager*, Berlin., 130 p.

Kwader, T. (1986). The use of geophysical logs for determining formation water quality. *Ground Water.*, v. 24., p. 11-15.

Lambe, T.W. and Whitman (1969). Soil Mechanics, *Wiley and Sons.*

Liesch, B.A. (1969). Resistivity methods to locate aquifers. *Public Works.*, v. 100., p. 82-83.

Lohman, S.W. (1972). Groundwater Hydraulics. *US Geological Survey prof. paper.*, p. 708-770.

Longsworth, L.G. (1945). The diffusion of electrolytes and macromolecules in solution, An. *New York Acad. Sci.*, v. 46, art. 5., p. 209-346.

Lovell, M.A. (1983). Resistivity-Thermal conductivity porosity relationship for marine sediment. Ph.d thesis, University of Wales.

Lovell, M.A. (1985). Thermal Conductivity and Permeability assessment by electrical resistivity measurements in marine sediments.
Marine Geotechnology, v. 6, no. 2.

Lusczynski, N.J. (1961). Head and flow of groundwater of variable density. *Jour. Geophysical Research.*, v. 66., p. 4247-4256.

Lusczynski, N.J. and Swarzenski, W.V. (1962) Fresh and salty groundwater in Long Island, New York. *Proc. Amer. Soc. of Civil Engrs.*, HY., 4., p. 174-194.

Lusczynski, N.J. and Swarzenski, W.V. (1966). Salt water encroachment in Southern Nassau and South eastern Queens counties, Long Island, New York. *US Geological Survey Water-Supply Paper 1613-F*, p. 76.

Maillet, R. (1947). The fundamental equations of electrical prospecting. *Geophysics*, 12., p. 529-556.

Mallick, K. and Verma, R.K. (1979). Time-domain electromagnetic sounding computation of multilayered response and the problem of equivalence in interpretation. *Geophs. Prospec.*, 27(1), p. 137-155.

Marlette, R.R. (1952). Field determinations of the transmissibility and storage coefficients of the Platte Valley aquifer near Ashland, Nebraska. Unpublished M.S. thesis. Dept. of Civil Engrs., University of Nebraska-Lincoln.

Merkel, R.H. (1973). Acid mine Drainage in groundwater. *Ground Water.*, v. 10, no. 5., p. 38-42.

McGinnis, L.D. and Kempton, J.P. (1961). Integrated seismic, resistivity and geologic studies of glacial deposits. *Illinois Geological Survey Circular 323.*

McNeill, J.D. (1980). Applications of transient electromagnetic techniques. *Geonics Ltd.*, Tech Note TN-7.

Meidar, T. (1960). An electrical resistivity survey for groundwater. *Geophysics.*, v. 25, no. 5, p. 1077-1093.

Meinzer, O.E. (1945). Problems of the perennial yield of artesian aquifers. *Economic Geology.*, 40(3)., p. 159-163.

Mills, L.R. and Ryder, P.D. (1977). Salt water intrusion in the Floridan aquifer, coastal Citrus and Hernando Counties, Florida, 1975. *US Geological Survey Water-Resources Investigations.*, p. 77-100.

Mills, T., Hoekstra, P., Blohm, M.W. and Evans, L. (1988). Time domain electromagnetic soundings for mapping sea water intrusion in Monterey county, CA. *Ground Water.*, 26, p. 771-782.

Milsom, J., (1989). Field Geophysics. Ist edition. Halsted Press, Division of *John Wiley & Sons*, Inc., New York., p.80.

Noel, M. and Walker, R. (1990). Development of an electrical resistivity tomography system for imaging archaeological structures. *Archaeometry*, E. Pernicka and G.A. Wagner (eds.), p. 767-776. Birkhauser, Basel.

Noel, M. and Xu, B. (1991). Archaeological investigation by electric resistivity tomography: a preliminary study. *Geophysical Journal International*, 107., p.95-102.

Nomitsu, T., Toyohara, Y. and Kamimoto, R. (1927). On the contact surface of fresh and salt water near a sandy sea-shore. *Mem. college Sc., Kyoto Imp. Uni., Ser. A.*, v. 10, no. 7, p. 279-303.

Ohrt, F. (1947). Water development and salt water intrusion on Pacific Islands. *Jour. Amer. Works Assoc.*, v. 39., p. 979-988.

Orellana, E. and Mooney, H.M., (1966). Master Tables and Curves for Vertical Electric Soundings over Layered Structures. *Interciencia*, Madrid, p. 34.

Park, S.K. and Dicky (1989). Accurate estimation of conductivity of water from geoelectrical measurements. A new way to correct for clays. *Ground Water.*, 27(6), p. 786-792.

Patnode, H.W. and Wyllie, M.R.J. (1950). The presence of conductive solids in reservoir rocks as a factor in electric log interpretation. *Jour. of Petroleum Technology.*, v. 189, p. 47-52.

Patra, H.P. and Mallick, K. (1980). Geosounding Principles 2. *Elsevier Publishing Co.*, New York.

Pennink, J.M.K. (1905). Investigations for groundwater supplies. *Trans. Amer. Soc. Cir. Eng.*, v. 54-D, p. 169-181.

Perlmutter, N.M. and Geraghty, J.J. (1963). Geology and Groundwater Conditions in

Southern Nassau and Southeastern Queens Counties, Long Island, N.Y. *US Geological Survey Water Supply Paper 1613-A*, 205 p.

Pinder, G.F. and Cooper, H.H. Jr. (1970). A numerical technique for calculating the transient position of the salt water front. *Water Resources Research.*, v. 6, p. 875-882.

Pointon, W.K. and Hart, (1982). Glaciogenic deposits along the eastern Menai Straits. Unpubl. M.Sc. thesis, City of London, Polytechnic.

Raudikivi, A.J. and Callander, R.A. (1976). Analysis of Groundwater Flow. *Edward Arnold (Publishers) Ltd.*, ISBN 0-7131-3364-3., p. 214.

Reichel, W. (1969). Analytical Chemistry., *Acs. L.*, 41(13)., p. 1886-1969.

Revelle, R. (1941). Criteria for recognition of seawater in groundwater. *Trans. Amer. Geophys. Union.*, v. 22, pt. 3., p. 593-597.

Reynold, W.D. and Elrick, D.E. (1986). A method for simultaneous in-situ measurement in the vadose zone of field saturated hydraulic conductivity sorptivity and the conductivity pressure head relationship. *Groundwater Monitoring Review.* p. 84-95.

Rose, H.E. (1950). Fluid flow through beds of granular material. *Proc. Conf. Instn. Phy.*, p. 136.

Rumer, R.R. and Harleman, D.R.F. (1963). Intruded salt water wedge in porous media. *Jour. Hydraulics Div., Amer. Soc. Civil Engrs.*, v. 89, no. HY6, p. 193-220.

Sandberg, S.K. and Jagel (1993). Examples of resolution improvement in geoelectrical soundings applied to groundwater investigations. *Geophysical Prospecting.*, 41, p. 213.

Scheidegger, A.E. (1974). The physics of flow through porous media. Third Edition, University of Toronto Press.

Schmorak, S. and Mercado, A. (1969). Upconing of fresh-sea water interface below pumping wells, field study. *Water resources Research.*, v. 5., p. 1290-1311.

Schröder, N. (1970). Interpretation of depth to salt water by application of electrical soundings. *Geoexploration.*, 8., p. 113-116.

Sen, P.N., Scala, C. and Cohen, M.H. (1981). A self similar model for sedimentary rocks with application to the dielectric constant of fused glass beads. *Geophysics.*, 46(5)., p. 781-795.

Shima, H. (1990). Two dimensional automatic resistivity inversion technique using alpha centers. *Geophysics*, 55., p. 682-694.

Slichter, C.S. (1899). Theoretical investigation of the motion of groundwater 19th annual report. *US Geological Survey*., 2., p. 305.

Solymer, Z.V. and Illobachie, B.C. (1986). Permeability determination in an alluvial dam foundation. *Geotechnique*., 36, N. 1., p. 95-108.

Stewart, M., Lizanec, T. and Layton, M. (1982). Application of DC resistivity surveys to regional hydrogeoogic investigations, Collier County, Florida. *South Florida press*, West Palm Beach.

Stewart, M. and Gay, M.C. (1986). Evaluation of transient electromagnetic soundings for deep detection of conductive fluids. *Ground Water*., v. 24., p. 351-356.

Swartz, J.H. (1937). Resistivity studies of some salt water boundaries in the Hawaiian Islands. *Trans. Amer. Geophysical Union*., v. 18., p. 387-393.

Swartz, J.H. (1939). Part II. Geophysical investigations in the Hawaiian Islands. *American Geophysical Union Transactions*., v. 20., p. 292.

Taylor Smith, D. (1971). Acoustic and electric techniques for sea floor sediment identification. *Proc. Int. Symp. on Engineering properties of sea floor soils and their geophysical identification.* (Seattle, Washington)., p. 253-267.

Terzaghi, C. (1925). Principles of soil mechanics: determination of permeability of clay. *Engineering News Record*., v. 95., p. 832-836.

Thiem, G. (1906). Hydrolgische Methoden. *Gebhardt*, Leipzig., p. 56.

Todd, D.K. (1974). Salt water intrusion and its control. *Jour. Amer. Water Works Assoc.*, v. 66., p. 180-187.

Todd, D.K. (1980). Groundwater Hydrology. 2nd edition. *John Wiley and Sons*, New York., p. 245.

Toyohara, Y. (1935). A study on the coastal groundwater at Yumingahama, Tottori. *Mem. College of Sci., Kyoto Imp. Uni., Ser.A*., v. 18, no. 5., p. 295-309.

Truscott, E.D. (1970). ibid., 42(13)., p. 16557.

Urish, D.W. (1981). Electrical resistivity hydraulic conductivity relationships in glacial

outwash aquifers. *Water Resources Research.*, 17(5), p. 1401-1408.

U.S. Environmental Protection Agency, (1978). Electrical resistivity evaluations at solid waste disposal facilities. SW-729.

Van Dam, J.C., and Meulenkamp (1967). Some results of the geo-electrical resistivity method in groundwater investigations in the Netherlands. *Geophysical Prospecting.*, v. 15, no. 1., p. 92-115.

Van Der Veer, P. (1977). Analytical solution for steady surface in a coastal aquifer involving a phreatic surface with precipitation. *Journal of Hydrology.*, v. 34., p. 1-11.

Van Overmeeren, R.A. and Ritsema, I.L. (1988). Continuous vertical sounding. *First Break*, 6., p. 313-324.

Volker, A. and Dijkstra, J. (1955). Determination des salinities des eaux dans le sons-soldu Zuiderzee par prospection geophysique. *Geophysical Prospecting.*, v. 111, no. 2, p. 111.

Water and Power Development Agency, Pakistan, (1970). Water logging and Salinity. *Annual Report.*

Water and Power Development Agency, Pakistan, (1988). Water logging and Salinity. *Annual Report.*

Water and Power Development Agency, Pakistan, (1989). Water logging and Salinity. *Annual Report.*

Welsh Water Authority. Dee and Clwyd River Division (personal communication).

Wentworth, C.K. (1939). Specific gravity of seawater and the Ghijben-Herzberg ratio. *Trans. Amer. Geophys. Union.*, v. 20, pt. 4., p. 690-692.

Wentworth, C.K. (1951). The process and progress of saltwater encroachment. *Intl. Assoc. Sci. Hydrology Publ.*, 33., p. 238-248.

Wiest, R.J.M. DE. (1965). Geohydrology. John Wiley and Sons, Inc., New York, p. 297 (Chapter 7).

Windle, D. and Wroth, C.P. (1975). Electrical resistivity method for determining volume change, that occur during a pressuremeter test. Proc. Speciality Conf. On In-situ Measurement of Soil Properties. *Am. Soc. Civil Engrs.* Raileigh, N.C. June 1-4., p. 497-510.

Winsauer, W.O., Shearin, A.M., Masson P.H. and Williams, M. (1952). Resistivities of brine saturated sands in relation to pore geometry, Bull., Am. Assoc. Pet. Geol., 36, p. 253.

Worthington, P.F. (1973). Estimation of the permeability of a Bunter Sandstone aquifer from laboratory investigation and borehole resistivity measurement. *Water and Water Engineering.*, p. 251-257.

Worthington, P.F., (1975). Quantitative geophysical investigation of granular aquifer. *Geophysical Surveys.*, 2., p. 313-366.

Worthington, P.F., (1976). Hydrogeophysical equivalency of water salinity porosity and matrix conduction in arrenaceous aquifers. *Ground Water.*, v. 14, no. 4., p. 224-232.

Worthington, P.F., (1977). Geophysical investigations of groundwater resources in the Kalahari Basin. *Geophysics.*, v. 42, no. 1., p. 87-92.

Wyllie, M.R.T. and Spangler, (1952). Application of electrical resistivity measurements to problems of fluid flow in porous media. *Bull- AAPE.*, v. 36, no. 2, p. 359-403.

Zohdy, A.A.R., Eaton, G.P. and Maybey, D.R. (1974). Application of surface geophysics to groundwater investigations. *U.S. Geological Survey.*, p.116.

APPENDICES

DATA SET: ABER10B

CLIENT: UCNW
LOCATION: ABER
COUNTY: GWYNEDD
PROJECT:GROUNDWATER
ELEVATION: 0.0
SOUNDING COORDINATES: X: 0.0 Y: 0.0

DATE: 3.6.92
SOUNDING: 10B
AZIMUTH: //BEACH
EQUIPMENT: T-METER

Wenner Configuration

FITTING ERROR 3.5 PERCENT

L	RESISTIVITY (ohm-m)	THICKNESS (meters)	ELEVATION (meters)	LONG. COND. (Siemens)	TRANS. RES. (ohm-m^2)
1	100.0	0.500*	-0.500	0.005	50.00
2	2090.0	1.50 *	-2.00	6.470E-04	3477.50
3	45.00	2.80 *	-4.80	0.0622	126.00
4	15.00*	2.40 *	-7.20	0.160	36.00
5	614.30	8.10	-15.30	0.0113	7412.90
6	111.30	17.00	-32.30	0.1350	1671.70
7	15.00				

'*' INDICATES FIXED PARAMETER

PARAMETER BOUNDS FROM EQUIVALENCE ANALYSIS

	LAYER	MINIMUM	BEST	MAXIMUM
RHO	1	82.00	100.00	111.00
	2	1182.90	2090.00	4961.80
	3	40.00	45.00	52.00
	4	15.00	15.00	15.00
	5	64.55	614.30	3210.00
	6	101.00	111.00	121.01
	7	11.21	15.00	18.05
THICK	1	0.500	0.500	0.500
	2	1.500	1.500	1.500
	3	2.800	2.800	2.800
	4	2.400	2.400	2.400
	5	4.360	8.100	10.50
	6	15.941	17.000	17.85
DEPTH	1	0.500	0.500	0.500
	2	2.000	2.000	2.000
	3	4.800	4.800	4.800
	4	7.200	7.200	7.200
	5	11.560	15.300	17.70
	6	27.501	32.300	35.55

Appendix Table 6A. Equivalence bounds (DC resistivity) sounding results at site Aber 10B.

DATA SET: ABER10B

CLIENT: UCNW
LOCATION: ABER
COUNTY: GWYNEDD
PROJECT:GROUNDWATER
ELEVATION: 0.0
SOUNDING COORDINATES: X: 0.0 Y: 0.0

DATE: 3.6.92
SOUNDING: 10B
AZIMUTH: //BEACH
EQUIPMENT: MAXMIN
COIL SEPARATION: 50.00 m

Horizontal Coplanar Loops

FITTING ERROR 0.90 PERCENT

L	RESISTIVITY (ohm-m)	THICKNESS (meters)	ELEVATION (meters)	CONDUCTANCE (Siemens)	RESISTANCE (ohm)
1	101.4	0.500*	-0.500	0.0049	50.74
2	1593.0	1.50 *	-2.00	0.0018	4769.60
3	40.00	2.80 *	-4.80	0.0700	112.00
4	15.00*	2.40 *	-7.20	0.160	36.99
5	550.10	9.90	-17.10	0.0178	5391.70
6	126.00	15.50	-32.60	0.2530	4022.40
7	20.00				

'*' INDICATES FIXED PARAMETER

PARAMETER BOUNDS FROM EQUIVALENCE ANALYSIS

	LAYER	MINIMUM	BEST	MAXIMUM
RHO	1	90.00	101.40	104.340
	2	159.36	1593.60	15936.560
	3	35.00	40.00	45.00
	4	15.00	15.00	15.00
	5	135.01	550.10	5501.890
	6	116.00	126.00	141.01
	7	11.21	20.00	40.05
THICK	1	0.500	0.500	0.500
	2	1.500	1.500	1.500
	3	2.800	2.800	2.800
	4	2.400	2.400	2.400
	5	8.90	9.900	10.840
	6	14.20	15.50	20.20
DEPTH	1	0.500	0.500	0.500
	2	2.000	2.000	2.000
	3	4.800	4.800	4.800
	4	7.200	7.200	7.200
	5	16.10	17.100	18.040
	6	30.30	32.60	38.240

Appendix Table 6B. Equivalence bounds (EM) sounding results at site Aber 10B.

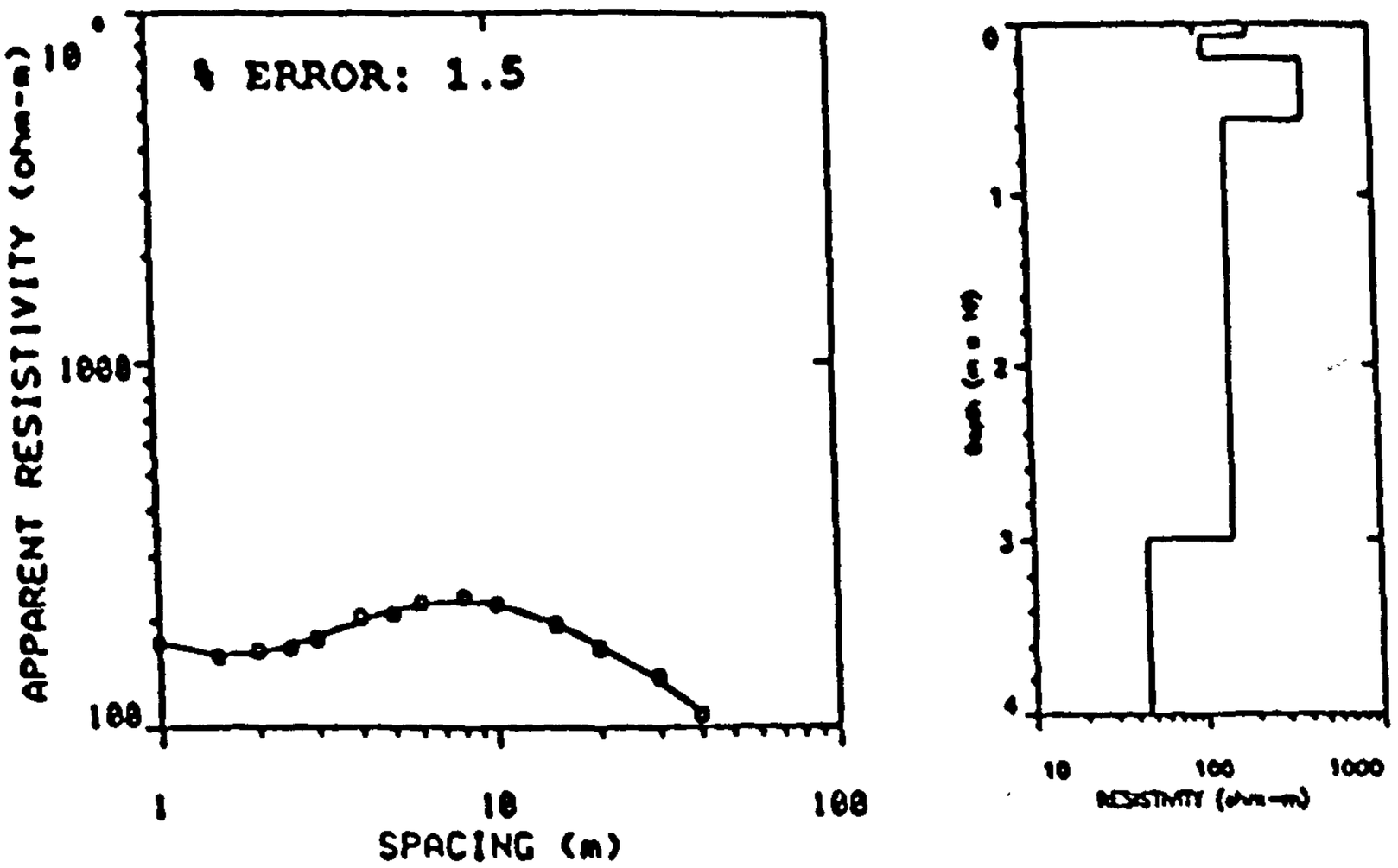

.a.

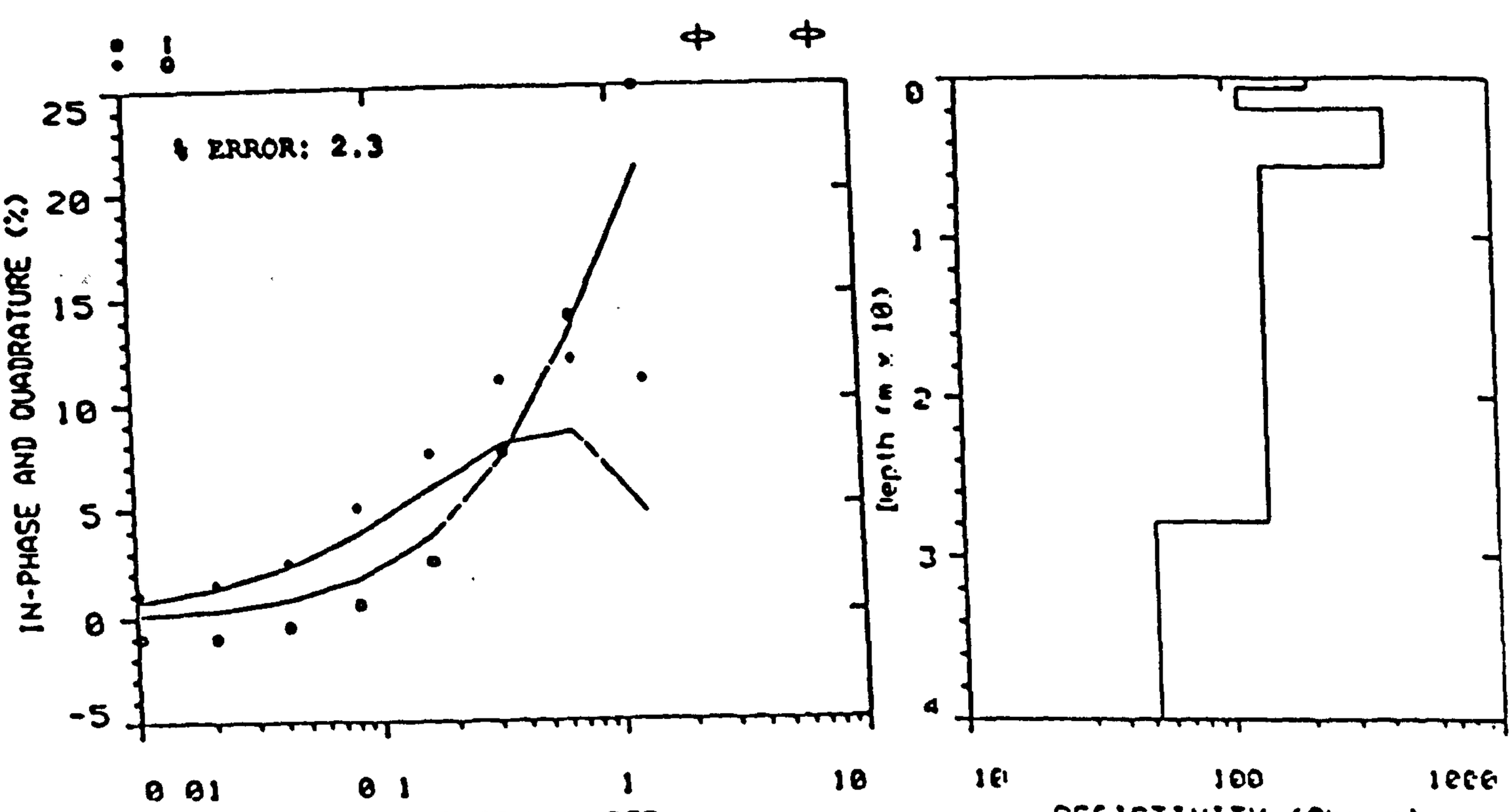

.b.

Appendix Figure 6C. Vertical electric sounding curve (a) and electromagnetic sounding curve (b) at site 3C based on field data points.

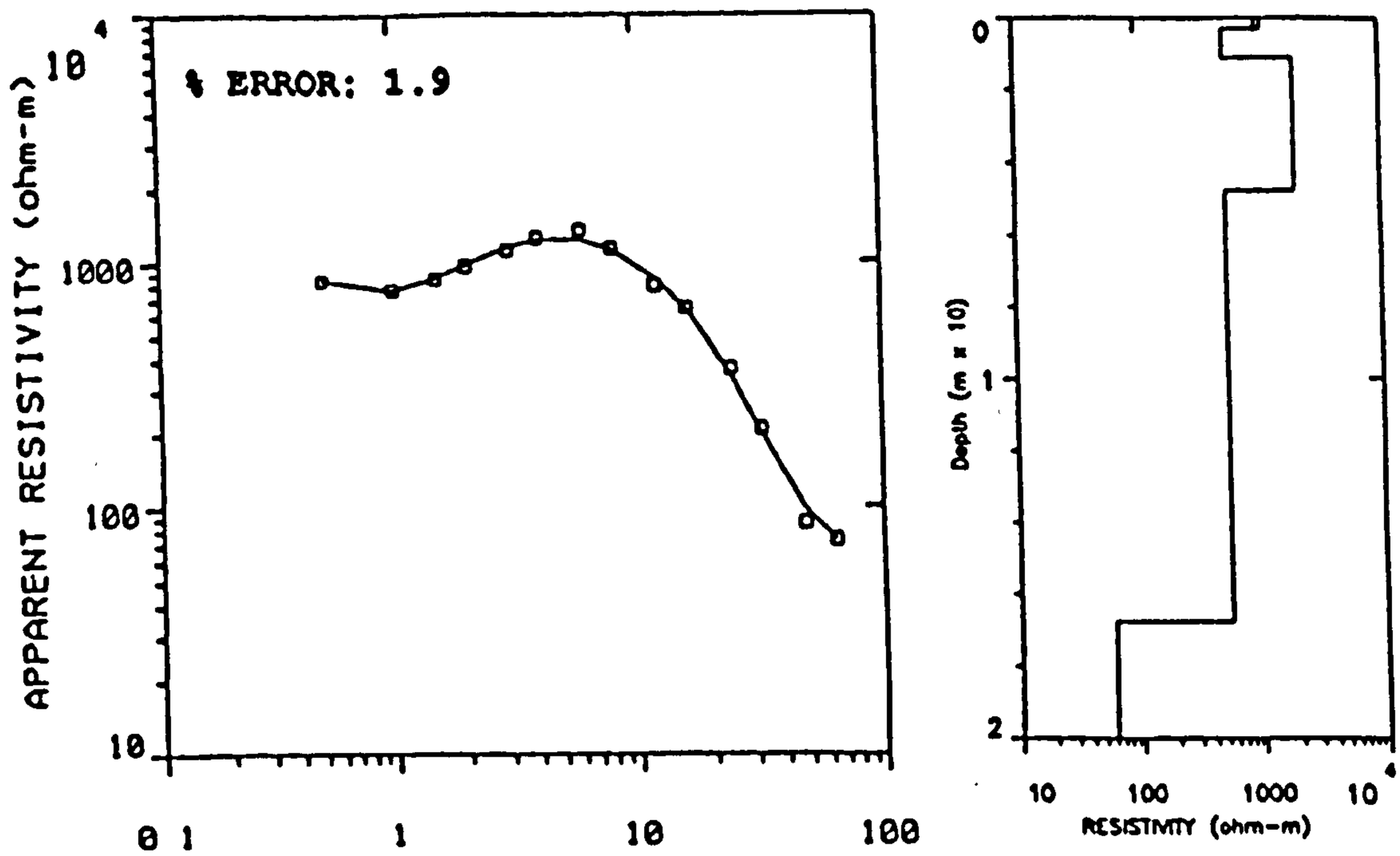

Appendix Figure 6D. Vertical electric sounding curve at site 2B based on field data points.

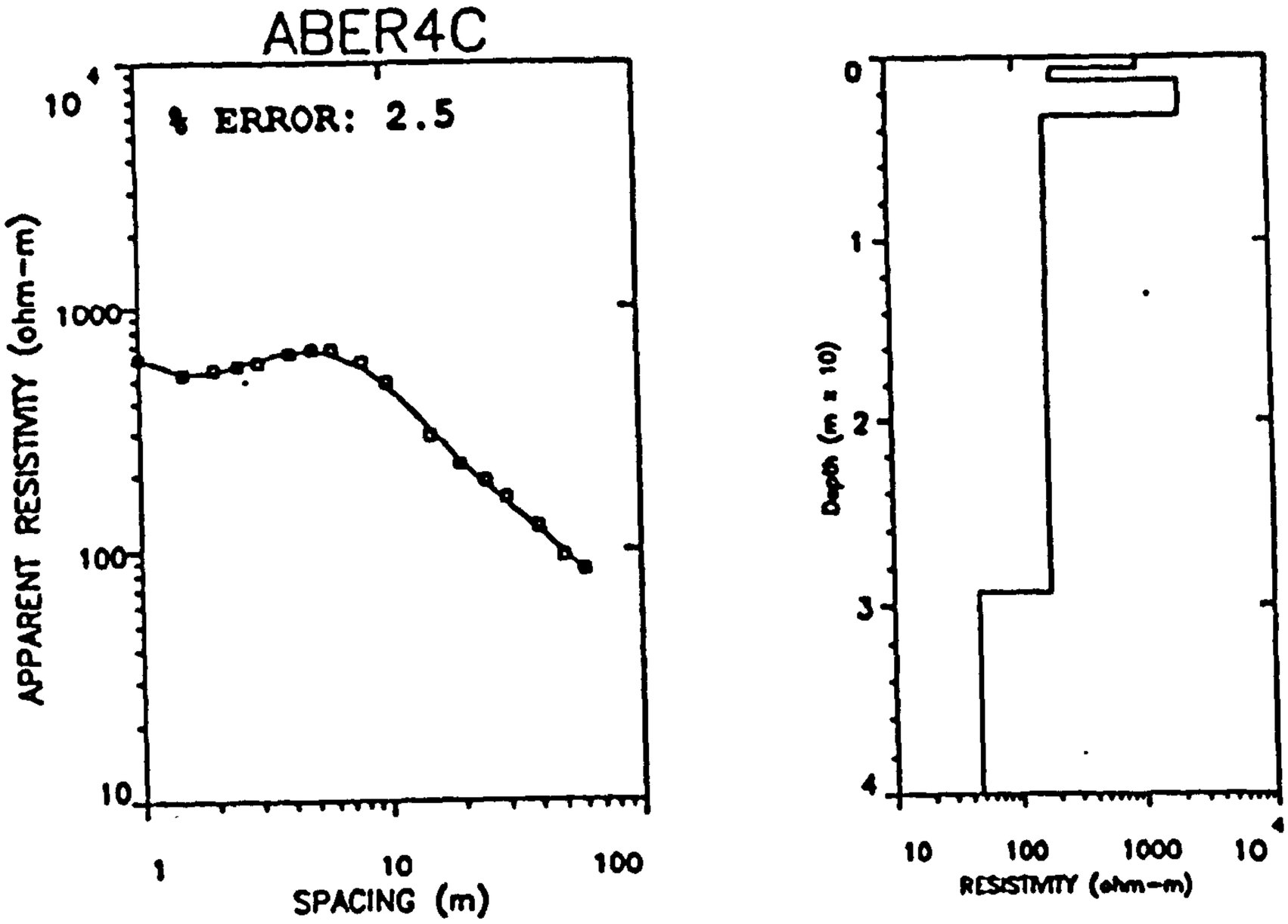

.a.

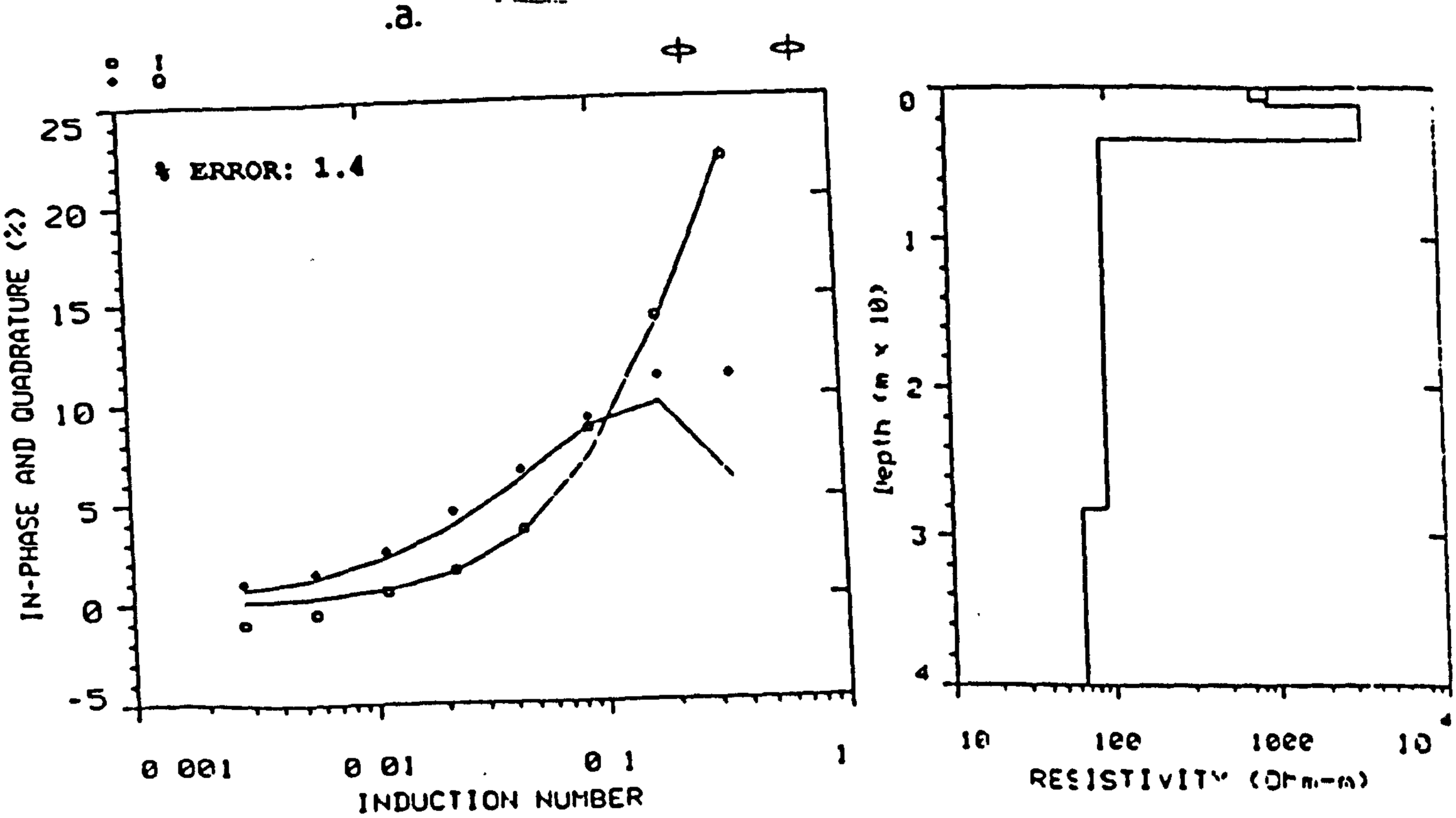

.b.

Appendix Figure 6E. Vertical electric sounding curve (a) and electromagnetic sounding curve (b) at site 4C based on field data points.

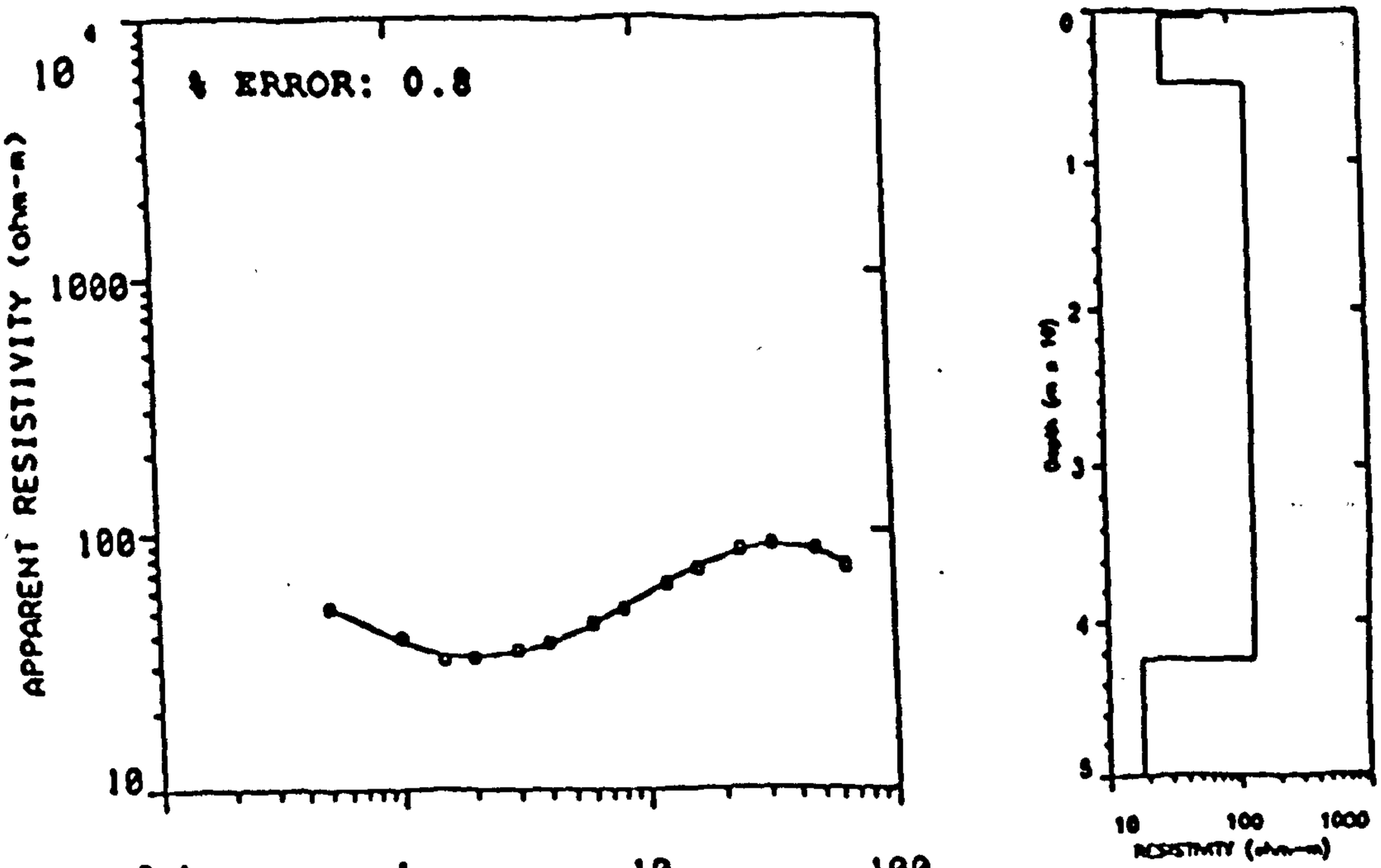

.a.

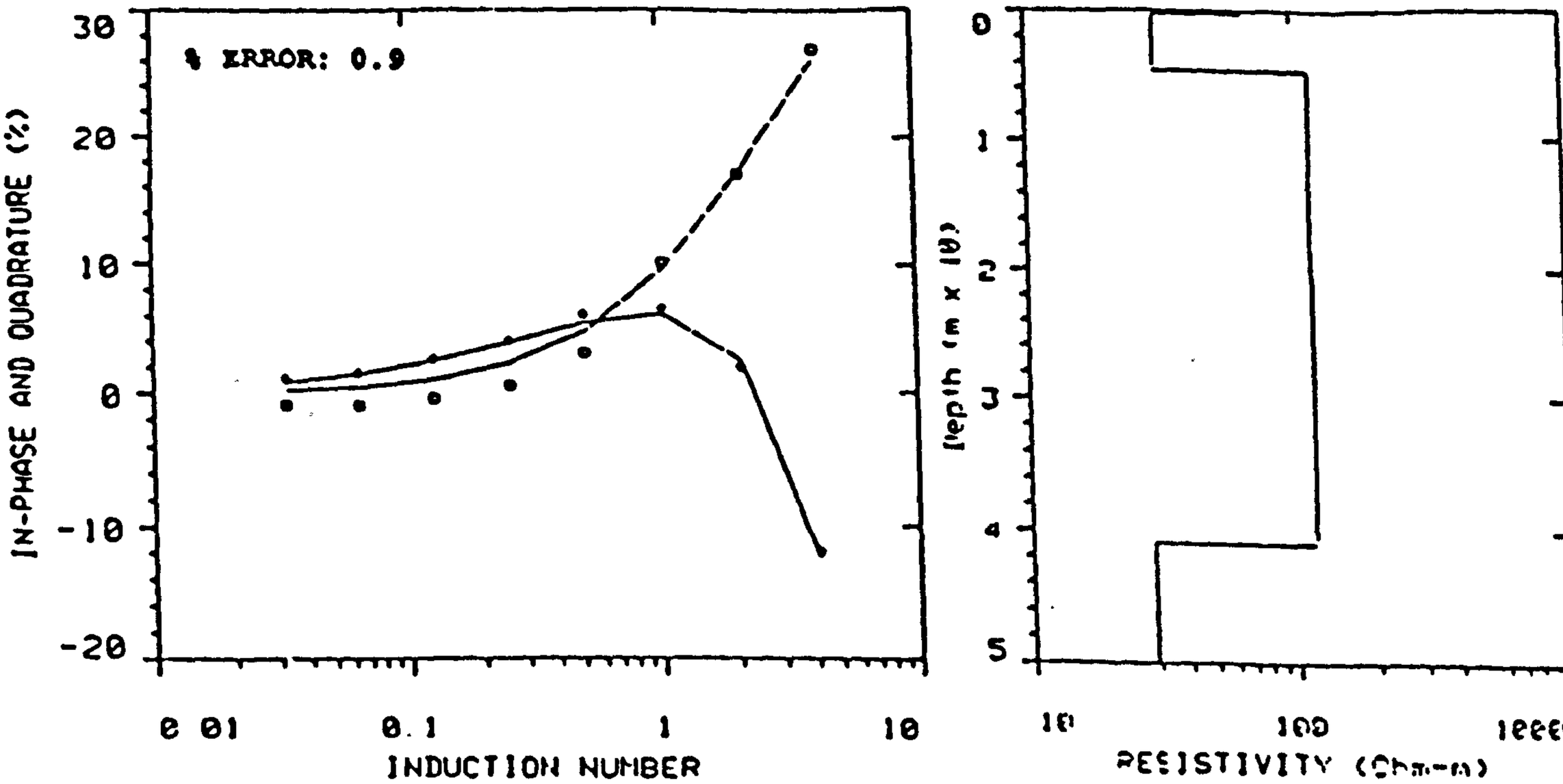

.b.

Appendix Figure 6F. Vertical electric sounding curve (a) and electromagnetic sounding curve (b) at site 5B based on field data points.

DATA SET: MTRTH3C

CLIENT: UCNW
LOCATION: MALLTRAETH
COUNTY: GWYNEDD
PROJECT: GROUNDWATER
ELEVATION: 0.0
SOUNDING COORDINATES: X: 0.0 Y: 0.0

DATE: 1.4.92
SOUNDING: 3C
AZIMUTH: //BEACH
EQUIPMENT: TERRA-MR

Wenner Configuration

FITTING ERROR 2.6 PERCENT

L	RESISTIVITY (ohm-m)	THICKNESS (meters)	ELEVATION (meters)	LONG. COND. (Siemens)	TRANS. RES. (ohm-m^2)
1	1.440	3.29	-3.29	2.28	4.76
2	1.97	10.71	- 14.00	5.74	20.25
3	142.03				

'*' INDICATES FIXED PARAMETER

PARAMETER BOUNDS FROM EQUIVALENCE ANALYSIS

	LAYER	MINIMUM	BEST	MAXIMUM
RHO	1	1.370	1.444	1.523
	2	1.551	1.970	2.266
	3	67.233	142.030	887.05
THICK	1	2.131	3.291	4.957
	2	10.001	10.711	12.826
DEPTH	1	2.131	3.298	4.957
	2	12.132	14.002	17.783

Appendix Table 7C. Equivalence bounds (DC resistivity) sounding results at site Malltraeth 3C.

DATA SET: MTRTH3C

CLIENT: UCNW
LOCATION: MALLTRAETH
COUNTY: GWYNEDD
PROJECT:GROUNDWATER
ELEVATION: 0.0
SOUNDING COORDINATES: X: 0.0 Y: 0.0

DATE: 1.4.92
SOUNDING: 3C
AZIMUTH: //BEACH
EQUIPMENT: MAXMIN
COIL SEPARATION: 50.00 m

Horizontal Coplanar Loops

FITTING ERROR 3.90 PERCENT

L	RESISTIVITY (ohm-m)	THICKNESS (meters)	ELEVATION (meters)	CONDUCTANCE (Siemens)	RESISTANCE (ohm)
1	1.11	4.40	-4.40	4.62	12.09
2	2.26	11.41	-15.81	6.87	10.98
3	142.00				

'*' INDICATES FIXED PARAMETER

PARAMETER BOUNDS FROM EQUIVALENCE ANALYSIS

	LAYER	MINIMUM	BEST	MAXIMUM
RHO	1	0.939	1.11	2.37
	2	1.551	2.26	7.58
	3	135.34	142.002	250.02
THICK	1	4.31	4.400	4.45
	2	11.20	11.411	12.01
DEPTH	1	4.31	4.40	4.45
	2	15.51	15.811	16.46

Appendix Table 7H. Equivalence bounds (EM) sounding results at site Malltraeth 3C.

DATA SET:MBYCN6I'

CLIENT: UCNW
LOCATION: MORFA BYCHN
COUNTY: -
PROJECT:GROUNDWATER
ELEVATION: 0.0
SOUNDING COORDINATES: X: 0.0 Y: 0.0

DATE: 7.4.92
SOUNDING: 6I'
AZIMUTH: //BEACH
EQUIPMENT: TERRA-MR

Wenner Configuration

FITTING ERROR 2.43 PERCENT

L	RESISTIVITY (ohm-m)	THICKNESS (meters)	ELEVATION (meters)	LONG. COND. (Siemens)	TRANS. RES. (ohm-m^2)
1	4.00	1.91	-1.91	0.418	6.21
2	12.01	7.50	-9.41	0.652	64.94
3	54.90				

'*' INDICATES FIXED PARAMETER

PARAMETER BOUNDS FROM EQUIVALENCE ANALYSIS

	LAYER	MINIMUM	BEST	MAXIMUM
RHO	1	3.64	4.00	4.11
	2	8.08	12.01	13.26
	3	49.44	54.90	63.51
THICK	1	1.31	1.91	2.12
	2	5.23	7.50	8.74
DEPTH	1	1.31	1.91	2.12
	2	6.54	9.41	10.86

Appendix Table 8I. Equivalence bounds (DC resistivity) sounding results at site Morfa Bychan 6I'.